

IMFUFA **tekst**

- I, OM OG MED MATEMATIK OG FYSIK

Mathematical Modeling of the Hypothalamic-Pituitary-Adrenal Axis

Frank Vinther and Morten Andersen
March 2010

nr. 469 - 2010



Mathematical Modeling of the Hypothalamic-Pituitary-Adrenal Axis

By: Frank Vinther and Morten Andersen

In this thesis two mathematical models of the hypothalamic-pituitary-adrenal-axis (HPA-axis) are built using well known physiological mechanisms. The HPA-axis controls the secretion of the hormones CRH, ACTH and cortisol. The regulation of these hormones are important to human health. These hormones are the variables in two systems of coupled non-linear differential equations that constitute the models. The models include a negative feedback of cortisol on ACTH. The first model has a negative feedback from cortisol on CRH corresponding to the 'standard biology textbook' description of the HPA -axis. The second model allows a feedback from cortisol on CRH to be positive or negative depending on the cortisol concentration by including mechanisms from hippocampus.

For parameter values in a physiologically relevant range it is investigated if the models are capable of guaranteeing solutions with reasonable levels in hormone concentration. It is investigated if the models are capable of producing the ultradian oscillations that are observed in data of hormone concentrations. It is investigated if an external imposed function on the differential equation governing the CRH concentration can

cause the circadian rhythm that is seen in the concentrations of ACTH and cortisol.

Previous papers of the HPA-axis [1] and [2] claim to make models showing ultradian oscillations. We analyze the two models and find significant drawbacks that must be elaborated for a successful model taking care of the physiological mechanisms of the HPA-axis.

Results of analytical investigation of our models

For both models the results of the investigation is that all solutions end in a trapping region in the positive octant of \mathbf{R}^3 , thus guaranteeing reasonable levels in hormone concentration. Within this trapping region there exists at least one fixed point. The first model has a unique fixed point. The unique fixed point is locally stable for all physiological choices of parameters. Therefore no Hopf bifurcation is possible as an explanation for the ultradian oscillations in data. For the second model more than one fixed point is possible. The stability of a fixed point is categorized depending on the sign of the feedback on CRH at the fixed point.

A sufficient, easily applicable criteria for a unique, globally stable fixed point is formulated for a more general model. This can be applied on the two specific models.

Results of numerical investigation of our models

In the case of a unique fixed point this is asymptotically stable for all reasonable parameter values and initial conditions. Perturbating the parameters in the second model makes the system undergo a bifurcation where two new fixed points emerge. In the case of three fixed points there is one unstable fixed point and two asymptotically stable fixed points. For all reasonable values of parameters and initial conditions the solutions converge towards one of the two stable fixed points. Thus for reasonable parameter values neither of the models are capable of producing the ultradian oscillations.

The analytical criteria for a globally stable fixed point is fulfilled for some set of parameters within physiologically relevant range for both models.

An external input in the differential equation governing CRH is capable of showing circadian oscillations in the ACTH and cortisol concentration.

Mathematical Modeling of the Hypothalamic-Pituitary-Adrenal Axis

Morten Andersen
Frank Vinther

Supervisor
Johnny T. Ottesen

MASTER THESIS - MATHEMATICS
NSM, IMFUFA, FALL 2009



ROSKILDE UNIVERSITETSCENTER
INSTITUT FOR NATUR, SYSTEMER OG MODELLER

Preface

This project report is a master thesis in mathematics for two persons at Roskilde University. The thesis is thus counting 20 ECTS points per person. The thesis is in the category 'Mathematical Model Building' and concerns deterministic models of the hypothalamic-pituitary-adrenal (HPA)-axis.

In our early study of the literature for the thesis our eyes fell upon papers by Kyrylov et al., [1], and by Jelić et al., [2]. Here models reproducing the dynamics of the HPA-axis are formulated. Therefore we appreciate that Vadim Kyrylov invited one of the authors of this project on a visit to discuss mathematical modeling of the HPA-axis.

We thank Jan Vistisen and Lars Arvastson from the medical company H. Lundbeck A/S for being very helpful with many aspects regarding the modeling of the HPA-axis.

The collaboration with H. Lundbeck A/S has given us the fortunate opportunity of access to data of hormone levels in healthy and unhealthy (depressed) persons. To our knowledge deterministic mathematical models of the HPA-axis has not previously been compared to such data. A successful model could therefore be used on the healthy group as well as on the unhealthy group(s). The outcome could be that some parameters of the mathematical model are significantly different among the groups. Then the model could be used for a better understanding of the mechanisms causing depression.

It has been very motivating to us that a successful model may help improve the understanding of the HPA-axis that is important to human health.

A special thanks to our supervisor, Johnny Tom Ottesen, for thorough feedback, interest and relevant suggestions through the project.

Contents

Contents	vi
1 Method and readers guide	1
2 Introduction	4
2.1 Introduction to the physiology of the hypothalamic-pituitary-adrenal axis	4
2.2 Mathematical modeling of the dynamics of the HPA-axis	6
2.3 Brief presentation of previous models	9
2.4 Our model	14
2.5 Description of included mechanisms of our model	16
2.6 Problem formulation	16
3 Introduction to the mathematics of differential equations	18
3.1 Method for solving a system of linear differential equations	19
3.2 Three dimensional system of linear differential equations	21
3.3 Three dimensional system of non-linear differential equations	22
3.4 Bifurcations	23
3.5 Bifurcation and stability of a fixed point	25
3.6 Banach Fixed Point Theorem	27
4 Previous models	28
4.1 Discussion of the paper of Kyrylov et al.	28
4.2 Applying the RHC on a linear three dimensional model of Kyrylov et al.	32
4.3 Discussion of the paper by Jelic et al.	38
5 Modeling the HPA-axis	42
5.1 Modeling the HPA-axis without hippocampus	42
5.2 Hill function	45
5.3 Implementing the feedback functions	49
5.4 Jelic-like approach	50
5.5 Description of the obtained system of nonlinear differential equations . .	51
5.6 Existence and uniqueness of solutions, trapping region, existence and number of fixed points	52
5.7 $x_3(t) > 0$ after finite time and for all future time.	54
6 Analytic analysis of the system without hippocampus	60
6.1 Scaling of the system of differential equations	60
6.2 The system with $\mu = 1, \rho = 1$	64

7	Stability of a fixed point for a system with positive feedback from cortisol on CRH	68
8	A model including the mechanisms from hippocampus	70
8.1	Simplifications using physiological reasoning	72
8.2	Scaling of the differential equations	72
8.3	Existence and uniqueness of solutions, non negative concentrations, confining set and existence of fixed points	73
8.4	Stability of fixed point(s)	75
9	Considerations regarding general systems with bounded feedback functions	78
9.1	Expansion of trapping region	80
9.2	Bounding of solutions inside trapping region using solutions of linear systems	82
9.3	Sufficient criteria for a globally stable fixed point	84
9.4	Sufficient criteria for using Banach Fixed Point Theorem	90
10	Estimation of parameters	94
10.1	The parameter values in the scaled system without hippocampus	98
10.2	Parameters of the model including hippocampus	100
11	Numerical investigations	104
11.1	The system without hippocampus	104
11.2	Variation of parameters in the system without hippocampus	109
11.3	The system including mechanisms from hippocampus	114
11.4	Summary of numerical analysis of the system including hippocampal mechanisms	123
11.5	Including external function to model the circadian rhythm	123
12	Discussion	130
12.1	Most general results	130
12.2	Results of model including hippocampal dynamics	131
12.3	Results of the model excluding hippocampal mechanisms	132
12.4	Comparing the results to state of the art models	133
12.5	Typical mathematical approaches when non linear differential equations are used for modeling	134
12.6	Inclusion of circadian rhythm	135
12.7	Conclusion	135
13	Discussion: Modeling of HPA axis including time delay	136
13.1	Inclusion of time delay in our system	139
A	Proof of the Routh Hurwitz Criteria	142
B	Matlab codes	146
B.1	Fast Fourier transformation	146
B.2	Calculation of parameters	151
B.3	Main file used for the numerical analysis	152

B.4 Files loaded by the main file used for numerical analysis	160
Bibliography	162

1 Method and readers guide

In this chapter we seek to give the reader an insight into the structure of this thesis.

First we introduce the reader to the rather complex biology of the HPA-axis in chapter 2. This introduction serve as the platform for our mathematical model. The standard biology textbook description of the HPA-axis regards a system where three hormones interact and two negative feedbacks are present. Some mathematical models of the HPA-axis include more mechanisms that may be of importance. We aim at the simplest model showing the desired behaviour. Therefore we will construct and analyze two models. One only including the 'standard biology textbook' mechanisms of the HPA axis and a more advanced model.

Our two models are deterministic. For a deterministic model a solution can be found numerically given a set of initial conditions and parameters. Perturbing a parameter may lead to qualitatively different dynamics which can be investigated numerically and analytically (locally). The included mechanisms of the HPA-axis result in expressions including parameters in the mathematical model. This means the behaviour of the mathematical model can be analyzed as different mechanisms of the physiology are given more or less weight. Since the three kinds of hormones of the HPA axis are coupled it is hard to distinguish cause and effect in for the physiology of the HPA-axis. However for a deterministic model it may be possible to describe the effect of e.g. a malfunctioning feedback.

In chapter 2 we also show masked data kindly provided by H. Lundbeck A/S. This should give the reader an idea of the dynamics a model should be able to reproduce. A brief presentation of two state of the art models (paper [2] and paper [1]) of the HPA axis is also given in this chapter. Here we focus on categorizing the arguments regarding physiology and mathematical modeling. We focus here on the advantages of the two models.

In chapter 3 we introduce the most widely used mathematical theory in this thesis. We focus on deterministic models. Therefore this chapter mainly concerns theory regarding ordinary differential equations.

Since the mathematical theory is now introduced we can in chapter 4 give a more in depth analysis of [2] and [1]. This analysis reveals problematic parts of each model that must be improved. The purpose of this chapter is to show typical models of the HPA-axis. Also this chapter shows that modeling of the HPA-axis is incomplete justifying that more work is needed.

In chapter 5 the first of our two models is constructed and analyzed. An important part of the model relies on receptor dynamics that are crucial for feedback mechanisms. The analytical investigation does not constitute a complete investigation of the system dynamics (which is often the case for non linear systems of differential equations). However the analysis does not give reason to expect the system has the desired dynamics.

The second model is constructed and analyzed in chapter 8. The use of receptor dynamics is also in focus for the second model.

The two mathematical models are analyzed and some important properties are common for both systems. The arguments for this is also quite similar in the two cases. However this emphasize the potential in a formulation a more general model where the same results apply. This is interesting since a wider range of models is then covered. This is explored in chapter 9. Here a criteria is formulated that guaranties global stability, thus outruling the existence of limit cycles. This arguments is easy to use for a specific system where parameters are known.

Some results of this projects hold solely by knowing the sign of the included parameters. However some results are a categorization of system dynamics. This depends on the actual values of the parameters of the system. Therefore chapter 10 concerns estimation of parameters. This leads to a set of default parameters for our two models. However it is a general problem when modeling the HPA-axis to get reliable parameters.

In chapter 11 the dynamics of our two models are investigated numerically using Matlab. First using the default parameters. Then typically one parameter is perturbed and the rest of parameters are fixed at default values. This is valuable information since the parameter estimation leaves room for improvement. Therefore the behaviour of the model using perturbed parameters are of interest.

It is a common assumption of the papers modeling the HPA-axis that a circadian pattern can be separated from a faster dynamics. In chapter 11 we will include this circadian input in simulations. All Matlab codes can be found in appendix B.

Chapter 12 summarize the results of this project. Here we start with the most general results for our models and proceed with the results that characterize specific models. The results are compared to state of the art models.

Since no successful model is found chapter 13 concerns including time delay in the model. This is justified by a 'transport time' for a hormone to reach its place of action. Models (paper [3] and [4]) including time delay have rejected that time delay explains the physiologic observed behaviour. However we point out a crucial shortcoming of their argumentation. We therefore suggest further studies should be made on a model including time delay.

2 Introduction

2.1 Introduction to the physiology of the hypothalamic-pituitary-adrenal axis

A hormone is a 'messenger molecule' released into the bloodstream where it flows with the blood and then binds to a specific target receptor in the body tissue. This thesis will concern a mathematical model with hormone concentrations as variables. More precisely the hormones of the hypothalamic-pituitary-adrenal (HPA) axis. The HPA axis is a biological system connecting three areas in the human body by mainly three hormones, this is illustrated in figure 2.1 and figure 2.2.

The HPA axis plays an important role under stressed conditions by raising the concentration of the HPA axis hormones which leads to energy directed to the organism[4]. The return to the basal hormone levels after a while is an important feature of the system when it is working properly.

We will now give a short description of the HPA axis, see figure 2.2. Corticotropin releasing hormone (CRH) is secreted in hypothalamus and reaches another area in the brain - the anterior pituitary. Here CRH stimulates the secretion of adrenocorticotrophic hormone (ACTH) from the pituitary gland. ACTH moves with the bloodstream and when it reaches the adrenal glands it stimulates secretion of cortisol. The standard textbook description is that cortisol inhibits the secretion of CRH in the pituitary (performs a negative feedback). Cortisol also performs a negative feedback on the secretion of ACTH in the hypothalamus as shown in figure 2.2[5]. It has been suggested that there can be a struggle between a resulting positive and a negative feedback on the CRH secretion from cortisol[2, 6] which will be discussed later.

Stress causes the body to increase the level of cortisol which stimulates e.g. formation and secretion of glucose that is important 'fuel' for the body[5]. Keeping cortisol concentration within a certain range is important for various reasons. As an example a maintained, high level of cortisol (hypercortisolism) can cause depression, diabetes, visceral obesity or osteoporosis[6]. Too low concentration is neither desirable since it can result in a disturbed memory formation or life-threatening adrenal crisis[6]. The regulation of the HPA axis is thus important to be healthy. More factors influence the system but the three hormones mentioned constitute the backbone of the HPA axis[5] and will therefore constitute the variables of the model considered in this project.

The cortisol concentration has a daily pattern. It is typically low between 8 p.m. and 2 a.m. and rises to peak in the period 6-10 a.m.[2]. CRH is secreted in a pattern with a frequency of one to three secretory periods per hour (often referred to as ultradian oscillations)[7]. Throughout the literature [8] and our data we see circadian as well as ultradian oscillations in the hormone concentration of ACTH and cortisol. Therefore circadian as well as ultradian oscillations are present in the system.

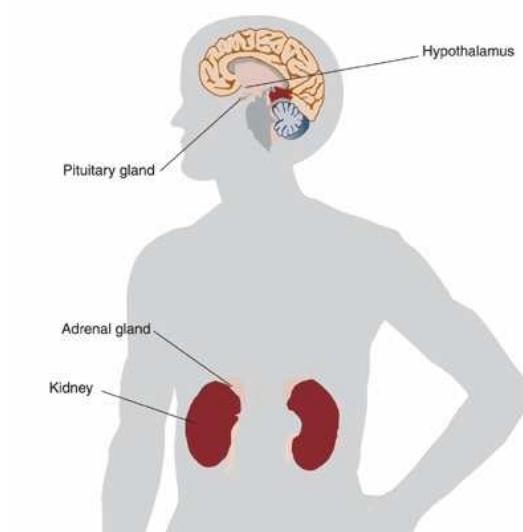


Figure 2.1: The location of the hypothalamus, the pituitary and the adrenal glands that constitute the HPA axis along with the ACTH, CRH and cortisol interactions.

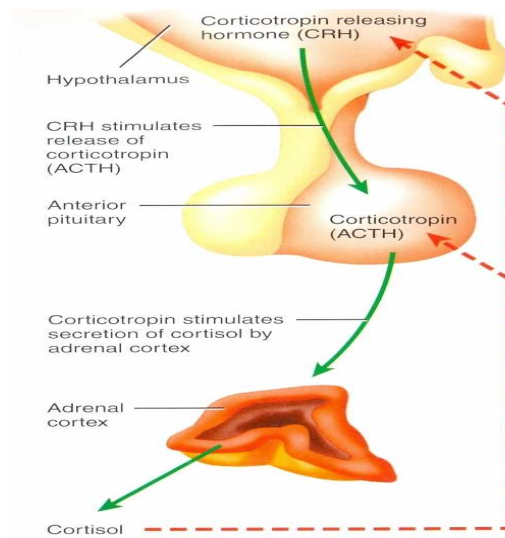


Figure 2.2: The HPA-axis from [5]. The green lines show a positive stimulation. The red lines indicate that elevated cortisol concentration inhibits secretion of CRH as well as a direct inhibition of secretion of ACTH.

The frequency of the ultradian oscillations is rather insensitive to stress whereas the amplitude increases[7]. Examples of data with circadian and ultradian oscillations can be seen in the figures 2.3 and 2.4.

2.2 Mathematical modeling of the dynamics of the HPA-axis

Understanding of the interplay between the various mechanisms of the HPA axis is interesting and important since the system has an important function. Since several feedback mechanisms are working simultaneously in the HPA axis cause and effect may be hard to distinguish. A mathematical model may help to separate cause and effect and can be an important tool for pointing out different ways in which a malfunctioning can occur.

The aim of this project is to make a mathematical model of the dynamics of the HPA axis using mechanism based differential equations including physical interpretable parameters. The model should be simple enough to allow computation but still sufficiently advanced that it captures the important mechanisms. The approach here is to start on solid ground with a simple model and in case of failure proceed in a detective like manner to more complex models.

Known structures that the model should reflect are

- Feedbacks of cortisol on ACTH and CRH.
- Circadian rhythm of hormone concentrations.
- Ultradian oscillations in hormone concentration.

A differential equation model of the HPA-axis can typically be represented by a compartment diagram where significant elements of the HPA-axis are symbolized with boxes and the influence from one box to another is represented by arrows and a plus or minus depending on whether the presence of a substance stimulate or inhibits the production of another substance, see figure 2.5.

Perspectives of a useful model

If a successful model is found it is interesting to investigate the dependence on the included parameters. Parts of the behavior of the model might be more robust to perturbations of some parameters than others. It would be interesting to couple specific values of parameters to measurable quantities in humans. If so the model may be used to determine parameters that are specific to individual patients and thereby give an indication of malfunctioning physiological mechanisms. For example the concentration of cortisol is relevant to depression and there exists depression characterized with a high concentration of cortisol (high cortisol depressive) and similarly a low cortisol depressive group exists. Some values of one or more parameters may characterize one group and values of other parameters may characterize another group. This could help identifying the mechanisms or causes leading to depression.

A field lacking reliable data

It is a general problem to get reliable, physically reasonable parameter values for the HPA axis since it is hard to perform measurements on for instance the CRH concentration in hypothalamus. Therefore it is an ambitious but interesting goal to make a reliable model. A reason not to consider this too ambitious is the access to data of

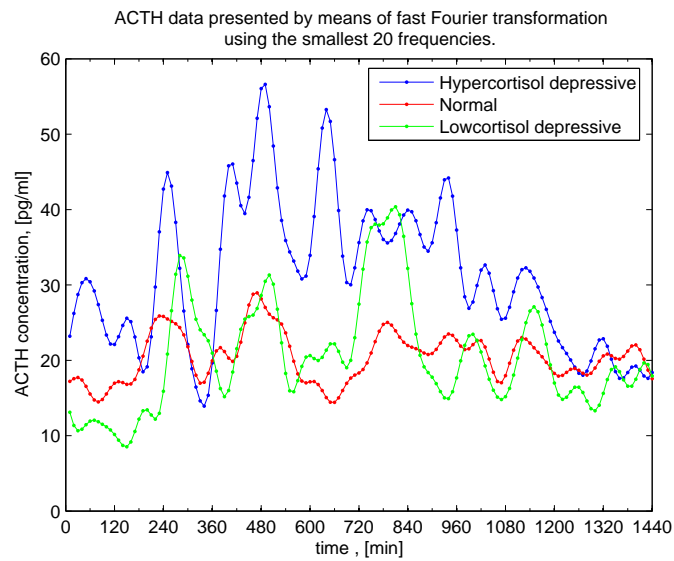


Figure 2.3: Example of ACTH data of three individuals from the hypercortisol depressed group, the low cortisol depressed group and a normal person. Time $t=0$ corresponds to midnight. Data was sampled every tenth minutes through 24 hours.

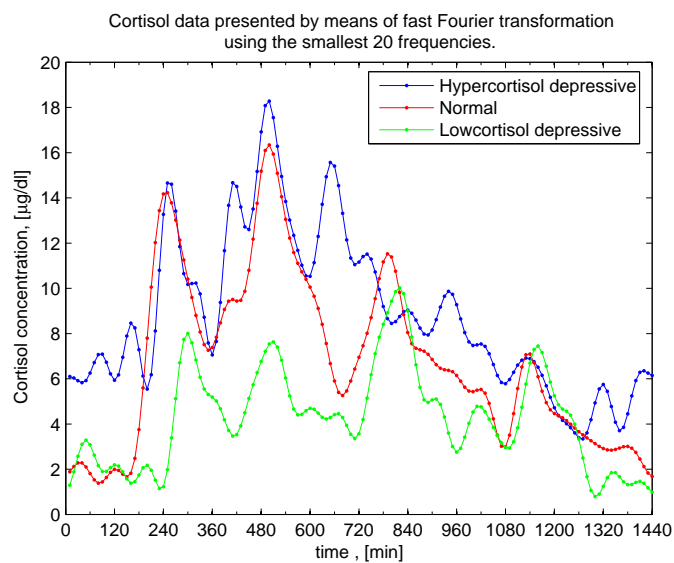


Figure 2.4: Example of cortisol data corresponding to the individuals represented in figure 2.3. Time $t=0$ corresponds to midnight. Data was sampled every tenth minutes through 24 hours.

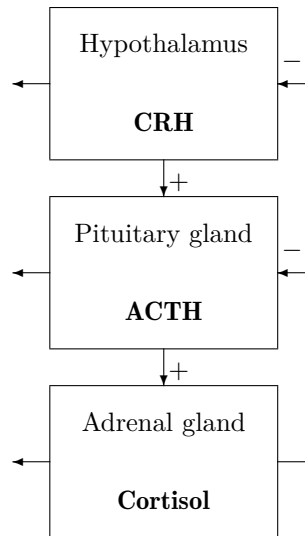


Figure 2.5: A compartment model of the HPA-axis corresponding to figure 2.2.

ACTH and cortisol concentrations of a high cortisol depressive group, a low cortisol depressive and a normal group. Confidential data is kindly provided by H. Lundbeck A/S and is originally from Carroll et al.[9].

This data contains 7 hypercortisol depressive persons, 5 low cortisol depressive persons and 17 not depressed control persons. The measurements are performed every tenth minute through 24 hours and the time $t=0$ corresponds to midnight. Meals were given at 7.30, 12.00 and 18.00 and in waking hours the subjects were allowed to rest in bed or chair. No sleep were allowed in waking hours but listening to radio, watching television or reading was permitted. In order not to violate the confidentiality of the data we have chosen to transform the data by means of fast Fourier transformation(the Matlab code is presented in appendix B.1). The 145 different measurements give us a total of 73 different frequencies when using fast fourier transformation. An example of the data where only the 20 lowest frequencies is included (in order to mask the data sufficiently) is shown in figure 2.3 and figure 2.4. The three individuals shown in figure 2.3 and figure 2.4 corresponds to individual 5, 10 and 27 in the confidential attachment.

We would like the reader to notice the circadian oscillation in ACTH and cortisol as well as the ultradian oscillations. The original aim of the project is to form a mathematical model with physiologically interpretable parts that results in solutions showing these oscillations. We cannot hope to find evidence for faster oscillations than three an hour since sampling every 10th minutes leads to the smallest observable period of 20 minutes(using discrete Fourier analysis).

2.3 Brief presentation of previous models

There are rather few differential equations models of the HPA axis. The various models may be considered consisting of two parts. One is the physiology e.g. the description of the HPA axis using biological terms and one is the modelling e.g. the translation of the biology into mathematics and especially differential equations. Of course these two parts are not independent but criticism or credit of a model may be categorised into either physiology or mathematical modelling.

Papers using nonlinear, coupled differential equations to model the HPA axis are made by Kyrilov et al.[1] and Jelic et al.[2]. These have been of great inspiration to us and of course a project concerning the modelling of the HPA axis must include an overview of previous models. This section serves as an overview of the two models categorizing the parts unique to each model into *physiology* or *mathematical modeling*. This categorization helps determining the difference in the considered physiological mechanisms of each model as well as helps clarifying if the mathematical model properly describes the proposed physiological mechanisms. Both papers describe the physiology as the standard textbook description (section 2) but also more details to the physiology are added. We will present the reader to a more in depth critique of the two models [1, 2] in chapter 4. Chapter 4 will therefore be a justification of why we consider neither the model of [1] nor [2] to capture enough relevant physiological aspects of the HPA axis. We will use what we consider the best aspects of each model and make our own model of the HPA axis. The brief presentation in this section will not include any differential equations since the tools for analyzing these will be illustrated in chapter 3.

The approach of Kyrylov et al.

Here we will give an brief presentation of [1].

Physiology

A compartment formulation of the model is shown in figure 2.6. The included hormones of the HPA axis are CRH, ACTH, free cortisol, albumin bound cortisol and corticosteroid-binding-globulin (CBG) bound cortisol. The diagram has the characteristics of figure 2.5 but several new mechanisms are introduced. An impact from the central nervous system (CNS) on hypothalamus is included and used to give a circadian input on the derivative of CRH. The cortisol dynamics is a bit more complicated than in figure 2.5 since it can be in free form or two bound forms. The bound forms of cortisol only interact with the free form thus not making the system too complicated. It is worth noting that CRH have a direct positive stimulation on cortisol. This stimulation is passing ACTH which we have not seen elsewhere.

Mathematical modeling

The variables of the mathematical model are the five hormones. The mathematical modeling is divided into three steps. First a linear differential model is considered, then non linearities are imposed and finally the circadian input on the derivative of CRH is added.

- First step.

The overall idea is that a linear systems of differential equations can be used when the concentrations of the hormones of the model have moderate, positive values¹. The linear system should show an unstable and oscillatory behaviour. A numerical investigation of the linear system is performed, where some parameters are considered known and the rest are varied within ranges given by orders of the known parameters. The unknown parameters are varied independently within their respective ranges in each simulation and the stability is investigated (If there exists an eigenvalue of the linear system with positive real part the system is unstable. If all eigenvalues are negative the system is stable). The linear system results in unstable and oscillating behaviour in more than 90 percent of the simulated cases. This give the system its ultradian oscillations.

- Second step.

Two artificial nonlinear mechanism are imposed on the linear system. The first is an upper limit on hormone release rate and the second nonlinearity ensures that the hormone concentrations can not become negative. These two physically relevant properties are included in the model by introducing nonlinear functions that obey these characteristics.

- Third step.

The circadian oscillations are introduced by adding a forcing function affecting the derivative of the CRH concentration which then causes circadian variation on the other hormones due to the coupling of the differential equations.

Kyrylov et al. consider their model successful since it represents the physiological behavior of ultradian oscillations and a circadian(imposed) rhythm. Also they consider

¹ Normally a linear approximation of a non linear system of differential equations is only useful close to a steady state solution. However there is no investigation of steady state solution in [1]. For an explanation of steady state solution see chapter 3

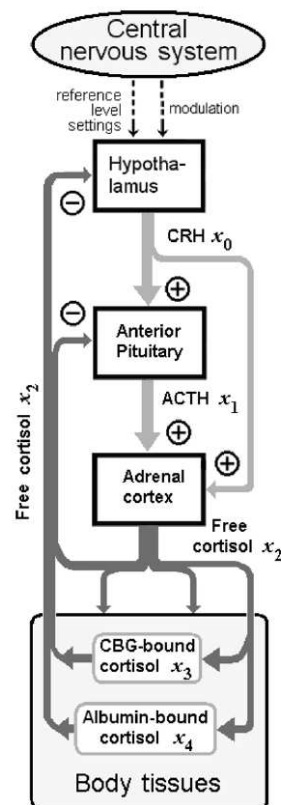


Figure 2.6: The compartment diagram of Kyrylov et al. from [1]. The central nervous system can stimulate the secretion of CRH from hypothalamus. A direct CRH- cortisol stimulation is included which is not the case in diagram 2.5. The negative feedback from this diagram is also included. Two bound forms of cortisol interacts with the free form.

the model more robust to perturbation of the parameters which makes it more reliable than previous models in their view. Actually their model resulted in a whole body simulator that should be used for education of students in biology and medicine.

Some points about the approach of Kyrylov et al. should be noted.

- Physiology.
 - Five hormones of the HPA axis are considered with two bound forms of cortisol included.
 - A direct CRH -cortisol stimulation is included.
- Mathematical modeling.
 - The linear equations of the system shows unstable, oscillatory behavior which is responsible for the ultradian oscillations in the system.

- The non linearities are chosen to ensure the hormone release rate is bounded and negative concentrations do not occur.
- The circadian rhythm is introduced as an external input to hypothalamus affecting the derivative of the concentration of CRH. This is done additively with a time varying cosine function as input. Thus the system becomes non autonomous when this is introduced. The circadian rhythm then 'spreads' to the ACTH and cortisol concentrations automatically since the differential equations are coupled.

The approach of Jelic et al.

The physiology

Hormones have to bind to receptors in order to cause an effect. Taking this approach Jelic et al. put forward a set of chemical reactions upon which their differential equations build. A compartment diagram of the system is shown in figure 2.7. The negative feedback of cortisol on CRH and ACTH takes place through glucocorticoid receptors (GR) in hypothalamus and pituitary. Stress acts on the system through hippocampus (a component of the brain). The circadian rhythm is expressed through the hypothalamic suprachiasmatic nucleus (SCN) that is considered an external factor influencing CRH secretion [2]. [2] describes the dynamics associated with cortisol binding to the mineral corticoid receptors (MR) and the GR in hippocampus. Whereas GR is present in both hippocampus, hypothalamus and the pituitary glands, MR is present particularly in hippocampus [10].

Cortisol binding to MR in hippocampus leads to a negative feedback on the secretion of CRH while cortisol binding to GR in hippocampus cause a positive feedback on the secretion on CRH [2]. Glucocorticoids have a ten fold higher affinity for MR than for GR. Therefore Jelic et al. propose that MR regulates the HPA-axis activity under normal conditions while both MR and GR play a role under high level cortisol conditions since the number of MR is limited [2]. The hormones Jelic et al. suggest are governing the dynamics of the HPA axis are CRH, ACTH, cortisol and aldosterone. Aldosterone is a mineralocorticoid (affecting balance of minerals) whereas cortisol is a glucocorticoid. Aldosterone and cortisol are both secreted from the adrenal glands. Cortisol can bind to both MR and GR but aldosterone has very little affinity for GR but binds to MR [2]. The main reason to include aldosterone in the model is its role as 'placeholder' meaning it is occupying MR in hippocampus resulting in fewer available MR to be occupied by cortisol. If the number of receptors is the limiting factor and the amount of aldosterone is increased thus leading to more binding of aldosterone by hippocampal MR then fewer MR would be available to cortisol thus weakening the negative feedback and strengthening the positive feedback. Jelic et al. claim to be the first to include aldosterone in a model of the HPA axis and we have not seen later models include this. (However the dynamics of aldosterone is in the mathematical model reduced by assuming that $\frac{d\text{aldosterone}}{dt} = 0$. This means the effect on pushing the balance of cortisol feedback is also disregarded).

Mathematical model

The approach in [2] is to write a reaction scheme for the variables. The reaction scheme is not adjusted which can be seen from the fact that the reaction scheme is not stoichio-

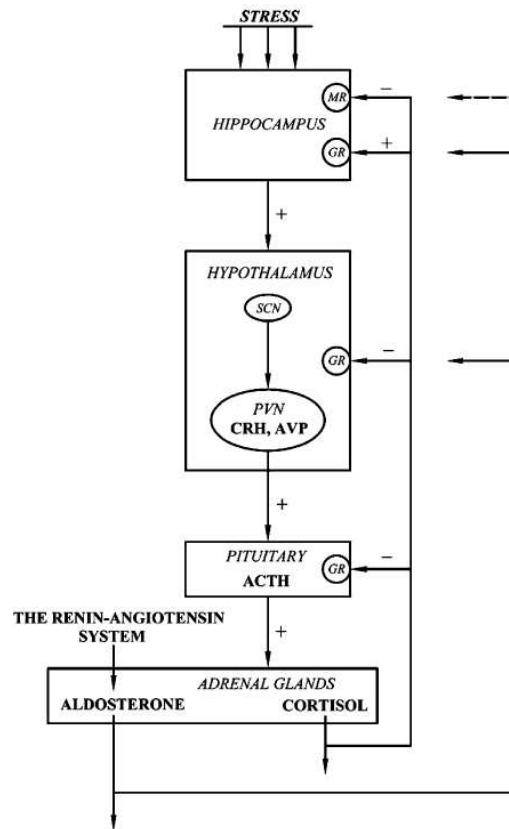


Figure 2.7: The compartment diagram from [2]. Cortisol exerts negative feedback on ACTH and CRH through GR. Also hippocampus is included since cortisol has a feedback on CRH acting through hippocampus. This is positive for cortisol binding to hippocampal GR and negative for cortisol binding to hippocampal MR.

metric correct. Using the law of mass action² the reaction scheme can be transformed into differential equations. This means the mathematical model is crucially dependent on the reaction scheme. However there is no reference nor derivation of the reaction scheme in [2]. Since four hormones are considered the result is four differential equations. The obtained differential equation for $d\text{CRH}/dt$ only depends on CRH (and some parameters). This means the feedback from cortisol is not included in the mathematical model. A (non trivial) assumption about a slow dynamics of CRH and aldosterone compared to the dynamics of ACTH and cortisol leads to the statement $d\text{aldosterone}/dt = d\text{CRH}/dt = 0$ thus effectively reducing the number of differential equations from four to two, i.e. resulting in a two dimensional system. The crucial non linearity of the two equations (in order to hope for oscillating solutions) comes from a reaction where one ACTH molecule

² The law of mass action is explained in section 5.2

reacts with two cortisol thus becoming three cortisol molecules. This should reflect the positive feedback from cortisol acting through hippocampal GR.

The Poincaré Bendixson theorem³ can ensure existence of a stable limit cycle which is an important tool for two dimensional systems (a stable limit cycle is a periodic solution, see chapter 3, with neighbouring solutions that are not periodic. The neighbouring solutions must converge to the limit cycle). For the chosen set of parameters a limit cycle exists which gives the ultradian oscillations in the system.

Important points from [2] are

- Physiology.
 - Cortisol exerts negative feedback on CRH in hypothalamus and ACTH in the pituitary through GR.
 - Cortisol exerts feedback on hippocampal receptors that influence the HPA-axis. There are two kind of receptors and one cause a positive feedback and the other cause a negative feedback.
 - Aldosterone is included but no bound forms of cortisol are included.
- Mathematical modeling.
 - The reaction scheme leads directly to the final, non linear differential equations.
 - The negative feedback from cortisol on CRH is not included.
 - The investigated system is significantly reduced from the physiological description since only the dynamics of two hormones are considered.
 - The investigated system consists of two coupled, non linear differential equations of cortisol and ACTH based on a reaction scheme and the law of mass action.
 - Parameters are chosen so that the Poincaré Bendixson Theorem guarantees a stable limit cycle which cause the ultradian oscillations of the system.
 - The circadian rhythm appears additively to the differential equation of ACTH. First the circadian rhythm is constant but for a numerical investigation a time dependent trigonometric function is used. Then the model becomes non autonomous.

2.4 Our model

Our model of the HPA-axis is building on [1] and [2] and section 2.

Including relevant physiology as described by Jelic and Kyrylov

Comments on physiology from Kyrylov et al.

CBG binds approximately 90 percent of the cortisol and is thus the major binder of cortisol. The binding and dissociation is very fast[10]. A saturation is visible for concentrations above $25 \mu\text{g}/\text{dl}$ but this limit is above realistic concentration[11]. *‘Because CBG is the major cortisol-binding protein the free cortisol in plasma is almost linearly related to the total cortisol at normal concentrations’*[11]. About 7 percent of plasma cortisol is bound to albumin (at 37 degrees Celcius). No saturation of albumin bound cortisol is present. Since cortisol has a faster association and dissociation from albumin

³ The Poincaré Bendixson theorem is explained in chapter 3

than from CBG we consider the albumin bound cortisol and the free cortisol to be in equilibrium [11]. We can therefore disregard the dynamics of the CBG-bound cortisol and the albumin bound cortisol. The free cortisol is considered a constant fraction of the total amount of cortisol. Since it is only the free cortisol that is capable of interacting with the rest of the HPA-axis it is really the free cortisol that is of most interest.

We have not been able to get good verification on the direct CRH-cortisol stimulation which is the major reason to disregard it. We will not include this in our final model but still some analysis is done on a system including the CRH-cortisol stimulation (in chapter 4.2). This analysis shows that the behaviour of the system with CRH-cortisol stimulation is in some sense controlled by the system without CRH-cortisol stimulation. This means that we have some control with what happens by disregarding this term.

Comments on physiology from Jelic et al.

The aldosterone included in [2] will not be included in our model. This is because [2] argues that the dynamics of this is fast compared to the rest of axis. Also in [2] aldosterone is included as a placeholder of MR thus leaving fewer available to cortisol though cortisol is more dominant in binding MR than aldosterone. We do not know how many receptors are available anyway so this constant fraction of aldosterone occupying receptors is not considered important.

We will pursue the idea from [2] that cortisol exerts negative feedback through GR in hypothalamus and pituitary. The positive feedback of cortisol on CRH acting through hippocampal GR and the negative feedback of cortisol on CRH through hippocampal MR is an interesting mechanism. We have no information about possible hormones in hippocampus i.e. if there should be included a hormone in hippocampus that acts on hypothalamus we do not know what this should be. Therefore inclusion of hippocampal dynamics will be as extra feedbacks on CRH in hypothalamus. However this includes some speculation. Therefore the system without hippocampus must be investigated thoroughly before including hippocampal dynamics. Furthermore the system without hippocampus is the most understood and thereby more thoroughly investigated than the system including hippocampal dynamics.

What mathematical modeling by Kyrylov and Jelic can be used in our model

Since we include three hormones the mathematical model consists of three coupled differential equations. In both papers the ultradian oscillations of the system is a behaviour that is caused by the dynamics within the HPA axis and not due to an external forcing function. We will therefore purpose a system of three nonlinear, coupled, autonomous differential equations and look for conditions such that the solutions of the system is oscillating. These oscillations should resemble the ultradian oscillations seen in data. In both papers the circadian input is included as a 'forcing function' when the analysis of the autonomous system is completed. We will follow this approach by including a circadian input on the positive stimulation on the derivative of CRH, thus making the system non autonomous.

Comments on Jelic et. al

According to [12] one of the parameters in [2] are wrong by a factor of 1000 to be physiologically relevant. The physiologically relevant choice of parameters do not lead

to a limit cycle for the system.

The interesting approach of Jelic et al. using the Poincaré Bendixson Theorem ensured existence of a limit cycle. Unfortunately the Poincaré Bendixson Theorem is only usable for two dimensional systems. Jelic et al. get the final differential equations 'for free' once the reaction scheme is written. Unfortunately the reaction can not be verified and the negative feedback from cortisol on CRH is not included which is a major problem.

Comments on Kyrylov et. al

Since we have little trust in the reaction scheme from [2] we will pursue the approach of Kyrylov et al. by starting with a simple model. However increased complexity should be included as close to the physiological mechanisms as possible. Therefore another way of introducing non linearities is desirable.

2.5 Description of included mechanisms of our model

After this motivation of how to model the HPA axis we will now shortly summarize the compartment diagram of our model. We actually have two models. The first does not contain hippocampal dynamics (figure 2.8) but the second adds the hippocampal dynamics upon the first (figure 2.9).

The overall structure of the system with hippocampus is as follows. In hypothalamus corticotropin-releasing hormone (CRH) is secreted which causes secretion of adrenocorticotrophic hormone (ACTH) from the pituitary gland. ACTH causes secretion of hormones from the adrenal gland including cortisol. The circuit for cortisol now consists of an amount that is distributed in body tissues but there is also a negative feedback on the ACTH secretion from the pituitary gland as well as a negative feedback on the CRH secretion from hypothalamus.

For the model including hippocampus two more feedbacks from cortisol are added on the secretion of CRH. A positive feedback acting through hippocampal GR and a negative feedback acting through hippocampal MR. Since cortisol has different affinity for the two receptors their overall stimulation from hippocampus may depend on the concentration of cortisol.

Now the reader has been introduced to both the physiology and previously made mathematical models upon which we have found inspiration. Therefore the exact aim of this thesis can be formulated as:

2.6 Problem formulation

Do our models of the HPA-axis constructed using well known physiological mechanisms and physiological parameter values show the following behaviour.

- Do the models guarantee reasonable levels in hormone concentration?
- Are the models capable of producing ultradian oscillations in hormone concentrations without external, time varying input?
- Can an external imposed function cause the observed circadian rhythm?

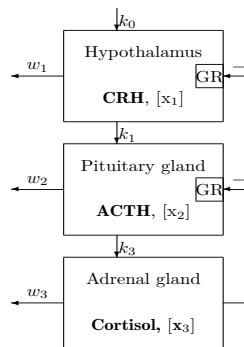


Figure 2.8: Compartment diagram of the HPA-axis without hippocampus included.

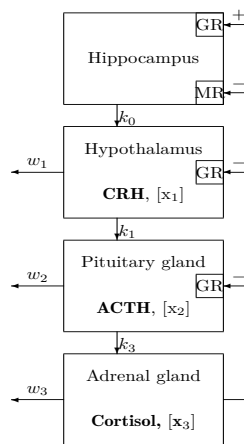


Figure 2.9: Compartment diagram of the HPA-axis with hippocampus included

3 Introduction to the mathematics of differential equations

This chapter concerns the mathematical tools mostly used throughout this project. This chapter will therefore serve as both a mathematical introduction to general results about systems of differential equations as well as a chapter we can refer to. If the reader is familiar with theory concerning differential equations this chapter may be skipped.

Of interest is now a system of autonomous differential equations

$$\dot{\mathbf{x}} \equiv \frac{d\mathbf{x}}{dt} = \mathbf{f}(\mathbf{x}), \quad \mathbf{x}(t_0) = \mathbf{x}_0, \quad \mathbf{f}: E \subseteq \mathbb{R}^n \rightarrow \mathbb{R}^n, \quad E \text{ open.} \quad (3.1)$$

First we state the following theorem about existence and uniqueness of solutions to equation 3.1 that ensures that solution curves cannot intersect where \mathbf{f} is sufficiently smooth[13].

Theorem 3.1: Existence and uniqueness

Let each of the functions $f_1(x_1, \dots, x_n), \dots, f_n(x_1, \dots, x_n)$ have continuous partial derivatives with respect to x_1, \dots, x_n . Then, the initial-value problem $\dot{\mathbf{x}} = \mathbf{f}(\mathbf{x}), \mathbf{x}(t_0) = \mathbf{x}_0$ has one, and only one solution $\mathbf{x} = \mathbf{x}(t)$, for every \mathbf{x}_0 in \mathbb{R}^n .

The solution may exist only on a finite interval. When f is a nonlinear function in the variables x_1, \dots, x_n one can not in general expect that explicit solution formulas for x_1, \dots, x_n can be found. Therefore it is interesting to consider numerical methods to find solutions and qualitative properties of the solutions.

A steady state solution, \mathbf{x}_{ss} , is a solution where all the variables are constant in time thus defined as

$$\mathbf{f}(\mathbf{x}_{ss}) = \mathbf{0}. \quad (3.2)$$

\mathbf{x}_{ss} is also called a fixed point of the system. If a solution at some time equals a steady state solution, it must remain a steady solution for all future times. How the solutions in the vicinity of a steady state solution behave is therefore of interest. There are two definitions regarding stability - (Lyapunov, local) stability and asymptotical local stability. If any solution is close to the steady state solution at some time, then they must stay close for all future times if the fixed point should be called stable. This is the content of the definition of stability [14].

Definition 3.1: Stability

Let \mathbf{x}_{ss} be a steady state solution of $\dot{\mathbf{x}} = \mathbf{f}(\mathbf{x})$. \mathbf{x}_{ss} is called (Lyapunov, locally) stable if for any other solution $\mathbf{x}(t)$ it is true that $\forall \epsilon > 0 \exists \delta > 0$ such that $\|\mathbf{x}_{ss} - \mathbf{x}(t_0)\| < \delta \Rightarrow \forall t > t_0$ it is true that $\|\mathbf{x}_{ss} - \mathbf{x}(t)\| < \epsilon$.

For a solution to be asymptotically stable it has to be stable and any close solution has to converge to it as time increases. This is stated in the following definition[14].

Definition 3.2: Asymptotic stability

Let \mathbf{x}_{ss} be a steady state solution of $\dot{\mathbf{x}} = \mathbf{f}(\mathbf{x})$. \mathbf{x}_{ss} is called (locally) asymptotically stable if \mathbf{x}_{ss} is stable and there exists $\delta > 0$ such that

$$\|\mathbf{x}_{ss} - \mathbf{x}(t_0)\|_2 < \delta \Rightarrow \lim_{t \rightarrow \infty} \|\mathbf{x}_{ss} - \mathbf{x}(t)\|_2 = 0.$$

Steady state solutions are one kind of special solutions of interest. Another is periodic solutions. Periodic solutions can be the mathematical explanation of behaviour with a pattern that repeats itself. The definition is from [14].

Definition 3.3: Periodic solution

A periodic solution $\phi(t)$ is a non-constant solution to the set of differential equations equation 3.1 with the property $\exists T > 0$ such that $\forall t$ where $\phi(t)$ is defined it holds that $\phi(t + T) = \phi(t)$. The smallest T where $\phi(t)$ has this property is called the period of the solution.

Thus a fixed point is not a periodic solution.

The existence and uniqueness theorem simplifies the possible dynamics especially in two dimensions. What can happen if the solutions are caught in a bounded region where there is no fixed point? The answer is given by the theorem of Poincaré - Bendixon and concerns the long term behavior of a solution [13].

Theorem 3.2: Poincaré-Bendixon

Suppose that a solution $x = x(t)$, $y = y(t)$ of the system of differential equations

$$\frac{dx}{dt} = f(x, y), \quad \frac{dy}{dt} = g(x, y) \quad (3.3)$$

remains in a bounded region of the plane which contains no equilibrium points of equation 3.3. Then, its orbit must spiral into a simple closed curve, which is itself the orbit of a periodic solution of equation 3.3.

The Poincaré-Bendixon theorem gives sufficient criteria for the existence of periodic solutions but only in two dimensions.

3.1 Method for solving a system of linear differential equations

In this section we present a way to solve a system of autonomous linear differential equations with constant coefficients. There is a close connection between stability of linear systems and non linear system which is the motivation for this section. Also the focus on modeling using linear systems in [1] gives reason to focus on this. This method for solving the system is called the eigenvalue-eigenvector method[13].

We consider a system of first order linear autonomous differential equations with constant coefficients given as

$$\dot{\mathbf{x}} = \frac{d\mathbf{x}}{dt} = \mathbf{A}\mathbf{x} + \mathbf{B}, \quad \mathbf{x}(t_0) = \mathbf{x}_0. \quad (3.4)$$

where $\mathbf{x} = (x_1, x_2, \dots, x_n)$ and \mathbf{A} is an n by n matrix with entries of real constants and \mathbf{B} is a vector of size n by 1 with real constant entries. The general solution of equation 3.4 is a particular solution to equation 3.4 plus the general solution of the homogeneous system (equation 3.4 with $\mathbf{B} = \mathbf{0}$)[15]. A simple way of finding a particular solution is solving the fixed point equation $\mathbf{0} = \mathbf{A}\mathbf{x}_p + \mathbf{B}$ which is a linear algebra problem.

The following focus on finding the general solution to the homogeneous equation

$$\dot{\mathbf{x}} = \mathbf{A}\mathbf{x}. \quad (3.5)$$

First we observe that

$$\frac{d}{dt}e^{\lambda t}\mathbf{v} = \lambda e^{\lambda t}\mathbf{v} \quad (3.6)$$

and

$$\mathbf{A}(e^{\lambda t}\mathbf{v}) = e^{\lambda t}\mathbf{A}\mathbf{v}. \quad (3.7)$$

Dividing through with $e^{\lambda t}$ gives

$$\mathbf{A}\mathbf{v} = \lambda\mathbf{v}, \quad (3.8)$$

or equivalently

$$(\mathbf{A} - \mathbf{I}\lambda)\mathbf{v} = \mathbf{0}. \quad (3.9)$$

A nonzero vector \mathbf{v} satisfying equation 3.8 is called an eigenvector of \mathbf{A} with eigenvalue λ .

Equation 3.9 has nonzero solutions \mathbf{v} only if the characteristic polynomial $P(\lambda)$ is zero, that is

$$P(\lambda) = \det(\mathbf{A} - \mathbf{I}\lambda) = 0. \quad (3.10)$$

Therefore the eigenvalues of \mathbf{A} are the roots of the characteristic polynomial. The eigenvectors are the vectors satisfying

$$(\mathbf{A} - \mathbf{I}\lambda)\mathbf{v} = \mathbf{0} \quad (3.11)$$

thus \mathbf{v} depends on λ . We now observe that if \mathbf{v} is an eigenvector with eigenvalue λ then

$$\mathbf{A}(c\mathbf{v}) = c\mathbf{A}\mathbf{v} = c\lambda\mathbf{v} = \lambda(c\mathbf{v}) \quad (3.12)$$

for any constant $c \neq 0$. Therefore any multiple of an eigenvector of \mathbf{A} is again an eigenvector of \mathbf{A} .

If \mathbf{A} is an $n \times n$ matrix with n linearly independent eigenvectors $\mathbf{v}^1, \dots, \mathbf{v}^n$, with distinct, real eigenvalues $\lambda_1, \dots, \lambda_n$ then every solution to equation 3.5 is a linear combination of solutions $c_i e^{\lambda_i t} \mathbf{v}^i$ with $i \in 1, \dots, n$ [13].

$$\mathbf{x}(t) = c_1 e^{\lambda_1 t} \mathbf{v}^1 + c_2 e^{\lambda_2 t} \mathbf{v}^2 + \dots + c_n e^{\lambda_n t} \mathbf{v}^n. \quad (3.13)$$

This is called the general solution of equation 3.5. The constant real coefficients c_1, \dots, c_n can be found from the initial condition $\mathbf{x}(t_0) = \mathbf{x}_0$.

When $\dot{\mathbf{x}} = \mathbf{A}\mathbf{x}_{ss} = \mathbf{0}$, \mathbf{x}_{ss} is called a fixed point for 3.5 and we now comment on the stability. If $\lambda_i < 0$ $i \in \{1, \dots, n\}$ then from 3.13 it can easily be seen that $\mathbf{x}(t) \rightarrow \mathbf{x}_{ss}$ for $t \rightarrow \infty$ but if just one of the eigenvalues are positive this will not be the case thus making sure that \mathbf{x}_{ss} is unstable. Thus the eigenvalues of the matrix \mathbf{A} play a central role when stability is considered.

μ_{max}	σ	solution behaviour
$\mu_{max} > 0$	$\sigma = 0$	unstable, non-oscillating
$\mu_{max} > 0$	$\sigma \neq 0$	unstable, oscillating
$\mu_{max} = 0$	$\sigma \in \mathbb{R}$	stable, oscillating
$\mu_{max} < 0$	$\sigma = 0$	asymptotically stable, non-oscillating
$\mu_{max} < 0$	$\sigma \neq 0$	asymptotically stable, oscillating

Table 3.1: The system behaviour depending on the largest eigenvalue of \mathbf{A} , $\lambda_{max} = \mu_{max} + i\sigma$, $\mu, \sigma \in \mathbb{R}$

There are ways to obtain a general solution even though there are repeated eigenvalues or complex eigenvalues. For a complex eigenvalue, $\lambda = \mu + i\sigma$, $\mu, \sigma \in \mathbb{R}$ then $e^{\lambda t} = e^{\mu t}(\cos(\sigma t) + i \sin(\sigma t))$ is complex. Since the original problem was real a real solution is desired. It turns out that one can find two constant vectors with n real entries \mathbf{u} and \mathbf{w} such that solutions can be formed by $e^{\mu t} \cos(\sigma t)\mathbf{u}$ and $e^{\mu t} \sin(\sigma t)\mathbf{w}$ [15]. This means that for a complex eigenvalue two solutions can be found and they each have a factor that describe growth or decay related to the real part of the eigenvalue ($e^{\mu t}$) and a factor describing an oscillation ($\cos(\sigma t)$ or $\sin(\sigma t)$). In practice this is not a periodic oscillation since the amplitude is typically not constant - for a decreasing amplitude it is often called a damped oscillation. Note that the period of oscillation is $2\pi/\sigma$ thus the imaginary part of a complex eigenvalue determines the period of oscillation.

It follows from equation 3.13 that the eigenvalue, λ_{max} , with the largest real part determines the long time behaviour of the solution meaning that it controls the stability and whether this happens as a pure exponential decay or growth or if oscillations are also present. If λ_{max} has positive real part and has a nonzero imaginary part the solution will be unstable and converging towards an oscillating solution, i. e a periodic solution. If λ_{max} has positive real part and zero imaginary part, the solution will be unstable and not oscillating. If λ_{max} has a real part equal to zero the solution will be stable and oscillating. If λ_{max} has negative real part the solution is asymptotically stable and oscillating only if the imaginary part of λ_{max} is nonzero. The different types of system behaviour are shown in table 3.1.

3.2 Three dimensional system of linear differential equations

Since our project mainly concerns a three dimensional system of differential equations we will now turn our attention toward this. Thus we have a vector \mathbf{x} with nonnegative entries defined as $\mathbf{x} = (x_1, x_2, x_3)$

We consider the system of homogeneous, linear differential equations with constant, real coefficients given by

$$\frac{d\mathbf{x}}{dt} = \mathbf{A}\mathbf{x}. \quad (3.14)$$

The characteristic polynomial of the 3 by 3 matrix \mathbf{A} then can be written in the form

$$P_A(\lambda) = \lambda^3 + \alpha_1\lambda^2 + \alpha_2\lambda + \alpha_3 \quad (3.15)$$

The solutions to this equation are the eigenvalues of the system. Using numerical tools like Matlab, the sign of the eigenvalues for a given 3 by 3 matrix can easily be determined numerically. A way to do this analytical is to use the Routh-Hurwitz Criteria (RHC) that gives equivalence between relations on the coefficients of the characteristic polynomial and the sign of the eigenvalues of the system. Here is RHC only stated for a polynomial of third degree [[14]].

Theorem 3.3: Routh Hurwitz Criteria.

Let $P(\lambda) = \lambda^3 + \alpha_1\lambda^2 + \alpha_2\lambda + \alpha_3$, $\alpha_1, \alpha_2, \alpha_3 \in \mathbb{R}$. Then all of the roots of $P(\lambda)$ are negative or have negative real part if and only if $\alpha_1 > 0$, $\alpha_3 > 0$ and $\alpha_1 \cdot \alpha_2 > \alpha_3$.

A proof of the RHC is formulated in A.

3.3 Three dimensional system of non-linear differential equations

We now wish to turn our attention to non-linear three dimensional systems of autonomous differential equations. That is in general the equations

$$\dot{\mathbf{x}} = \mathbf{f}(\mathbf{x}), \quad \mathbf{f}: \mathbb{R}^3 \rightarrow \mathbb{R}^3, \quad \mathbf{x}(t_0) = \mathbf{x}_0. \quad (3.16)$$

Important information is determination of fixed points and the behavior of solutions close to steady state. The basic idea is that we can approximate the nonlinear system well by a linear system for solutions close to steady state. The idea of looking at the behaviour of the solutions close to steady state is possible because the solutions typically depend continuously on the initial values as stated in the next theorem [16].

Theorem 3.4: Continuously dependency on initial values

Let $U \subset \mathbb{R}^n$ be open and let $\mathbf{f}: U \rightarrow \mathbb{R}^n$ with $\mathbf{f} \in C^1$. Let $\mathbf{x}_0 \in U$ and $t_0 \in \mathbb{R}$.

Then the solutions $\phi_t(\mathbf{x}_0)$ of 3.1 depend continuously on the initial value \mathbf{x}_0 .

In the following we demand that f_i is C^2 with respect to each x_j with $i, j \in \{1, 2, 3\}$. We call the steady state solutions \mathbf{x}_{ss} and define the new variable $\mathbf{z} = \mathbf{x} - \mathbf{x}_{ss}$ and use Taylors theorem[17] to linearize equation 3.16 around \mathbf{x}_{ss} . Thus

$$\dot{\mathbf{z}} = \dot{\mathbf{x}} = \mathbf{A}\mathbf{z} + \mathbf{g}(\mathbf{z}), \quad (3.17)$$

where $\mathbf{g}(\mathbf{z})$ is a polynomial of degree not less than two, and \mathbf{A} is the Jacobian matrix, \mathbf{J} , evaluated at \mathbf{x}_{ss} . The Jacobian is given by

$$\mathbf{J} = \begin{pmatrix} \frac{\partial f_1}{\partial x_1} & \frac{\partial f_1}{\partial x_2} & \frac{\partial f_1}{\partial x_3} \\ \frac{\partial f_2}{\partial x_1} & \frac{\partial f_2}{\partial x_2} & \frac{\partial f_2}{\partial x_3} \\ \frac{\partial f_3}{\partial x_1} & \frac{\partial f_3}{\partial x_2} & \frac{\partial f_3}{\partial x_3} \end{pmatrix}. \quad (3.18)$$

Now to evaluate the stability of equation 3.16 we look at a small perturbation from steady state. That is small values of \mathbf{z} . Only keeping first order terms of equation 3.17 yields

$$\dot{\mathbf{z}} = \mathbf{A}\mathbf{z}. \quad (3.19)$$

Now this is a linear system and therefore all the results about stability presented in section 3.2 apply to this system. The question is what the stability of the linear system tells us about the fixed point of the original nonlinear system. This is determined from the largest real part of the eigenvalues of \mathbf{A} . If this is strictly positive the fixed point of the original nonlinear system is unstable and if the largest real part of the eigenvalues is strictly negative the original nonlinear system has a stable fixed point¹. In case the largest real part is zero there is not enough information in the linear system to determine the stability of the non linear fixed point. This is what the next theorem is about only stated in terms of the coefficients of the characteristic polynomial instead of the eigenvalues directly. The theorem is from [14] and is formulated in terms of the coefficients of the characteristic polynomial like the Routh Hurwitz Criteria thus we name it RHC for a non linear systems. Here the theorem will only be stated for a three dimensional system.

Theorem 3.5: Routh Hurwitz Criteria for Nonlinear System

Suppose \mathbf{x}_{ss} is a fixed point of equation 3.16. Denote the characteristic equation of the eigenvalues at the fixed point as $0 = \lambda^3 + \alpha_1\lambda^2 + \alpha_2\lambda + \alpha_3$, $\alpha_1, \alpha_2, \alpha_3 \in \mathbb{R}$.

If $\alpha_1 > 0 \wedge \alpha_3 > 0 \wedge \alpha_1 \cdot \alpha_2 > \alpha_3$ then the fixed point is asymptotically stable.

If $\alpha_1 < 0 \vee \alpha_3 < 0 \vee \alpha_1 \cdot \alpha_2 < \alpha_3$ then the fixed point is unstable.

3.4 Bifurcations

In this thesis we will be interested in the qualitative behaviour of the solutions to a system of differential equations. A parameter often enters a differential equation as an unspecified constant. However the system may have dramatically different behaviour if the constant is set to one value instead of another. A bifurcation is here defined as a qualitative change of the solutions for any initial condition (a qualitative change of the phase space) as a parameter is varied. A qualitative change is for example that the number of fixed points or limit cycles changes or that the stability of a fixed point changes. For a system where parameters are only known to a certain precision or may only be estimated it is important to be aware of the different types of behaviour the system may exhibit if different values for the parameters are chosen.

¹ The Hartman-Grobman theorem can be used if no eigenvalues of the Jacobian evaluated at a fixed point are zero. This requires the concept of topologically equivalent which requires the concept of homeomorphism. A homeomorphism is a bijective, continuous function with a continuous inverse. Two dynamical systems $\dot{\mathbf{x}} = \mathbf{f}(\mathbf{x})$ defined on $U \in \mathbb{R}^n$ and $\dot{\mathbf{x}} = \mathbf{g}(\mathbf{x})$ defined on $V \in \mathbb{R}^n$ are topologically equivalent if there exists a homeomorphism $h : U \rightarrow V$ such that h maps the solution curves of the vector field f onto the solution curves of g and by that keeps the orientation of the time of the solution curve. The Hartman-Grobman theorem states that when no real part of the eigenvalues of the linearized system at a fixed point are zero then there exist a neighbourhood of the fixed point where the nonlinear and the linearized system are topologically equivalent[16]. Topological equivalence is central in the definition of a structural stable vector field. The strict definition of a bifurcation value (that we will introduce more loosely in section 3.4) is a parameter value that causes a vector field to be not structurally stable[16].

Examples

An example is now given where a change in one parameter leads to creation or destruction of fixed points. Consider

$$\frac{dx}{dt} = \mu - x^2, x, \mu \in \mathbb{R} \quad (3.20)$$

If $\mu > 0$ there are two fixed points namely $x_{ss1} = -\sqrt{\mu}$, and $x_{ss2} = \sqrt{\mu}$. If $\mu = 0$ there is one fixed point $x_{ss3} = 0$ and if $\mu < 0$ there are no fixed points. Using the earlier described method the stability of the fixed is classified using the eigenvalues of the Jacobian evaluated at the fixed points. The Jacobian is $J = -2x$ thus for $\mu > 0$ the eigenvalue corresponding to x_{ss1} is $2\sqrt{\mu} > 0$ thus \mathbf{x}_{ss1} is an unstable fixed point. The eigenvalue for x_{ss2} is $-2\sqrt{\mu} < 0$ thus \mathbf{x}_{ss2} is a stable fixed point. When $\mu = 0$ the eigenvalues of the Jacobian is 0 so the linearization cannot tell us about the fixed point here. This kind of bifurcation is called a saddle-node (fold, turning-point, blue sky) bifurcation. The different behavior of equation 3.20 for different μ is shown in figure 3.1.

It is no coincidence that for an eigenvalue of the Jacobian equal to zero a bifurcation occurs. According to [18] the term bifurcation was originally used to describe the 'splitting' of equilibrium solutions of differential equations as a parameter vector is varied. This means that for some parameter value there can exist several branches of equilibrium solutions and a meeting point for two or more branches defines the 'splitting'. Now the implicit function theorem[17] is very convenient to determine when $f(\mathbf{x}, \mu) = 0$ can be solved in terms of $\mathbf{x}(\mu)$. When this is the case there is locally only one solution to $f(\mathbf{x}, \mu) = 0$ out ruling the possibility of e.g. a saddle node bifurcation where no fixed point of the system turns into two fixed points as a parameter is varied. If a change in the value of a parameter cause the Jacobian at a fixed point to have a zero eigenvalue then the parameter is at a bifurcation value[18]. This can be seen in the saddle node bifurcation at the value $(x, \mu) = (0, 0)$ where the steady state solution in any neighbourhood can be described by two different functions namely $x_+ = \sqrt{\mu}$ and $x_- = -\sqrt{\mu}$. However it is exactly for $(x, \mu) = (0, 0)$ that the implicit function theorem does not ensure that x can be uniquely solved as a function of μ .

A change of a stability of a fixed point may cause the existence of a limit cycle as the next example sketches. Consider a two dimensional system including a parameter λ

$$\frac{dx}{dt} = f(x, y, \lambda), \frac{dy}{dt} = g(x, y, \lambda), x(0) = x_0, y(0) = y_0, (x, y, \lambda) \in \mathbb{R}^2. \quad (3.21)$$

Let there be a bounded region where the solution curves are confined such that solutions starting in the region stay there and let there be one fixed point in this bounded region. It may be so that for one value of λ this fixed point is stable and for another fixed point it is unstable. In the latter case the bounded region without the fixed point constitute a bounded region where solution curves are confined since the flow points away from the fixed point. Then the theorem of Poincaré -Bendixon ensures a limit cycle exists. This example illustrates that a bifurcation can lead to sufficient conditions for the existence of a limit cycle.

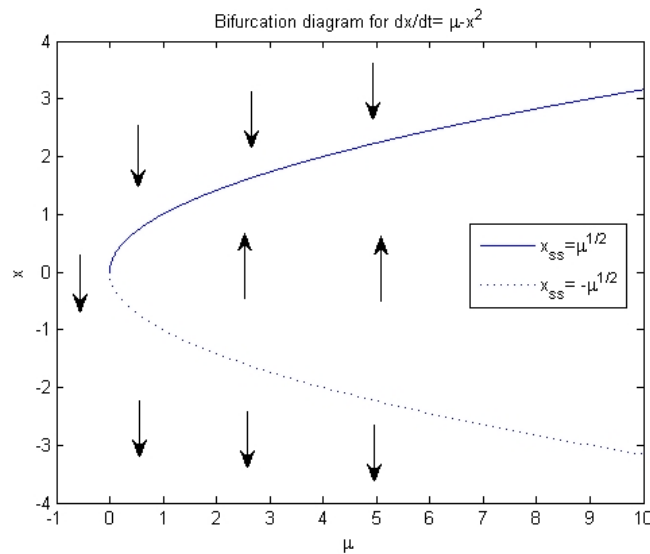


Figure 3.1: Diagram showing the number of fixed points and their stability parametrized by the parameter μ of the differential equation $\dot{x} = \mu - x^2$. The arrows indicate if x increase or decrease for a given (μ, x) . The solid line corresponds to a stable set of fixed points (the arrows point towards it) and the dotted line corresponds to an unstable set of fixed points (the arrows point away from it). It can be seen that for positive μ there exists two steady state solution - one stable and one unstable. For μ less than zero no steady state solution exists.

Existence and uniqueness for parameter dependent system

How do the dependency of parameters interplay with the previous, important theorems like the existence and uniqueness theorem? In other words how can we relate knowledge about $\mathbf{f}(\mathbf{x})$ to $\mathbf{f}(\mathbf{x}, \boldsymbol{\mu})$, where $\boldsymbol{\mu}$ is now an r -dimensional parameter vector when we want to describe variations in the solutions as $\boldsymbol{\mu}$ is varied continuously? This can be done by expanding the original n 'th dimensional system with that of an $n + r$ dimensional system where the parameters are now variables with a simple dynamic. Denoting $dx_{n+i}/dt = d\mu_i/dt = 0$ with $i \in \{1, \dots, r\}$ and $x_{n+i}(t_0) = \mu_{0,i}$ the existence and uniqueness theorem can be applied. Also continuous dependency from parameters follow from the theorem of continuous dependency on initial values theorem 3.4.

3.5 Bifurcation and stability of a fixed point

How can a stable fixed point become unstable when varying a parameter? This can happen in two different ways. First all the real parts of the eigenvalues are negative then (as the parameter is varied) either one (or more) real valued eigenvalues goes from negative values through zero and then becomes positive. Or a pair of complex conjugate eigenvalues with a real part that goes from negative through zero to being positive while the remaining eigenvalues have negative real parts. The latter is defined

as a Hopf bifurcation and is interesting because a periodic solution is the outcome of such a bifurcation.

Following the approach of [19] we consider the autonomous system

$$\dot{\mathbf{x}} = \mathbf{f}(\mathbf{x}, \mu) \quad \mathbf{f}: \mathbb{R}^n \rightarrow \mathbb{R}^n \quad (3.22)$$

Assume a fixed point, \mathbf{x}_{ss} , exists and all eigenvalues have negative real part. Assume that μ is varied which causes a set of complex conjugate eigenvalues $\lambda_{1,2}(\mu) = \alpha(\mu) \pm i\sigma(\mu)$, $\alpha(\mu) \in \mathbb{R}$, $\sigma(\mu) \in \mathbb{R}$ to vary such that the real part crosses the imaginary axis. This means the real part of $\lambda_{1,2}$ goes from negative to positive values causing the fixed point going from stable state to unstable state. Denote $\mu = \mu_c$ for $\alpha(\mu_c) = 0$ (μ_c is called the Hopf bifurcation value) and assume the following holds in a neighborhood around μ_c

- $\sigma(\mu_c) \neq 0$.
- $\alpha(\mu) < 0$ for $\mu < \mu_c$.
- $\alpha(\mu) > 0$ for $\mu > \mu_c$.

Then in a small neighbourhood around μ_c for $\mu > \mu_c$ the steady state is unstable by growing oscillations and a limit cycle periodic solution exists around \mathbf{x}_{ss} . The period of the limit cycle is $2\pi/\sigma(\mu_c)$. [19]

This is good news when modeling a biological system and sufficient criteria for a limit cycle is desired. However note that

- The amplitude of the limit cycle may be small.
- The neighborhood of μ_c where the limit cycle exists may be small.

This means that this approach is more related to 'mathematical existence' than to observed behavior of realistic values of a biological system with sustained oscillations. In our approach this means that if the criteria just mentioned for a limit cycle to exist is fulfilled then simulations must be performed in order to see if the limit cycle is visible.

Existence and Uniqueness of Non Autonomous System

A system of differential equations depending explicitly on time obeys an existence and uniqueness theorem (the theorem is from [20]). The expression *maximal interval of existence* enters the theorem which we will therefore explain first. $\phi(t, t_0, \mathbf{x}_0)$ is a solution to the initial value problem equation 3.23 on an interval I containing t_0 if ϕ is a C^1 function of t on I and satisfies equation 3.23 for each $t \in I$. A function $\Phi(t, t_0, \mathbf{x}_0)$ is called a continuation of ϕ if Φ is a solution to equation 3.23 on a larger open interval containing I and $\Phi(t, t_0, \mathbf{x}_0) = \phi(t, t_0, \mathbf{x}_0)$ for $t \in I$. The interval, I , is called the *maximal interval of existence* if ϕ has no continuation to a larger interval.

Theorem 3.6: Existence and uniqueness for non autonomous system

Let $U \in \mathbb{R} \times \mathbb{R}^n$ be open and $\mathbf{f}: U \rightarrow \mathbb{R}^n$ and consider the initial value problem

$$\dot{\mathbf{x}} = \mathbf{f}(t, \mathbf{x}) \quad \mathbf{x}(t_0) = \mathbf{x}_0 \quad (3.23)$$

If $\mathbf{f} \in C^k(U, \mathbb{R}^n)$ with $k \geq 1$ then there exists a unique solution $\phi(t, t_0, \mathbf{x}_0)$ of the initial-value problem defined on a maximal interval of existence; moreover, ϕ is C^k in (t, t_0, \mathbf{x}_0) .

3.6 Banach Fixed Point Theorem

In this project the Banach Fixed Point Theorem turns out to be an important theorem in order to guarantee global stability of a fixed point.

Definition 3.4

Suppose (D, d) is a complete metric space and $H : D \rightarrow D$ is any function. If $|H(x) - H(y)| \leq p|x - y|$ for $0 < p < 1 \forall x, y \in D$ then H is called a contraction.

Theorem 3.7: Banach Fixed Point Theorem

Let (D, d) be a non empty complete metric space. Let $H : D \rightarrow D$ be a contraction mapping on D . Then there exists exactly one fixed point of H i.e. there exists exactly one x_{ss} such that $x_{ss} = H(x_{ss})$. For any $x_0 \in D$ the sequence $x_{n+1} = H(x_n)$ converges and its limit is x_{ss} .

The Banach fixed point theorem is also called the Principle of Contraction Mapping and the theorem can be found in [21].

4 Previous models

In this chapter we will give an in depth discussion of two state of the art models for modeling the HPA axis. Namely the models made by Kyrylov et al.[1] and Jelic et al.[2]. The papers were introduced in section 2.3. Now we have introduced the mathematical tools of most need when building and analyzing models using differential equations. Therefore it is now time for digging into more details of the two models.

4.1 Discussion of the paper of Kyrylov et al.

Now we will specify the model of Kyrylov et al.[1] that was introduced in section 2.3. The compartment diagram for this model is shown in figure 2.6. The purpose of this section is to focus on some points where improvement deserves to be made. Since the model relies on some numerical test cases we later investigate parts of the model analytically. In [1] the modeling of the HPA axis is basically separated in three steps. First a linear model is presented and is assumed to be valid when the variables have moderate positive values. Whenever any variable is close to zero, or approaches its upper physiological limit nonlinearities are required. Second step is the inclusion of these nonlinearities. When a 'reasonable' linear model is found nonlinearities related to finite secretion rate and a demand of non negative hormone concentrations are introduced. The third step in the modeling is introducing a time dependent input on the CRH concentration thus imposing the daily oscillation on the system.

The variables for the model are concentrations of CRH, ACTH, free cortisol, albumin bound cortisol and CBG bound cortisol. In the differential equations normalized concentrations are used. Thus y_0 represents CRH, y_1 represents ACTH, y_2 represents free cortisol, y_3 and y_4 represents the two protein-bound forms(see figure 2.6). It should be noticed that y_i is the concentration of hormone i divided by the mean concentration of hormone i .

The linear system

With some minor changes in the notation compared to the notation of Kyrylov et al., the linear differential model is given by equation 4.1

$$\dot{\mathbf{y}} = \begin{pmatrix} -a_{00} & 0 & -a_{02} & 0 & 0 \\ a_{10} & -a_{11} & -a_{12} & 0 & 0 \\ a_{20} & a_{21} & -a_{22} & a_{23} & a_{24} \\ 0 & 0 & a_{32} & -a_{33} & 0 \\ 0 & 0 & a_{42} & 0 & -a_{44} \end{pmatrix} \mathbf{y} + \begin{pmatrix} c_0 \\ 0 \\ 0 \\ 0 \\ 0 \end{pmatrix} \quad (4.1)$$

All fifteen parameters are positive numbers. The direct cortisol-CRH stimulation by-passing ACTH is chosen as 20% of the stimulation from ACTH on cortisol meaning that

$a_{20} = 1/5 a_{21}$. Now Kyrylov et al. wisely choose to relate as many parameters as possible to values found in literature. a_{ii} represents the self-elimination factors. These are considered known from the literature. For the value of the parameters $a_{22}, a_{23}, a_{24}, a_{32}, a_{33}, a_{42}$ and a_{44} , they choose to use the values given by Liu et al.[22]¹.

Kyrylov et al. now wishes to determine the numerical value of the remaining parameters. This is done by what they call logical inference. *'A logical assumption can be made that the stimulatory action of CRH on the pituitary is possible only if the transfer gain a_{10} is at least of same order of magnitude as the self-elimination factor $|a_{11}|$ (or likely even greater). A similar assumption applies to $a_{21}, |a_{22}|, a_{02}, a_{12}$ '*[1]. Our interpretation of this is that since all hormones of the HPA axis are capable of increase as well as decrease this should be contained in a mathematical model. Since we are now considering a normalized hormone concentration the values are close to one. Therefore the coefficients must be of same order such that the derivative of a concentration is capable of attaining positive as well as negative values.

Kyrylov et al. assumes that the value of c_0 is approximately equal to a_{00} . The remaining parameters can be described as

$$\begin{aligned} a_{10} &= b \cdot a_{11} \\ a_{21} &= c \cdot a_{22} \\ a_{12} &= d \cdot a_{11} \\ a_{02} &= e \cdot a_{00}. \end{aligned} \tag{4.2}$$

Where b, c, d, e are assumed to have values as $b, c \in [1; 1000]$ and $d, e \in [1; 100]$. Kyrylov et al. uses the above mentioned parameters in his numerical experiment. This is to consider b, c, d, e as independent random variables from a uniform distribution in their respective intervals and then check whether or not the solutions of the linear system is unstable and oscillating (if the eigenvalue with largest real part is positive and the imaginary part is non-zero). The result is, that the system is unstable and oscillating in $91.2 \pm 2.5\%$ of the cases. However we consider this crucially dependent on the domains of b, c, d, e . $b, c \in [1; 100]$ compared to $b, c \in [1; 1000]$ is halving the number of unstable oscillating solutions. Thus the domain of b, c, d, e deserve to be chosen with great care and reason. We make an analytical investigation of the system without the bound forms of cortisol in the next section showing a relation between b, c, d, e determining when the solutions are unstable and oscillating. If 'logical interference' can be understood as a way of ensuring that neither the positive nor the negative term in each of the equations in array 4.1 totally dominates there seems to be a problem. E.g. a_{10} and a_{12} can not be chosen independently of each other as we will now discuss. First we rewrite array

¹ Liu et al. investigates a model with the same variables as Kyrylov et al. but with 33 parameters. The parameters are found using trial and error but the final equations are compared to important physiological behaviour of the HPA axis such as hormone half life and association constants of cortisol with proteins. Thereby some optimization of the parameter set is found though we think it is fair to say that this approach lacks credibility.

4.1 with the parameters given in array 4.2.

$$dy_0/dt = a_{00}(-y_0 - ey_2) + c_0 \quad (4.3)$$

$$dy_1/dt = a_{11}(by_0 - y_1 - dy_2) \quad (4.4)$$

$$dy_2/dt = a_{22}(1/5cy_0 + cy_1 - y_2) + a_{23}y_3 + a_{24}y_4 \quad (4.5)$$

$$dy_3/dt = a_{32}y_2 - a_{33}y_3 \quad (4.6)$$

$$dy_4/dt = a_{42}y_2 - a_{44}y_4. \quad (4.7)$$

Now considering for instance the second equation

$$dy_1/dt = a_{11}(by_0 - y_1 - dy_2). \quad (4.8)$$

We want to illustrate an undesirable consequence of the fact that Kyrylov et al. allow the parameters to be chosen independently. We want to make a rough estimate of an upper bound for b for a given d in order to avoid the same sign of dy_1/dt for all realistic hormone concentration. From the figures 2.3 and 2.4 it seems fair to assume that the concentrations do not fluctuate more than a factor 5 from the mean value. Thus if we want to make a rough estimate on an upper bound on b such that y_1 is not always increasing we solve for b in the 'best case scenario' where the y_0 attain a low value ($1/5$) and y_1 and y_2 attain a large value (5).

$$dy_1/dt = a_{11} \left(b_{max} \frac{1}{5} - 5 - 5d \right) = 0 \Leftrightarrow b_{max} = 25(1 + d). \quad (4.9)$$

Since d is chosen as a random number in $[1;100]$ an outcome could be $d = 9$. Then by equation 4.9 $b_{max} = 250$. However since b is a random number in $[1;1000]$ a realization of a simulation could be $b = 500$. But then $dy_1/dt > 0$ at all times where the model applies. Kyrylov et al. states that the negative feedback should be capable of overcoming the forward gain but this cannot be the case for this outcome of the random numbers b, c, d, e . Now the values of y_0, y_1 and y_2 should rather be chosen as values closer to 1 (than $1/5$ and 5) since the model only applies for moderate values of the concentrations. Putting a more narrow bound on the concentration further stresses the problem of choosing the parameters independently.

Introduction of non linearities

The second step in the modeling is introducing non linearities. These are introduced to avoid negative concentrations and to ensure that the hormone release rate is bounded. This is done by multiplying two functions - one take care of non negative concentrations and one take care of an upper limit of the derivatives of the concentrations.

Let x_i denote the concentration of the i 'th hormone and \dot{x}_i denote the derivative of the concentration. The function making sure concentrations do not become negative is given by

$$r_i(\dot{x}_i, x) = \begin{cases} 1 - \exp\left(\frac{S_0 x_i^2}{\dot{x}_i (\epsilon - x_i)^2}\right), & \text{if } (x_i < \epsilon) \wedge (\dot{x}_i < 0) \\ 1, & \text{otherwise} \end{cases}. \quad (4.10)$$

Here S_0 is of order 10^{-2}min^{-1} and denotes an upper limit for hormone release rate, which is assumed to be proportional to the size of the gland. ϵ is a small positive

constant later put equal to $1/2$ (we consider this a fitting parameter). The non-linearity introduced to model finite release rate is given by

$$h_i(\dot{x}_i) = \begin{cases} \frac{x_i}{1 + \frac{x_i}{S_0} (1 - \exp(-\frac{x_i}{S_0}))}, & \text{if } \dot{x}_i > 0 \\ \dot{x}_i, & \text{if } \dot{x}_i \leq 0 \end{cases} \quad (4.11)$$

Now these nonlinearities are brought into play by defining the functions

$$g_i(\dot{x}_i, x_i) = h_i(\dot{x}_i) \cdot r_i(\dot{x}_i, x_i). \quad (4.12)$$

With these non-linearities Kyrylov et al. obtain the non linear equations of the HPA-axis.

$$dy_0/dt = g_0(a_{00}(-y_0 - ey_2), y_0) + c_0 \quad (4.13)$$

$$dy_1/dt = g_1(a_{11}(by_0 - y_1 - dy_2), y_1) \quad (4.14)$$

$$dy_2/dt = g_2(a_{22}(1/5cy_0 + cy_1 + y_0) + a_{23}y_3 + a_{24}y_4, y_2) \quad (4.15)$$

$$dy_3/dt = g_3(a_{32}y_2 - a_{33}y_3, y_3) \quad (4.16)$$

$$dy_4/dt = g_4(a_{42}y_2 - a_{44}y_4, y_4). \quad (4.17)$$

The inclusion of nonlinearities are imposed on the linear system. We believe that it would be a strengthening of the model if the nonlinearity was introduced in a less arbitrary way relying more on physiological facts. Kyrylov et al. mention that these functions are just one of many possible functions that give the desired behaviour. Note that if $x > \epsilon$ and $\dot{x} < 0$ the non linear system equals the linear system thus the non linearities fulfill the purpose of kicking in when concentrations become too close to zero. It is worth noting that h is only a function of \dot{x}_i and not on x_i and h is positive for positive \dot{x}_i . This means that only the release rate of a concentration is bounded - not the concentration itself.

Now a 'robustness' analysis is performed. *'In each experiment, only one parameter was varied by decreasing or increasing its default value until the model behaviour undergoes qualitative changes, such as ending in unstable or decaying oscillations'*[1]. However it is unclear to us how the criteria of 'qualitative changes' is investigated. For the linear system the stability was determined by the eigenvalues of the system. The meaning of stability of the non linear system is more unclear since there is no preceding analysis of fixed points which is where 'substitution' of the non linear system with a linear system (given by the Jacobian) makes sense. It could be that the qualitative changes were found from looking at the graphs of the solution curves (found numerically). If the solution curves have 'nice' oscillations the system could be considered stable with oscillations. If this approach is used then also initial values of the system should be varied since one set of initial values could lead to bounded oscillations and some could lead to unbounded solutions.

Default values of the parameters must be chosen in order to perform the robustness analysis. For some parameter values there is quite a difference between the values considered in the linear model and the non linear model. We have previously argued that the parameters of the linear model were chosen in a problematic way. However the reasons to have discrepancies between the parameters of the linear model and the parameters of the non linear model is unclear. Examples of this different choice of

parameters will now be given. It is our belief that the default parameters should reflect the parameters of the linear system or require a new argument if new ones should be chosen. Especially since the linear system equals the nonlinear system when concentrations are larger than ϵ and decreasing. However for the linear case $c_0 = a_{00}$ but for the non linear system the default parameter value of c_0 is 0.443 and $a_{00} = 0.00843$ meaning that $c_0 = 52.6 \cdot a_{00}$. This discrepancy is not commented in [1]. Furthermore Kyrylov et al. reach the conclusion that the system will not have stable oscillations when $c_0 < 0.223 \approx 26a_{00}$. This is when all other parameter values are held fixed at their default values. This means that the system is not capable of showing the desired behaviour when the parameter c_0 is more than 26 times times the value in the linear case. This discrepancy is neither commented in [1]. Furthermore Kyrylov et al. argue in the linear case that the parameter a_{21} should be found as $a_{21} = c \cdot a_{22}$ where $c \in [1; 1000]$. However Kyrylov et al. end up with the default values $a_{22} = 0.957$ and $a_{21} = 0.0310$. Thus for the non linear case the $c = 0.03$ is the default value of c . Therefore there is quite a discrepancy between the parameter values for the linear system and the non linear system.

Introducing diurnal rhythm

The third step in the modeling is the time dependent input on the derivative of CRH. To model the circadian rhythm a cosine function with a 24 hour period is introduced. This function is implemented into the external generating factor, c_0 .

Summary

Summarizing the criticism for the linear system as well as for the non linear system:

- The parameters of the linear system are varied independently of each other leading to possible derivatives with constant sign for realistic concentrations.
- The differences between the parameters in the linear and the nonlinear model are unexplained.
- The nonlinearities are not closely related to a physical mechanism but are introduced as functions obeying non negative hormone concentrations and finite secretion rate.

4.2 Applying the RHC on a linear three dimensional model of Kyrylov et al.

Preceding the five dimensional model of Kyrylov et al. [1] a three dimensional model was formulated without the bound forms of cortisol [23](this is an unpublished paper from a conference). The approach is very similar to the five dimensional model. First a linear model is considered where unknown parameters are estimated using 'logical interference' and domains for these parameters are considered as independent random variables from the respective domains when simulations are performed. This means that the half lives of CRH, ACTH and cortisol are used to estimate four other parameters. No parameters in this model is taken from Liu et al.

A numerical investigation of the eigenvalues of the linear system is performed. One negative real eigenvalue and a set of complex conjugate roots with positive real part is the predominant result. Later non linearities are introduced (using different functions

than in [1] but the approach is the same) in order to avoid negative concentrations and to put an upper limit on hormone release rates e.g. a bound on the derivative of the hormones. Finally a circadian rhythm is imposed on the CRH concentration that 'spreads' to ACTH and cortisol. The approach and results of the five dimensional model and the three dimensional model are thus very similar. The direct CRH cortisol is not included. However after analyzing the system without this part we can include it and compare the case with and without CRH -cortisol stimulation. If the dynamics of the bound forms of cortisol are fast ($dy_3/dt = dy_4/dt = 0$) for the five dimensional model it reduces to the three dimensional (except for direct the CRH-cortisol stimulation). Due to our reasoning in section 2.3 we believe it is fair to consider the dynamics of the bound forms fast compared to the rest of the HPA-axis.

We now make an analytical investigation of the three dimensional linear system that is numerically investigated by Kyrlyov et al. This serves two purposes. Kyrlyov et al is interested in when the system is unstable and oscillating and this is investigated as four parameters are varied independently and at the same time. We find a relation between the four parameters expressing when the system is unstable and oscillating. It turns out that only two parameters are important for this (the four parameters are grouped such that there is only two degrees of freedom). The analytical result is thus halving the number of 'important' parameters. We stated earlier how crucial the domains of b, c, d, g are for the stability of the linear system. With the analytical investigation we can say exactly how the values of b, c, d, g influence on the stability of the system.

The analysis is based on RHC. We have \mathbf{x} as a vector in \mathbb{R}^3 denoting the concentration of CRH, ACTH and cortisol. The linear system is then given by equation 4.18 (noted the indexes now start at (1,1) where the previous model of Kyrlyov the indices began with (0,0)).

$$\dot{\mathbf{x}} = \begin{pmatrix} a_{11} & 0 & a_{13} \\ a_{21} & a_{22} & a_{23} \\ 0 & a_{32} & a_{33} \end{pmatrix} \mathbf{x} + \begin{pmatrix} a_{14} \\ a_{24}(t) \\ 0 \end{pmatrix} \quad (4.18)$$

$a_{31} = 0$ since the direct path from CRH to cortisol is not included in this model. We will in the next section estimate the stability of the system including this stimulation ($a_{31} > 0$) using the result we are about to find for the system without the direct CRH-cortisol stimulation. $a_{24}(t)$ is only included to make external ACTH injections possible and is thus 0 when ACTH is not injected.

a_{21}	$=$	$-b \cdot a_{22}$
a_{32}	$=$	$-c \cdot a_{33}$
a_{13}	$=$	$d \cdot a_{11}$
a_{23}	$=$	$g \cdot a_{22}$

Table 4.1: The off diagonal elements of A where $b, c, d, g > 0$

We are considering the matrix A^2 .

$$A = \begin{pmatrix} a_{11} & 0 & a_{13} \\ a_{21} & a_{22} & a_{23} \\ 0 & a_{32} & a_{33} \end{pmatrix} \quad (4.19)$$

In the work of Kyrylov[1] the diagonal elements are considered well-known components of A . From the half lives of CRH, ACTH and cortisol, the diagonal elements can be found from the relation $a_{ii} = -\ln 2 / \text{half life}$. The half lives vary from individual to individual but also within each individual the half lives vary for example due to functioning of the liver. For example the half life for CRH is in the range 10-90 minutes. We will make consequences of the choice of the half lives visible by keeping the analysis in terms of a_{ii} instead of inserting a numerical value. Due to the mechanisms of the system the signs of the entries of the matrix are known. The diagonal has purely negative entries since each element describes a self elimination effect. a_{21} must be positive to describe that an increase in CRH causes increase on ACTH. Using the same argument on the ACTH impact on CRH, a_{32} must be positive. Since cortisol has a negative feedback on both CRH and ACTH, a_{13} and a_{23} must be negative. As done by Kyrylov we now introduce four positive parameters b, c, d, g through table 4.1. Inserting this in A we get

$$A = \begin{pmatrix} a_{11} & 0 & d \cdot a_{11} \\ -b \cdot a_{22} & a_{22} & g \cdot a_{22} \\ 0 & -c \cdot a_{33} & a_{33} \end{pmatrix}. \quad (4.20)$$

Here Kyrylov et al. make a large number of numerical cases with b, c, d, g in the domain from $[1; 1000]$ and then considers the different cases of stability outcomes. The approach we use instead is describing the characteristic polynomial directly in terms of b, c, d, g . The eigenvalues are found from the equation $\det(\mathbf{A} - \lambda \mathbf{I}) = \mathbf{0}$ which is equivalent to $\det(\lambda \mathbf{I} - \mathbf{A}) = \mathbf{0}$. To get the equation on a form with the coefficient

² Due to the described mechanisms of the system the signs of the entries of A are well known. This may lead the attention to qualitative analysis of A , where the stability of all matrices having the same signs as the entries of A are considered. So the stability of A is then guaranteed if $Q_A = \text{sign}(A)$ is stable, where

$$Q_A = \begin{pmatrix} - & 0 & - \\ + & - & - \\ 0 & + & - \end{pmatrix}$$

Necessary conditions for Q to be stable are given in [14]. Q_A does not meet all these conditions which means that we cannot use this approach. For example we would need $Q_{A_{12}} < 0$ which is not the case. This means that not all matrices with the same sign of the entries as A are stable. Unfortunately this means that we can deduce nothing about the stability of A in this way.

for λ^3 equal to one directly we define the characteristic polynomial of the matrix \mathbf{A} , $P_A(\lambda) = \det(\lambda \mathbf{I} - \mathbf{A})$. This is easily calculated using equation 4.20.

$$P_A(\lambda) = \lambda^3 - (a_{11} + a_{22} + a_{33}) \lambda^2 + (a_{11}a_{22} + a_{22}a_{33} + a_{11}a_{33} + \gamma a_{22}a_{33}) \lambda - (a_{11}a_{22}a_{33} + \gamma a_{11}a_{22}a_{33} + \delta a_{11}a_{22}a_{33}). \quad (4.21)$$

where

$$\gamma = cg \quad (4.22)$$

and

$$\delta = bcd. \quad (4.23)$$

Before actually using the RHC it is worth noticing the role of b, c, d, g . The reason for introducing γ and δ is because b, c, d, g do not play a role individually as much as in the terms of the products indicated by γ and δ . Therefore it is already obvious that the qualitative behaviour of the system initially described by 4 parameters only depends on two parameters. This is an interesting simplification obtained using this approach.

Describing the the characteristic polynomial as

$$P_A(\lambda) = \lambda^3 + \alpha_1 \lambda^2 + \alpha_2 \lambda + \alpha_3, \quad (4.24)$$

we see that the coefficients are

$$\alpha_1 = -(a_{11} + a_{22} + a_{33}) \quad (4.25)$$

$$\alpha_2 = a_{11}a_{22} + a_{22}a_{33} + a_{11}a_{33} + \gamma a_{22}a_{33} \quad (4.26)$$

$$\alpha_3 = -(a_{11}a_{22}a_{33} + \gamma a_{11}a_{22}a_{33} + \delta a_{11}a_{22}a_{33}) \quad (4.27)$$

We see that $\alpha_1 > 0$, $\alpha_2 > 0$ and $\alpha_3 > 0$ are always satisfied. This is due to the fact that all the diagonal elements of the matrix are negative and γ and δ are positive. For a non negative λ this means using equation 4.24

$$P_A(\lambda) = \lambda^3 + \alpha_1 \lambda^2 + \alpha_2 \lambda + \alpha_3 \geq 0 + 0 + 0 + \alpha_3 > 0. \quad (4.28)$$

Then there is no real, non negative root of P_A .

The criteria determining stability is now according to RHC if $\alpha_1 \cdot \alpha_2 > \alpha_3$ is true. When the inequality holds the system is stable and when the inequality is false the system is unstable. But since there can be no real, non negative root in the case of instability we are guaranteed that the largest real part of the eigenvalues belong to an eigenvalue with non zero imaginary part. This means that if the system is unstable it is guaranteed to have growing oscillations.

Expanding $\alpha_1 \cdot \alpha_2 > \alpha_3$ using equation 4.25, equation 4.26 and equation 4.27 and isolating δ gives

$$\delta < \frac{a_{22} + a_{33}}{a_{11}} \gamma + \frac{a_{22}a_{11}^2 + a_{33}^2a_{22} + a_{33}^2a_{11} + 2a_{33}a_{22}a_{11} + a_{33}a_{22}^2 + a_{22}^2a_{11} + a_{33}a_{11}^2}{a_{11}a_{22}a_{33}} \quad (4.29)$$

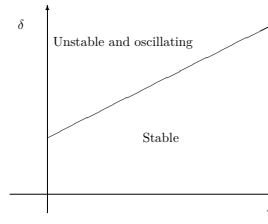


Figure 4.1: The unstable, oscillating solutions of the three dimensional linear system without direct CRH-cortisol stimulation are characterized by having (γ, δ) - values above the graph.

Variable	Half life, [min]	$a_{ii} = -\ln 2/\text{half life}, [1/\text{min}]$
CRH	30	-0.023
ACTH	17	-0.041
Cortisol	80	-0.009

Table 4.2: Half lives as given in [23].

Thus when inequality 4.29 holds the solutions of P_A are asymptotically stable. Using only the qualitative information, $a_{11} < 0$, $a_{22} < 0$ and $a_{33} < 0$ it can be seen that 4.29 can be written in the form

$$\delta < c_1(w_{11}, w_{22}, w_{33})\gamma + c_2(w_{11}, w_{22}, w_{33}), \quad (4.30)$$

where $c_1(w_{11}, w_{22}, w_{33})$ and $c_2(w_{11}, w_{22}, w_{33})$ are positive constants for fixed values of the half lives of CRH, ACTH and cortisol. This is illustrated on figure 4.1 The stable cases are found as (γ, δ) below the graph. Considering the half lives of CRH, ACTH and cortisol known and fixed (the same assumption as Kyrylov et al.) then c_1 and c_2 can be calculated and inequality 4.30 are dependent only on the two parameters γ and δ . An obvious advantage of this approach is that it gives one inequality with two parameters determining the stability of the system.

Comparing RHC results to the results of Kyrylov et al.

First we try using the half lives used by Kyrylov et al.. Parameters considered known in [23] are listed in table 4.2 with the resulting values for the diagonal elements.

Using the numerical values from table 4.2 in inequality 4.29 we get a numerical version of inequality 4.29 to be

$$\delta < 2.17\gamma + 12.07 \quad (4.31)$$

Using the definitions of δ and γ and inserting in inequality (4.31) we get

$$bcd < 2.17cg + 12.07. \quad (4.32)$$

Thus for increasing values of b and d the system is 'more unstable' and for increasing value of g the system is 'more' stable. In the numerical experiment done by Kyrylov et al b, c, d, g are chosen randomly from a uniform distribution with values in $[1; 100]$. This results in 96% unstable, oscillating cases. For b, c, d, g chosen randomly between 1 and 10 the results is 72% untable oscillating cases. This is qualitatively in agreement with inequality 4.32.

When we build a non linear, threedimensional model of the HPA axis how can we use the analytical results from the three dimensional system? The solutions near fixed points are well described by a linear system given by the Jacobian of the non linear system evaluated at the fixed point value. Any nonlinear system where cortisol exerts negative feedback on CRH and ACTH and no direct CRH-cortisol stimulation is present will have Jacobian with the same sign matrix as A . The stability of the fixed point e.g. the stability of the solution close to the fixed point is now determined from the eigenvalues of the Jacobian evaluated at the fixed point. Due to our analysis the stability of the fixed point depends solely on the sign of $\alpha_1\alpha_2 - \alpha_3$.

Using RHC Approach on the 3D System with Direct CRH-Cortisol Link

Now RHC will be used on the three dimensional linear system including positive CRH-cortisol stimulation since this is the only difference between the three dimensional linear system and the five dimensional linear system for fast dynamics of the bound forms of cortisol. The only difference from the previous system is $a_{31} > 0$ (before $a_{31} = 0$). Only changing the matrix A by changing a_{31} from zero to a positive number we define the matrix \hat{A} by

$$\hat{A} = \begin{pmatrix} a_{11} & 0 & d \cdot a_{11} \\ -b \cdot a_{22} & a_{22} & g \cdot a_{22} \\ a_{31} & -c \cdot a_{33} & a_{33} \end{pmatrix}. \quad (4.33)$$

Since \hat{A} resembles A , the comparison to already analyzed system will be stressed. When making the characteristic polynomial one finds a determinant

$$\det(\lambda I - \hat{A}) = 0. \quad (4.34)$$

The determinant can now be found using row expansion (cofactor expansion) of the last row. This means that

$$\begin{aligned} P_{\hat{A}}(\lambda) &= \det(\lambda I - \hat{A}) && \Leftrightarrow \\ P_{\hat{A}}(\lambda) &= (-1)^{3+1} a_{31} \cdot \det \begin{pmatrix} 0 & d \cdot a_{11} \\ \lambda - a_{22} & g \cdot a_{22} \end{pmatrix} + P_A(\lambda) && \Leftrightarrow \\ P_{\hat{A}}(\lambda) &= -d \cdot a_{31} a_{11} (\lambda - a_{22}) + P_A(\lambda) && \Leftrightarrow \\ P_{\hat{A}}(\lambda) &= d \cdot a_{31} a_{11} a_{22} - d \cdot a_{31} a_{11} \lambda + P_A(\lambda). && (4.35) \end{aligned}$$

The coefficients of the two first terms in equation 4.35 are positive and the coefficients for P_A are positive as well. Therefore the coefficients for $P_{\hat{A}}$ are positive so the real roots of $P_{\hat{A}}$ are negative. This means once again that unstable solutions of the linear system is guaranteed to be oscillating.

Inserting the expression of $P_A(\lambda)$ from equation 4.21 in terms of the three α 's from 4.25, 4.26 and 4.27 we get

$$P_{\hat{A}}(\lambda) = d \cdot a_{31}a_{11}a_{22} - d \cdot a_{31}a_{11}\lambda + \lambda^3 + \alpha_1\lambda^2 + \alpha_2\lambda + \alpha_0, \quad (4.36)$$

which can be written as

$$P_{\hat{A}}(\lambda) = \lambda^3 + \alpha_1\lambda^2 + (-d \cdot a_{31}a_{11} + \alpha_2)\lambda + (d \cdot a_{31}a_{11}a_{22} + \alpha_3), \quad (4.37)$$

Before applying Theorem 3.3 we first we make some new names for the coefficients:

$$\beta_1 = \alpha_1 \quad (4.38)$$

$$\beta_2 = -d \cdot a_{31}a_{11} + \alpha_2 \quad (4.39)$$

$$\beta_3 = d \cdot a_{31}a_{11}a_{22} + \alpha_3. \quad (4.40)$$

Since $\alpha_1 > 0, \alpha_3 > 0, d > 0, a_{31} > 0$ we have $\beta_1 > 0$ and $\beta_3 > 0$ so the two first conditions of Theorem 3.3 are satisfied. The third condition requires $\beta_1\beta_2 > \beta_3$ which can be expanded using equation 4.38, equation 4.39 and equation 4.40.

$$\alpha_1(-d \cdot a_{31}a_{11} + \alpha_2) > d \cdot a_{31}a_{11}a_{22} + \alpha_3. \quad (4.41)$$

This can be rewritten as

$$\alpha_1\alpha_2 + da_{31}a_{11}(-\alpha_1 - a_{22}) > \alpha_3. \quad (4.42)$$

Now it is time to use the definition of α_1 from equation 4.25 which then reduces the parenthesis so equation 4.42 can be written

$$\alpha_1\alpha_2 + da_{31}a_{11}(a_{33} + a_{11}) > \alpha_3. \quad (4.43)$$

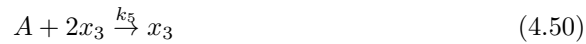
The second term $da_{31}a_{11}(a_{33} + a_{11})$ is strictly positive. The asymptotic stability of the solution of A is guaranteed if and only if $\alpha_1\alpha_2 > \alpha_3$. Therefore we see that any stable case for A guarantees the stability of \hat{A} . This means that the stable cases for A constitute a subset of the stable cases for the matrix \hat{A} . This does not mean that the unstable cases for A guarantees \hat{A} to be unstable. We see that changing the system from A to \hat{A} expands the number of stable cases which means that this change in the system increases the 'chance' of being stable. This may be valuable information even if it is really the system described by \hat{A} that is the more interesting. Especially because P_A can be described with only two parameters (γ and δ) while $P_{\hat{A}}$ also has d as parameter.

4.3 Discussion of the paper by Jelic et al.

Since the paper made by Jelic et al.[2] have been a great inspiration to us we will in this section present their approach of modeling the HPA-axis. This shall serve to the reader both as an insight in the modeling of the HPA axis and a justification of some of our later reasoning. In the last section of this chapter we will give a brief critique of this approach.

The compartment diagram of the system is shown in figure 2.7. To make it easier for the reader to relate this model to previous information about the HPA axis we have chosen to use our notation of the variables.

The following chemical reactions to model the HPA-axis are assumed to be valid in the paper.



Where x_1 represents CRH, x_2 represents ACTH, x_3 represents cortisol A represents aldosterone. P_1 and P_2 represents the products of ACTH and cortisol elimination.

Here equation 4.49 is modeling the positive feedback through hippocampal GR since two cortisol molecules are involved in a reaction where three cortisol molecules is the outcome. Equation 4.50 is modeling the overall negative feedback through hippocampal MR. These two reactions leads to the non linearities of the mathematical model. Thus the mathematical model depends heavily on these two reactions.

By means of the *law of mass action*³ the reaction scheme is used to write the following differential equations for the system⁴ (a denotes the concentration of aldosterone).

$$\frac{dx_1}{dt} = k_0 - k_1x_1 \quad (4.53)$$

$$\frac{dA}{dt} = k_m + k_3x_2 - k_5Ax_3^2 \quad (4.54)$$

$$\frac{dx_2}{dt} = k_1x_1 - k_2x_2 - k_3x_2 - k_4x_2x_3^2 - k_6x_2 \quad (4.55)$$

$$\frac{dx_3}{dt} = k_2x_2 + k_4x_2x_3^2 - k_5Ax_3^2 - k_7x_3. \quad (4.56)$$

Note that the derivative of CRH only contains parameters and the CRH concentration. This means that the feedback from cortisol on CRH is not included which we consider very problematic. Jelic et al. assume that CRH and aldosterone have much slower dynamics than ACTH and cortisol e.g. they assume $dx_3/dt = 0$ ⁵ and $dA/dt = 0$.

³ The concept of *law of mass action* will be elaborated in chapter 5.2.

⁴ The Jacobian of this system has obviously continuous entries. This guarantees existence and uniqueness of solutions by the existence and uniqueness theorem, theorem 3.1

⁵ It seems very unnecessary to assume $\frac{dx_1}{dt} = 0$ since the differential equation for CRH is uncoupled to the rest of the equations and is solvable since it is a linear differential equation with constant coefficient and a constant inhomogeneous term. Solving the differential equation using the tools from chapter 3

Thus the overall dynamics of the two-dimensional "faster" system can be modeled by

$$\frac{dx_2}{dt} = k_0 - k_2x_2 - k_3x_2 - k_4x_2x_3^2 - k_6x_2 \quad (4.58)$$

$$\frac{dx_3}{dt} = k_2x_2 + k_4x_2x_3^2 - k_m - k_3x_2 - k_7x_3. \quad (4.59)$$

Then the number of parameters is reduced by putting the differential equations into dimensionless form. Through mathematical analysis the number and stability of fixed points is investigated. Jelic et al. demand an oscillating behaviour of the cortisol concentration. As a function of the parameters the a fixed point is capable of undergoing a Hopf bifurcation. The Poincaré-Bendixon theorem ensures that there exists a limit cycle. This give the desired oscillations of the solutions. Finally the circadian rythm is included by changing k_0 from a konstant to a periodic function with a 24 hour period.

Criticism of Jelic et al.

We find overall approach to model the HPA axis through chemical reactions interesting. The detailed description of the biology within the HPA axis is impressive. Jelic et al. point out different feedback mechanisms (MR, GR) throughout the HPA-axis and try to model these. However the reaction scheme lacks validation especially the parts leading to the crucial equation 4.49 and equation 4.50.

The argument that CRH is not oscillating with an amplitude and frequency that is comparable to that of ACTH and cortisol is not in correspondence to what we have read in the literature. [1, 5, 24] argue for oscillations between twenty minutes and two hours. This is with a relative amplitude that is comparable with that of ACTH and cortisol. We therefore consider $dx_1/dt = 0$ a problematic assumption.

A previous project investigating this system[12] have done simulations with the parameter values proposed by Jelic et al.. These simulations leads to concentration levels of ACTH that are wrong by a factor of 1000. This must be noticed as problematic.

The overall critique of the article can be summarized in the following points.

- The chemical reactions leading to the mathematical model is not validated.
- No feedback from cortisol on CRH is present in the mathematical model.
- The assumption that leads to a two dimensional system is problematic.
- The outcome when scaling the equations numerically is wrong by up to a factor of 1000. Thus the interesting dynamics (explaining the ultradian oscillations) happens in parameter range far away from what is considered physiologically relevant.

and the initial condition $x_1(0) = x_{10}$ we get

$$x_1(t) = x_{10}e^{-k_1t} + \frac{k_0}{k_1} (1 - e^{-k_1t}). \quad (4.57)$$

5 Modeling the HPA-axis

In the introduction we introduced the reader to the physiology of the HPA-axis. Furthermore we have introduced the reader to how previous state of the art models have been made. The information we have gathered through our studies in literature will now be combined to make our own mathematical model of the HPA-axis.

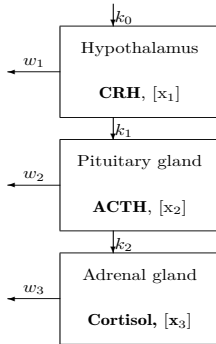


Figure 5.1: HPA-axis without feedback mechanisms

differential equations into non autonomous differential equations. Since the system is non linear this decoupling of input to the system and inherent system dynamics may however be problematic.

As seen in the previous models the standard approach to model the HPA-axis is not to include hippocampus. We have chosen to pursue this approach in our first model of the HPA-axis. We have chosen to build the model step by step because we believe that this gives the reader the best insight in the process of building the model¹.

When the model is complete it will be somehow complex. To be able to compute relevant analytic results about parts of the model we will try to reduce the number of parameters by means of physiological reasoning.

We follow the approach of [1, 2] searching for criteria such that the HPA-axis show an oscillatory behaviour without the external circadian rhythm. Therefore we will investigate the obtained system for oscillations when the circadian input is constant. If this is achieved we will mimic the circadian rhythm with a periodic function of time which has also been the approach in previous works [1–3, 6]. That is that the input to the system through k_0 will no longer be constant but time dependent thus turning the resulting

5.1 Modeling the HPA-axis without hippocampus

This model is based on the negative feedback mechanisms in hypothalamus and in the pituitary glands through the glucocorticoid receptors (GR) located here. In this chapter we will account for the way we include these feedback mechanisms in our mathematical model. Without the feedback mechanisms the model looks as in figure 5.1 and a simple

¹ If the reader wants to skip the modeling, the final differential equations of the HPA axis not including hippocampus is array 5.33. A short description of the obtained model is found in section 5.5.

system of linear differential equations is given by equation array 5.1.

$$\begin{aligned}\frac{dx_1}{dt} &= k_0 - w_1x_1 \\ \frac{dx_2}{dt} &= k_1x_1 - w_2x_2 \\ \frac{dx_3}{dt} &= k_2x_2 - w_3x_3.\end{aligned}\tag{5.1}$$

All the k 's and w 's are positive constants and the k 's model positive stimulation of the hormone concentration while the w_i 's model the elimination of the hormone concentration.

Now we will implement the feedback mechanisms. Let us start with the negative feedback from the cortisol concentration to hypothalamus. When we implement this in figure 5.1 it will look as in figure 5.2. This feedback mechanism should be modeled in such a way that the higher concentration of cortisol the larger feedback on the system. In other words the body is telling itself to produce less cortisol, if there is plenty. We have chosen to model this effect in the following way. In the differential equations 5.1 k_0 is the parameter that feeds the system from hippocampus. It would therefore be natural to multiply k_0 with a function of the cortisol concentration, $f(x_3)$, that for high concentrations reduce or perhaps even shut down the feed-forward into hypothalamus. This will in time reduce the amount of cortisol. It is clear that the function should be constructed in such a way that when the concentration of cortisol decreases it opens up the pathway again working like a kind of valve. Let us for now implement this in equation 5.1 through the function $f(x_3)$

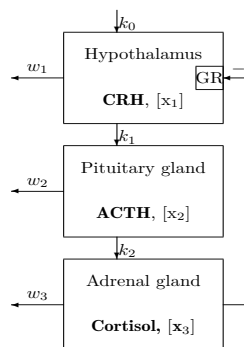


Figure 5.2: The feedback mechanism in hypothalamus included

$$\begin{aligned}
\frac{dx_1}{dt} &= k_0 f(x_3) - w_1 x_1 \\
\frac{dx_2}{dt} &= k_1 x_1 - w_2 x_2 \\
\frac{dx_3}{dt} &= k_2 x_2 - w_3 x_3 .
\end{aligned}
\tag{5.2}$$

The criteria that $f(x_3)$ gives a negative feedback is that $df(x_3)/dx_3 < 0$ for all $x_3 > 0$ [19]. In a similar way we will include the other feedback mechanisms. It will be our assumption that a feedback in a compartment works directly on the input to this compartment. These are all shown on figure 5.3 and the differential equations for this system is written in equation 5.3.

$$\begin{aligned}
\frac{dx_1}{dt} &= k_0 f(x_3) - w_1 x_1 \\
\frac{dx_2}{dt} &= k_1 x_1 g(x_3) - w_2 x_2 \\
\frac{dx_3}{dt} &= k_3 x_2 - w_3 x_3 .
\end{aligned}
\tag{5.3}$$

Now we have the differential equations with both feedback mechanisms. So now it is time to see how the feedback functions can be reasonably defined.

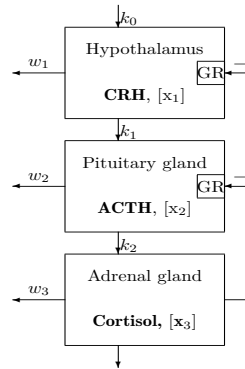


Figure 5.3: All feedback mechanisms included

5.2 Hill function

The basic assumption for the feedback functions is that a feedback must be implemented through a receptor. These receptors form the bottleneck of the process and the result is a feedback function where a saturation is present.

In this section we will assume that the chemical law known as the *law of mass action* is valid[25]. This law states that the rate which a chemical reaction occurs is proportional to the product of concentration of reactants and the rate constant. As an illustration of this we give the following example. Given the chemical stoichiometric balanced reaction scheme



where bold capital letters denote the reactants, small letters denote the number of reactants and k denote the rate constant. Then the rate of change of the concentration of product C will be given as

$$\frac{dC}{dt} = kA^a B^b, \quad (5.5)$$

where the capital letters denote the concentration of the reactants.

Now let us concentrate on a system of a specific kind of receptors. In this system there is a concentration of free receptors, $X(t) \geq 0$, and occupied receptors, $Y(t) \geq 0$. These receptors are not allowed to leave the system meaning that $X(t)+Y(t)$ is constant. Into the system is a flow of molecule concentration, $A(t) \geq 0$, that are able to be caught by the free receptors which then become occupied receptors with rate constant k_1 . The occupied receptors shall only be thought of as being occupied by this single kind of molecule which it can release to become a free receptor again. This will happen at a different rate constant, k_{-1} . Furthermore the occupied receptors shall be able to transform the incoming molecules to a new molecule, $B(t) \geq 0$, with rate constant k_2 and then release it to leave the system. The occupied receptor will then become unoccupied. As a chemical reaction this can be written as



where α is the number of molecules that are reacting with one free receptor, and β is the number of new molecules that are produced by the receptor.

Using the law of mass action we can write up the differential equations describing the change in concentrations.

$$\begin{aligned} \frac{dA}{dt} &= -k_1 A^\alpha X + k_{-1} Y \\ \frac{dX}{dt} &= -k_1 A^\alpha X + k_{-1} Y + k_2 Y \\ \frac{dY}{dt} &= k_1 A^\alpha X - k_{-1} Y - k_2 Y \\ \frac{dB}{dt} &= \beta k_2 Y. \end{aligned} \quad (5.7)$$

We will now use the fact that the sum of the free and occupied receptors are constant thus $X(t) + Y(t) = r$ where r is a constant. Substituting this into equation array 5.7 we end up with the following equations

$$\begin{aligned}\frac{dA}{dt} &= -k_1 A^\alpha r + (k_1 A^\alpha + k_{-1}) Y \\ \frac{dY}{dt} &= k_1 A^\alpha r - (k_1 A^\alpha + k_{-1} + k_2) Y \\ \frac{dB}{dt} &= \beta k_2 Y.\end{aligned}\tag{5.8}$$

In a biological system such as a gland or a cell the number of incoming molecules is usually much larger than the number of receptors. Therefore it is reasonable to think of the receptors as working at maximum capacity so that their occupancy rate is approximately constant ($dY/dt = 0$). This is known as the *quasi-equilibrium hypothesis*[14]. Solving $dY/dt = 0$ in the second equation of array 5.8 and isolating Y we get

$$Y = \frac{k_1 A^\alpha r}{k_1 A^\alpha + k_2 + k_{-1}}.\tag{5.9}$$

Putting this expression into the third equation of array 5.8 we obtain the rate of outgoing molecules

$$\frac{dB}{dt} = k_2 Y = \frac{k_1 A^\alpha r k_2}{k_1 A^\alpha + k_2 + k_{-1}}.\tag{5.10}$$

Since the rate constants are positive we can simplify this to

$$\frac{dB}{dt} = \beta \frac{A^\alpha r k_2}{A^\alpha + \frac{k_2 + k_{-1}}{k_1}} = \beta \frac{A^\alpha r k_2}{A^\alpha + \left(\sqrt[\alpha]{\frac{k_2 + k_{-1}}{k_1}}\right)^\alpha}.\tag{5.11}$$

Substituting in the following quantities $k_{max} = \beta r k_2$ and $k_n = \sqrt[\alpha]{(k_2 + k_{-1})/k_1}$, gives the following expression for the products rate of change as a function of incoming molecules

$$\frac{dB}{dt} = k_{max} \frac{A^\alpha}{A^\alpha + k_n^\alpha}.\tag{5.12}$$

The supremum of equation 5.12 is k_{max} . This is the limit as the incoming concentration tends to infinity. Furthermore it is seen that $dB/dt = k_{max}/2$ for $A = k_n$.

In figure 5.4 the Hill function is seen for different values of k_{max} .

Affinity

In biology and chemistry dissociation constants or affinity is used to describe how likely a chemical/biological reaction takes place[26].

Given concentrations of reactants and products as for example in equation array 5.6 the association constant (affinity constant) is defined as the ratio between concentrations in equilibrium[26]. That is in a simple chemical reaction such as



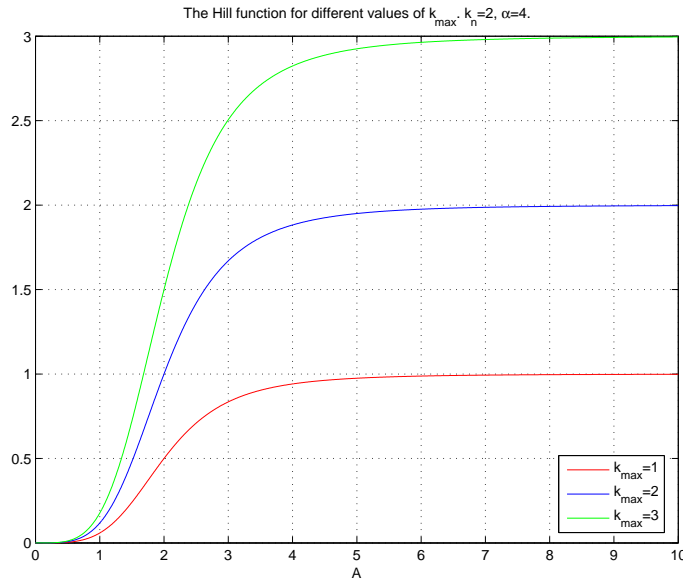


Figure 5.4: The Hill function shown with different values of k_{max} . The values of α and k_n is: $\alpha = 4$ and $k_n = 2$

the association constant, K_a , for $2H$ and O , and thereby the affinity of $2H$ and O becoming H_2O , is given by

$$K_a = \frac{[H_2O]}{[H^2] \cdot [O]}. \quad (5.14)$$

The demand for the occupied receptors to be in equilibrium (the quasi-steady state hypothesis) is from array 5.7

$$k_1 A^\alpha X - (k_{-1} + k_2) Y = 0 \Leftrightarrow \frac{Y}{A^\alpha \cdot X} = \frac{k_1}{k_{-1} + k_2}. \quad (5.15)$$

The affinity for αA to occupy the receptor is according to previous definition therefore given by

$$K_a = \frac{Y}{A^\alpha \cdot X} = \frac{k_1}{k_{-1} + k_2} = \frac{1}{k_n^\alpha}, \quad (5.16)$$

since $k_n = \sqrt[\alpha]{(k_2 + k_{-1})/k_1}$ (in equation 5.12). Obviously k_n^α determines the affinity.

In figure 5.5 the Hill function is shown for different values of k_n .

Inflection point

In mathematics this kind of function is an example of a sigmoid function and in biology it is called a Hill function. In certain cases it is of some interest to know at which value the rate of change of a function of this type changes from growing to decreasing. These inflection points will occur when the second derivative is zero. For $\alpha \geq 2$ the second

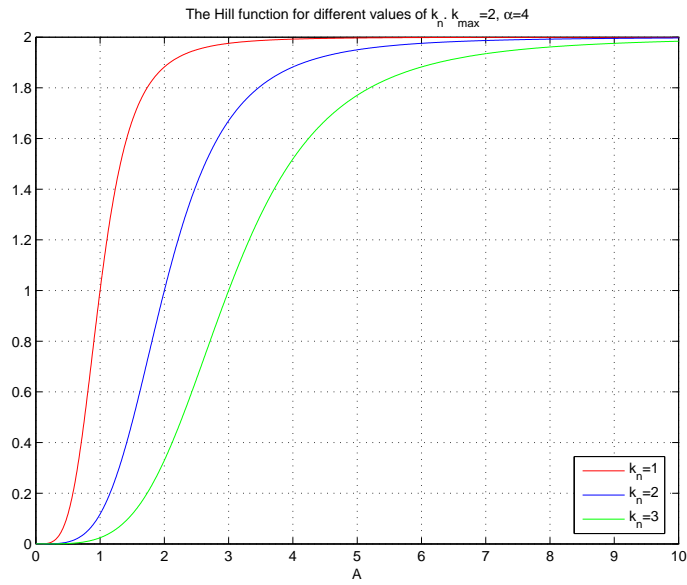


Figure 5.5: The Hill function shown with different values of k_n . $k_{max} = 2$ and $\alpha = 4$.

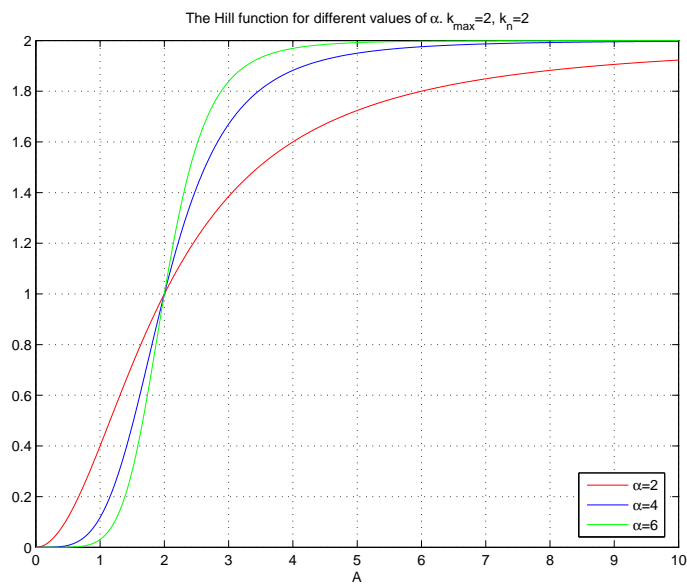


Figure 5.6: The Hill function shown with different values of α . The values of k_{max} and k_n is: $k_{max} = 2$ and $k_n = 2$.

derivative of equation 5.12 is

$$\frac{d^2}{dA^2} \left(k_{max} \frac{A^\alpha}{A^\alpha + k_n^\alpha} \right) = k_{max} \alpha k_n^\alpha A^{\alpha-2} \frac{(\alpha-1)(A^\alpha + k_n^\alpha) - 2\alpha A^\alpha}{(A^\alpha + k_n^\alpha)^3}. \quad (5.17)$$

Equating this expression to zero (and using A_I to denote the inflection point value of A) gives that

$$(\alpha-1)(A_I^\alpha + k_n^\alpha) - 2\alpha A_I^\alpha = 0, \quad (5.18)$$

which occur when

$$A_I = k_n \left(\frac{\alpha-1}{\alpha+1} \right)^{1/\alpha}. \quad (5.19)$$

As seen from this expression the inflection point, will converge toward k_n for large values of α .

A possible way to gather information about the constants would be to look at the gradient of the Hill function at the inflection point. As seen on figure 5.5 it is possible to get a fairly accurate estimate of the largest gradient. It is obvious that the largest gradient occur at the inflection point. Now we know the value of the concentration A from equation 5.19. The gradient is calculated from equation 5.12 as

$$\frac{d}{dA} \frac{dB}{dt} = \frac{d}{dA} \left(k_{max} \frac{A^\alpha}{A^\alpha + k_n^\alpha} \right) = k_{max} \alpha \frac{A^{\alpha-1} k_n^\alpha}{(A^\alpha + k_n^\alpha)^2}. \quad (5.20)$$

Inserting the concentration of A from equation 5.19 into equation 5.20 we obtain

$$\begin{aligned} \left. \frac{d}{dA} \frac{dB}{dt} \right|_{k_n \left(\frac{\alpha-1}{\alpha+1} \right)^{1/\alpha}} &= k_{max} \alpha \frac{\left(k_n \left(\frac{\alpha-1}{\alpha+1} \right)^{1/\alpha} \right)^{\alpha-1} k_n^\alpha}{\left(\left(k_n \left(\frac{\alpha-1}{\alpha+1} \right)^{1/\alpha} \right)^\alpha + k_n^\alpha \right)^2} \\ &= \frac{k_{max}}{4\alpha k_n} (\alpha^2 - 1) \left(\frac{\alpha+1}{\alpha-1} \right)^{1/\alpha}. \end{aligned} \quad (5.21)$$

This means that α is determining the place of the inflection point and the magnitude of the gradient at the inflection point. An illustration of this is seen in figure 5.6. As seen in equation 5.21 the magnitude of the gradient at the inflection point also depends on the values of k_{max} and k_n . This can be seen in figure 5.4 and figure 5.5.

5.3 Implementing the feedback functions

The previous section gave an indication about how a receptor works on a microscopic level. But in fact we do not know exactly how the chemical process is throughout the HPA-axis. Therefore we will implement the feedback functions in a more phenomenological way.

We will assume that a feedback in a compartment works in a way that reduces gain pathway (the term corresponding to positive stimuli of the hormone) at that specific compartment. Furthermore we assume that the processes in the HPA-axis are irreversible meaning that any flow shown on the compartment diagrams are not allowed to be reverted. Furthermore we assume that a negative feedback can not become a positive feedback.

5.4 Jelic-like approach

As explained in the introduction there are several receptors in the brain that are regulating the hormone secretion. We will now implement the Hill-functions into the feedback mechanisms. To do this we look at the compartment with CRH and write up the chemical reactions similar to the way Jelic et al.[2] write up their reactions. We assume cortisol is reacting with the receptors and substance B is produced. B reacts with CRH to form the neutral substance C which is no longer able to contribute to the dynamics of the HPA-axis. Then the chemical reactions would look like in equation array 5.22



The law of mass action then states that change in x_1 is given by

$$\frac{dx_1}{dt} = k_0 - c_1 x_1 B - w_1 x_1 . \quad (5.23)$$

As described in the previous section the amount of produced B is given by

$$k_{max} \frac{x_3^\alpha}{x_3^\alpha + k_n^\alpha} . \quad (5.24)$$

And the amount that is used is

$$c_1 x_1 B . \quad (5.25)$$

This leads to the following differential equation for A

$$\frac{dB}{dt} = k_{max} \frac{x_3^\alpha}{x_3^\alpha + k_n^\alpha} - c_1 x_1 B . \quad (5.26)$$

Now we use the *quasi-equilibrium hypothesis*. This means we assume the reaction between x_1 and B is fast compared to the other dynamics of the HPA-axis. Then B is used in approximately the same rate as it is produced.

$$\frac{dB}{dt} = 0 \Leftrightarrow k_{max} \frac{x_3^\alpha}{x_3^\alpha + k_n^\alpha} = c_1 x_1 B . \quad (5.27)$$

Inserting this result in equation 5.23 gives

$$\frac{dx_1}{dt} = k_0 - k_{max} \frac{x_3^\alpha}{x_3^\alpha + k_n^\alpha} - w_1 x_1 . \quad (5.28)$$

To avoid a feedback function reverting the flow in the system k_{max} is not allowed to attain values larger than k_0 .

$$k_{max} = \mu k_0 , \quad (5.29)$$

with $\mu \in [0, 1]$. Inserting in equation 5.28.

$$\frac{dx_1}{dt} = k_0 \left(1 - \mu \frac{x_3^\alpha}{x_3^\alpha + k_n^\alpha} \right) - w_1 x_1 . \quad (5.30)$$

This kind of approach to model a feedback mechanism has been widely used throughout literature[3, 4, 27]. We should check explicitly that the feedback function does fulfill the criteria for a negative feedback meaning that the derivative with respect to x_3 takes only negative values.

$$\frac{d}{dx_3} \left(1 - \mu \frac{x_3^\alpha}{x_3^\alpha + k_n^\alpha} \right) = -\mu \frac{\alpha k_n^\alpha x_3^{\alpha-1}}{(x_3^\alpha + k_n^\alpha)^2}. \quad (5.31)$$

Thus for $x_3 > 0$ this is indeed negative.

In a similar way we model the negative feedback in the pituitary gland which gives the equations in array 5.32

$$\begin{aligned} \frac{dx_1}{dt} &= k_0 \left(1 - \mu \frac{x_3^\alpha}{x_3^\alpha + c_1^\alpha} \right) - w_1 x_1 \\ \frac{dx_2}{dt} &= k_1 \left(1 - \rho \frac{x_3^\beta}{x_3^\beta + c_2^\beta} \right) x_1 - w_2 x_2 \\ \frac{dx_3}{dt} &= k_2 x_2 - w_3 x_3. \end{aligned} \quad (5.32)$$

Now c_1 , c_2 , α and β are determined by the stoichiometric chemical reaction scheme. Since both feedbacks correspond to cortisol binding to GR we assume $c_1 = c_2 \equiv c$ and $\alpha = \beta$. μ is dependent on the stoichiometric chemical reaction, k_0 and the size of the receptor of which we do not have any information. The same is the case with ρ . Therefore these parameters will still be included in the final equations given by array 5.33

$$\begin{aligned} \frac{dx_1}{dt} &= k_0 \left(1 - \mu \frac{x_3^\alpha}{x_3^\alpha + c^\alpha} \right) - w_1 x_1 \\ \frac{dx_2}{dt} &= k_1 \left(1 - \rho \frac{x_3^\alpha}{x_3^\alpha + c^\alpha} \right) x_1 - w_2 x_2 \\ \frac{dx_3}{dt} &= k_2 x_2 - w_3 x_3. \end{aligned} \quad (5.33)$$

Actually there will most certainly be more than one receptor in each compartment. Therefore one could argue that it would be more reasonable to assume many receptors are controlling each feedback at the same time. But if many small receptors obey the same chemical reactions and the receptors have different capacities, a_i , then the differential equation for CRH would look as

$$\frac{dx_1}{dt} = k_0 \left(1 - \frac{\sum_i a_i}{k_0} \frac{x_3^\alpha}{x_3^\alpha + c^\alpha} \right) - w_1 x_1$$

Denoting $\sum_i a_i/k_0 = \mu$ we end up with the same differential equations as in array 5.33. Therefore nothing is lost by modeling all receptors as one big receptor.

5.5 Description of the obtained system of nonlinear differential equations

The system of differential equations 5.33 with strictly positive k_0 , k_1 , k_2 , w_1 , w_2 , w_3 and $\mu, \rho \in]0, 1]$ and α as an integer value will be in focus for the next section. Since it has

taken some pages to end up with this system it may help summarizing the mechanisms of the system. The derivative of CRH (x_1) has a positive term $k_0 \left(1 - \mu \frac{x_3^\alpha}{x_3^\alpha + c^\alpha}\right)$ where a negative feedback from cortisol (x_3) inhibits the positive stimulation for increasing cortisol. There is a similar negative feedback mechanism from cortisol in the equation describing the derivative of ACTH (x_2) where the positive term is 'proportional' to the CRH concentration. Again increasing concentration of cortisol inhibits the positive stimulation. The positive stimulation on the derivative of cortisol is linear in ACTH thus the more ACTH the more cortisol is produced. The change in all the hormone concentrations have a loss depending linearly on the concentration itself. This description of our model match well the qualitative description of the HPA axis as shown in figure 2.2.

5.6 Existence and uniqueness of solutions, trapping region, existence and number of fixed points

Our model without hippocampus (equation array 5.33) is given by three coupled, non linear, autonomous differential equations. In this section we will show results about existence and uniqueness of solutions, bounded region for the solutions, the existence and number of fixed points.

Existence and uniqueness of solutions

To use the existence and uniqueness theorem (theorem 3.1) we should calculate all the partial derivatives of the right hand sides of the equations 5.33 and investigate whether these are continuous. Since we are only caring about non negative concentrations this is the case and quite simple to show so we will omit the calculations. Therefore the existence and uniqueness theorem apply and we are guaranteed that there is one and only one solution for a given initial condition.

Guarantee of non negative concentrations

Let us start with some observations regarding existence of an invariant solution set of array 5.33. By invariant solution set is meant that if a solution is in the set at some time then it will stay in there for all future times. Since non negative hormone concentrations as well as infinite concentrations are unphysiological it is a criterion that reasonable initial conditions does not lead to solutions with negative concentrations or solutions diverging to infinity. This can be avoided if solutions starting in a bounded region in the non negative octant of \mathbb{R}^3 stay in that region for all future time. Let us start with an argument that solutions starting with non negative concentrations stay non negative for all future time and deal with the boundedness afterwards. We are going to use that $\forall x_3 \geq 0$ then $1 - \mu \frac{x_3^\alpha}{x_3^\alpha + c^\alpha} > 0$ for $\mu \in [0, 1]$. Similarly $1 - \rho \frac{x_3^\alpha}{x_3^\alpha + c^\alpha}$ is always positive for $\rho \in [0, 1]$. If x_1 is zero there is only a positive term in the differential equation governing x_1 no matter the values of x_2 and x_3 . Therefore for any nonnegative initial value of x_1 , x_1 never become negative. Similar reasoning applies for the two other differential equations where the only negative term of the derivative vanishes when the concentration considered is zero. Thus the octant in \mathbb{R}^3 with nonnegative entries is an invariant solution set.

Existence of trapping region(s)

Now we argue that there exists a bounded subset of the non negative octant of \mathbb{R}^3 that is an invariant solution set to the equations 5.33. This is called a trapping region meaning that no solution can 'escape' from this region if it is once in it. This is also needed when two dimensional systems are considered and one wants to use the Poincaré Bendixon theorem. It may be the hardest part in applying the theorem and sometimes requires 'good ideas' in how to construct boundaries where the flow does not point out of set. Here it seems more straightforward fortunately. For dynamical systems in general there could be a trapping region but this would not rule out interesting dynamics outside the trapping region. However for our system there exists a trapping region and all solutions enter the trapping region in finite time which means the trapping region contains the interesting part of the system dynamics. We will start showing the existence of trapping region(s) given by equation 5.34 and a 'minimal' trapping region given by equation 5.35.

Since $0 < 1 - \mu \frac{x_3^\alpha}{x_3^\alpha + c^\alpha} \leq 1$ then from the first equation of array 5.33 we have $dx_1/dt \leq k_0 - w_1 x_1$. Therefore if $x_1 > k_0/w_1$ then $dx_1/dt < 0$ and if $x_1 = k_0/w_1$ then $dx_1/dt \leq 0$. Thus a bound, M_{x_1} , for x_1 can be chosen as $M_{x_1} = k_0/w_1 + \epsilon_1 \forall \epsilon_1 \geq 0$. This is very convenient because then x_1 is bounded no matter what values x_2 and x_3 attains. But the fact that x_1 is bounded can be used to make a bound on x_2 and after that on x_3 . Carrying out the argument in detail we see that $0 < 1 - \rho \frac{x_3^\alpha}{x_3^\alpha + c^\alpha} \leq 1$ and $dx_2/dt < 0$ if $x_2 > k_1/w_2 x_1$ (and $dx_2/dt \leq 0$ if $x_2 = k_1/w_2 x_1$). Since x_1 is bounded this means that x_2 is also bounded. A bound for x_2 is $M_{x_2} = k_1/w_2 M_{x_1} + \epsilon_2 \forall \epsilon_2 \geq 0$. If $x_3 > w_3/k_2 x_2$ then $dx_3/dt < 0$. Defining $M_{x_3} \equiv k_2/w_3 M_{x_2} + \epsilon_3 \forall \epsilon_3 > 0$ then $dx_3/dt < 0$ for $x_2 \in [0; k_0 k_1/w_1 w_2]$ and $x_3 = M_{x_3}$ (and $\dot{x}_3 \leq 0$ for $x_3 = w_3/k_2 M_{x_2}$ and $x_2 \in [0; k_0 k_1/w_1 w_2]$).

This shows there exists a bounded set in which solutions will stay in if they are once in there - a 'trapping region'.

$$\begin{aligned} W(\epsilon_1, \epsilon_2, \epsilon_3) &= [0; M_{x_1}(\epsilon_1)] \times [0; M_{x_2}(\epsilon_2)] \times [0; M_{x_3}(\epsilon_3)] \\ &= \left[0; \frac{k_0}{w_1} + \epsilon_1\right] \times \left[0; \frac{k_0 k_1}{w_1 w_2} + \frac{k_1}{w_2} \epsilon_1 + \epsilon_2\right] \times \left[0; \frac{k_0 k_1 k_2}{w_1 w_2 w_3} + \frac{k_1 k_2}{w_2 w_3} \epsilon_1 + \frac{k_2}{w_3} \epsilon_2 + \epsilon_3\right] \\ &\equiv I_1(\epsilon) \times I_2(\epsilon_1, \epsilon_2) \times I_3(\epsilon_1, \epsilon_2, \epsilon_3) \quad \forall \epsilon_1, \epsilon_2, \epsilon_3 > 0. \end{aligned} \tag{5.34}$$

For any $\epsilon_1 > 0, \epsilon_2 > 0, \epsilon_3 > 0$ we have shown that the flow is pointing into $W(\epsilon_1, \epsilon_2, \epsilon_3)$ on the boundaries where no concentration is zero. Now we were a bit strict demanding that the derivative of a variable should be negative for sufficiently large values of the variable. It is sufficient for the derivative to be zero. If this is used one can omit the ϵ 's from the estimation of boundaries. This means that $W(0, 0, 0)$ is also a trapping region as well as e.g. $W(\epsilon_1, 0, 0) \forall \epsilon_1 > 0$. We denote this trapping region by $V = W(0, 0, 0)$ thus

$$V = [0; k_0/w_1] \times [0; k_0 k_1/w_1 w_2] \times [0; k_0 k_1 k_2/w_1 w_2 w_3]. \tag{5.35}$$

Note that the argumentation for the trapping region is such that $I_1(\epsilon_1)$ is a trapping region for $x_1(t)$ for all non negative values of x_2 and x_3 . $I_1(\epsilon_1) \times I_2(\epsilon_1, \epsilon_2)$ is a trapping region for $x_1(t)$ and $x_2(t)$ for all non negative values of x_3 .

It has now been shown that for initial conditions in the nonnegative octant the system have solutions living in a bounded region with nonnegative hormone concentrations. This is physiological correct and a problem that other models such as [1] have

to fix with additional non-linearities. We have now shown existence of several trapping regions of our system and now we focus on showing that all solutions enter the trapping region in finite time.

5.7 $x_3(t) > 0$ after finite time and for all future time.

In order to show that any non negative solution outside V enters V in finite time we need that $x_3(t) > 0$ after finite time and for all future time. This section is dedicated to show $x_3(t) > 0$ after finite time and for all future time.

Assume we have an arbitrary nonnegative initial condition $\mathbf{x}(t_0) = \mathbf{x}_0 = (x_{10}, x_{20}, x_{30})$. We now want to construct a trapping region for the solution with initial condition \mathbf{x}_0 . Here there are two cases that needs to be considered regarding x_{10} . These are $x_{10} > k_0/w_1$ or $0 \leq x_{10} \leq k_0/w_1$. We take care of this by defining $\epsilon_1 = \max\{x_{10} - k_0/w_1, 0\}$. Then the solution with initial condition \mathbf{x}_0 is trapped in the region $W(\epsilon_1, 0, 0)$. In this trapping region we can now make an estimation for the differential equations using linear differential equations. Since $I_3(\epsilon_1, 0, 0)$ is compact, $1 - \rho \frac{x_3^\alpha}{c^\alpha + x_3^\alpha}$ and $1 - \mu \frac{x_3^\alpha}{c^\alpha + x_3^\alpha}$ attains minimum and maximum values by the extreme value theorem [17]. Since the expressions are decreasing in x_3 the minimum L_1 and L_2 are found as the expression evaluated at the right endpoint of $I_3(\epsilon_1, 0, 0)$.

$$\begin{aligned} L_1 &= 1 - \mu \frac{M_{x_3}^\alpha}{c^\alpha + M_{x_3}^\alpha} > 0 \\ L_2 &= 1 - \rho \frac{M_{x_3}^\alpha}{c^\alpha + M_{x_3}^\alpha} > 0. \end{aligned} \quad (5.36)$$

We construct a linear system of differential equations that will be used for a bound on the solutions of the non linear system.

$$\begin{aligned} \dot{x}_1' &= L_1 k_0 - w_1 x_1' \\ \dot{x}_2' &= L_2 k_1 x_1' - w_2 x_2' \\ \dot{x}_3' &= k_2 x_2' - w_2 x_3'. \end{aligned} \quad (5.37)$$

and $\mathbf{x}'(t_0) = \mathbf{x}_0$ Using this to compare the original, non linear coupled system of differential equations restricted to $W(\epsilon_1, 0, 0)$ we obtain.

$$\begin{aligned} \dot{x}_1' &\leq x_1 \\ \dot{x}_2' &\leq x_2 \\ \dot{x}_3' &\leq x_3. \end{aligned} \quad (5.38)$$

The idea of comparing the non linear system with a linear system that can be solved is contained in the following lemma

Lemma 5.1

Let $f : \mathbb{R} \rightarrow \mathbb{R}$, $g : \mathbb{R} \rightarrow \mathbb{R}$ and $f, g \in C^1$ and $f(t_0) = g(t_0)$. If $\forall t_0 \leq t < \infty$ $df(t)/dt \leq dg(t)/dt$ then $f(t) \leq g(t) \forall t \geq t_0$.

Proof

Since $df(t)/dt$ and $dg(t)/dt$ are continuous, they are integrable on a closed, bounded interval [17]. Using the comparison theorem for integrals [17] we get

$$\int_{t_0}^t \frac{df(x)}{dx} dx \leq \int_{t_0}^t \frac{dg(x)}{dx} dx. \quad (5.39)$$

Using the fundamental theorem of calculus [17] this equals

$$f(t) - f(t_0) \leq g(t) - g(t_0). \quad (5.40)$$

Since by assumption $f(t_0) = g(t_0)$ we have

$$f(t) \leq g(t), \quad \forall t \geq t_0. \quad (5.41)$$

□

Then lemma 5.2 trivially

Lemma 5.2

If $x'(t_0) = x(t_0) = x''(t_0)$ and $x_1' \leq x_1 \leq x_1''$ for all $t \geq t_0$ then $x'(t) \leq x(t) \leq x''(t) \forall t \geq t_0$.

Solving the linear system (array 5.37) we get

$$\begin{aligned} x_1(t)' &= d_{11}e^{-w_1t} + \frac{k_0}{w_1}L_1 \\ x_2(t)' &= d_{21}e^{-w_1t} + d_{22}e^{-w_2t} + \frac{k_0k_1}{w_1w_2}L_1L_2 \\ x_3(t)' &= d_{31}e^{-w_1t} + d_{32}e^{-w_2t} + d_{33}e^{-w_3t} + \frac{k_0k_1k_2}{w_1w_2w_3}L_1L_2. \end{aligned} \quad (5.42)$$

where the d_{ij} 's are real constants that can be found from the initial conditions and the eigenvectors of the homogeneous system of array 5.37.

Since $\frac{k_0k_1k_2}{w_1w_2w_3}L_1L_2 > 0$ and all terms involving exponentials are converging to 0 for increasing t then there exists a $T_0 < \infty$ such that $x_3'(t) > 0 \forall t > T_0$ (actually any infinitesimal small time is sufficient since we only allow non negative initial conditions). By bounding $x_3(t)$ using $x_3'(t)$ it is clear that $x_3(t) > 0 \forall t > T_0$.

All non negative initial conditions lead to solutions entering V in finite time for $\mu, \rho \in]0; 1]$.

The two lemmas 5.1 and 5.3 can be used to show that if a differential equation can be bounded by another differential equation and the solution to the latter attains a certain value in finite time then the same holds for the original differential equation. This means that the lemmas are used to 'squeeze' the solution of a differential equation with a solution of another differential equation.

Lemma 5.3

Let $f : \mathbb{R} \rightarrow \mathbb{R}$, $g : \mathbb{R} \rightarrow \mathbb{R}$ and $f, g \in C^1$ and $f(t_0) = g(t_0)$. Let $t_0 \leq T' \leq a < \infty$ and $\forall t \in [t_0, a]$ $f(t) \leq g(t)$ and $g(T' + t_0) = b$ and $g(t)$ decreasing on $[0; T']$. Then there exists T with the property that $0 \leq T \leq T'$ such that $f(T + t_0) = b$.

Proof

Since $f(t) \leq g(t) \forall t \in [t_0, a]$ then first consider $f(T' + t_0) = g(T' + t_0) = b$. This means we can choose $T = T'$. Secondly we have to consider $f(T' + t_0) < g(T' + t_0) = b$. Since $f(t_0) = g(t_0) > b$ and since f is continuous we have by the intermediate theorem [17] that there exists T such that $0 < T < T'$ with $f(T + t_0) = b$. \square

The two lemmas are 'very intuitive understandable' if figure 5.7 is considered.

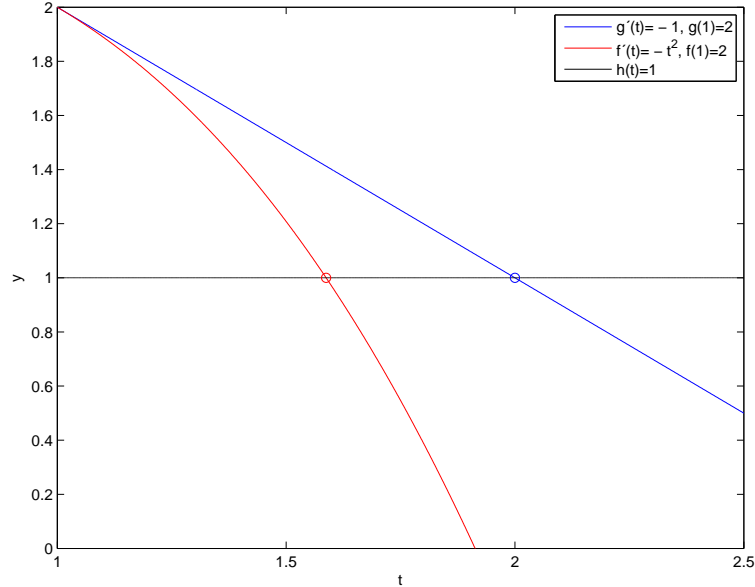


Figure 5.7: Illustration of lemma 5.1 and lemma 5.3. The derivative of f is smaller than that of g . If the two functions are equal at some t_0 (here at (1,2)) and if g has the value $b = 1$ at some later, finite time then there also exists a finite time such that f has the value 1.

For $\mu, \rho \in]0; 1]$ we will show that all solutions with non negative initial conditions that are not contained in V will enter V in finite time. Since we have shown V is a trapping region any solution entering V stays in there. Assume an initial condition $\mathbf{x}(t_0) = \mathbf{x}_0 = (x_{10}, x_{20}, x_{30})$ is given. From the argument above we know that there exists a finite time T_0 such that $x_3(t) > 0$ for $t \geq T_0$. Therefore we consider $\mathbf{x}(t)$ for $t \geq T_0$.

The proof that any solution enters V in finite time is now split in steps. First it is shown that $x_1(t)$ enters $I_1(0)$ in finite time and x_1 is then trapped. Then we can show that it takes finite time for x_2 to be trapped in $I_2(0, 0)$ and then it can be shown that x_3 is trapped after finite time in $I_3(0, 0, 0)$.

- Proof that $x_1(T_0 + T_1) \in [0; k_0/w_1]$ for some $0 \leq T_0 + T_1 < \infty$.
If $x_1(T_0) \in [0; k_0/w_1]$ then for $T_1 = 0$ the proof is finished. For $x_1(T_0) > k_0/w_1$ consider the closed, bounded interval $x_1 \in [k_0/w_1, x_1(T_0)]$. Since $x_3 > 0$, $\mu > 0$

then $1 - \mu \frac{x_3^\alpha}{x_3^\alpha + c^\alpha} < 1$. Therefore $dx_1/dt < 0$ for $x_1 \in [k_0/w_1; x_1(T_0)]$ (see array 5.33). This is sufficient to ensure that $x_1(t)$ enters the desired region in finite time, but it takes a little more work to prove it.

Since dx_1/dt is a continuous function on the closed, bounded interval $[k_0/w_1; x_1(T_0)]$ then dx_1/dt obtains a maximum by the extreme value theorem [17]. Denote the maximum by M_1 . Since $dx_1/dt < 0$ for all x_1 in the considered interval then $M_1 < 0$. Now we have that $\forall x_1 \in [k_0/w_1; x_1(T_0)]$ then $dx_1/dt \leq M_1 < 0$. Now we define the function y_1 by $y_1(T_0) = x_1(T_0)$ and $dy_1/dt = M_1$. Solving the differential equation we get $y(t) = M_1 t + x_1(T_0) - M_1 T_0$. Now we can calculate when y_1 enters $I_1(0)$ by solving $y(T'_1 + T_0) = k_0/w_1$

$$T'_1 = \frac{k_0/w_1 - x_1(T_0)}{M_1} > 0. \quad (5.43)$$

Thus in finite time $y_1(T_0 + T'_1) \in [0; k_0/w_1]$. By lemma 5.1 and lemma 5.3 there exist a finite time T_1 such that $x_1(t_0 + T_1) \in [0; k_0/w_1]$. Since $I_1(0)$ is a trapping region for x_1 for all non negative values of x_2 and x_3 then we can now proceed looking at x_2 considering x_1 trapped.

- Proof that $x_2 \in [0; k_0 k_1/w_1 w_2]$ in finite time.

For all non negative initial conditions of x_2 we consider dx_2/dt after the time $T_0 + T_1$. If $x_2(T_0 + T_1) \in [0; k_0 k_1/w_1 w_2]$ then we are done. Thus consider the case that $x_2 > k_0 k_1/w_1 w_2$. $x_3(t) > 0$, $\rho \in]0, 1]$ so $0 < 1 - \rho x_3^\alpha/x_3^\alpha + c^\alpha < 1$ so $\forall x_2 \in [k_0 k_1/w_1 w_2; x_2(T_0 + T_1)]$ then $dx_2/dt < 0$. We just repeat the argument from the case with x_1 that dx_2/dt thus has a maximum, M_2 , on the closed interval $[k_0 k_1/w_1 w_2; x_2(T_0 + T_1)]$ by the extreme value theorem and M_2 is strictly less than 0. Defining $y_2(T_0 + T_1) = x_2(T_0 + T_1)$ and $y'_2 = M_2$ we solve the differential equation for y_2 . $y_2(t) = M_2 t + x_2(T_0 + T_1) - M_2(T_0 + T_1)$. Solving $y_2(T_0 + T_1 + T'_2) = k_0 k_1/w_1 w_2$ for T'_2 we get

$$T'_2 = \frac{k_0 k_1/w_1 w_2 - x_2(T_0 + T_1)}{M_2} > 0. \quad (5.44)$$

This means that after the finite time $T_0 + T_1 + T'_2$ then $y_2(t) \in [0; k_0 k_1/w_1 w_2]$. $x_2(t)$ enters the set as least as fast as y_2 by lemma 5.1 and lemma 5.3. This means there exists $0 \leq T_2 < T'_2$ such that $x_2(T_0 + T_1 + T_2) \in [0; k_0 k_1/w_1 w_2] \forall t > T_0 + T_1 + T_2$. Since $\dot{x}_2 < 0$ for $x_2 = k_0 k_1/w_1 w_2$ then $x_2(t) \in [0; k_0 k_1/w_1 w_2[$ for $t > T_0 + T_1 + T_2 + \delta$, $\forall \delta > 0$.

- Proof that $x_3 \in [0; k_0 k_1 k_2/w_1 w_2 w_3]$ after finite time. If $x_3(T_0 + T_1 + T_2 + \delta) \in [0; k_0 k_1 k_2/w_1 w_2 w_3]$ then we are done. If $x_3(T_0 + T_1 + T_2 + \delta) > k_0 k_1 k_2/w_1 w_2 w_3$ then we have that $dx_3/dt < 0$ for $x_3 \in [k_0 k_1 k_2/w_1 w_2 w_3; x_3(T_0 + T_1 + T_2 + \delta)]$. By the extreme value theorem $M_3 < 0$ is the minimum of \dot{x}_3 on $[k_0 k_1 k_2/w_1 w_2 w_3; x_3(T_0 + T_1 + T_2 + \delta)]$ so we can once again make a differential equation in y_3 with solutions entering $[0; k_0 k_1 k_2/w_1 w_2 w_3]$ in finite time. Since x_3 decreases faster than y_3 it takes a finite time for x_3 to enter $[0; k_0 k_1 k_2/w_1 w_2 w_3]$. The details are similar to the case with x_1 and x_2 .

Now it has been shown that any solution enters V in finite time for $\mu, \rho \in]0, 1]$. For $x_1 \notin I_1(0)$ it may be that $\dot{x}_2 > 0$ and $\dot{x}_3 > 0$. This shows $dist(x_2, I_2(0, 0))$ may be increasing for some time until $x_1 \in I_1(0)$. Thus even though all solutions outside V

enter V in finite time this does not mean that any coordinate of a solution approach the trapping region for all times.

Existence and number of fixed points

Now we investigate the existence and number of the fixed points of the system. There exists one and only one steady state solution which we will now show from array 5.33. The conditions for steady state is given by equations 5.45-5.47

$$x_{1ss} = \frac{k_0}{w_1} \left(1 - \mu \frac{x_{3ss}^\alpha}{x_{3ss}^\alpha + c^\alpha} \right) \quad (5.45)$$

$$x_{2ss} = \frac{k_0 k_1}{w_1 w_2} \left(1 - \mu \frac{x_{3ss}^\alpha}{x_{3ss}^\alpha + c^\alpha} \right) \left(1 - \rho \frac{x_{3ss}^\alpha}{x_{3ss}^\alpha + c^\alpha} \right) \quad (5.46)$$

$$x_{3ss} = \frac{k_0 k_1 k_2}{w_1 w_2 w_3} \left(1 - \mu \frac{x_{3ss}^\alpha}{x_{3ss}^\alpha + c^\alpha} \right) \left(1 - \rho \frac{x_{3ss}^\alpha}{x_{3ss}^\alpha + c^\alpha} \right). \quad (5.47)$$

The right hand side of equation 5.47 has the value $\frac{k_0 k_1 k_2}{w_1 w_2 w_3} > 0$ for $x_{3ss} = 0$ and is decreasing as a function of x_{3ss} . The left hand side has the value 0 for $x_{3ss} = 0$ and is increasing linearly as a function of x_{3ss} . This guarantees the existence of a unique x_{3ss} . Then there is exactly one fixed point since equation 5.45 and equation 5.46 determines x_{1ss} and x_{2ss} from x_{3ss} . Since $x_{1ss}, x_{2ss}, x_{3ss}$ are non negative we are guaranteed that the fixed point is contained in V since all solutions enter V in finite time.

Note that we have used no assumptions regarding the numerical values of the included parameters. Only the sign of the parameters have been used for the argument. This means a unique fixed point exists for any numerical values of the parameters. As parameters may be varied no additional fixed points is created. This means there can be no saddle node bifurcation for this system. In terms of bifurcations of fixed points the only thing left to happen is a change of the stability of the fixed point in terms of the parameters. This will be in focus for the next sections.

6 Analytic analysis of the system without hippocampus

In this chapter we will simplify the system by scaling the variables and thereby reducing the number of parameters from nine to six. We will then perform an analytic investigation of this system. The investigation treat local stability of the fixed point.

6.1 Scaling of the system of differential equations

Scaling of differential equations may be convenient in order to reduce the number of parameters by grouping the original parameters. Here we will allow the time and the three time dependent variables to be scaled with a scaling constant that we will specify later in order to get a system with fewer parameters. Let d_0, d_1, d_2, d_3 be constants that we will later specify and define θ, X_1, X_2, X_3 by the equations

$$\begin{aligned}\theta &\equiv d_0 t \\ x_1 &\equiv d_1 X_1 \\ x_2 &\equiv d_2 X_2 \\ x_3 &\equiv d_3 X_3.\end{aligned}\tag{6.1}$$

This is substituted into array 5.33 and the chain rule is used. Using the first equation of array 5.33 as example we first look at the left side

$$\frac{dx_1}{dt} = d_1 \frac{dX_1}{dt} = d_1 \frac{dX_1}{d\theta} \frac{d\theta}{dt} = d_1 d_0 \frac{dX_1}{d\theta}.\tag{6.2}$$

Substituting on the right side of the first equation of array 5.33 gives

$$\frac{dx_1}{dt} = k_0 \left(1 - \mu \frac{d_3^\alpha X_3^\alpha}{c^\alpha + d_3^\alpha X_3^\alpha} \right) - w_1 d_1 X_1\tag{6.3}$$

Now it is just a matter of setting the two expressions 6.2, 6.3 equal to each other and isolate $dX_1/d\theta$

$$\frac{dX_1}{d\theta} = \frac{k_0}{d_0 d_1} \left(1 - \mu \frac{d_3^\alpha X_3^\alpha}{c^\alpha + d_3^\alpha X_3^\alpha} \right) - \frac{w_1}{d_0} X_1.\tag{6.4}$$

This approach is used on the two other differential equations as well.

$$\begin{aligned}\frac{dX_1}{d\theta} &= \frac{k_0}{d_0 d_1} \left(1 - \mu \frac{d_3^\alpha X_3^\alpha}{c^\alpha + d_3^\alpha X_3^\alpha} \right) - \frac{w_1}{d_0} X_1 \\ \frac{dX_2}{d\theta} &= \frac{k_1 d_1}{d_0 d_2} \left(1 - \rho \frac{d_3^\alpha X_3^\alpha}{c^\alpha + d_3^\alpha X_3^\alpha} \right) X_1 - \frac{w_2}{d_0} X_2 \\ \frac{dX_3}{d\theta} &= \frac{k_2 d_2}{d_0 d_3} X_2 - \frac{w_3}{d_0} X_3.\end{aligned}\tag{6.5}$$

Now this may not seem simpler than the original system 5.33 but remember we still have the option of choosing d_0, d_1, d_2 and d_3 in an appropriate manner. It seems to be a good idea to choose $d_3 = c$ in order to simplify the fractions with x_3 involved. We can use the last three degrees of freedom to make the first coefficient in each equation equal unity.

$$\begin{aligned}1 &= \frac{k_0}{d_0 d_1} \\ 1 &= \frac{k_1 d_1}{d_0 d_2} \\ 1 &= \frac{k_2 d_2}{d_0 d_3}.\end{aligned}\tag{6.6}$$

Solving for d_0, d_1, d_2 we get

$$\begin{aligned}d_0 &= \left(\frac{k_0 k_1 k_2}{c} \right)^{1/3} \\ d_1 &= \left(\frac{c k_0^2}{k_1 k_2} \right)^{1/3} \\ d_2 &= \left(\frac{c^2 k_0 k_1}{k_2^2} \right)^{1/3} \\ d_3 &= c.\end{aligned}\tag{6.7}$$

All the scalings constants are thus positive. What about the dimensions of d_0, d_1, d_2 ? From array 5.33 we see that c has dimension of concentration, k_0 has dimension concentration divided by time and k_2 and k_3 have dimension inverse time. Considering array 6.7 this means d_0 has dimension of inverse time, d_1, d_2, d_3 have dimension of concentration. Recalling the defining equations for the scaled variables 6.1 we get

$$\begin{aligned}\theta &= \left(\frac{k_0 k_1 k_2}{c} \right)^{1/3} t \\ x_1 &= \left(\frac{c k_0^2}{k_1 k_2} \right)^{1/3} X_1 \\ x_2 &= \left(\frac{c^2 k_0 k_1}{k_2^2} \right)^{1/3} X_2 \\ x_3 &= c X_3.\end{aligned}\tag{6.8}$$

Since the concentrations are all non negative and the scaling factors are positive we have that X_1, X_2, X_3 are non negative. The time is scaled by a positive constant thus

an increase in time corresponds to an increase in θ . Note that X_1, X_2, X_3 and θ are all dimensionless. Now we can write array 6.5 in a way with fewer parameters by defining positive parameters $\tilde{w}_1, \tilde{w}_2, \tilde{w}_3$ by

$$\begin{aligned}\tilde{w}_1 &\equiv \frac{w_1}{d_0} \\ \tilde{w}_2 &\equiv \frac{w_2}{d_0} \\ \tilde{w}_3 &\equiv \frac{w_3}{d_0}.\end{aligned}\tag{6.9}$$

This means \tilde{w}_1, \tilde{w}_2 and \tilde{w}_3 are dimensionless. Putting all the substitutions into array 6.5 we obtain the dimensionless system

$$\begin{aligned}\frac{dX_1}{d\theta} &= 1 - \mu \frac{X_3^\alpha}{1 + X_3^\alpha} - \tilde{w}_1 X_1 \\ \frac{dX_2}{d\theta} &= \left(1 - \rho \frac{X_3^\alpha}{1 + X_3^\alpha}\right) X_1 - \tilde{w}_2 X_2 \\ \frac{dX_3}{d\theta} &= X_2 - \tilde{w}_3 X_3.\end{aligned}\tag{6.10}$$

Comparing to 5.33 we see that this version of the system has 6 parameters which is 3 less than the original system. We are now interested in finding the stability of the fixed point of this system for different parameter values. To simplify notation we introduce Y as

$$Y \equiv \frac{X_3^\alpha}{1 + X_3^\alpha}.\tag{6.11}$$

We have X_3 non negative and thus $Y \in [0, 1[$. Now the steady state condition is that all the left hand sides in 6.10 equal zero leading to (using the notation $Y_{ss} \equiv \frac{X_{3ss}^\alpha}{1 + X_{3ss}^\alpha}$)

$$\begin{aligned}X_{1ss} &= \frac{1}{\tilde{w}_1} (1 - \mu Y_{ss}) \\ X_{2ss} &= \frac{1}{\tilde{w}_2} (1 - \rho Y_{ss}) X_{1ss} = \frac{1}{\tilde{w}_1 \tilde{w}_2} (1 - \rho Y_{ss}) (1 - \mu Y_{ss}) \\ X_{3ss} &= \frac{1}{\tilde{w}_3} X_{2ss} = \frac{1}{\tilde{w}_1 \tilde{w}_2 \tilde{w}_3} (1 - \rho Y_{ss}) (1 - \mu Y_{ss}).\end{aligned}\tag{6.12}$$

This is equivalent to array 5.47 thus we are sure that exactly one fixed point exists.

Now we make the Jacobian of 6.10 where we use that $dY/dX_3 = \alpha X_3^{\alpha-1}/(1+X_3^\alpha)^2 = \alpha Y^2 X_3^{-\alpha-1}$ (for $X_3 \neq 0$)

$$\mathbf{J} = \begin{pmatrix} -\tilde{w}_1 & 0 & -\mu \alpha Y^2 X_3^{-\alpha-1} \\ 1 - \rho Y & -\tilde{w}_2 & -\alpha \rho X_1 Y^2 X_3^{-\alpha-1} \\ 0 & 1 & -\tilde{w}_3 \end{pmatrix}\tag{6.13}$$

In order to determine the stability of the fixed point we need to find the eigenvalues of the Jacobian, matrix 6.13, evaluated at the fixed point given by the equations 6.12.

The algebra is easier if we wait with actually inserting the steady state values but just denote with ss that the variables are evaluated at the steady state.

$$-\det(J_{ss} - \lambda I) = \lambda^3 + \alpha_1 \lambda^2 + \alpha_2 \lambda + \alpha_3, \quad (6.14)$$

where

$$\begin{aligned} \alpha_1 &= \tilde{w}_1 + \tilde{w}_2 + \tilde{w}_3 \\ \alpha_2 &= \rho \alpha X_{1ss} Y_{ss}^2 X_{3ss}^{-\alpha-1} + \tilde{w}_1 \tilde{w}_2 + \tilde{w}_1 \tilde{w}_3 + \tilde{w}_2 \tilde{w}_3 \\ \alpha_3 &= \mu \alpha Y_{ss}^2 X_{3ss}^{-\alpha-1} - \mu \rho \alpha Y_{ss}^3 X_{3ss}^{-\alpha-1} + \alpha \rho \tilde{w}_1 X_{1ss} Y_{ss}^2 X_{3ss}^{-\alpha-1} + \tilde{w}_1 \tilde{w}_2 \tilde{w}_3. \end{aligned} \quad (6.15)$$

Since the sign matrix of J is the same as a model previously described in section 4.2 then α_1, α_2 and α_3 must be strictly positive to guarantee stability. This can also be seen by inspection since the only negative term entering is for α_3 . Rewriting α_3

$$\alpha_3 = \mu \alpha Y_{ss}^2 X_{3ss}^{-\alpha-1} (1 - \rho Y_{ss}) + \alpha \rho \tilde{w}_1 X_{1ss} Y_{ss}^2 X_{3ss}^{-\alpha-1} + \tilde{w}_1 \tilde{w}_2 \tilde{w}_3. \quad (6.16)$$

Since $0 \leq Y_{ss} < 1$ and $0 \leq \rho \leq 1$ then $1 - \rho Y_{ss} \geq 0$. This means $\alpha_3 > 0$. Therefore the fixed point is asymptotically stable if $\alpha_1 \alpha_2 - \alpha_3 > 0$ and unstable if $\alpha_1 \alpha_2 - \alpha_3 < 0$ by theorem 3.5.

$$\begin{aligned} \alpha_1 \alpha_2 - \alpha_3 &= \frac{\alpha \rho X_{1ss} Y_{ss}^2}{X_{3ss}^{\alpha+1}} (\tilde{w}_2 + \tilde{w}_3) + \tilde{w}_1 \tilde{w}_3^2 + \tilde{w}_2 \tilde{w}_3^2 + 2 \tilde{w}_1 \tilde{w}_2 \tilde{w}_3 \\ &\quad + \tilde{w}_2^2 \tilde{w}_3 + \tilde{w}_1 \tilde{w}_2^2 + \tilde{w}_1^2 \tilde{w}_2 + \tilde{w}_1^2 \tilde{w}_3 + \frac{\alpha \mu Y_{ss}^2}{X_{3ss}^{\alpha+1}} (-1 + \rho Y_{ss}). \end{aligned} \quad (6.17)$$

The last term is negative since $\rho Y_{ss} < 1$ and it is the only negative term. We now focus on this term and denote it by H

$$H \equiv \frac{\alpha \mu Y_{ss}^2}{X_{3ss}^{\alpha+1}} (-1 + \rho Y_{ss}). \quad (6.18)$$

Now it is time to use the condition given by the steady state 6.12 thus replacing X_{3ss} by an expression in Y_{ss} leading to

$$\begin{aligned} H &= \frac{\alpha \mu Y_{ss}^2}{\left(\frac{1}{\tilde{w}_1 \tilde{w}_2 \tilde{w}_3} (1 - \rho Y_{ss}) (1 - \mu Y_{ss}) \right)^{\alpha+1}} (-1 + \rho Y_{ss}) \Leftrightarrow \\ H &= - \frac{(\tilde{w}_1 \tilde{w}_2 \tilde{w}_3)^{\alpha+1} \alpha \mu Y_{ss}^2}{(1 - \rho Y_{ss})^\alpha (1 - \mu Y_{ss})^{\alpha+1}}. \end{aligned} \quad (6.19)$$

The question is how small H can get? We have that μ and ρ can vary in $[0,1]$. But since $Y_{ss} \in [0,1[$ it can be seen directly from 6.19 that $\mu = \rho = 1$ makes the denominator closest to zero in terms of μ and ρ and at the same time maximizing the numerator in terms of μ and ρ . Thus the 'worst case scenario' is when μ and ρ equals one. This scenario will therefore be considered in section 6.2.

$$H = - \frac{(\tilde{w}_1 \tilde{w}_2 \tilde{w}_3)^{\alpha+1} \alpha \mu Y_{ss}^2}{(1 - \rho Y_{ss})^\alpha (1 - \mu Y_{ss})^{\alpha+1}} \geq - \frac{(\tilde{w}_1 \tilde{w}_2 \tilde{w}_3)^{\alpha+1} \alpha Y_{ss}^2}{(1 - Y_{ss})^{2\alpha+1}}. \quad (6.20)$$

Note that if the negative feedback on CRH from cortisol is disregarded this corresponds to $\mu = 0$. But then $H = 0$ so the stability analysis simplifies since $\alpha_1\alpha_2 - \alpha_3$ is always positive then. This means the fixed point is stable for all non negative values of α .

6.2 The system with $\mu = 1, \rho = 1$

As mentioned in the previous section the fixed point is most likely to be unstable for $\mu = \rho = 1$. Therefore we will in this section investigate this scenario. We investigate if realistic values of α cause an unstable fixed point i.e. $\alpha_1\alpha_2 - \alpha_3 > 0$.

Inserting $\mu = \rho = 1$ in equation 6.17

$$\begin{aligned} \alpha_1\alpha_2 - \alpha_3 = & \frac{\alpha X_{1ss} Y_{ss}^2}{X_{3ss}^{\alpha+1}} (\tilde{w}_2 + \tilde{w}_3) + \tilde{w}_1 \tilde{w}_3^2 + \tilde{w}_2 \tilde{w}_3^2 + 2\tilde{w}_1 \tilde{w}_2 \tilde{w}_3 \\ & + \tilde{w}_2^2 \tilde{w}_3 + \tilde{w}_1 \tilde{w}_2^2 + \tilde{w}_1^2 \tilde{w}_2 + \tilde{w}_1^2 \tilde{w}_3 + \frac{\alpha Y_{ss}^2}{X_{3ss}^{\alpha+1}} (-1 + Y_{ss}). \end{aligned} \quad (6.21)$$

Since the first term on the right side is non negative ¹

$$\begin{aligned} \alpha_1\alpha_2 - \alpha_3 \geq & \tilde{w}_1 \tilde{w}_3^2 + \tilde{w}_2 \tilde{w}_3^2 + 2\tilde{w}_1 \tilde{w}_2 \tilde{w}_3 \\ & + \tilde{w}_2^2 \tilde{w}_3 + \tilde{w}_1 \tilde{w}_2^2 + \tilde{w}_1^2 \tilde{w}_2 + \tilde{w}_1^2 \tilde{w}_3 + \frac{\alpha Y_{ss}^2}{X_{3ss}^{\alpha+1}} (-1 + Y_{ss}). \end{aligned} \quad (6.23)$$

Introduce the variable Z ,

$$Z \equiv \frac{1}{1 + X_3^\alpha} \Leftrightarrow X_3 = \left(\frac{1 - Z}{Z} \right)^{1/\alpha}. \quad (6.24)$$

Since $X_3 \in [0, \infty)$ then $Z \in (0, 1]$. Since $Y = X_3^\alpha / (1 + X_3^\alpha)$ then $Z = 1 - Y$. Inserting for Z in terms of Y_{ss} and X_{3ss} in equation 6.23.

$$\begin{aligned} \alpha_1\alpha_2 - \alpha_3 \geq & \tilde{w}_3^2 \tilde{w}_2 + \tilde{w}_3^2 \tilde{w}_1 + 2 \tilde{w}_3 \tilde{w}_2 \tilde{w}_1 + \tilde{w}_3 \tilde{w}_2^2 + \tilde{w}_2^2 \tilde{w}_1 + \tilde{w}_3 \tilde{w}_1^2 \\ & + \tilde{w}_2 \tilde{w}_1^2 - \alpha X_{3ss}^{2+1/\alpha} (1 - Y_{ss})^{1-1/\alpha}. \end{aligned} \quad (6.25)$$

Consider again the steady state condition array 6.12 with $\mu = \rho = 1$.

¹ It is sufficient for our argument to throw away the first term in inequality 6.21. However note that if the first and last term is combined we get $\frac{\alpha Y_{ss}^2}{X_{3ss}^{\alpha+1}} (X_{1ss}(\tilde{w}_2 + \tilde{w}_3) - 1 + Y_{ss})$. If the expression in the brackets is non negative then the fixed point is stable. Using $X_{1ss} = 1/\tilde{w}_1(1 - Y_{ss})$ the fixed point is stable if

$$\frac{\tilde{w}_2 + \tilde{w}_3}{\tilde{w}_1} (1 - Y_{ss}) - 1 + Y_{ss} \geq 0.$$

Since $1 - Y > 0$ then if

$$\tilde{w}_2 + \tilde{w}_3 \geq \tilde{w}_1, \quad (6.22)$$

the fixed point is stable for all non negative values of α .

$$\begin{aligned}
X_{1ss} &= \frac{1}{\tilde{w}_1} (1 - Y_{ss}) \\
X_{2ss} &= \frac{1}{\tilde{w}_2} (1 - Y_{ss}) X_1 = \frac{1}{\tilde{w}_1 \tilde{w}_2} (1 - Y_{ss})^2 \\
X_{3ss} &= \frac{1}{\tilde{w}_3} X_2 = \frac{1}{\tilde{w}_1 \tilde{w}_2 \tilde{w}_3} (1 - Y_{ss})^2.
\end{aligned} \tag{6.26}$$

The parameter γ is defined

$$\gamma \equiv \frac{1}{\tilde{w}_1 \tilde{w}_2 \tilde{w}_3}. \tag{6.27}$$

Now the steady state condition will be used. Expressing the last equation in array 6.26 in terms of Z using equation 6.24 we have

$$\left(\frac{1 - Z_{ss}}{Z_{ss}} \right)^{1/\alpha} = \gamma Z_{ss}^2. \tag{6.28}$$

This is equivalent to

$$\frac{1 - Z_{ss}}{\gamma} = (1 - Z_{ss})^{1-1/\alpha} Z_{ss}^{2+1/\alpha}. \tag{6.29}$$

Inserting equation 6.29 in equation 6.25

$$\begin{aligned}
\alpha_1 \alpha_2 - \alpha_3 &\geq \tilde{w}_3^2 \tilde{w}_2 + \tilde{w}_3^2 \tilde{w}_1 + 2 \tilde{w}_3 \tilde{w}_2 \tilde{w}_1 + \tilde{w}_3 \tilde{w}_2^2 + \tilde{w}_2^2 \tilde{w}_1 + \tilde{w}_3 \tilde{w}_1^2 \\
&\quad + \tilde{w}_2 \tilde{w}_1^2 - \alpha \frac{1 - Z_{ss}}{\gamma}.
\end{aligned} \tag{6.30}$$

Since $0 < Z \leq 1 \Leftrightarrow -1 < -1 + Z \leq 0$ we have $-(1 - Z_{ss}) = -1 + Z_{ss} > -1$ thus we can write

$$\begin{aligned}
\alpha_1 \alpha_2 - \alpha_3 &> \tilde{w}_3^2 \tilde{w}_2 + \tilde{w}_3^2 \tilde{w}_1 + 2 \tilde{w}_3 \tilde{w}_2 \tilde{w}_1 + \tilde{w}_3 \tilde{w}_2^2 + \tilde{w}_2^2 \tilde{w}_1 + \tilde{w}_3 \tilde{w}_1^2 \\
&\quad + \tilde{w}_2 \tilde{w}_1^2 - \alpha \frac{1}{\gamma}.
\end{aligned} \tag{6.31}$$

Using the definition of γ from equation 6.27 this is equivalent to

$$\begin{aligned}
\alpha_1 \alpha_2 - \alpha_3 &> \tilde{w}_3^2 \tilde{w}_2 + \tilde{w}_3^2 \tilde{w}_1 + 2 \tilde{w}_3 \tilde{w}_2 \tilde{w}_1 + \tilde{w}_3 \tilde{w}_2^2 + \tilde{w}_2^2 \tilde{w}_1 + \tilde{w}_3 \tilde{w}_1^2 \\
&\quad + \tilde{w}_2 \tilde{w}_1^2 - \tilde{w}_1 \tilde{w}_2 \tilde{w}_3 \alpha.
\end{aligned} \tag{6.32}$$

The right hand side is symmetric in \tilde{w}_1, \tilde{w}_2 and \tilde{w}_3 . We want to find out if there are some α for which there are only stable solutions meaning the right hand side is positive. Due to symmetry of the right side of equation 6.32 we can assume $\tilde{w}_1 \geq \tilde{w}_2 \geq \tilde{w}_3$. Then δ_1 and δ_2 are defined through the equations

$$\tilde{w}_1 = \delta_1 \tilde{w}_3 \tag{6.33}$$

$$\tilde{w}_2 = \delta_2 \tilde{w}_3, \tag{6.34}$$

where $\delta_1 \geq \delta_2 \geq 1$. Inserting in equation 6.32 and a few rearrangements give

$$\alpha_1 \alpha_2 - \alpha_3 > \tilde{w}_3^3 (\delta_2 + \delta_1 + \delta_2^2 + \delta_1^2 + \delta_2 \delta_1 (\delta_1 + \delta_2 - (\alpha - 2))) . \quad (6.35)$$

Thus we define

$$F(\delta_1, \delta_2) \equiv \delta_2 + \delta_1 + \delta_2^2 + \delta_1^2 + \delta_2 \delta_1 (\delta_1 + \delta_2 - (\alpha - 2)) . \quad (6.36)$$

For what values of α is $F > 0$? Obviously if $\alpha \leq 2$ F is always positive since it is then a sum of positive and non negative terms. For large δ_1 or δ_2 it is true that $\delta_1 + \delta_2 - (\alpha - 2) > 0$. Thus we restrict our attention to $(\delta_1, \delta_2) \in [1, \alpha - 2] \times [1, \alpha - 2]$. A minimum exists by the extreme value theorem [17] and should be found at a critical point or boundary point. First we calculate the value at the boundary point (1, 1)

$$F(1, 1) = 8 - \alpha < 0 \text{ if and only if } \alpha > 8 . \quad (6.37)$$

So we know that for values of α larger than 8, the system may be unstable. But what about values between 2 and 8? Calculating F at one boundary line

$$F(\delta_1, 1) = 2\delta_1^2 + (4 - \alpha)\delta_1 + 2 . \quad (6.38)$$

This gives a second order polynomial in δ_1 . Calculating the discriminant

$$d = (4 - \alpha)^2 - 4 \cdot 2 \cdot 2 = \alpha(\alpha - 8) , \quad (6.39)$$

so for $\alpha \in (0, 8)$, $d < 0$ meaning $F(\delta_1, 1) > 0$. Since F is symmetric in δ_1 and δ_2 the same holds on the boundary line $F(1, \delta_2)$. On the two remaining boundary lines F is always positive.

The critical points are found

$$\frac{\partial F}{\partial \delta_1} = 1 + 2\delta_1 + 2\delta_1\delta_2 + \delta_2^2 - (\alpha - 2)\delta_2 = 0 \quad (6.40)$$

$$\frac{\partial F}{\partial \delta_2} = 1 + 2\delta_2 + 2\delta_1\delta_2 + \delta_1^2 - (\alpha - 2)\delta_1 = 0 . \quad (6.41)$$

Multiplying equation 6.40 by δ_1 and multiplying equation 6.41 by δ_2 and subtracting

$$\delta_1 - \delta_2 + 2(\delta_1^2 - \delta_2^2) + \delta_1\delta_2(\delta_1 - \delta_2) = 0 . \quad (6.42)$$

If $\delta_1 > \delta_2$ equation 6.42 is obviously never satisfied. If $\delta_1 = \delta_2$ then equation 6.42 always holds. This is now used in equation 6.40

$$\frac{\partial F}{\partial \delta_1} = 3\delta_1^2 - (\alpha - 4)\delta_1 + 1 = 0 . \quad (6.43)$$

Calculating the discriminant

$$d_2 = (\alpha - 4)^2 - 4 \cdot 3 = \alpha^2 - 8\alpha + 4 . \quad (6.44)$$

This gives a new second order polynomial with α as variable with solutions trivially found as

$$\alpha = 4 - 2\sqrt{3} \text{ or } \alpha = 4 + 2\sqrt{3} . \quad (6.45)$$

$4 - 2\sqrt{3} < 2$ then the first solution is not interesting since we already found the system to be stable for values of $\alpha \leq 2$. $8 > 4 + 2\sqrt{3} > 7$. Thus $\alpha_{min} = 4 + 2\sqrt{3}$ in order to have a critical point (we have not argued that the critical point necessarily is where F obtains its minimum value). Using integer values for α we have now shown for $\alpha < 8$ F is positive. If we should consider all positive, real values for α , we would still require $\alpha > 7$ in order to have a chance that F could be negative. This means that for $\alpha \in \{1, \dots, 7\}$ the unique fixed point of array 6.10 is stable. This means that the system has only stable solutions of the linearized system close to the unique steady state solution.

Therefore we can conclude that the system 5.33 has exactly one fixed point and it is stable for $\mu, \rho \in [0, 1], \alpha \in [1, 7]$. For larger values of α the fixed point could be stable as well as unstable².

Summary of chapter 6

The results of this chapter can be summarized as

- The system without hippocampus is scaled. The scaled system have six parameters which is three less than the original system.
- If there is no feedback from cortisol of the production of CRH($\mu=0$) the unique fixed point will be locally stable for all values of α .
- The fixed point is most likely to be locally unstable if $\mu = \rho = 1$. In this 'worst case scenario' we have showed that the unique fixed point is guaranteed to be locally stable for $\alpha \in \{1, \dots, 7\}$. For values of $\alpha > 7$ the unique fixed point can be stable as well as unstable.

² A more general proof of this result can be seen in [28]

7 Stability of a fixed point for a system with positive feedback from cortisol on CRH

Including hippocampal mechanisms in the differential equation governing CRH may lead to positive feedback from cortisol on CRH at a fixed point. In this section we will analyze the stability of a fixed point if the cortisol exerts a positive feedback on CRH. In case of multiple feedbacks from cortisol on CRH this means that at the steady state point the positive feedback dominates the negative feedback. Recall that a positive feedback from cortisol to CRH means $\partial f_1/\partial x_3 > 0$ and a negative feedback means $\partial f_1/\partial x_3 < 0$. Thus a dominating positive feedback at a fixed point means that $\partial f_1/\partial x_3 > 0$. The Jacobian at the fixed point is on the form

$$J = \begin{pmatrix} -a_{11} & 0 & a_{13} \\ a_{21} & -a_{22} & -a_{23} \\ 0 & a_{32} & -a_{33} \end{pmatrix}. \quad (7.1)$$

Here all a_{ij} 's are positive and the positive feedback from cortisol to CRH means that $a_{13} > 0$. Forming the characteristic polynomial we have

$$P(\lambda) = \lambda^3 + \alpha_1\lambda^2 + \alpha_2\lambda + \alpha_3. \quad (7.2)$$

The coefficients equal

$$\alpha_1 = a_{11} + a_{22} + a_{33} \quad (7.3)$$

$$\alpha_2 = a_{11}a_{22} + a_{11}a_{33} + a_{22}a_{33} + a_{32}a_{23} \quad (7.4)$$

$$\alpha_3 = a_{11}a_{22}a_{33} + a_{11}a_{23}a_{32} - a_{13}a_{21}a_{32}. \quad (7.5)$$

We see that $\alpha_1 > 0, \alpha_2 > 0$ but we do not know in general if α_3 is positive or negative. In order to use theorem 3.5 we need to calculate the sign of $\alpha_1\alpha_2 - \alpha_3$ as well.

$$\alpha_1\alpha_2 - \alpha_3 = (a_{22} + a_{33})\alpha_2 + a_{11}^2(a_{22} + a_{33}) + a_{13}a_{21}a_{32}. \quad (7.6)$$

Therefore $\alpha_1\alpha_2 - \alpha_3 > 0$. Thus for all the systems on the form 7.1 the stability can be determined solely by looking at the sign of α_3 . Instability is thus guaranteed for $\alpha_3 < 0$ and stability is guaranteed for $\alpha_3 > 0$. If $\alpha_3 < 0$ then $P(0) < 0$ and since the leading coefficient of $P(\lambda)$ is positive, then $P(\lambda)$ is positive for sufficiently large λ , say for $\lambda \geq M$. Now $P(\lambda)$ is continuous and $P(0) < 0$ and $P(M) > 0$ so by the intermediate value theorem [17] there exists $\lambda' \in]0, M[$ such that $P(\lambda') = 0$. This means that in the case of instability $P(\lambda)$ has a positive, real root. What about the other roots? Could it be that the system also has complex roots with non zero imaginary part and positive real part such that oscillations are present of solutions close to the fixed point? The

answer is no which we will now show. The situation is $\alpha_1 > 0, \alpha_2 > 0$ and $\alpha_3 < 0$ and there exists a positive real root, λ_1 of $P(\lambda)$. Factorizing P we get

$$\begin{aligned} P(\lambda) &= (\lambda - \lambda_1)(\lambda - \lambda_2)(\lambda - \lambda_3) \Leftrightarrow \\ P(\lambda) &= \lambda^3 - (\lambda_1 + \lambda_2 + \lambda_3)\lambda^2 + (\lambda_1\lambda_2 + \lambda_1\lambda_3 + \lambda_2\lambda_3)\lambda - \lambda_1\lambda_2\lambda_3. \end{aligned} \quad (7.7)$$

What can be said about λ_2 and λ_3 ? Expanding $P(\lambda)$ and comparing to equation 7.2 we see that

$$-(\lambda_1 + \lambda_2 + \lambda_3) = \alpha_1 \Leftrightarrow \lambda_2 + \lambda_3 = -\alpha_1 - \lambda_1 < 0. \quad (7.8)$$

Considering the case λ_2 complex with non zero imaginary part then also the complex conjugate is root. Since λ_1 is real then λ_3 must be the complex conjugate of λ_2 . Then $\lambda_2 + \lambda_3 = 2 \operatorname{Re}(\lambda_2) = 2 \operatorname{Re}(\lambda_3)$. By inequality 7.8 then if complex eigenvalues exist with non zero imaginary part then the real part must be negative. If λ_2 and λ_3 are real then at least one of them is negative by inequality 7.8.

Summary of a positive feedback from cortisol on CRH at the fixed point.

- If $\alpha_3 > 0$ then the fixed point is stable.
- If $\alpha_3 < 0$ then at least 1 eigenvalues of the Jacobian at the steady state is real and positive. If complex roots with non zero imaginary parts exists then they have negative real part.
- No Hopf bifurcation occurs for α_3 going from negative to positive values.

Note that the case with no feedback from cortisol on CRH corresponds to $a_{13} = 0$. This will always give a stable system since then $\alpha_1 > 0, \alpha_3 > 0, \alpha_1\alpha_2 - \alpha_3 > 0$.

8 A model including the mechanisms from hippocampus

Now we have shown a range of models that do not account for the dynamics of the HPA axis.

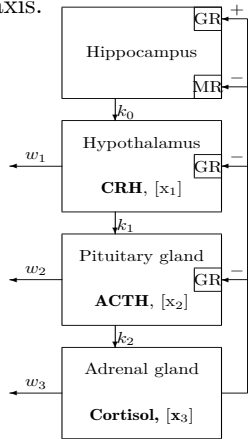


Figure 8.1: Compartment diagram with hippocampus included

It is therefore time to include the mechanisms of hippocampus. Here cortisol binding to GR in hippocampus cause a positive stimulation on the production of CRH in hypothalamus while cortisol binding to MR in hippocampus cause a inhibition of the production of CRH in hypothalamus[2]. Still the direct negative feedback from cortisol on CRH in hypothalamus is also present. The model is shown in figure 8.1. Since there is no known hormone in hippocampus we will not include an extra variable. We keep modeling the feedback as a factor influencing the positive input on the compartment where the feedback occurs. This means that all the three feedbacks modeled at CRH from cortisol should be introduced as a factor acting on k_0 . This means that we get $k_0 F(x_3)$, where $F(x_3)$ is a function taking care of the three feedbacks. We add the three feedbacks similar to the approach of e.g. Conrad et al.[6]. We choose $F(x_3)$ as

$$F(x_3) = 1 - \mu \frac{x_3^\alpha}{x_3^\alpha + c_1^\alpha} + \phi \frac{x_3^\beta}{x_3^\beta + c_2^\beta} - \psi \frac{x_3^\gamma}{x_3^\gamma + c_3^\gamma} \quad (8.1)$$

Here the negative feedback acting directly on hypothalamus through GR is still on the form $-\mu \frac{x_3^\alpha}{x_3^\alpha + c_1^\alpha}$, where $\mu \in [0; 1]$. $-\mu$ is the limit corresponding to the largest negative feedback. c_1^α is the affinity for cortisol and GR in hypothalamus, and α is an integer. Similar interpretations apply for the two other feedbacks. $\phi \frac{x_3^\beta}{x_3^\beta + c_2^\beta}$ is the positive feedback acting through hippocampal GR. $-\psi \frac{x_3^\gamma}{x_3^\gamma + c_3^\gamma}$ is the negative feedback acting through hippocampal MR. All parameters entering F are positive but will later be specified such that $F \geq 0$. Note that $\phi = \psi = 0$ corresponds to the model without hippocampal mechanisms. Implementing $F(x_3)$ into the set of differential equations gives

$$\begin{aligned}
\frac{dx_1}{dt} &= k_0 \left(1 - \mu \frac{x_3^\alpha}{x_3^\alpha + c_1^\alpha} + \phi \frac{x_3^\beta}{x_3^\beta + c_2^\beta} - \psi \frac{x_3^\gamma}{x_3^\gamma + c_3^\gamma} \right) - w_1 x_1 \\
\frac{dx_2}{dt} &= k_1 \left(1 - \rho \frac{x_3^\delta}{x_3^\delta + c_4^\delta} \right) x_1 - w_2 x_2 \\
\frac{dx_3}{dt} &= k_2 x_2 - w_3 x_3.
\end{aligned} \tag{8.2}$$

From section 5.2 it is clear that α , β , γ , δ , c_1 , c_2 and c_3 are determined from the chemical stoichiometric equations and the fractions μ , ϕ , ψ and ρ depend on the size of the receptors as well.

When we define the function in this way we satisfy the demand that the process is irreversible. Furthermore the overall response to the feedback mechanisms now depend on the chemical stoichiometric equations and on the size of the receptors, which sounds reasonable. But we accept that a function that satisfy the demand of being irreversible can be constructed differently seen from a mathematical point of view.

For example one could introduce an unknown substance concentration x_0 in hippocampus. Modeling the system in analogy with the previous model one would get

$$\begin{aligned}
\frac{dx_0}{dt} &= k_{00} \left(1 + \phi \frac{x_3^\beta}{x_3^\beta + c_2^\beta} - \psi \frac{x_3^\gamma}{x_3^\gamma + c_3^\gamma} \right) - w_0 x_0 \\
\frac{dx_1}{dt} &= k_0 \left(1 - \mu \frac{x_3^\alpha}{x_3^\alpha + c_1^\alpha} \right) x_0 - w_1 x_1 \\
\frac{dx_2}{dt} &= k_1 \left(1 - \rho \frac{x_3^\delta}{x_3^\delta + c_4^\delta} \right) x_1 - w_2 x_2 \\
\frac{dx_3}{dt} &= k_2 x_2 - w_3 x_3.
\end{aligned} \tag{8.3}$$

Assuming a quasi steady state in x_0 one would get

$$\begin{aligned}
\frac{dx_1}{dt} &= \frac{k_{00} k_0}{w_0} \left(1 - \mu \frac{x_3^\alpha}{x_3^\alpha + c_1^\alpha} \right) \left(1 + \phi \frac{x_3^\beta}{x_3^\beta + c_2^\beta} - \psi \frac{x_3^\gamma}{x_3^\gamma + c_3^\gamma} \right) - w_1 x_1 \\
\frac{dx_2}{dt} &= k_1 \left(1 - \rho \frac{x_3^\delta}{x_3^\delta + c_4^\delta} \right) x_1 - w_2 x_2 \\
\frac{dx_3}{dt} &= k_2 x_2 - w_3 x_3.
\end{aligned} \tag{8.4}$$

Neglecting higher order terms of the Hill functions the system in array 8.4 corresponds to the system in array 8.2. This means that for small values of cortisol these are approximately identical. For simplicity we will model the mechanisms from hippocampus as in array 8.2.

8.1 Simplifications using physiological reasoning

The number of independent parameters for the equations in array 8.2 will now be reduced using physiological reasoning. First we assume that the chemical stoichiometric equations are the same for the identical GR in hippocampus, hypothalamus and in the adrenal gland. This assumption gives in accordance with equation 5.12 that, $c_1 = c_2 = c_4$ and $\alpha = \beta = \delta$. We define $c \equiv c_1$. Furthermore it has been suggested that cortisol have ten times higher affinity for MR than for GR throughout the entire HPA-axis[29], meaning that $c^\alpha = 10c_3^\beta$. This is found in rats so we will allow this number to vary thus keeping c_3 as a parameter for now. The model including hippocampal mechanisms can be written

$$\begin{aligned}\frac{dx_1}{dt} &= k_0 \left(1 - \mu \frac{x_3^\alpha}{x_3^\alpha + c^\alpha} + \phi \frac{x_3^\alpha}{x_3^\alpha + c^\alpha} - \psi \frac{x_3^\gamma}{x_3^\gamma + c_3^\gamma} \right) - w_1 x_1 \\ \frac{dx_2}{dt} &= k_1 \left(1 - \rho \frac{x_3^\alpha}{x_3^\alpha + c^\alpha} \right) x_1 - w_2 x_2 \\ \frac{dx_3}{dt} &= k_2 x_2 - w_3 x_3.\end{aligned}\tag{8.5}$$

Now we have not been very specific about all the domains for the parameters. If we let $\mu \in [0; 1]$, we see that for $\phi = \psi = 0$ the model is the one already investigated in detail in the previous sections and the hippocampus model is then indeed a generalization of the previous considered model. However we must be careful that $1 - \mu \frac{x_3^\alpha}{x_3^\alpha + c^\alpha} + \phi \frac{x_3^\alpha}{x_3^\alpha + c^\alpha} - \psi \frac{x_3^\gamma}{x_3^\gamma + c_3^\gamma} \geq 0$ in order to make sure that an initial condition with positive concentrations cannot result in solutions with negative concentrations. A way to make sure this is the case could be to make sure that the negative feedbacks does not add up to more than 1. This could be done by having $\mu \in [0; 1]$ and $\psi \in [0; 1 - \mu]$. Now we have a model where we require $k_0, k_1, k_2, w_1, w_2, w_3, c, c_3$ positive, ϕ non negative and α and δ are integers. Mathematically the positive feedback in hippocampus and the negative feedback in hypothalamus can be combined since the two expressions have the same functional form but with different coefficient. Defining ξ as $\xi \equiv \phi - \mu$. Since $\mu \in [0; 1]$ and $\phi \geq 0$ then $\xi \geq -1$. The set of equations can then be written are

$$\begin{aligned}\frac{dx_1}{dt} &= k_0 \left(1 + \xi \frac{x_3^\alpha}{x_3^\alpha + c^\alpha} - \psi \frac{x_3^\gamma}{x_3^\gamma + c_3^\gamma} \right) - w_1 x_1 \\ \frac{dx_2}{dt} &= k_1 \left(1 - \rho \frac{x_3^\alpha}{x_3^\alpha + c^\alpha} \right) x_1 - w_2 x_2 \\ \frac{dx_3}{dt} &= k_2 x_2 - w_3 x_3.\end{aligned}\tag{8.6}$$

8.2 Scaling of the differential equations

We use the same scaling as in section 6.1. Defining $\tilde{c}_3 \equiv c_3/d_3$ the equations in array 8.6 becomes

$$\begin{aligned}\frac{dX_1}{d\theta} &= \left(1 + \xi \frac{X_3^\alpha}{1 + X_3^\alpha} - \psi \frac{X_3^\gamma}{\tilde{c}_3^\gamma + X_3^\gamma}\right) - \tilde{w}_1 X_1 \\ \frac{dX_2}{d\theta} &= \left(1 - \rho \frac{X_3^\alpha}{1 + X_3^\alpha}\right) X_1 - \tilde{w}_2 X_2 \\ \frac{dX_3}{d\theta} &= X_2 - \tilde{w}_3 X_3.\end{aligned}\tag{8.7}$$

Thus the dynamics of the autonomous system is governed by nine parameters. The cost of including hippocampal feedbacks is three extra parameters.

8.3 Existence and uniqueness of solutions, non negative concentrations, confining set and existence of fixed points

A lot of the same reasoning applies for the system with as well as without hippocampal mechanisms. The system of coupled differential equations 8.7 obeys the criteria posed for existence and uniqueness of solutions (theorem 3.1) for non negative variables.

In order to make sure negative concentrations can not occur for non negative initial conditions we require that $1 + \xi - \psi \geq 0$. This is fulfilled for the previous stated restrictions on ξ and ψ that for $\xi \in [-1; 0]$ then $\psi \in [0; 1 + \xi]$ and for $\xi > 0$ then $\psi \in [0; 1]$. Then all derivatives have only non negative terms when the respective concentration equal zero. Thereby non negative initial conditions cannot lead to solutions with negative concentrations.

Even though there is now a positive feedback on CRH this is still included through a saturation mechanism. This means we can still find an upper bound for x_1 where $dx_1/dt \geq 0$. If we have a trapping region for x_1 we also have one for x_2 and x_3 as in the case without hippocampus. We look at two cases $\xi \in [-1; 0]$ and $\xi > 0$ to determine a trapping region.

- $\xi \in [-1; 0]$.

$$\xi \in [-1; 0] \Rightarrow \left(1 + \xi \frac{X_3^\alpha}{1 + X_3^\alpha} - \psi \frac{X_3^\gamma}{\tilde{c}_3^\gamma + X_3^\gamma}\right) \leq 1. \text{ For } X_1 \geq 1/\tilde{w}_1 \text{ then } dX_1/dt \leq 0.$$

Having $X_2 \geq 1/\tilde{w}_1 \tilde{w}_2$ and $X_1 \in [0; 1/\tilde{w}_1]$ means $dX_2/dt \leq 0$. For $X_3 \geq 1/\tilde{w}_1 \tilde{w}_2 \tilde{w}_3$ and $X_2 \in [0; 1/\tilde{w}_1 \tilde{w}_2]$ and $X_1 \in [0; 1/\tilde{w}_1]$ then $dX_3/dt \leq 0$. Initial conditions with values in $(X_1, X_2, X_3) \in [0; 1/\tilde{w}_1] \times [0; 1/\tilde{w}_1 \tilde{w}_2] \times [0; 1/\tilde{w}_1 \tilde{w}_2 \tilde{w}_3]$ will lead to solutions staying in this set for all future time.

- $\xi > 0$.

$$\xi > 0 \Rightarrow \left(1 + \xi \frac{X_3^\alpha}{1 + X_3^\alpha} - \psi \frac{X_3^\gamma}{\tilde{c}_3^\gamma + X_3^\gamma}\right) \leq 1 + \xi \text{ Then for } X_1 \geq (1 + \xi)/\tilde{w}_1 \text{ then } dX_1/dt \leq 0. \text{ Using similar reasoning as for } \xi \in [0; 1] \text{ we get the trapping region } (X_1, X_2, X_3) \in [0; (1 + \xi)/\tilde{w}_1] \times [0; (1 + \xi)/\tilde{w}_1 \tilde{w}_2] \times [0; (1 + \xi)/\tilde{w}_1 \tilde{w}_2 \tilde{w}_3].$$

Existence of fixed points

Setting all the left hand sides of the equations 8.7 equal to zero give the following criteria for a fixed point

$$X_{3ss} = \frac{1}{\tilde{w}_1 \tilde{w}_2 \tilde{w}_3} \left(1 + \xi \frac{X_{3ss}^\alpha}{1 + X_{3ss}^\alpha} - \psi \frac{X_{3ss}^\gamma}{\tilde{c}_3^\gamma + X_{3ss}^\gamma}\right) \left(1 - \rho \frac{X_{3ss}^\alpha}{1 + X_{3ss}^\alpha}\right). \tag{8.8}$$

We form the functions

$$L(X_3) = X_3 \quad (8.9)$$

and

$$R(X_3) = \frac{1}{\tilde{w}_1 \tilde{w}_2 \tilde{w}_3} \left(1 + \xi \frac{X_3^\alpha}{1 + X_3^\alpha} - \psi \frac{X_3^\gamma}{\tilde{c}_3^\gamma + X_3^\gamma} \right) \left(1 - \rho \frac{X_3^\alpha}{1 + X_3^\alpha} \right). \quad (8.10)$$

If a value of X_3 obeys $L(X_3) = R(X_3)$ then this value of X_3 is a fixed point value and denoted X_{3ss} . $R(X_3)$ is non negative and equals $1/\tilde{w}_1 \tilde{w}_2 \tilde{w}_3$ for $X_3 = 0$. Since each of the terms of $R(X_3)$ are bounded then the right hand side is bounded. $L(X_3)$ is obviously zero for $X_3 = 0$ and has no bound for increasing X_3 . By the intermediate value theorem [17] there now exists at least one X_3' such that the $L(X_3') = R(X_3')$. This means there exists at least one steady state solution of the system of equations 8.7.

Number of fixed points

How can we know how many steady state solutions there are? One way is for a given set of parameters to plot $L(X_3)$ and $R(X_3)$ for X_3 in its trapping region. The number of intersections of the two graphs corresponds to the number of fixed points. For some realizations of this approach it seems that $L(X_3)$ grows faster than $R(X_3)$. This means we can form a criteria for the existence of a unique fixed point. If $L(X_3)$ always has a larger slope than $R(X_3)$ then for values of X_3 larger than a steady state value, then $L(X_3)$ will always be greater than $R(X_3)$ which means there can only be one steady state value. Thus $dR(X_3)/dX_3 < 1$ for X_3 in its confining region is a sufficient criteria for a unique existence of a fixed point.

$$\begin{aligned} \frac{dR}{dX_3} = & \frac{1}{\tilde{w}_1 \tilde{w}_2 \tilde{w}_3} \left(\left(\xi \alpha \frac{X_3^{\alpha-1}}{(1 + X_3^\alpha)^2} - \psi \gamma \frac{c^\gamma X_3^{\gamma-1}}{(\tilde{c}_3^\gamma + X_3^\gamma)^2} \right) \left(1 - \rho \frac{X_3^\alpha}{1 + X_3^\alpha} \right) \right. \\ & \left. + \left(1 + \xi \frac{X_3^\alpha}{1 + X_3^\alpha} - \psi \frac{X_3^\gamma}{\tilde{c}_3^\gamma + X_3^\gamma} \right) \left(-\rho \alpha \frac{X_3^{\alpha-1}}{(1 + X_3^\alpha)^2} \right) \right) \end{aligned} \quad (8.11)$$

A rough estimate on 8.11 can give sufficient criteria for a unique steady state solution.

$$\frac{dR}{dX_3} \leq \frac{1}{\tilde{w}_1 \tilde{w}_2 \tilde{w}_3} \left(\xi \alpha \frac{X_3^{\alpha-1}}{(1 + X_3^\alpha)^2} - \psi \gamma \frac{c^\gamma X_3^{\gamma-1}}{(\tilde{c}_3^\gamma + X_3^\gamma)^2} \right) \left(1 - \rho \frac{X_3^\alpha}{1 + X_3^\alpha} \right) \quad (8.12)$$

If the expression in the first set of brackets are non positive then $dR/dX_3 \leq 0 < 1$. If the expression in the first set of brackets is positive (this require $\xi > 0$) then since $0 < 1 - \rho \frac{X_3^\alpha}{1 + X_3^\alpha} \leq 1$

$$\frac{dR}{dX_3} \leq \frac{1}{\tilde{w}_1 \tilde{w}_2 \tilde{w}_3} \left(\xi \alpha \frac{X_3^{\alpha-1}}{(1 + X_3^\alpha)^2} - \psi \gamma \frac{c^\gamma X_3^{\gamma-1}}{(\tilde{c}_3^\gamma + X_3^\gamma)^2} \right) \quad (8.13)$$

Considering the expression in the brackets (we already considered $X_3 = 0$ so now $X_3 > 0$) with $\xi > 0$

$$\xi \alpha \frac{X_3^{\alpha-1}}{(1 + X_3^\alpha)^2} - \psi \gamma \frac{c^\gamma X_3^{\gamma-1}}{(\tilde{c}_3^\gamma + X_3^\gamma)^2} \leq \xi \alpha \frac{X_3^{\alpha-1}}{(1 + X_3^\alpha)^2} < \xi \alpha \quad (8.14)$$

This leads to a bound for $\frac{dR}{dX_3}$ solely expressed by parameters for $\xi > 0$.

$$\frac{dR}{dX_3} < \frac{\xi\alpha}{\tilde{w}_1\tilde{w}_2\tilde{w}_3} \quad (8.15)$$

Therefore if

$$\frac{\xi\alpha}{\tilde{w}_1\tilde{w}_2\tilde{w}_3} \leq 1, \quad (8.16)$$

for $\xi > 0$ a unique fixed point is guaranteed. If $\xi \in [-1; 0]$ then by inequality 8.12 $\frac{dR}{dX_3} \leq 0$ so $\xi \leq 0$ guarantees a unique fixed point. This case is equivalent to the system without hippocampus since $R(X_3)$ is then a decreasing function and $L(X_3)$ is increasing. This means there can be no more than one fixed point.

8.4 Stability of fixed point(s)

To find the stability of a fixed point of the system of differential equations 8.7 we need the Jacobian evaluated at the fixed point. We define a_{13} as

$$a_{13} = \partial f_1 / \partial X_3 |_{ss} = \xi\alpha \frac{X_{3ss}^{\alpha-1}}{(1 + X_{3ss}^\alpha)^2} - \psi\gamma \frac{c_3^\gamma X_{3ss}^{\gamma-1}}{(c_3^\gamma + X_{3ss}^\gamma)^2} \quad (8.17)$$

We know from the previous analysis that the sign of a_{13} is crucial for the type of instability that may occur as well as whether we should look at the sign of α_3 or the sign of $\alpha_1\alpha_2 - \alpha_3$ to determine the stability. The Jacobian at steady state of the system 8.7 can be written (recall $Y = \frac{X_3^\alpha}{1+X_3^\alpha}$)

$$\mathbf{J} = \begin{pmatrix} -\tilde{w}_1 & 0 & a_{13} \\ 1 - \rho Y_{ss} & -\tilde{w}_2 & -\alpha\rho X_{1ss} X_{3ss}^{-\alpha-1} Y_{ss}^2 \\ 0 & 1 & -\tilde{w}_3 \end{pmatrix} \quad (8.18)$$

We form the characteristic polynomial as

$$P(\lambda) = \lambda^3 + \alpha_1\lambda^2 + \alpha_2\lambda + \alpha_3 \quad (8.19)$$

where

$$\begin{aligned} \alpha_1 &= \tilde{w}_1 + \tilde{w}_2 + \tilde{w}_3 \\ \alpha_2 &= \tilde{w}_1\tilde{w}_2 + \tilde{w}_1\tilde{w}_3 + \tilde{w}_2\tilde{w}_3 + \rho\alpha X_{1ss} X_{3ss}^{-\alpha-1} Y_{ss}^2 \\ \alpha_3 &= \tilde{w}_1\tilde{w}_2\tilde{w}_3 + \alpha\rho\tilde{w}_1 X_{1ss} X_{3ss}^{-\alpha-1} Y_{ss}^2 - a_{13}(1 - \rho Y_{ss}). \end{aligned} \quad (8.20)$$

Here $-a_{13}(1 - \rho Y_{ss})$ is the only term entering α_1 , α_2 and α_3 that may be negative. Leaning on the knowledge from the general case we split the analysis in the cases $a_{13} > 0$, $a_{13} < 0$ and $a_{13} = 0$.

- If $a_{13} > 0$.
 - If $\alpha_3 > 0$ then the fixed point is stable
 - If $\alpha_3 < 0$ then the fixed point is unstable and there exists a positive, real eigenvalue of the Jacobian at the fixed point. If the remaining two eigenvalues are complex with non zero imaginary part then their real part is negative.

- If $a_{13} < 0$.
 - If $\alpha_1\alpha_2 - \alpha_3 > 0$ then the system is stable.
 - If $\alpha_1\alpha_2 - \alpha_3 < 0$ then the system is unstable with a set of complex conjugate eigenvalues with positive real part and non vanishing imaginary part and the last eigenvalue is real and negative.

$$\begin{aligned} \alpha_1\alpha_2 - \alpha_3 = & (\tilde{w}_2 + \tilde{w}_3)(\tilde{w}_1\tilde{w}_2 + \tilde{w}_1\tilde{w}_3 + \tilde{w}_2\tilde{w}_3 \\ & + \rho\alpha X_{1ss}X_{3ss}^{-\alpha-1}Y_{ss}^2) + \tilde{w}_1^2(\tilde{w}_2 + \tilde{w}_3) \\ & + a_{13}\left(1 - \rho\frac{X_{3ss}^\alpha}{1 + X_{3ss}^\alpha}\right). \end{aligned} \quad (8.21)$$

Here the last term is the only negative term.

We can make a lower bound for $\alpha_1\alpha_2 - \alpha_3$. If this turns out to be positive then no Hopf bifurcation is possible. Since we are in the situation $a_{13} < 0$ we can make the following estimate

$$\begin{aligned} \alpha_1\alpha_2 - \alpha_3 \geq & (\tilde{w}_2 + \tilde{w}_3)(\tilde{w}_1\tilde{w}_2 + \tilde{w}_1\tilde{w}_3 + \tilde{w}_2\tilde{w}_3) \\ & + \tilde{w}_1^2(\tilde{w}_2 + \tilde{w}_3) + a_{13}. \end{aligned} \quad (8.22)$$

Considering a_{13} from equation 8.17 with the restriction $a_{13} < 0$ we can make an estimate dependent on the sign of ξ .

$$a_{13} \geq -\psi\gamma/c_3 \geq -\gamma/c_3 \quad \text{for } \xi \geq 0, \quad (8.23)$$

and

$$a_{13} \geq \xi\alpha - \psi\gamma/c_3 > -\alpha - \gamma/c_3 \quad \text{for } \xi < 0, \quad (8.24)$$

Using this in the estimation of $\alpha_1\alpha_2 - \alpha_3$ we get

$$\begin{aligned} \alpha_1\alpha_2 - \alpha_3 \geq & (\tilde{w}_2 + \tilde{w}_3)(\tilde{w}_1\tilde{w}_2 + \tilde{w}_1\tilde{w}_3 + \tilde{w}_2\tilde{w}_3) \\ & + \tilde{w}_1^2(\tilde{w}_2 + \tilde{w}_3) - \psi\gamma/c_3 \quad \text{for } \xi \geq 0. \end{aligned} \quad (8.25)$$

$$\begin{aligned} \alpha_1\alpha_2 - \alpha_3 \geq & (\tilde{w}_2 + \tilde{w}_3)(\tilde{w}_1\tilde{w}_2 + \tilde{w}_1\tilde{w}_3 + \tilde{w}_2\tilde{w}_3) \\ & + \tilde{w}_1^2(\tilde{w}_2 + \tilde{w}_3) - \psi\gamma/c_3 + \xi\alpha \quad \text{for } \xi < 0. \end{aligned} \quad (8.26)$$

In order to have $\alpha_1\alpha_2 - \alpha_3 < 0$ we have the necessary condition (using inequalities 8.25 and 8.26). For $\xi \geq 0$

$$\gamma/c_3 \geq \psi\gamma/c_3 \geq (\tilde{w}_2 + \tilde{w}_3)(\tilde{w}_1\tilde{w}_2 + \tilde{w}_1\tilde{w}_3 + \tilde{w}_2\tilde{w}_3) + \tilde{w}_1^2(\tilde{w}_2 + \tilde{w}_3). \quad (8.27)$$

And for $\xi < 0$

$$\gamma/c_3 + \alpha \geq \psi\gamma/c_3 - \xi\alpha \geq (\tilde{w}_2 + \tilde{w}_3)(\tilde{w}_1\tilde{w}_2 + \tilde{w}_1\tilde{w}_3 + \tilde{w}_2\tilde{w}_3) + \tilde{w}_1^2(\tilde{w}_2 + \tilde{w}_3). \quad (8.28)$$

Thus when a numerical estimate for \tilde{w}_1, \tilde{w}_2 and \tilde{w}_3 are found inequalities 8.27 and 8.28 give a lower bound on γ or $\gamma + \alpha$. It is a necessary condition for a Hopf bifurcation to occur that γ respectively $\gamma + \alpha$ is larger than this lower bound.

- If $a_{13} = 0$.
 - The fixed point is stable.

9 Considerations regarding general systems with bounded feedback functions

Now we have considered a model of the HPA axis including as well as excluding hippocampal mechanisms. Quite a lot of similar arguments were used to analyze the two models. This gives inspiration to impose some criteria on a very general system of differential equations governing the HPA axis. Only imposing some rather mild conditions on the general feedback functions from cortisol on ACTH and CRH we can state some general results. After a scaling of the concentrations and time the general system of differential equations (excluding circadian input on the derivative on CRH) can be written in dimensionless form

$$\begin{aligned}\frac{dX_1}{dt} &= F_1(X_3) - w_1 X_1 \\ \frac{dX_2}{dt} &= F_2(X_3) X_1 - w_2 X_2 \\ \frac{dX_3}{dt} &= X_2 - w_3 X_3.\end{aligned}\tag{9.1}$$

with constants $w_1, w_2, w_3 > 0$, $F_1, F_2 : \mathbb{R}_+ \cup \{0\} \mapsto \mathbb{R}_+ \cup \{0\}$, $F_1, F_2 \in C^1$, $\forall X_3 \in \mathbb{R}_+ \cup \{0\}$, $\sup(F_1(X_3)) \leq M_1$, $\sup(F_2(X_3)) \leq M_2$, $F_1(0) > 0$, $F_2(0) > 0$. This means F_1 and F_2 are bounded functions mapping non negative real numbers into non negative real numbers. For the HPA axis F_1 and F_2 are general feedback functions and the posed criteria for these functions is fulfilled for the feedback functions considered in this project. The criteria that F_1 and F_2 are bounded can be justified by saturation of receptors. When no cortisol is present then the feedbacks must not close the stimulation of hormone production. This justifies $F_1(0) > 0$ and $F_2(0) > 0$. Note that our models with as well as without hippocampus satisfies the criteria posed for this general model. This section shows that many results found for our two models are characteristic for all models on the form 9.1. Also a criteria for a globally stable fixed point is found which has not been mentioned for the previous models.

Existence and uniqueness of solutions

Since $F_1(X_3), F_2(X_3) \in C^1$ the system given in array 9.1 fulfills the criteria for the existence and uniqueness (theorem 3.1) for non negative values of X_1, X_2, X_3 so we are guaranteed that no solution curves cross.

All non negative initial values lead to non negative solutions

For $i \in \{1, 2, 3\}$ there is only one negative term in the expression for \dot{X}_i and this negative term has X_i as a factor. Therefore $\dot{X}_i \geq 0$ for $X_i = 0$ and the other two hormones are

non negative. This ensures that non negative initial conditions lead to solutions that are non negative for all future time.

Existence of a fixed point

The fixed point condition is

$$X_{1ss} = \frac{F_1(X_{3ss})}{w_1} \quad (9.2)$$

$$X_{2ss} = \frac{F_1(X_{3ss})F_2(X_{3ss})}{w_1w_2} \quad (9.3)$$

$$X_{3ss} = \frac{F_1(X_{3ss})F_2(X_{3ss})}{w_1w_2w_3}. \quad (9.4)$$

This means that for each fixed point value of X_3 the steady state value of X_1 and X_2 can be calculated using equation 9.2 and equation 9.3. The equation that may be hard to solve is 9.4 since this may not be explicitly solvable for X_3 . However we can say something about existence of a solution and then approximate the solution numerically.

First we define the functions

$$L(X_3) \equiv X_3 \quad (9.5)$$

and

$$R(X_3) \equiv \frac{F_1(X_3)F_2(X_3)}{w_1w_2w_3}. \quad (9.6)$$

If a value X'_3 has the property that $L(X'_3) = R(X'_3)$ then $X'_3 = X_{3ss}$. Finding steady states values is equivalent to find intersections between the graphs of L and R . Note that since F_1 and F_2 are bounded this means we have a bound for R as

$$\forall X_3 \geq 0 \quad R(X_3) \leq \frac{M_1M_2}{w_1w_2w_3} \equiv M_3. \quad (9.7)$$

Now choose $P = M_3 + \epsilon$ for any $\epsilon > 0$. Then

$$L(P) = M_3 + \epsilon > M_3 \geq R(P) \quad (9.8)$$

Now define the function $h : \mathbb{R}_+ \cup \{0\} \mapsto \mathbb{R}$

$$h(X_3) = L(X_3) - R(X_3). \quad (9.9)$$

Note that since L and R are continuous so is h and note that $h(0) = L(0) - R(0) < 0$ and $h(P) = L(P) - R(P) > 0$. Then by the intermediate theorem[17] there exists a $X'_3 \in]0; P[$ such that $h(X'_3) = 0 \Leftrightarrow L(X'_3) = R(X'_3)$. This means that we are sure there exists at least one fixed point of the system. Since $R(X_3) \leq M_3$ and $R(0) > 0$ we are guaranteed that any non negative fixed point value of X_3 is in the interval $]0; M_3] =]0; \frac{M_1M_2}{w_1w_2w_3}]$. Then any fixed point is in the set $]0; \frac{M_1}{w_1}] \times]0; \frac{M_1M_2}{w_1w_2}] \times]0; \frac{M_1M_2}{w_1w_2w_3}]$.

Sufficient criteria for only one fixed point

We now discuss a sufficient criteria that there only exists one fixed point of the system. Let X'_{3ss} denote the smallest existing fixed point for now. If $L(X_3)$ is increasing faster than $R(X_3)$ for all non negative X_3 this means that for values of X_3 larger than X'_{3ss} then $L(X_3) > R(X_3)$ which ensures that there can only be one fixed point. Since $dL(X_3)/dt = 1$ a sufficient criteria for only one fixed point is $dR(X_3)/dt < 1$ which is equivalent to

$$\forall X_3 \geq 0 \quad \frac{dF_1}{dX_3} F_2 + F_1 \frac{dF_2}{dX_3} < w_1 w_2 w_3. \quad (9.10)$$

If the feedback functions, F_1 and F_2 , corresponds to negative feedbacks then $\frac{dF_1}{dX_3} < 0$ and $\frac{dF_2}{dX_3} < 0$. Since F_1 and F_2 only takes non negative values this means that $\frac{dF_1}{dX_3} F_2 + F_1 \frac{dF_2}{dX_3} \leq 0 < w_1 w_2 w_3$ so purely negative feedbacks guarantee there exists exactly one fixed point.

Trapping region

We see that for $X_1 = \frac{M_1}{w_1}$ then $\dot{X}_1 \leq 0$. This means that $[0; \frac{M_1}{w_1}]$ is a trapping region for X_1 . Using this region for X_1 we can find a trapping region for X_2 and after that we can find one for X_3 . For $X_1 \in [0; \frac{M_1}{w_1}] \equiv J_1$ and $X_2 = \frac{M_1 M_2}{w_1 w_2}$ then $\dot{X}_2 \leq 0$. For $X_2 \in [0; \frac{M_1 M_2}{w_1 w_2}] \equiv J_2$ and $X_3 = \frac{M_1 M_2}{w_1 w_2 w_3}$ then $\dot{X}_3 \leq 0$ so for $X_1 \in J_1$ and $X_2 \in J_2$ and $X_3 \in [0; \frac{M_1 M_2}{w_1 w_2 w_3}] \equiv J_3$ then $X_1(t), X_2(t)$ and $X_3(t)$ are trapped in J_1, J_2 and J_3 . This means we have the trapping region U

$$U \equiv J_1 \times J_2 \times J_3. \quad (9.11)$$

Note that any fixed point is contained in the trapping region.

9.1 Expansion of trapping region

This section concerns that we can expand the trapping region which is needed in the next section. Here it is shown that any solution with non negative initial conditions get arbitrarily close to U in finite time. Therefore we make a larger box by for each $i \in (1, 2, 3)$ we add an amount to each positive end point of J_i .

$\forall \epsilon \geq 0$ define $\epsilon_2(\epsilon)$ and $\epsilon_3(\epsilon)$ as

$$\epsilon_2(\epsilon) \equiv 2 \frac{M_2}{w_2} \epsilon \quad (9.12)$$

$$\epsilon_3(\epsilon) \equiv 3 \frac{M_2}{w_2 w_3} \epsilon. \quad (9.13)$$

and define

$$\begin{aligned} \tilde{W}(\epsilon) &\equiv \left[0; \frac{M_1}{w_1} + \epsilon \right] \times \left[0; \frac{M_1 M_2}{w_1 w_2} + \epsilon_2(\epsilon) \right] \times \left[0; \frac{M_1 M_2}{w_1 w_2 w_3} + \epsilon_3(\epsilon) \right] \\ &\equiv I_1(\epsilon) \times I_2(\epsilon) \times I_3(\epsilon) \quad \forall \epsilon \geq 0. \end{aligned} \quad (9.14)$$

It is clear that $U = \tilde{W}(0)$. Now we want to show that $\tilde{W}(\epsilon)$ is a trapping region. Since it is already clear that $\tilde{W}(0)$ is a trapping region we will now only consider $\epsilon > 0$. For $\epsilon > 0$ (in contrast to $\epsilon \geq 0$) it turns out that the flow points into the trapping region whereas if $\epsilon = 0$ there could be zero speed on the boundary.

The argument is very similar to the argument that U is a trapping region. For $X_{1m} \equiv \max\{I_1(\epsilon)\} = \frac{M_1}{w_1} + \epsilon$ then $\dot{X}_{1m} \leq M_1 - w_1 \left(\frac{M_1}{w_1} + \epsilon\right) = -w_1\epsilon < 0$. For $X_1 \in I_1(\epsilon)$ we get for $X_{2m} \equiv \max\{I_2(\epsilon)\} = \frac{M_1 M_2}{w_1 w_2} + \epsilon_2$ that $\dot{X}_{2m} \leq M_2 \left(\frac{M_1}{w_1} + \epsilon\right) - w_2 \left(\frac{M_1 M_2}{w_1 w_2} + \epsilon_2(\epsilon)\right) = -M_2\epsilon < 0$. For $X_{3m} = \max\{I_3(\epsilon)\} = \frac{M_1 M_2}{w_1 w_2 w_3} + \epsilon_3(\epsilon)$ and $X_2 \in I_2(\epsilon)$ then $\dot{X}_3 \leq \left(\frac{M_1 M_2}{w_1 w_2} + \epsilon_2(\epsilon)\right) - w_3 \left(\frac{M_1 M_2}{w_1 w_2 w_3} + \epsilon_3(\epsilon)\right) = \epsilon_2(\epsilon) - w_3 \epsilon_3(\epsilon) = -\frac{M_2}{w_2} \epsilon < 0$.

Note that there is a 'hierarchy' that can not be reversed when the trapping region is found. $I_1(\epsilon)$ is a trapping region for X_1 for all values of X_2 and X_3 . A trapping region for X_2 exists when X_1 is bounded, and similarly we need a bound for X_2 in order to construct a trapping region for X_3 . So for $X_1 \in I_1(\epsilon)$ then X_1 is trapped. For $(X_1, X_2) \in I_1(\epsilon) \times I_2(\epsilon)$ then X_1 and X_2 are trapped and for $\mathbf{X} \in \tilde{W}(\epsilon)$ then X_1, X_2 and X_3 are trapped.

All solutions get arbitrarily close to U in finite time and then they stay close to U .

For any $\delta > 0$ we can choose $\epsilon > 0$ such that the distance between points in $\tilde{W}(\epsilon)$ and U is less than δ . We can prove that for any $\epsilon > 0$ any solution enters $\tilde{W}(\epsilon)$ in finite time (however the time depends on the initial condition). Since $\tilde{W}(\epsilon)$ is a trapping region this means the solution stays less than δ from U for all future time. This outlines the content of this section.

A solution is arbitrary close to U and stays close to U means for any $\delta > 0$ and a finite time $T_4 < \infty$ exists such that for $t > T_4$ it is true that $\text{dist}(X(t), U) \leq \delta$. The infinity norm (or the sub-norm) is defined as^[17]

$$\|\mathbf{X}\|_\infty \equiv \max\{|X_1|, |X_2|, |X_3|\}. \quad (9.15)$$

Proposition 9.1

For a fixed δ there exists ϵ such that if $\mathbf{X}(t) \in \tilde{W}(\epsilon)$ then the distance between $\mathbf{X}(t)$ and U is at most δ .

Proof

Fix $\delta > 0$. Define $m \equiv \max\{1, 2\frac{M_2}{w_2}, 3\frac{M_2}{w_2 w_3}\}$. Then choose $\epsilon = \delta/m > 0$. Now we have that the maximal distance between U and $X(t) \in \tilde{W}(\epsilon)$ is $\text{dist}(\mathbf{X}(t), \tilde{W}) \leq \text{dist}(U, \tilde{W}(\epsilon)) = \max\{\epsilon, \epsilon_2, \epsilon_3\} = m\epsilon = \delta$. \square

Since $\tilde{W}(\epsilon)$ is a trapping region then if the solution is once in $\tilde{W}(\epsilon)$ it stays in there for all future time.

Proposition 9.2

For any $\epsilon > 0$ then any initial condition leads to a solution in $\tilde{W}(\epsilon)$ after finite time.

¹ Similar reasoning could have been used to show the same result using other norms

Proof

Fix $\epsilon > 0$. Assume we have an arbitrary non negative initial condition $\mathbf{X}(t_0) = \mathbf{X}_0 = (X_{10}, X_{20}, X_{30})$. If $X_{10} > \frac{M_1}{w_1} + \epsilon$ form the compact interval $K_1 \equiv [\frac{M_1}{w_1} + \epsilon; X_{10}]$. We see that $\dot{X}_1 < 0$ on K_1 .

Since \dot{X}_1 is continuous then by the extreme value theorem [17] \dot{X}_1 has a maximum $m_1 < 0$ on K_1 . Using lemma 5.1 and lemma 5.3 there exists a finite time T_1 such that $X_1(t_0 + T_1) \in I_1(\epsilon)$ and then X_1 stays in this region for all future time. The worst case is that $X_2(t_0 + T_1)$ is not yet in \tilde{W} and then we will have to repeat the argument. If $X_2(t_0 + T_1) \in I_2(\epsilon)$ it will stay in this interval. Therefore consider $X_2(t_0 + T_1) > \frac{M_1 M_2}{w_1 w_2} + \epsilon_2$. Then $K_2 \equiv [\frac{M_1 M_2}{w_1 w_2} + \epsilon_2; X_2(t_0 + T_1)]$ is compact. It is clear that $\dot{X}_2 < 0$ on K_2 . By the extreme value theorem then \dot{X}_2 has a minimum $m_2 < 0$ on K_2 . Then by lemma 5.1 and lemma 5.3 there exists a finite time T_2 such that $X_2(t_0 + T_1 + T_2) \in I_2(\epsilon)$ and then X_2 stays in this region for all future time.

The similar argument for X_3 is that if $X_3(t_0 + T_1 + T_2) > \frac{M_1 M_2}{w_1 w_2 w_3} + \epsilon_3$ form the compact interval K_3 as $K_3 \equiv [X_3(t_0 + T_1 + T_2); \frac{M_1 M_2}{w_1 w_2 w_3} + \epsilon_3]$. Since $X_2 \in I_2(\epsilon)$ then $\dot{X}_3 < 0$ for $X_3 > \frac{M_1 M_2}{w_1 w_2 w_3}$. This means $\dot{X}_3 < 0$ on K_3 and by the extreme value theorem there exists a maximum m_3 of \dot{X}_3 with $m_3 < 0$ on K_3 . Then by lemma 5.1 and lemma 5.3 there exists a finite time T_3 such that for $X_3(t_0 + T_1 + T_2 + T_3) \in I_3(\epsilon)$.

This means that for any $\epsilon > 0$ for any non negative initial condition, it takes finite time, $T_4 = t_0 + T_1 + T_2 + T_3$, until the solution is contained in $\tilde{W}(\epsilon)$. Since $\tilde{W}(\epsilon)$ is a trapping region the solution will stay in $\tilde{W}(\epsilon)$ for all future time. \square

This shows that the dynamics of the system is somewhat simple for solutions outside U but note that X_2 and X_3 may be increasing for some time for some initial conditions outside U .

9.2 Bounding of solutions inside trapping region using solutions of linear systems

For the general model of the HPA axis (array 9.1) we consider $\tilde{W}(\tilde{\delta})$. We have shown that any solution enters the trapping region $\tilde{W}(\tilde{\delta})$ in finite time. Fix $\tilde{\delta} > 0$. Denote

$$\delta \equiv 3 \frac{M_2}{\tilde{w}_2 \tilde{w}_3} \tilde{\delta}. \quad (9.16)$$

and

$$I_3(\tilde{\delta}) = \left[0; \frac{M_1 M_2}{\tilde{w}_1 \tilde{w}_2 \tilde{w}_3} + \delta \right] \equiv D_0. \quad (9.17)$$

Assume $F_1(X_3) > 0$ $F_2(X_3) > 0$, $\forall X_3 \in D_0$. Since $\tilde{W}(\tilde{\delta})$ is compact the continuous functions $F_1(X_3)$ and $F_2(X_3)$ attain maximum and minimum values by the extreme value theorem [17].

$$\begin{aligned}
&\text{For } X_3 \in D_0 \\
&U_1 \equiv \max\{F_1(X_3)\} \leq M_1 \\
&L_1 \equiv \min\{F_1(X_3)\} > 0 \\
&U_2 \equiv \max\{F_2(X_3)\} \leq M_2 \\
&L_2 \equiv \min\{F_2(X_3)\} > 0.
\end{aligned}$$

Here the assumption $F_1(X_3) > 0$, $F_2(X_3) > 0$, $\forall X_3 \in D_0$ assures $L_1 > 0$, $L_2 > 0$. Now we make a bound of the solutions of the system using linear differential equations. The approach is very similar to approach in section 5.7 why we will not go into too many details again.

$$\begin{aligned}
\dot{X}_1' &\equiv L_1 - \tilde{w}_1 X_1' \\
\dot{X}_2' &\equiv L_2 X_1' - \tilde{w}_2 X_2' \\
\dot{X}_3' &\equiv X_2' - \tilde{w}_3 X_3'
\end{aligned} \tag{9.18}$$

$$\begin{aligned}
\dot{X}_1'' &\equiv U_1 - \tilde{w}_1 X_1'' \\
\dot{X}_2'' &\equiv U_2 X_1'' - \tilde{w}_2 X_2'' \\
\dot{X}_3'' &\equiv X_2'' - \tilde{w}_3 X_3''.
\end{aligned} \tag{9.19}$$

The initial conditions are $\mathbf{X}(t_0) = \mathbf{X}'(t_0) = \mathbf{X}''(t_0)$. Using this to compare the original, non linear coupled system of differential equations by a linear system given by array 5.33 restricted to $\tilde{W}(\tilde{\delta})$.

$$\begin{aligned}
\dot{X}_1' &\leq \dot{X}_1 \leq \dot{X}_1'' \\
\dot{X}_2' &\leq \dot{X}_2 \leq \dot{X}_2'' \\
\dot{X}_3' &\leq \dot{X}_3 \leq \dot{X}_3''.
\end{aligned} \tag{9.20}$$

Solving the linear system (array 9.18) we get

$$\begin{aligned}
X_1'(t) &= d_{11} e^{-\tilde{w}_1 t} + \frac{1}{\tilde{w}_1} L_1 \\
X_2'(t) &= d_{21} e^{-\tilde{w}_1 t} + d_{22} e^{-\tilde{w}_2 t} + \frac{1}{\tilde{w}_1 \tilde{w}_2} L_1 L_2 \\
X_3'(t) &= d_{31} e^{-\tilde{w}_1 t} + d_{32} e^{-\tilde{w}_2 t} + d_{33} e^{-\tilde{w}_3 t} + \frac{1}{\tilde{w}_1 \tilde{w}_2 \tilde{w}_3} L_1 L_2.
\end{aligned} \tag{9.21}$$

Similarly the linear system (array 9.19) is solved

$$\begin{aligned}
X_1''(t) &= c_{11} e^{-\tilde{w}_1 t} + \frac{1}{\tilde{w}_1} U_1 \\
X_2''(t) &= c_{21} e^{-\tilde{w}_1 t} + c_{22} e^{-\tilde{w}_2 t} + \frac{1}{\tilde{w}_1 \tilde{w}_2} U_1 U_2 \\
X_3''(t) &= c_{31} e^{-\tilde{w}_1 t} + c_{32} e^{-\tilde{w}_2 t} + c_{33} e^{-\tilde{w}_3 t} + \frac{1}{\tilde{w}_1 \tilde{w}_2 \tilde{w}_3} U_1 U_2.
\end{aligned} \tag{9.22}$$

All c_{ij} 's and d_{ij} 's are constants that depends on the initial conditions and the eigenvectors of the homogeneous part of array 9.18 and array 9.19. By lemma 5.2

$$\begin{aligned} X_1'(t) &\leq X_1(t) \leq X_1''(t) \quad \text{for } t \geq t_0 \\ X_2'(t) &\leq X_2(t) \leq X_2''(t) \quad \text{for } t \geq t_0 \\ X_3'(t) &\leq X_3(t) \leq X_3''(t) \quad \text{for } t \geq t_0. \end{aligned} \quad (9.23)$$

This means for any $\epsilon_1 > 0$ there exists a $T_1 < \infty$ such that

$$X_3(t) \in \left[-\epsilon_1 + \frac{1}{\tilde{w}_1 \tilde{w}_2 \tilde{w}_3} L_1 L_2; \epsilon_1 + \frac{1}{\tilde{w}_1 \tilde{w}_2 \tilde{w}_3} U_1 U_2 \right] \quad \text{for } t > T_1. \quad (9.24)$$

9.3 Sufficient criteria for a globally stable fixed point

Define the function H

$$H(X_3) \equiv \frac{F_1(X_3)F_2(X_3)}{\tilde{w}_1 \tilde{w}_2 \tilde{w}_3}. \quad (9.25)$$

$$H : D_0 \mapsto D_0. \quad (9.26)$$

This means $H(X_3)$ is the restriction of $R(X_3)$ to D_0 . Now we assume H is a contraction on D_0 (and still H is positive on D_0) which means we assume there exists $1 > p > 0$ such that $|H(y_1) - H(y_2)| \leq p|y_1 - y_2| \quad \forall y_1, y_2 \in D_0$. This ensures a unique fixed point of the non linear system of differential equations. Moreover any solution in D_0 converge to the unique fixed point of the system which will be proven in this section. Defining

$$0 < \epsilon_c = \frac{1}{2} \min \left\{ \delta + \frac{M_1 M_2 - U_1 U_2}{\tilde{w}_1 \tilde{w}_2 \tilde{w}_3}, \frac{1}{\tilde{w}_1 \tilde{w}_2 \tilde{w}_3} L_1 L_2 \right\}, \quad (9.27)$$

then

$$D_1 \equiv \left[-\epsilon_1 + \frac{1}{\tilde{w}_1 \tilde{w}_2 \tilde{w}_3} L_1 L_2; \epsilon_1 + \frac{1}{\tilde{w}_1 \tilde{w}_2 \tilde{w}_3} U_1 U_2 \right] \subseteq D_0, \quad 0 < \epsilon_1 \leq \epsilon_c. \quad (9.28)$$

The choice of ϵ_c ensures $D_1 \subseteq D_0$.

Thus from equation 9.24 there exists a finite time T_1 such that $X_3(t) \in D_1 \subseteq D_0, \forall t > T_1$.

Now a sequence of sets is defined by D_n

$$\begin{aligned} u_n &\equiv \max \{ H(x_n) : x_n \in D_n \} \\ l_n &\equiv \min \{ H(x_n) : x_n \in D_n \} \end{aligned} \quad (9.29)$$

And

$$D_{n+1} \equiv [-\epsilon_n + l_n; \epsilon_n + u_n], \quad 0 < \epsilon_n \leq \epsilon_c, \quad n \in \mathbb{N}_0. \quad (9.30)$$

D_n is well defined and compact and $D_n \subseteq D_0$.

Proof

The proof is done by induction. u_0 and l_0 are given by the expressions

$$\begin{aligned} u_0 &= \max \{ H(x_0) : x_0 \in D_0 \} \\ l_0 &= \min \{ H(x_0) : x_0 \in D_0 \} \end{aligned} \quad (9.31)$$

Since D_0 is compact and H is continuous then by the extreme value theorem [17] u_0 and l_0 are well defined and finite. This guarantees that D_1 is compact. Since $\epsilon_0 \leq \epsilon_c$ then $D_1 \subseteq D_0$. Now assume $D_n \subseteq D_0$ is compact. Then

$$\begin{aligned} u_n &= \max\{H(x_n) : x_n \in D_n\} \\ l_n &= \min\{H(x_n) : x_n \in D_n\} \end{aligned} \quad (9.32)$$

are well defined and finite by the extreme value theorem. Then D_{n+1} is compact.

$$D_{n+1} \equiv [-\epsilon_n + l_n; \epsilon_n + u_n], \quad 0 < \epsilon_n \leq \epsilon_c, \quad n \in \mathbb{N}_0, \quad (9.33)$$

Since by assumption $D_n \subseteq D_0$ then $l_n \geq l_0$ and $u_n \leq u_0$. This means

$$D_{n+1} \subseteq [-\epsilon_n + l_0; \epsilon_n + u_0], \quad 0 < \epsilon_n \leq \epsilon_c, \quad n \in \mathbb{N}_0, \quad (9.34)$$

This ensures $D_{n+1} \subseteq D_0$. \square

Due to the bounding of the solutions using linear systems we have shown that if $X_3(t_0) \in D_0$ then there exists $T_1 < \infty$ such that $X_3(t) \in D_1$ for $t > T_1$. Now we repeat the argument with bounding the solutions of the non linear differential equations by solutions to a linear system of differential equations. This means $\forall N < \infty$ there exists $T_N < \infty$ such that if $X_3(t_0) \in D_0$ then $X_3(t) \in D_N$ for $t > T_N$.

We now want to prove that D_n converges to $\{X_{3ss}\}$. The idea of the proof is based on the convergence of $y_{n+1} = H^n(y_0)$, $\forall y_0 \in D_0$ by the Banach Fixed Point Theorem. However there is also a large number of 'errors terms' that we have to control. This is done by using the contraction property of H as well as a decreasing, positive sequence of ϵ_n . This guarantees that any X_3 comes arbitrarily close to the unique fixed point defined by $y_{n+1} = H^n(y_0)$. This means that all solutions of the non linear differential equations converge to the unique fixed point of the system. We need the following two lemmas to prove this main result.

Lemma 9.1

Let p be the contraction constant for H . Then

$$H(a) - p|\epsilon| \leq H(y) \leq H(a) + p|\epsilon|, \quad \forall y \in [a; a + |\epsilon|] \subseteq D_0. \quad (9.35)$$

Proof

This is straightforward using the contraction property and the triangle inequality. Since H has non negative range

$$H(y) - H(a) = |H(y)| - |H(a)|. \quad (9.36)$$

Using the triangle inequality [17]

$$|H(y)| - |H(a)| \leq |H(y) - H(a)|. \quad (9.37)$$

Since $y \in D_0$ and $a \in D_0$ we use the contraction property

$$|H(y) - H(a)| \leq p|a - y| \leq p|\epsilon|. \quad (9.38)$$

Thus from 9.36, 9.37, 9.38

$$-p|\epsilon| \leq H(y) - H(a) \leq p|\epsilon|. \quad (9.39)$$

Adding $H(a)$ completes the proof. \square

Then it follows similarly

Lemma 9.2

Let p be the contraction constant for H . Then

$$H(a) - p|\epsilon| \leq H(y) \leq H(a) + p|\epsilon|, \quad \forall y \in [a - |\epsilon|; a] \subseteq D_0. \quad (9.40)$$

Lemma 9.1 and 9.2 means we can bound the maximum and minimum of H applied on a compact set by H evaluated at an end point of the set and the maximum distance between any two points in the set.

Introducing ϵ_0 .

$$0 < \epsilon_0 \leq p\epsilon_c. \quad (9.41)$$

Fix ϵ_0 . Then we can define $\epsilon_n > 0$.

$$\epsilon_n \equiv (1 - p)\epsilon_{n-1} = (1 - p)^n \epsilon_0. \quad (9.42)$$

To simplify notation we use

$$b \equiv 1 - p. \quad (9.43)$$

Since $p \in]0; 1[$ then $b \in]0; 1[$. Then we have

$$\epsilon_c > \epsilon_n = b^n \epsilon_0 > 0 \quad (9.44)$$

We introduce

$$A_n \equiv \epsilon_0 \sum_{i=0}^{n-1} b^i p^{n-1-i} > 0. \quad (9.45)$$

Since $b, p \in]0; 1[$ then $bp^n \leq b$ for $n \in \mathbb{N}_0$. This means

$$0 < \sum_{i=0}^{n-1} b^i p^{n-i} \leq \sum_{i=0}^{n-1} b^i = \frac{1 - b^n}{1 - b} \leq \frac{1}{1 - b}, \quad (9.46)$$

Using $b = 1 - p$

$$0 < A_n = \epsilon_0 \sum_{i=0}^{n-1} b^i p^{n-i} \leq \epsilon_0 \frac{1}{p}. \quad (9.47)$$

Define

$$\begin{aligned} \tilde{u}_n &= \max\{H^{n+1}(x_0) : x_0 \in D_0\} \\ \tilde{l}_n &= \min\{H^{n+1}(x_0) : x_0 \in D_0\}. \end{aligned} \quad (9.48)$$

\tilde{u}_n and \tilde{l}_n are well defined since repeated use of a continuous function on a compact set map into a compact set. The maximum and minimum of bounded sets exist and are finite by the extreme value theorem [17].

l_n and u_n are crucial for the range of D_{n+1} . Now we want to make bounds on l_n and u_n using \tilde{l}_n and \tilde{u}_n since we know the latter converges. In D_n 'error terms' (ϵ_n) are introduced at each step in the sequence. The following lemma helps bounding D_n by a series in the 'error terms' and a sequence $H^n(D_0)$ (corresponding to the span between l_n and u_n). This means the 'error terms' are separated from $H^n(D_0)$ and we can then estimate the two separately.

Lemma 9.3

If H is a contraction on D_0 and H is positive on D_0 then

$$D_n \subseteq \left[-A_n + \tilde{l}_n; A_n + \tilde{u}_n \right], \quad n \in \mathbb{N}. \quad (9.49)$$

Proof

The proof is by induction.

$$D_1 = [-\epsilon_0 + l_0; \epsilon_0 + u_0], \quad 0 < \epsilon_0 \leq \epsilon_c. \quad (9.50)$$

Since $l_0 = \tilde{l}_0$ and $u_0 = \tilde{u}_0$ and $A_1 = \epsilon_0$ a basis for the induction is justified. Now assume

$$D_n \subseteq \left[-A_n + \tilde{l}_n; A_n + \tilde{u}_n \right], \quad n \in \mathbb{N}. \quad (9.51)$$

We need to show

$$D_{n+1} \subseteq \left[-A_{n+1} + \tilde{l}_{n+1}; A_{n+1} + \tilde{u}_{n+1} \right], \quad n \in \mathbb{N}. \quad (9.52)$$

Note by 9.47

$$\left[-A_n + \tilde{l}_n; A_n + \tilde{u}_n \right] \subseteq \left[-\epsilon_0 \frac{1}{p} + \tilde{l}_n; \epsilon_0 \frac{1}{p} + \tilde{u}_n \right] \quad (9.53)$$

Because $H : D_0 \mapsto D_0$ then $\tilde{u}_n \leq \tilde{u}_0$ and $\tilde{l}_n \geq \tilde{l}_0$ due to the contraction property of H . Therefore

$$\left[-A_n + \tilde{l}_n; A_n + \tilde{u}_n \right] \subseteq \left[-A_n + \tilde{l}_0; A_n + \tilde{u}_0 \right]. \quad (9.54)$$

From inequality 9.47

$$\left[-A_n + \tilde{l}_n; A_n + \tilde{u}_n \right] \subseteq \left[-\epsilon_0 \frac{1}{p} + \tilde{l}_0; \epsilon_0 \frac{1}{p} + \tilde{u}_0 \right] \subseteq D_0 \quad (9.55)$$

We can therefore apply H on $\left[-A_n + \tilde{l}_n; A_n + \tilde{u}_n \right]$ and use the contraction property.

Now we consider $H(D_n)$ and using 9.51

$$H(D_n) \subseteq H \left(\left[-A_n + \tilde{l}_n; A_n + \tilde{u}_n \right] \right), \quad n \in \mathbb{N} \quad (9.56)$$

Then

$$H(D_n) \subseteq H\left([-A_n + \tilde{l}_n; \tilde{l}_n]\right) \cup H\left([\tilde{l}_n; \tilde{u}_n]\right) \cup H([\tilde{u}_n; A_n + \tilde{u}_n]), \quad n \in \mathbb{N} \quad (9.57)$$

Since H is continuous on the compact set $[-A_n + \tilde{l}_n; A_n + \tilde{u}_n]$ bounded extrema exist for each of the sets in equation 9.57. The simplest estimation is

$$\begin{aligned} H\left([\tilde{l}_n; \tilde{u}_n]\right) &= H\left([\min\{H^{n+1}(x_0)\}; \max\{H^{n+1}(x_0)\}]\right) \\ &= [\min\{H^{n+2}(x_0)\}; \max\{H^{n+2}(x_0)\}] = [\tilde{l}_{n+1}; \tilde{u}_{n+1}]. \end{aligned} \quad (9.58)$$

We can use the contraction property as shown in lemma 9.1 for bounding the two other sets of 9.57.

$$\begin{aligned} -pA_n + H(\tilde{l}_n) &\leq H(y_1) \leq pA_n + H(\tilde{l}_n), \quad \forall y_1 \in [-A_n + \tilde{l}_n; \tilde{l}_n] \\ -pA_n + H(\tilde{u}_n) &\leq H(y_2) \leq pA_n + H(\tilde{u}_n), \quad \forall y_2 \in [\tilde{u}_n; A_n + \tilde{u}_n]. \end{aligned} \quad (9.59)$$

Using the definitions of $l_n, u_n, \tilde{l}_n, \tilde{u}_n$,

$$\begin{aligned} \tilde{u}_{n+1} &= \max\{H^{n+2}(D_0)\} \geq H(\tilde{l}_n) = H(\min\{H^{n+1}(D_0)\}) \geq \min\{H^{n+2}(D_0)\} = \tilde{l}_{n+1} \\ \tilde{u}_{n+1} &= \max\{H^{n+2}(D_0)\} \geq H(\tilde{u}_n) = H(\max\{H^{n+1}(D_0)\}) \geq \min\{H^{n+2}(D_0)\} = \tilde{l}_{n+1}. \end{aligned} \quad (9.60)$$

Now we have an upper and a lower bound on each of the sets $H\left([-A_n + \tilde{l}_n; \tilde{l}_n]\right)$, $H\left([\tilde{l}_n; \tilde{u}_n]\right)$, $H([\tilde{u}_n; A_n + \tilde{u}_n])$, $n \in \mathbb{N}$. From 9.60, 9.59 and 9.57 we get

$$\begin{aligned} l_n &= \min\{H(D_n)\} \geq -pA_n + \tilde{l}_{n+1} \\ u_n &= \max\{H(D_n)\} \leq pA_n + \tilde{u}_{n+1}. \end{aligned} \quad (9.61)$$

We have by definition

$$D_{n+1} \equiv [-\epsilon_n + l_n; \epsilon_n + u_n], \quad 0 < \epsilon_n \leq \epsilon_c, \quad n \in \mathbb{N}_0, \quad (9.62)$$

Now we can bound D_{n+1} (equation 9.62)

$$D_{n+1} \subseteq [-\epsilon_n - pA_n + \tilde{l}_{n+1}; \epsilon_n + pA_n + \tilde{u}_{n+1}]. \quad (9.63)$$

Using the expressions for ϵ_n (equation 9.42) and A_n (equation 9.45)

$$\epsilon_n + pA_n = b^n \epsilon_0 + \epsilon_0 \sum_{i=0}^{n-1} b^i p^{n-i} = \epsilon_0 \sum_{i=0}^n b^i p^{n-i} = A_{n+1}. \quad (9.64)$$

Inserting in 9.63

$$D_{n+1} \subseteq [-A_{n+1} + \tilde{l}_{n+1}; A_{n+1} + \tilde{u}_{n+1}], \quad (9.65)$$

which completes the proof. \square

By equation 9.47

$$\left[-A_n + \tilde{l}_n; A_n + \tilde{u}_n\right] \subseteq \left[-\frac{\epsilon_0}{p} + \tilde{l}_n; \frac{\epsilon_0}{p} + \tilde{u}_n\right] \quad (9.66)$$

Lemma 9.4

If H is a contraction on D_0 and H is positive on D_0 then a unique fixed point exists of the system of differential equations. All solutions in $\tilde{W}(\tilde{\delta})$ converge to the fixed point.

Proof

There exists $T_n < \infty$ such that $X_3 \in D_n$ for $t > T_n$. Since H is a contraction on a complete metric space the Banach Fixed Point Theorem applies. This means that a unique fixed point exists of $y_{n+1} = H(y_n)$ for any $y_0 \in D_0$ i.e.

$$\lim_{n \rightarrow \infty} H^n(D_0) = \{X_{3ss}\}. \quad (9.67)$$

Fix $\tilde{\epsilon} > 0$. We need to show that for any $X_3(t_0) \in D_0$ there exists a $T_n < \infty$ such that $|X_3(t) - X_{3ss}| < \tilde{\epsilon}$, $\forall t > T_n$. Choose

$$\epsilon_0 = \min\left\{\frac{p}{5}\tilde{\epsilon}, p\epsilon_c\right\} > 0. \quad (9.68)$$

For any $N < \infty$ there exists a $T_N < \infty$ such that $X_3(t) \in D_N$, $\forall t > T_N$. By 9.67 there exists $N < \infty$ such that $|H^n(X_3(t_0)) - X_{3ss}| < \frac{\tilde{\epsilon}}{5}$, for $t > T_n$ (corresponding to $\forall n \geq N$), $\forall X_3(t_0) \in D_0$. This means

$$-\frac{\tilde{\epsilon}}{5} + X_{3ss} \leq \tilde{l}_n \leq \frac{\tilde{\epsilon}}{5} + X_{3ss} \quad \text{for } t > T_n. \quad (9.69)$$

and similarly

$$-\frac{\tilde{\epsilon}}{5} + X_{3ss} \leq \tilde{u}_n \leq \frac{\tilde{\epsilon}}{5} + X_{3ss} \quad \text{for } t > T_n. \quad (9.70)$$

Now we have by lemma 9.3

$$X_3 \in D_n \subseteq \left[-\epsilon_0 \frac{1}{p} + \tilde{l}_n; \epsilon_0 \frac{1}{p} + \tilde{u}_n\right] \quad \text{for } t > T_n, \forall X_3(t_0) \in D_0. \quad (9.71)$$

And 9.69 gives

$$X_3 \in D_n \subseteq \left[-\frac{\tilde{\epsilon}}{5} - \frac{\tilde{\epsilon}}{5} + X_{3ss}; \frac{\tilde{\epsilon}}{5} + \frac{\tilde{\epsilon}}{5} + X_{3ss}\right] \quad \text{for } t > T_n. \quad (9.72)$$

But now X_3 is contained in an interval of length less than $\tilde{\epsilon}$ and the interval contains X_{3ss} . Therefore $|X_3 - X_{3ss}| < \tilde{\epsilon}$ for $t > T_n$ for a $T_n < \infty$. Now we have proved that X_3 converges to X_{3ss} for any $X_3(t_0) \in D_0$.

When X_3 converges to X_{3ss} then $F_1(X_3)$ converge to $F_1(X_{3ss})$ and $F_2(X_3)$ converge to $F_2(X_{3ss})$ since F_1 and F_2 are continuous. Considering array 9.21 and array 9.22 this means that X_2' and X_2'' converge towards the same limit.

$$\lim_{t \rightarrow \infty} X_2' = \frac{F_1(X_{3ss})F_2(X_{3ss})}{\tilde{w}_1\tilde{w}_2} = \lim_{t \rightarrow \infty} X_2''. \quad (9.73)$$

Since X_2 is squeezed between the limit of X_2' and X_2'' .

$$\lim_{t \rightarrow \infty} X_2 = \frac{F_1(X_{3ss})F_2(X_{3ss})}{\tilde{w}_1\tilde{w}_2}. \quad (9.74)$$

Similar reasoning for X_1 means that

$$\lim_{t \rightarrow \infty} X_1 = \frac{F_1(X_{3ss})}{\tilde{w}_1}. \quad (9.75)$$

This means that all solutions with initial conditions in \tilde{W} converge to the unique fixed point of the non linear system of differential equations. \square

Since all solutions outside $\tilde{W}(\tilde{\delta})$ enter $\tilde{W}(\tilde{\delta})$ in finite time we are sure that if H is a contraction and positive on D_0 then all solutions converge to the fixed point solution.

This means that no periodic solution exists which we will now prove. There must be a positive distance between the fixed point and the periodic solution (if a periodic solution exists) because if a periodic solution ever equals the fixed point solution it will stay at the fixed point for all future time. Denote the infimum of the distance between the periodic solution and the fixed point by δ_1 . Since we have just proved that any solution converge to the fixed point then after some time all solutions are less than the distance δ_1 from the fixed point. This is a contradiction which means there cannot exist any periodic solutions in the trapping region.

9.4 Sufficient criteria for using Banach Fixed Point Theorem

How can we be sure that a given H is a contraction? This section focus on a sufficient criteria for applying Banach Fixed Point Theorem (theorem 3.6).

Lemma 9.5

Let $f : \mathbb{R}_+ \cup \{0\} \rightarrow \mathbb{R}_+ \cup \{0\}$ and let f be bounded by M and let f be C^1 . Then for any $c \geq 0$ let \tilde{f}_c denote the restriction of f to $D_c = [0; M + c]$. If $|d\tilde{f}_c/dx| < 1, \forall x \in D_c$ then \tilde{f}_c is a contraction and $x_{n+1} = \tilde{f}_c(x_n)$ converge to the unique fixed point of \tilde{f}_c for any $x_0 \in D_c$.

Proof

Fix $c \geq 0$ and assume $|d\tilde{f}_c/dx| < 1, \forall x \in D_c$. Note $\tilde{f} : D_c \rightarrow D_c$ since $\tilde{f}(D_c) \subseteq [0; M]$. Since $d\tilde{f}_c/dx$ is continuous on the compact set D_c then by the extreme value theorem there exists a minimum, p_1 , and maximum, p_2 , of $d\tilde{f}_c/dx$. Defining d

$$d \equiv \max\{|p_1|, |p_2|\}. \quad (9.76)$$

Fix any two points, $x_0, y_0 \in D_c$. By symmetry we can assume $y_0 \geq x_0$. Define $h_1(x_0) = h_2(x_0) = f(x_0)$ and $dh_1(x)/dx = d$ and $dh_2(x)/dx = -d$. Then we can solve the two differential equations.

$$\begin{aligned} h_1(x) &= d(x - x_0) + f(x_0) \\ h_2(x) &= -d(x - x_0) + f(x_0). \end{aligned} \quad (9.77)$$

By lemma 5.2

$$h_1(x) \geq f(x) \geq h_2(x) \quad \forall x \geq x_0. \quad (9.78)$$

Since $y_0 \geq x_0$ this holds especially for y_0

$$h_1(y_0) \geq f(y_0) \geq h_2(y_0). \quad (9.79)$$

Subtracting $f(x_0)$

$$h_1(y_0) - f(x_0) \geq f(y_0) - f(x_0) \geq h_2(y_0) - f(x_0). \quad (9.80)$$

Inserting $h_1(y_0)$ and $h_2(y_0)$ using array 9.77

$$d(y_0 - x_0) \geq f(y_0) - f(x_0) \geq -d(y_0 - x_0). \quad (9.81)$$

By [17] this means

$$|f(y_0) - f(x_0)| \leq d|y_0 - x_0|. \quad (9.82)$$

By assumption $d < 1$. Then we have shown that \tilde{f} is a contraction.

$\tilde{f}_c : D_c \rightarrow D_c$ and (d_2, D_c) is a complete metric space with metric given by the 2-norm and \tilde{f}_c is a contraction. Then by the Banach Fixed Point Theorem \tilde{f}_c has exactly one fixed point, x_{ss} , and the sequence $x_{n+1} = \tilde{f}_c(x_n)$ converge to x_{ss} for all $x_0 \in D_c$. \square

We have now proved that if $|dH/dX_3| < 1, \forall X_3 \in D_0 = \left[0; \frac{M_1 M_2}{\tilde{w}_1 \tilde{w}_2 \tilde{w}_3} + \delta\right]$ for any $\delta > 0$ then all solutions of the system of differential equations converge to the unique fixed point. However since $H \in C^1$ it is sufficient that $|dH/dX_3| < 1, \forall X_3 \in \left[0; \frac{M_1 M_2}{\tilde{w}_1 \tilde{w}_2 \tilde{w}_3}\right]$ for this conclusion.

Proof

Define

$$g(X_3) : \mathbb{R}_+ \cup \{0\} \mapsto \mathbb{R}_+ \cup \{0\} \quad (9.83)$$

$$g(X_3) \equiv |dH/dX_3|. \quad (9.84)$$

$g(X_3)$ is continuous and we assume $g(X_3) < 1, \forall X_3 \in \left[0; \frac{M_1 M_2}{\tilde{w}_1 \tilde{w}_2 \tilde{w}_3}\right]$. We choose

$$\epsilon \equiv \frac{1 - g\left(\frac{M_1 M_2}{\tilde{w}_1 \tilde{w}_2 \tilde{w}_3}\right)}{2} > 0. \quad (9.85)$$

Since $g(X_3)$ is continuous there exists $\delta > 0$ such that $\left|\frac{M_1 M_2}{\tilde{w}_1 \tilde{w}_2 \tilde{w}_3} - X_3\right| < \delta$ guarantees $\left|g\left(\frac{M_1 M_2}{\tilde{w}_1 \tilde{w}_2 \tilde{w}_3}\right) - g(X_3)\right| < \epsilon$. This means $\forall X_3$ that satisfies $\left|\frac{M_1 M_2}{\tilde{w}_1 \tilde{w}_2 \tilde{w}_3} - X_3\right| < \delta$ then

$$g(X_3) < \epsilon + g\left(\frac{M_1 M_2}{\tilde{w}_1 \tilde{w}_2 \tilde{w}_3}\right) = \frac{g\left(\frac{M_1 M_2}{\tilde{w}_1 \tilde{w}_2 \tilde{w}_3}\right) + 1}{2} < \frac{1 + 1}{2} = 1. \quad (9.86)$$

Thus $\forall X_3$ that satisfies $\left|\frac{M_1 M_2}{\tilde{w}_1 \tilde{w}_2 \tilde{w}_3} - X_3\right| < \delta$ then $|dH/dX_3| < 1$. This ensures there exists $\delta > 0$ such that $|dH/dX_3| < 1, \forall X_3 \in \left[0; \frac{M_1 M_2}{\tilde{w}_1 \tilde{w}_2 \tilde{w}_3} + \delta\right]$. \square

Summary of chapter 9

- Existence and uniqueness of solutions are guaranteed for the system 9.1 for non negative concentrations.
- A trapping region, U , exists. The trapping region can be expanded such that $\tilde{W}(\tilde{\delta})$ is a trapping region and $U \subset \tilde{W}(\tilde{\delta})$ for $\tilde{\delta} > 0$.
- All solutions of the non linear differential equations enter $\tilde{W}(\tilde{\delta})$ in finite time for $\tilde{\delta} > 0$. Then any solution get arbitrarily close to U in finite time. This outrules limit cycles outside U . (By similar reasoning that limit cycles do not exist when the fixed point is globally stable.)
- At least one fixed point exists and all fixed points are contained in U .
If $1/\tilde{w}_1\tilde{w}_2\tilde{w}_3 d(F_1F_2)/dX_3 < 1, \forall X_3 \in [0; M_1M_2/\tilde{w}_1\tilde{w}_2\tilde{w}_3]$ then a unique fixed point exists. This implies a unique fixed point exists if F_1 and F_2 are negative feedback functions.
- If $H = F_1(X_3)F_2(X_3)/\tilde{w}_1\tilde{w}_2\tilde{w}_3$ is a contraction and positive $\forall X_3 \in D_0$ then a unique fixed point exists of the system of differential equations. Any solution in $\tilde{W}(\tilde{\delta})$ converge to the fixed point. This means the fixed point is globally stable which outrules the possibility of limit cycles.
- $|dH/dX_3| < 1, \forall X_3 \in [0; \frac{M_1M_2}{\tilde{w}_1\tilde{w}_2\tilde{w}_3}]$ is a sufficient criteria for the existence a unique, globally stable fixed point of the differential equations. Whether this criteria is fulfilled or not depends on the parameters of the system.

10 Estimation of parameters

In this section we will give an estimate of the parameters in our models. This is important since for a given set of parameters we can categorize the behaviour of the systems due to our previous analysis. The overall idea is to assume that our model is realistic. Some parameters are well known. Other parameters are less known. The rest is almost totally unknown. We will present the three different categories of parameters below. Also we will make physiological reasoning to give a first estimate of the less known parameters.

Since we have been dealing mainly with two models one including the feedback mechanisms to hippocampus and a model that does not involve the mechanisms of hippocampus we will estimate parameters for both models. Since the latter of the two is the most common way of describing the HPA axis these parameters will be easiest to compare to the parameters of previously made models.

In the end of this section a first estimate will be given of all parameters of the two models. Then the idea is to make various simulations of the system and investigate the system dynamics with special focus on existence of limit cycles.

Many of the parameters are the same in the two models. We will start by giving an estimate of the model without hippocampus. Only the parameters that are not the same will be discussed when estimating parameters for the system with hippocampus.

The parameters will be compared to parameters of other model. However this may not be possible if two models are too dissimilar.

Parameters of the model without hippocampus

To remind the reader of the parameters in the system without hippocampus we have rewritten the system of unscaled differential equations (array 5.33) in array 10.1

$$\begin{aligned}\frac{dx_1}{dt} &= k_0 \left(1 - \mu \frac{x_3^\alpha}{x_3^\alpha + c^\alpha} \right) - w_1 x_1 \\ \frac{dx_2}{dt} &= k_1 \left(1 - \rho \frac{x_3^\alpha}{x_3^\alpha + c^\alpha} \right) x_1 - w_2 x_2 \\ \frac{dx_3}{dt} &= k_2 x_2 - w_3 x_3.\end{aligned}\tag{10.1}$$

- Well known parameters

From literature we have an estimate of the elimination constants from the half lives of the concentrations. We define w_i as $\ln(2)/half\ life$. This is widely used in modeling the HPA axis[1] although we realize that this is only a good approximation when the concentration of a given hormone x_i is much larger than the concentration of the other hormones x_j entering the differential equation.

When this is the case the differential equation for hormone x_i is approximately equal to

$$\dot{x}_i \approx -w_i x_i. \quad (10.2)$$

We have not deeply investigated how the half lives are measured but one way of pursuing this idea would be to measure the concentration of hormone x_i when a large dose of this hormone is injected into a person and if these measurements can be approximated by an exponential then calculate the half time for that.

From [10] the half life of human CRH in plasma is given to be about 4 min. This gives $w_1 = \ln(2)/4 = 0.17$.

The data provided by H. Lundbeck A/S can be used to estimate hormone half lives. The data originates from [9]. Here the hormone half life is calculated for different groups (healthy, high cortisol depressive, low cortisol depressive). We will estimate the parameters by using the data from the healthy group. The half life of ACTH for the healthy group is $19.9 \text{ min} \pm 4.2 \text{ min}$ (mean \pm standard deviation). The same have been done for cortisol and the result is $76.4 \text{ min} \pm 16.2 \text{ min}$ ¹. Because of the difficulties in measuring the concentration of CRH we have not been able to find a standard deviation in this hormone. But since the standard deviation is about $1/5$ of the mean value for ACTH and cortisol we let the relative standard deviation be similar for CRH. So that the half life of CRH is given by 4 ± 1 .

We assume the half life of a given hormone is normally distributed. A normal distribution with mean μ and standard deviation σ has 68% of the probability density located in the interval $[\mu - \sigma; \mu + \sigma]$. 99% of the probability density is located in $[\mu - 2\sigma; \mu + 2\sigma]$. We choose the default half life to be the mean value. Since the standard deviation for the half lives are close to $1/5$ of the mean value then varying the default value by $\pm 40\%$ covers the majority (99%) of physiologically relevant cases.

- Less known parameters

As explained in section 5.2 the exponents in the various Hill functions indicate how many cortisol molecules that react with one free receptor. [19] argues it would be unphysiological for such a parameter to attend values larger than eight. Savic et al.[3] model the HPA axis using $\alpha = 1$. We will make a first guess of $\alpha = 3 \pm 2$.

In [11] it is explained that GR is the most important receptor in regulating the HPA-axis. This suggests c^α has a value that ensures that the receptor is around the inflection point of the Hill function for reasonable values of cortisol concentration. We denote the mean value of free cortisol as \bar{x}_3 and we choose $c = \bar{x}_3$ as a first estimate.

- Unknown parameters

The saturation parameters μ and ρ are somehow unknown. The way the model is created gives that $\mu \in [0; 1]$ and $\rho \in [0; 1]$. To be able to investigate the possibility of a change in receptor capacity we will set $\mu = \rho = 0.5$ as a first guess for these parameters.

¹ The half lives of the two other groups are given in mean \pm standard deviation: Half life ACTH hypercortisolemic 15.7 ± 1.95 , half life ACTH non-hypercortisolemic 14.5 ± 1.1 , half life cortisol hypercortisolemic 79 ± 7.9 and half life non-hypercortisolemic 60.8 ± 13 .

Now we have determined a first estimate for the values of some of the parameters. We still need to give an estimate on k_i . To do this we will use the following reasoning.

The overall idea is that the system should be able to oscillate for physiologically reasonable values of parameters. This means that all the derivatives of the concentrations should be capable of changing sign for physiologically relevant hormone values. We therefore assume that the fixed point of the equations is located at the mean value of the concentrations. Therefore we are able to give an estimate of k_i . This is done by inserting the mean values of hormone concentrations and the values of the above mentioned parameters and equating the system of differential equations to zero. Letting \bar{x}_i denote the mean concentration of hormone i , k_i will be given by array 10.3

$$\begin{aligned} k_0 &= \frac{w_1 \bar{x}_1}{\left(1 - \mu \frac{\bar{x}_3^\alpha}{\bar{x}_3^\alpha + c^\alpha}\right)} \\ k_1 &= \frac{w_2 \bar{x}_2}{\left(1 - \rho \frac{\bar{x}_3^\alpha}{\bar{x}_3^\alpha + c^\alpha}\right) \bar{x}_1} \\ k_2 &= \frac{w_3 \bar{x}_3}{\bar{x}_2}. \end{aligned} \tag{10.3}$$

Note that for fixed μ, ρ, c, α then k_i/w_{i+1} is constant. This means that perturbing w_{i+1} by a factor changes k_i by the same factor.

The data of cortisol is the sum of bound and free cortisol. We are only interested in the free cortisol which in [10] is stated to be 3.9% of the total concentration in normal humans. And in [11] 3-10% of the total concentration is stated to be free. We will estimate the free cortisol to be 5% of the total amount.

The mean values of ACTH and cortisol come from our data[9]. We will use the data from the healthy control people and use the mean values of these. These values are given in array 10.4

$$\begin{aligned} \bar{x}_2 &= 21pg/ml \\ \bar{x}_3 &= 0.05 \cdot 6.11\mu g/dl = 3.055ng/ml. \end{aligned} \tag{10.4}$$

Since we have no data of CRH we take the mean of this hormone from the literature. From an investigation of plasma CRH we get that the mean plasma CRH level in normal subjects (26 individuals) was $1.64 \pm 0.43\text{pmol/l}$ [30]. From this we take the mean value of CRH to be 1.64pmol/l . The molecular weight of CRH in sheep is found to be 4670g/mol [11]. Doing the calculations we get that

$$\bar{x}_1 = 1.64 \cdot 4670 = 7.6588pg/ml. \tag{10.5}$$

Estimated parameters

Using the above parameters and reasoning we get our first guess of the parameters. The estimated parameters are given in table 10.1. They are calculated from the Matlab file given in appendix B.2. Along with our own parameters we have also gathered information of parameters used in other models. Where it is possible to compare any of these parameters to our own this is done. Two models are made by Liu et al. The first

Parameter	Default value	Liu et al.(1990)[31]	Liu et al.(1999)[22]	Savic et al.[4]
k_0	1.7696pg/ml·min	0.001917	-	-
k_1	0.127341/min	-	-	-
k_2	0.00131981/min	-	-	-
w_1	0.173291/min	0.0598	0.059	-
w_2	0.0348321/min	0.053	0.028	-
w_3	0.00907261/min	0.0138	0.67	-
ρ	0.5	-	-	0.72
μ	0.5	-	-	0.98
α	3	-	-	1
c	3.055ng/ml	-	-	-

Table 10.1: Default parameter values of the system without hippocampus.

model[31] only contains three concentrations. In [31] Liu et al. are assuming the free cortisol is always a constant fraction of the total amount of cortisol. This is leading to the use of total cortisol half life. In [22] Liu et al. have included the two bound forms of cortisol into the model thus leading to a five dimensional model. The decay constant given in table 10.1 is therefore now the decay constant for free cortisol which they allow much larger values than that of the total amount of cortisol.

In [22] 33 parameters are included. We do not consider differential equations of the model sufficiently related to physiological mechanisms as well as the huge number of parameters make the estimation quite doubtful. In both models Liu et al. is making the assumption that there are a constant input to the differential equations that is not influenced by the feedback from cortisol. In general we have not been able to compare this to our model. But in the case of [31] we can conclude that the number we relate to our k_0 is corresponding to the input on CRH when there is no cortisol in [31]. Our k_0 can be interpreted in the same way. In [22] they include multiple fast feedbacks on the concentrations. This leads to five coupled autonomous differential equations with 33 parameters. We have not been able to compare any of these except the half life coefficients.

Comparison to parameter values of Kyrlov et al.

As explained in section 4.1 Kyrlov et al. build a model from a linear system and impose non linearities. The linear system dominates for positive concentrations above a threshold value and nonincreasing concentrations. Since our system is defined to have steady state in the mean value of the concentrations we linearize our system around these values. This means that the values at the entries of the Jacobian taken in steady state can be compared to parameter values of Kyrlov et al..

$$J_{ss} = \begin{pmatrix} -0.1733 & 0 & -0.2172 \\ 0.0955 & -0.0348 & -0.1197 \\ 0 & 0.0013 & -0.0091 \end{pmatrix} = \begin{pmatrix} a_{00} & a_{01} & a_{02} \\ a_{10} & a_{11} & a_{12} \\ a_{20} & a_{21} & a_{22} \end{pmatrix}. \quad (10.6)$$

Now we can directly compare our values with those of Kyrlov et al. This is done in table 10.2 There is quite a difference between the parameters of the two models. Since

Parameter	Our value	Kyrylov et al.[1]
$-a_{00}$	0.1733	0.00843
a_{01}	0	0
$-a_{02}$	0.2172	0.440
a_{10}	0.0955	0.082
$-a_{11}$	0.0348	0.004
$-a_{12}$	0.1197	0.0668
a_{20}	0	0.0164
a_{21}	0.0013	0.031
$-a_{22}$	0.0091	0.0957

Table 10.2: Comparison between our values and them of Kyrylov et al.[1].

we have already discussed how we consider the model of Kyrylov et al. problematic we will not elaborate further on this comparison.

10.1 The parameter values in the scaled system without hippocampus

In section 6.1 we scaled the system into dimensionless units. The scaled system is given by array 10.7

$$\begin{aligned}
 \frac{dX_1}{d\theta} &= 1 - \mu \frac{X_3^\alpha}{1 + X_3^\alpha} - \tilde{w}_1 X_1 \\
 \frac{dX_2}{d\theta} &= \left(1 - \rho \frac{X_3^\alpha}{1 + X_3^\alpha} \right) X_1 - \tilde{w}_2 X_2 \\
 \frac{dX_3}{d\theta} &= X_2 - \tilde{w}_3 X_3.
 \end{aligned} \tag{10.7}$$

The parameters μ , ρ and α have the same value as in the unscaled system. The remaining variables and parameters are given by

$$\begin{aligned}
 \theta &\equiv d_0 t \\
 x_1 &\equiv d_1 X_1 \\
 x_2 &\equiv d_2 X_2 \\
 x_3 &\equiv d_3 X_3 \\
 \tilde{w}_1 &\equiv \frac{w_1}{d_0} \\
 \tilde{w}_2 &\equiv \frac{w_2}{d_0} \\
 \tilde{w}_3 &\equiv \frac{w_3}{d_0} \\
 d_0 &= \left(\frac{k_0 k_1 k_2}{c} \right)^{1/3} \\
 d_1 &= \left(\frac{c k_0^2}{k_1 k_2} \right)^{1/3} \\
 d_2 &= \left(\frac{c^2 k_0 k_1}{k_2^2} \right)^{1/3} \\
 d_3 &= c.
 \end{aligned}$$

These values can all be calculated using the parameters of the unscaled system given above, i.e

$$\theta = d_0 t = \left(\frac{k_0 k_1 k_2}{c} \right)^{1/3} t = 0.046003 \cdot t. \quad (10.8)$$

In table 10.3 the parameters of the scaled system are given

Parameter	Default values
\tilde{w}_1	3.7669
\tilde{w}_2	0.75716
\tilde{w}_3	0.19722
ρ	0.5
μ	0.5
α	3

Table 10.3: Parameter values for the scaled system without hippocampus.

10.2 Parameters of the model including hippocampus

To remind the reader of the parameters in the system including the mechanisms from hippocampus, the system is presented in array 10.9 (equal to array 8.6)

$$\begin{aligned}\frac{dx_1}{dt} &= k_0 \left(1 + \xi \frac{x_3^\alpha}{x_3^\alpha + c^\alpha} - \psi \frac{x_3^\gamma}{x_3^\gamma + c_3^\gamma} \right) - w_1 x_1 \\ \frac{dx_2}{dt} &= k_1 \left(1 - \rho \frac{x_3^\alpha}{x_3^\alpha + c^\alpha} \right) x_1 - w_2 x_2 \\ \frac{dx_3}{dt} &= k_2 x_2 - w_3 x_3.\end{aligned}\tag{10.9}$$

- Parameters that can be reused from the system without hippocampus

The parameters that we have no reason to believe is changing from the system without hippocampus is the half life of the different hormones α , $\mu(\xi = \phi - \mu)$, ρ and the mean value of the concentrations.

- Parameters still needed to estimated

Since nothing is indicating that the coefficients relating cortisol binding to MR and GR should be different a first guess will be that they are equal. The same reasoning that was applied to α will therefore also apply to γ . Therefore we believe that $\alpha = \gamma = 3 \pm 2$ would be good guess for a first estimate of these parameters.

As explained in the introduction it has been shown that cortisol has a ten times higher affinity for MR than for GR in mice, we will assume that this also applies to humans. This gives us that $c_3^\gamma = 1/10 c^\alpha$. Furthermore in [10] it is stated that the MR receptors in humans is nearly fully occupied at normal levels of corticosterone. Under the assumption that normal levels of cortisol imply normal levels of corticosterone. This is in good agreement with $c_3^\gamma = c^\alpha/10$.

The values of the parameters ξ and ψ are unknown. The way the model is created gives that $\psi \in [0; 1]$. Furthermore we would like the positive feedback to be able to overcome the negative feedback, thus $\phi > \mu$. If this is not the case it may be that a simpler model where the overall feedback is modeled as one negative feedback mechanism would apply as well. So for a first guess of these parameters we set $\psi = \rho = 0.5$ and $\xi = 2$.

To give an estimate of k_i we will use the same reasoning as when estimating these parameters in the system without hippocampus. Using the same notation k_i will be given by array 10.10

$$\begin{aligned}k_0 &= \frac{w_1 \bar{x}_1}{1 + \xi \frac{\bar{x}_3^\alpha}{\bar{x}_3^\alpha + c^\alpha} - \psi \frac{\bar{x}_3^\gamma}{\bar{x}_3^\gamma + c_3^\gamma}} \\ k_1 &= \frac{w_2 \bar{x}_2}{\left(1 - \rho \frac{\bar{x}_3^\alpha}{\bar{x}_3^\alpha + c^\alpha} \right) \bar{x}_1} \\ k_2 &= \frac{w_3 \bar{x}_3}{\bar{x}_2}.\end{aligned}\tag{10.10}$$

As in the previous section the parameters are given in table 10.4. These are also calculated using the Matlab file that can be seen in appendix B.2.

Parameter	Our values
k_0	0.85876 $\mu\text{g}/\text{ml} \cdot \text{min}$
k_1	0.12734 $1/\text{min}$
k_2	0.0013198 $1/\text{min}$
w_1	0.17329 $1/\text{min}$
w_2	0.034832 $1/\text{min}$
w_3	0.0090726 $1/\text{min}$
ρ	0.5
ψ	0.5
ξ	2
α	3
γ	3
c	3.055 ng/ml
c_3	1.418 ng/ml

Table 10.4: Parameter values for the system including hippocampus.

Parameters for the scaled system including hippocampus

As done in the system without hippocampus we will calculate the parameters in the scaled system from the parameters in the original system. To remind the reader the scaled system with hippocampus is given in array 10.11 (equal to array 8.7)

$$\begin{aligned}
 \frac{dX_1}{d\theta} &= \left(1 + \xi \frac{X_3^\alpha}{1 + X_3^\alpha} - \psi \frac{X_3^\gamma}{\tilde{c}_3^\gamma + X_3^\gamma} \right) - \tilde{w}_1 X_1 \\
 \frac{dX_2}{d\theta} &= \left(1 - \rho \frac{X_3^\alpha}{1 + X_3^\alpha} \right) X_1 - \tilde{w}_2 X_2 \\
 \frac{dX_3}{d\theta} &= X_2 - \tilde{w}_3 X_3.
 \end{aligned} \tag{10.11}$$

The only scaled variables and parameters that are not defined in the same way as in the system without hippocampus is

$$\tilde{c}_3 \equiv c_3/d_3. \tag{10.12}$$

Again we have calculated the scaled parameters using the Matlab file presented in appendix B.2. These are given in table 10.5

Parameter	Default values
\tilde{w}_1	4.7934
\tilde{w}_2	0.9635
\tilde{w}_3	0.2510
\tilde{c}_3	0.4642
ψ	0.5
ρ	0.5
ξ	2
γ	3
α	3

Table 10.5: Parameter values for the scaled system including hippocampus.

11 Numerical investigations

In this chapter we make various simulations of our system. The idea is to investigate the system for the possibility of oscillations of the solutions to the system. For the model with as without hippocampal mechanisms we use the default parameter values from chapter 10 as a basis for the numerical investigations. For each model we change one parameter while keeping the other fixed at default values. When perturbing a parameter we investigate if oscillating solutions of the system emerge. The numerical investigation is split into three different parts.

The first part concerns the system without hippocampus. In the second part we investigate the consequences of including the hippocampal feedback mechanisms. Finally we investigate how to include the circadian rhythm into the model.

All numerical investigations made in this chapter have been carried out using the matlab file given in appendix B.3. This file loads several other files. These files are presented in appendix B.4.

11.1 The system without hippocampus

In this section we will investigate the possibility of oscillations for the system without hippocampus.

First we investigate the system with parameter values given by the default parameters. On the graphs 11.1, 11.2 and 11.3 the different concentrations are plotted as a function of time. The initial conditions is given as $x_1(0) = 2\bar{x}_1$, $x_2(0) = 0.5\bar{x}_2$ and $x_3(0) = 1.5\bar{x}_3$. The parameters are chosen such that the steady state is at the mean value of each concentration $(\bar{x}_1, \bar{x}_2, \bar{x}_3) = (7.6588, 21, 3.055)$. As seen on the figures the concentrations converge to steady state.

In figure 11.4 we have shown a three dimensional plot of the system with default parameter values. In figure 11.5 a three dimensional plot of the scaled system with default parameter values is shown. As expected the dynamics of the scaled and the original system is similar. For this reason we will only investigate the scaled system. For the default parameter values the steady state solution of the scaled system will be given by array 11.1

$$\begin{aligned} X_{1ss} &= \frac{x_{1ss}}{d_1} = \frac{\bar{x}_1}{d_1} = 0.1991 \\ X_{2ss} &= \frac{x_{2ss}}{d_2} = \frac{\bar{x}_2}{d_2} = 0.1972 \\ X_{3ss} &= \frac{x_{3ss}}{d_3} = \frac{\bar{x}_3}{d_3} = 1. \end{aligned} \tag{11.1}$$

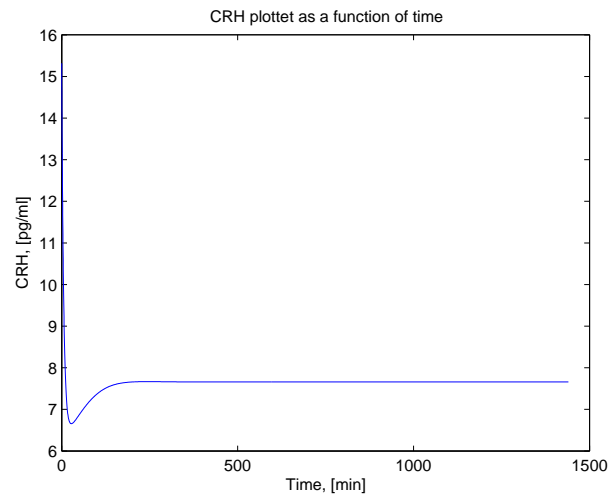


Figure 11.1: The CRH concentration plotted as a function of time. The parameters used are the default parameter values. The initial conditions are $x_1(0) = 2\bar{x}_1$, $x_2(0) = 0.5\bar{x}_2$ and $x_3(0) = 1.5\bar{x}_3$.

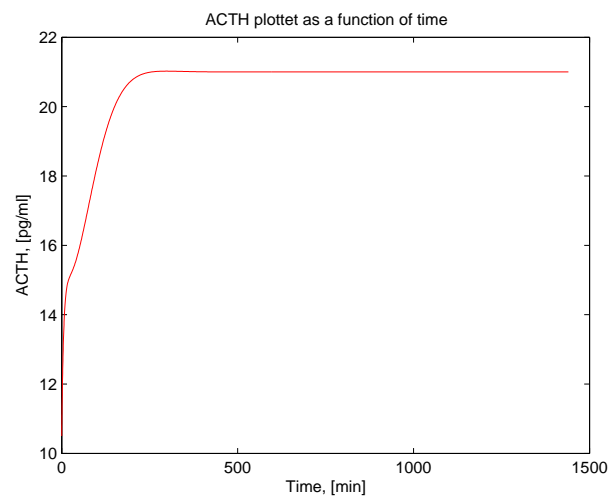


Figure 11.2: The ACTH concentration plotted as a function of time. The parameters used are the default parameter values. The initial conditions are $x_1(0) = 2\bar{x}_1$, $x_2(0) = 0.5\bar{x}_2$ and $x_3(0) = 1.5\bar{x}_3$.

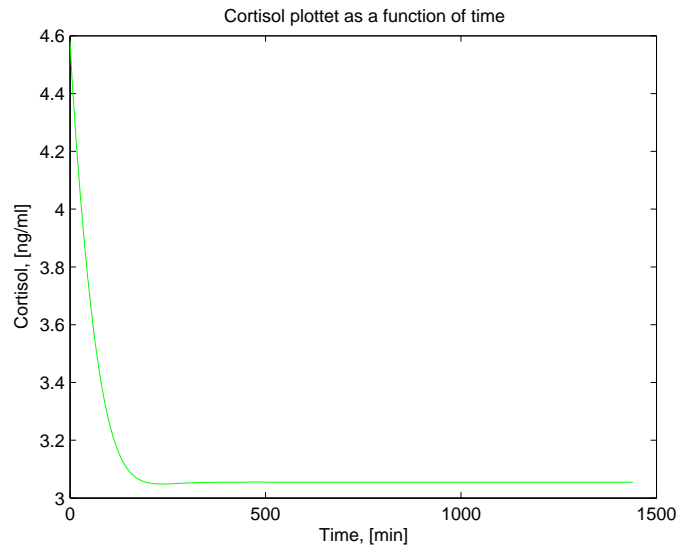


Figure 11.3: The cortisol concentration plotted as a function of time. The parameters used are the default parameter values. The initial conditions are $x_1(0) = 2\bar{x}_1$, $x_2(0) = 0.5\bar{x}_2$ and $x_3(0) = 1.5\bar{x}_3$.

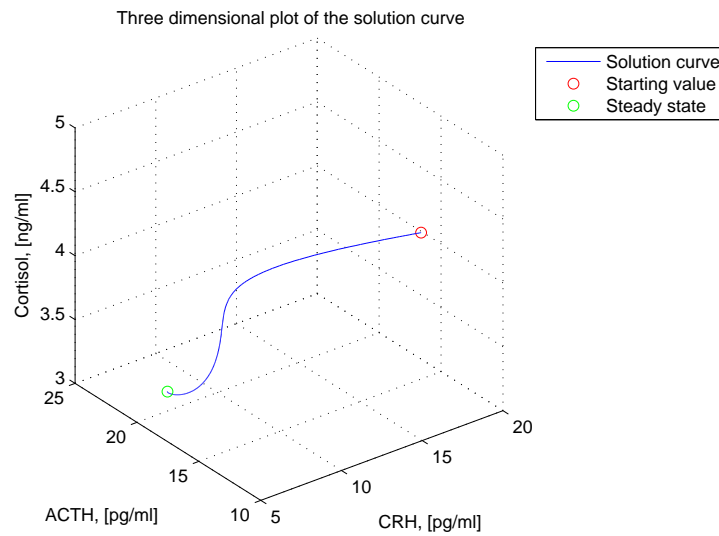


Figure 11.4: Three dimensional plot of concentrations. The parameters used are the default parameter values. The initial conditions are $x_1(0) = 2\bar{x}_1$, $x_2(0) = 0.5\bar{x}_2$ and $x_3(0) = 1.5\bar{x}_3$.

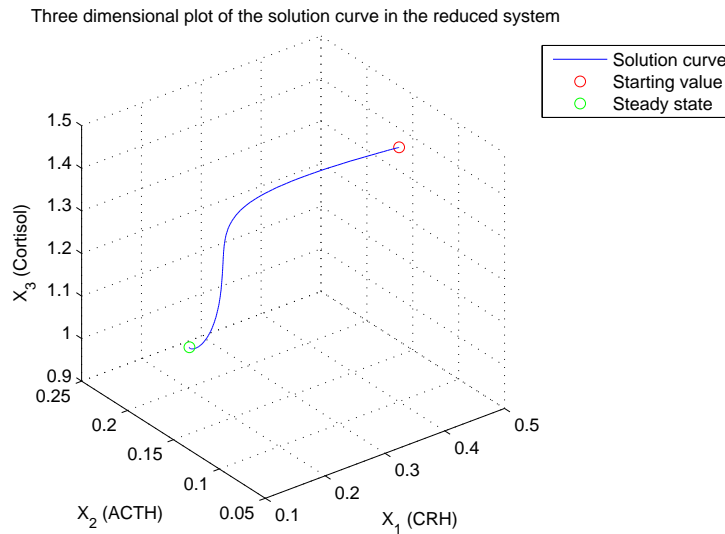


Figure 11.5: Three dimensional plot of the scaled system using the default parameter values. The initial conditions are $X_1(0) = 2\bar{x}_1/d_1$, $X_2(0) = 0.5\bar{x}_2/d_2$ and $X_3(0) = 1.5\bar{x}_3/d_3$.

In section 9.2 we have shown that all solutions of the system with the default parameter values will always enter the trapping region. The trapping region is given by

$$\tilde{V} \equiv [0; 1/\bar{w}_1] \times [0; 1/\bar{w}_1\bar{w}_2] \times [0; 1/\bar{w}_1\bar{w}_2\bar{w}_3]. \quad (11.2)$$

Using the default parameter values the trapping region is given by $[0; 0.2655] \times [0; 0.3506] \times [0; 1.7778]$. This means that the steady state solution is contained in the trapping region which is in accordance to previous results.

In figure 11.6 there is a plot of $H(X_3)$ alongside with $L(X_3)$. As shown in chapter 9 the intersection between $H(X_3)$ and $L(X_3)$ defines the unique steady state solution for X_3 .

In section 9.2 we showed that the system is globally stable if $H(x_3)$ is a contraction. We have also showed that if $|H'(X_3)| < 1$ for all $X_3 \in [0; 1/\bar{w}_1\bar{w}_2\bar{w}_3]$ then H is a contraction on $[0; 1/\bar{w}_1\bar{w}_2\bar{w}_3]$. For the model not including hippocampus $H'(X_3) < 0$ since H is a product of two functions that corresponds to negative feedback. The green ring in figure 11.6 is at $\max |H'(x_3)|$. Furthermore the value of $\min H'(X_3)$ is shown in the legend box. The value is less than -1. For this reason we cannot outrule the existence of limit cycles analytically. We cannot be sure that there are no limit cycles even though the steady state solution is stable. Therefore we have made a grid investigation of different initial conditions. This means we have made a grid of initial conditions in the region $[0; 2] \times [0; 2] \times [0; 2]$. The mask of the grid is 0.1. There are 20^3 different initial conditions inside this region illustrated with a green dot.

The differential equations was solved numerically and the last value (after what corresponds to three days) of the solutions was plotted as a blue dot. The steady state solution is plotted as a red ring. The grid investigation is shown in figure 11.7. Here

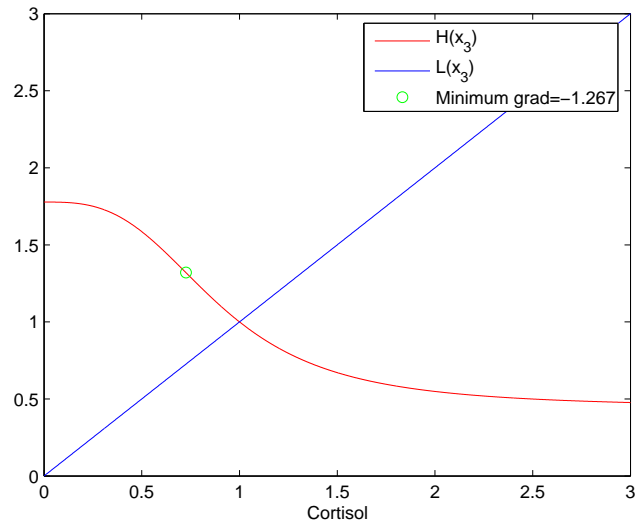


Figure 11.6: $H(X_3)$ shown along side $L(X_3)$ for the scaled system without hippocampus using the default parameter values.

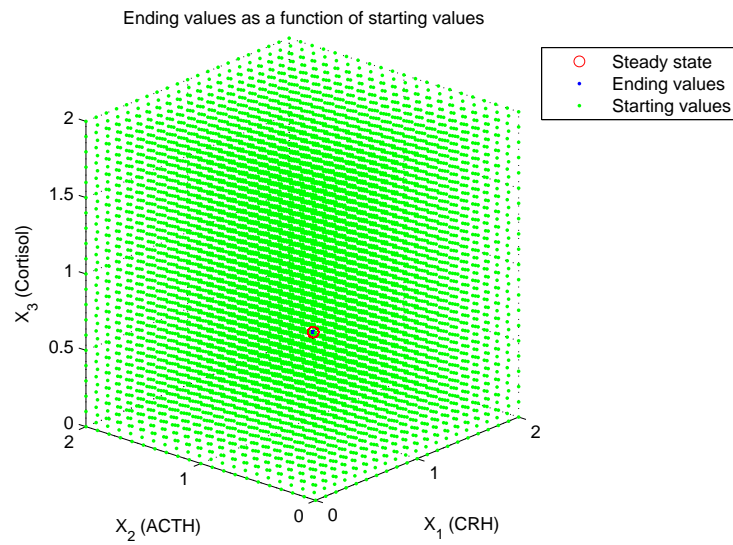


Figure 11.7: Grid investigation in the region $[0; 2] \times [0; 2] \times [0; 2]$. The trapping region is given by $[0; 0.2655] \times [0; 0.3506] \times [0; 1.7778]$

we see that initial conditions outside the trapping region lead to solutions entering the trapping region in accordance to previous mentioned results. Furthermore we see that all solutions converge to the steady state solution. This is no guarantee that no limit cycles exists inside the trapping region but the result seen in figure 11.7 gives an indication that it is unlikely.

11.2 Variation of parameters in the system without hippocampus

In this section we will make a variation in one parameter keeping the other fixed at their default value¹. Doing this for all the parameters will give an indication of the effect the parameter has on the solutions of the system. Since we know from section 5.6 that there exists only one steady state solution and that this is guaranteed to be locally stable this analysis will mainly concern which parameters that makes the system globally stable. That is we wish to investigate which parameters that makes $|H'(x_3)| < 1$. Furthermore it is clear that when we change the value of one parameter the steady state solution will change. Also an investigation of this change will be done.

Investigation of a change in w_i

We will start by investigating what will happen if we vary only the decay constants, w_i . Since $\tilde{w}_i = w_i/d_0$ changing w_i by a fraction will cause the same fractional change in \tilde{w}_i . Since

$$H(X_3) = \frac{1}{\tilde{w}_1\tilde{w}_2\tilde{w}_3} F_1(X_3)F_2(X_3), \quad (11.3)$$

we know that

$$\frac{dH(X_3)}{dX_3} = \frac{1}{\tilde{w}_1\tilde{w}_2\tilde{w}_3} \left(\frac{dF_1(X_3)}{dX_3} F_2(X_3) + \frac{dF_2(X_3)}{dX_3} F_1(X_3) \right). \quad (11.4)$$

If we now denote the default parameters as θ we know that for X_3 inside the trapping region

$$\max \left| \frac{\partial H(X_3, \theta)}{\partial X_3} \right| = 1.267. \quad (11.5)$$

Since only \tilde{w}_i is changing when w_i is changed we can make an equation that gives the fraction that w_i is allowed to change for the system to be guaranteed globally stable. Denoting the new set of parameters $\hat{\theta} = (\alpha, \mu, \rho, \hat{w}_1, \tilde{w}_2, \tilde{w}_3)^2$ we investigate the case

$$\frac{dH(X_3, \hat{\theta})}{dX_3} = -1. \quad (11.6)$$

This gives that for

$$\hat{w}_i > 1.267\tilde{w}_i \quad (11.7)$$

¹ A more thorough investigation must include an investigation of the dynamics in the nine dimensional parameter space. This is left to do for another project since we also investigate the behaviour for different initial conditions. Combining a variation of parameters with variation of initial condition is a huge task

² We denote the default parameters by the usual symbol e.g. ρ , and we denote a perturbed parameter by adding a 'hat' on top e.g. $\hat{\rho}$.

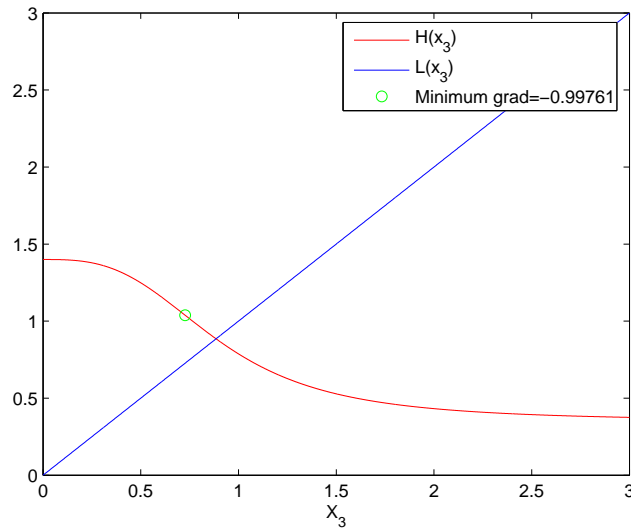


Figure 11.8: $H(X_3)$ plotted where $\hat{w}_1 = 1.27\tilde{w}_1$. All other parameter values are fixed at their default parameter values.

the system is globally stable. For now we assumed that only one parameter is varied. It is clear that this can also apply for the product of decay constants i.e. $\hat{w}_1\hat{w}_2\hat{w}_3 > 1.267w_1w_2w_3$. A graphical illustration of this $H(X_3)$ is shown in figure 11.8 where $\hat{w}_1 = 1.27\tilde{w}_1$.

Investigation of a change in α

As explained in section 5.2 the parameter α affects the magnitude of the gradient in the Hill function. Therefore we would expect that increasing α increases $\max |H'(X_3)|$. For $\alpha \neq 1$ this is indeed the case. When $\alpha = 1$ the Hill function changes shape from a sigmoid function to a function with no inflection point and steepest derivative in $X_3 = 0$. The effect on $H'(X_3)$ when varying α is written in table 11.1. It is seen that we do not get that $\max |H'(X_3)| < 1$ when changing α among positive integers. Thus

α	$\max H'(X_3) $
1	1.7778
2	1.0242
3	1.267
4	1.5699
5	1.8909

Table 11.1: $H'(X_3)$ as a function of α . All other parameters are fixed at their default values.

it is not possible for us to guarantee global stability.

Since the steady state of X_3 is defined to be at $X_{3ss} = 1$ the steady state solution does not change when we change the parameter α . In the not scaled system this corresponds to that the steady state solution of x_3 and the parameter c is defined to be equal. This assures that the fraction in Hill function always take the value $1/2$ for all values of α .

Investigation of a perturbation to ρ or μ

Last we analyze the effect of changes in the parameters μ or ρ . Because they enter into the equation of $H(X_3)$ in the same way we will treat them both at the same time.

We know from section 5.2 that these parameters also influence the steepness of the Hill function. Therefore we expect that the larger μ, ρ the larger a absolute value of $H'(X_3)$. This is indeed the case and we see that the largest absolute value of $H'(X_3)$ inside trapping region is 1.8033 when ρ or μ equal one and the other parameters are fixed at their default values. Also we see that we are guaranteed global stability when ρ or μ have values $\mu, \rho \leq 0.24$.

The effect of increasing ρ or μ on the steady state solution is a bit different. Since X_{1ss} is a function of ρ only through X_{3ss} and X_{3ss} is decreasing for increasing values of both μ and ρ it should be clear that the steady state solution for X_1 is increasing for increasing ρ . It is more subtle with X_{2ss} since this is a function of both of X_{3ss} and ρ . Numerical investigation show that also X_{2ss} is decreasing for increasing values of ρ . The case of varying μ is also subtle since all steady states depend explicitly on μ and the steady state of X_1 and X_2 also depend implicitly on μ through X_{3ss} . A numerical investigation was also made for variation in this parameter and the result is that for increasing μ all steady state values is decreasing. The results of variation in μ or ρ when all other parameters are fixed at their default values is shown in table 11.2.

μ	Steady state	ρ	Steady state
$\mu = 0.3$	(0.2215, 0.2116, 1.0731)	$\rho = 0.3$	(0.1921, 0.2116, 1.0731)
$\mu = 0.4$	(0.2096, 0.2041, 1.0349)	$\rho = 0.4$	(0.1957, 0.2041, 1.0349)
$\mu = 0.5$	(0.1991, 0.1972, 1.0000)	$\rho = 0.5$	(0.1991, 0.1972, 1.0000)
$\mu = 0.6$	(0.1897, 0.1909, 0.9681)	$\rho = 0.6$	(0.2023, 0.1909, 0.9681)
$\mu = 0.7$	(0.1813, 0.1852, 0.9391)	$\rho = 0.7$	(0.2053, 0.1852, 0.9391)

Table 11.2: The effect on steady state($X_{1ss}, X_{2ss}, X_{3ss}$) when varying μ or ρ while all other parameter values are fixed at their default values.

This ends the investigation of the parameters of the scaled system without hippocampus. Finally we wish to make some comments on the effect on the scaled parameters when changing the parameters in the unscaled system.

Since

$$\tilde{w}_i = \frac{w_i}{d_0} \quad (11.8)$$

and

$$d_0 = \left(\frac{k_0 k_1 k_2}{c} \right)^{1/3} \quad (11.9)$$

We see from the above analysis that an increase in k_i will lead to an increase in steady state concentrations in all variables X_i since all of \tilde{w}_i is decreased. This is of course expected since this corresponds to a larger input to the system.

Investigation of worst case scenario

We know that the system is locally stable for all reasonable parameter values and globally stable for $\max |H'(X_3)|$. One could think that the most chance of finding limit cycles in other areas of trapping region would be best if we change all the parameters in such a way that $\max |H'(X_3)|$ is much larger than one. We have mapped the influence on $H'(X_3)$ by changing one parameter at a time. Therefore we investigate the above mentioned by using the parameter values given in table 11.3. For the use of

Worst parameters
$\hat{w}_1 = 0.6\tilde{w}_1$
$\hat{w}_2 = 0.6\tilde{w}_2$
$\hat{w}_3 = 0.6\tilde{w}_3$
$\hat{\rho} = 1$
$\hat{\mu} = 1$
$\hat{\alpha} = 5$

Table 11.3: Worst case scenario of parameters.

the parameter values given in table 11.3 we have made a plot of $H(X_3)$ in figure 11.9. As seen $\max |H'(X_3)| = 14.4498$. The steady state solution is $(X_{1ss}, X_{2ss}, X_{3ss}) = (0.1628, 0.1319, 1.1143)$ and the trapping region is given by $[0; 0.4425] \times [0; 0.9739] \times [0; 8.2305]$. We have made a grid investigation in the region $[0; 10] \times [0; 10] \times [0; 10]$ using a grid mask of 0.4 and a numerical integration corresponding to three days. The investigation is seen in figure 11.10.

Summary of system without hippocampus

We have shown analytically that the unique fixed point is always locally stable for reasonable values of α which is also found in the simulations.

From the grid investigation we see that initial conditions 'far' from the fixed point converge to the fixed point. Thus it seems that the fixed point is globally stable from the simulations. Thus it is not likely that limit cycles exists.

When varying one parameter and keeping the other parameters fixed at their default values we can define a subspace of the parameter space where the fixed point system is globally stable. These parameters are $\hat{w}_i > 1.27\tilde{w}_i$ or if ρ or μ have values $\mu, \rho \leq 0.24$. We can also conclude that decreasing α decreases the gradient of H (except when $\alpha = 1$). Furthermore we have determined the behaviour of the value of the fixed point. Because $x_{3ss} = c$ perturbing α does not influence the value of the fixed point.

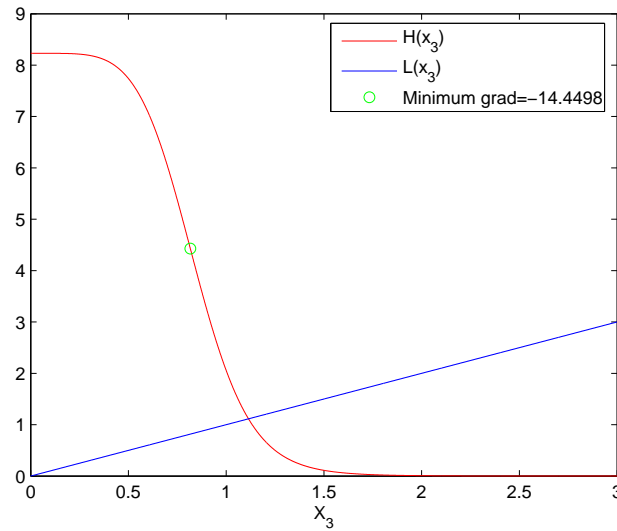


Figure 11.9: $H'(X_3)$ using the parameter values given in table 11.3 corresponding to the 'worst case scenario'.

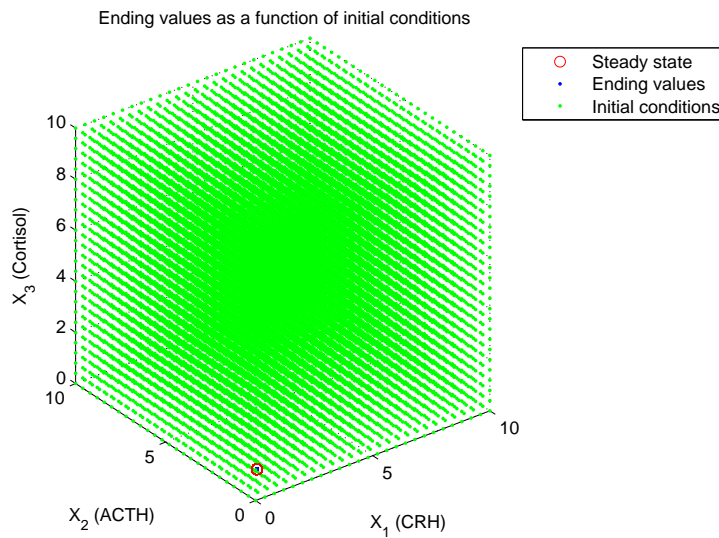


Figure 11.10: Grid investigation of the scaled system without hippocampal mechanisms. This figure shows the ending value as a function of initial conditions using the parameter values given in table 11.3 corresponding to the 'worst case scenario'. All initial conditions lead to solutions converging to the fixed point. The investigated region is $[0; 10] \times [0; 10] \times [0; 10]$ and the trapping region is $[0; 0.4425] \times [0; 0.9739] \times [0; 8.2305]$.

11.3 The system including mechanisms from hippocampus

In this section we will use the same approach as in the previous section. We will start by investigating the system with hippocampus with the default parameter values for this system as they are given in chapter 10. Then we will investigate the consequences of changing one parameter while keeping the other parameter values fixed at their default values. Since the behaviour of the scaled system is the same as the unscaled system we will only investigate the scaled system.

The trapping region of the scaled system including hippocampal mechanisms is given by

$$V = [0; (1+\xi)/\bar{w}_1] \times [0; (1+\xi)/\bar{w}_1\bar{w}_2] \times [0; (1+\xi)/\bar{w}_1\bar{w}_2\bar{w}_3]. \quad (11.10)$$

Using the default parameters this gives $[0; 0.6259] \times [0; 0.6496] \times [0; 2.5882]$.

To start with we plot $L(X_3)$ and $H(X_3)$ using the default parameter values. This is shown in figure 11.11. One intersection occurs. The unique steady state of the system using the default parameter values is $\mathbf{X}_{ss} = (0.3324, 0.2510, 1)$. Note $H(X_{3,ss})/dX_3 > 0$. This assures $F_1(X_{3,ss})/dX_3 > 0$. This means the fixed point may be stable or unstable with at least one positive eigenvalue and no complex eigenvalue with positive real part and non zero imaginary part exists. Written in the legend box is also the maximum gradient and the minimum gradient. The largest absolute value of the two is $0.57142 < 1$. We conclude that the system including hippocampal mechanisms has a globally stable fixed point and therefore no limit cycles exists when default parameters are used.

Because of the global stability we will now investigate the effect of changing the parameters. In this investigation we will focus mainly on how to maximize the possibility of ultradian oscillations. This requires $\max |H'(X_3)| > 1$ on $[0; (1+\xi)/\bar{w}_1\bar{w}_2\bar{w}_3]$.

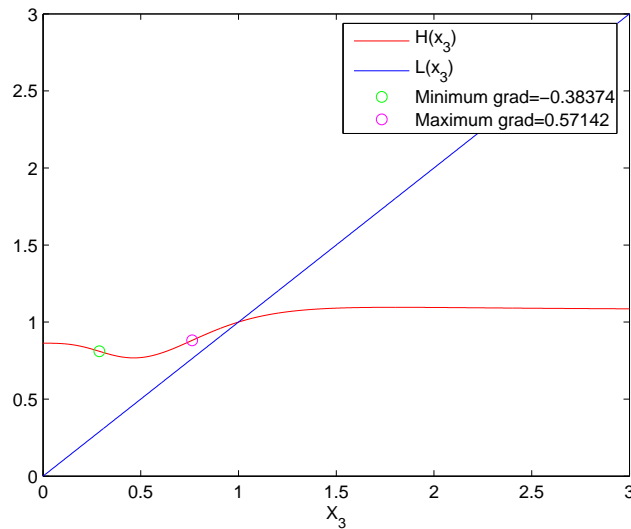


Figure 11.11: $H(X_3)$ plotted as a function of X_3 using the default parameter values for the scaled system with hippocampus i.e. the parameters given in table 10.4.

Investigation of a change in w_i

An increase in \tilde{w}_i will decrease the trapping region V (from equation 11.10). Furthermore we see in analogy to the calculations made for the system without hippocampal mechanisms that when all other parameters are fixed at their default values we are guaranteed global stability for

$$\hat{w}_1 \hat{w}_2 \hat{w}_3 > 0.57142 \tilde{w}_1 \tilde{w}_2 \tilde{w}_3. \quad (11.11)$$

Investigation of a change in α

First we will investigate the effect that α has on $\max |H'(X_3)|$. Since α still has an effect on the maximum gradient in the Hill functions we expect the maximum gradient will increase when α increases. But now it is not as simple as in the system without hippocampus. For the system including hippocampus α figures in both the negative feedback in the pituitary gland as well as in the negative feedback in hypothalamus and in the positive feedback in hippocampus. On figure 11.12 we have shown $H(X_3)$ with $\alpha = 1, 2, 3, 4, 5$.

We have investigated $\max |H'(X_3)|$ as a function of α for $\alpha = 1, 2, 3, 4, 5$. The results of the numerical investigations are given in table 11.4. For $\alpha \in 2, 3, 4$ the fixed point is guaranteed globally stable. As in the system without hippocampus changing the parameter α does not change the steady state solution of the system. This is also seen in figure 11.12 where the steady state of X_3 corresponds to the intersection between $L(X_3)$ and $H(X_3)$. It is worth noting there is only one intersection meaning there is only one fixed point for $\alpha \in \{1, 2, 3, 4, 5\}$.

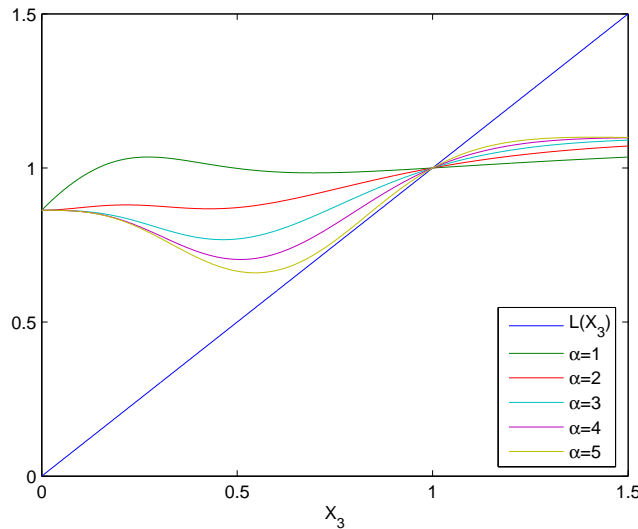


Figure 11.12: $L(X_3)$ and $H(X_3)$ for five different values of α . All other parameters are fixed at their default values.

α	$\max H'(X_3) $
1	1.2941
2	0.30161
3	0.57142
4	0.81411
5	1.0395

Table 11.4: $\max |H'(X_3)|$ as a function of α in the scaled system including hippocampal mechanisms. When all other parameters are fixed at their default values.

Investigation of a change in γ

Now we turn our attention to γ . This parameter also determines the steepness of a Hill function. But where α figured in both a positive feedback and a negative feedback function γ only figures in the negative feedback function in hippocampus. Therefore one would expect that the higher the value of γ the steeper decent in the beginning of $H(X_3)$ because γ is the power entering the Hill function with highest affinity. On figure 11.13 we have shown the graph of $H(X_3)$ with $\gamma \in 1, 2, 3, 4, 5$. In figure 11.13 it is seen that both $\max |H'(X_3)|$ and the intersection between $L(X_3)$ and $H(X_3)$ and thereby the steady state values is changing as a function of γ . Table 11.5 summarizes the investigation of these changes. It is worth noting that an increase in γ gives a decrease in the steady state concentrations. Fixing all other parameters at default values then for all reasonable values of γ we are guaranteed that H is a contraction.

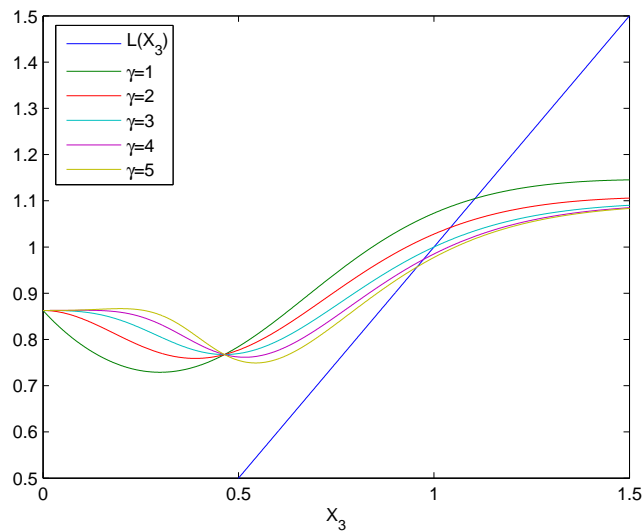


Figure 11.13: $L(X_3)$ and $H(X_3)$ for five different values of γ . When all other parameters are fixed at their default values.

γ	$\max H'(X_3) $	Steady state
1	0.92936	(0.4065, 0.2844, 1.1333)
2	0.5914	(0.3620, 0.2672, 1.0646)
3	0.57142	(0.3224, 0.2510, 1.0000)
4	0.59729	(0.1768, 0.1716, 0.6837)
5	0.63876	(0.1617, 0.1598, 0.6369)

Table 11.5: $\max |H'(X_3)|$ and the steady state solution as a function of γ in the scaled system including hippocampal mechanisms. All other parameters are fixed at their default values.

This guarantees a globally stable fixed point.

Investigation of a change in c_3

In figure 11.11 there is a characteristic well in $H(X_3)$ with a minimum for $X_3 \approx 0.5$. This valley comes from the negative feedback in hippocampus. The parameter \tilde{c}_3 determines the affinity for the negative feedback in hippocampus and thereby the value of X_3 for where the before mentioned valley is situated. A decrease in the parameter \tilde{c}_3 would mean an increasing affinity and thereby move this valley to the left. In figure 11.14 we show $H(X_3)$ when varying \tilde{c}_3 . Denoting the changed parameter by $\hat{\tilde{c}}_3$ we have changed the parameter such that $\hat{\tilde{c}}_3 = 1/2\tilde{c}_3$, $\hat{\tilde{c}}_3 = \tilde{c}_3$ and $\hat{\tilde{c}}_3 = 2\tilde{c}_3$. This corresponds to the affinity for cortisol binding to MR being respectively 20, 10 and 5 times that of GR. As seen on figure 11.14 \tilde{c}_3 is also determining the depth of the well. This is because the Hill functions enter into the overall feedback additively.

It can also be seen that \tilde{c}_3 has an effect on $H'(X_3)$ and the steady state solution. The effect is shown in table 11.6.

$\hat{\tilde{c}}_3$	$\max H'(X_3) $	Steady state
$1/2\tilde{c}_3$	1.4265	(0.2979, 0.2380, 0.9483)
\tilde{c}_3	0.57142	(0.3224, 0.2510, 1.0000)
$2\tilde{c}_3$	0.4271	(0.3881, 0.2837, 1.1306)

Table 11.6: $\max |H'(X_3)|$ and the steady state solution as a function of \tilde{c}_3 in the scaled system including hippocampal mechanisms. All other parameters are fixed at their default values.

Moreover the steady state solutions are locally stable.

Investigation of a change in ρ , ψ and ξ

As seen in the investigation of μ and ρ in the system without hippocampus the parameters in front of the Hill functions affect the steepness of $H'(X_3)$. Including the hippocampal mechanisms include a positive feedback with prefactor ξ thus an increase in ξ increase the largest positive gradient of $H(X_3)$ whereas an increase in ψ and ρ

give an increase in the absolute value of the largest negative gradient. Furthermore an increase in ξ cause an increase in the trapping region whereas the trapping region does not depend on ψ and ρ . To illustrate this we have made four graphs of $H(X_3)$ on figure 11.15. One where all values are at the default values. The rest only have on parameter perturbed: $\xi = 4$, $\rho = 1$ and $\psi = 1$. The effect of changing these parameters on $\max |H'(X_3)|$ and the steady state solution is written in table 11.7. Some combinations guarantees globally stable fixed points and some do not. However all steady state solutions are locally stable.

Parameter values	$\max H'(X_3) $	Steady state
$(\xi, \psi, \rho) = (2, 0.5, 0.5)$	0.57142	(0.3224, 0.2510, 1)
$(\xi, \psi, \rho) = (4, 0.5, 0.5)$	1.5988	(0.8404, 0.4883, 1.9455)
$(\xi, \psi, \rho) = (2, 1, 0.5)$	1.0921	(0.1379, 0.1337, 0.5327)
$(\xi, \psi, \rho) = (2, 0.5, 1)$	0.559	(0.2403, 0.1812, 0.722)

Table 11.7: The effect on $\max |H'(X_3)|$ and steady state when changing the parameters ξ , ψ or ρ . All other parameters are fixed at their default values.

Three steady state solutions

In this section we have investigated the behaviour of changing the parameters in the system including hippocampal mechanisms. It is obvious that we are able to change

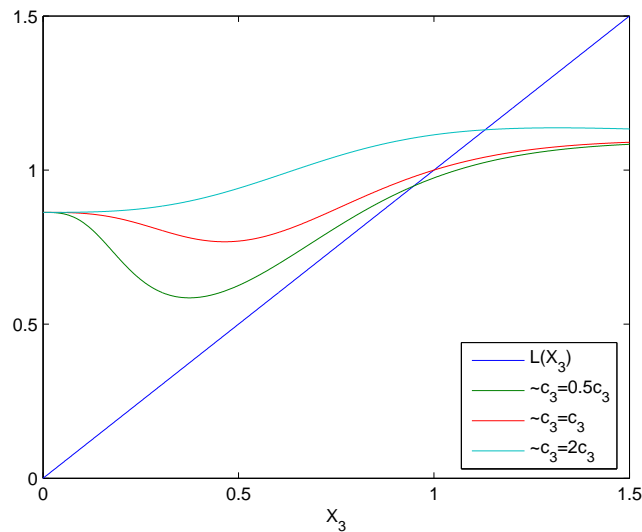


Figure 11.14: $H(X_3)$ shown when varying \tilde{c}_3 . All other parameters are fixed at their default values. Because of notational difficulties in matlab c_3 corresponds to \hat{c}_3 and c_3 corresponds to \tilde{c}_3 .

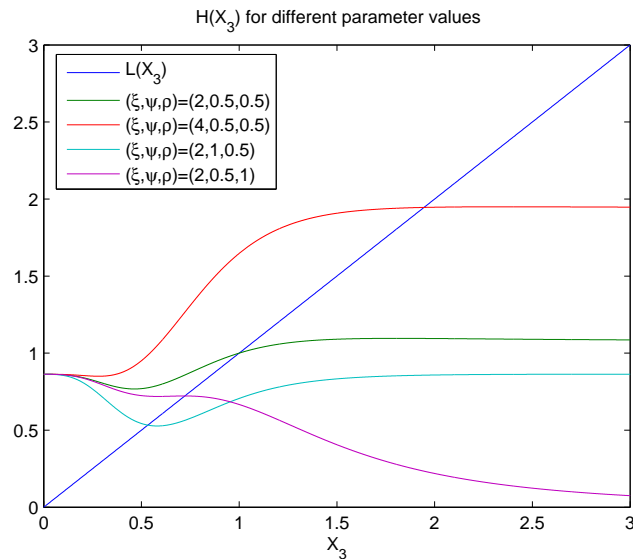


Figure 11.15: $H(X_3)$ for different values of (ξ, ψ, ρ) . All other parameters are fixed at their default values.

the parameters in such a way that there will be one, two or three intersections between $H(X_3)$ and $L(X_3)$. For what we believe to be reasonable parameter values we see only one intersection and thereby only one steady state solution which has been locally stable for all choice of parameter values. We will now investigate what dynamics that occur when there are three steady state solutions.

We start by using the default parameters and then use the knowledge about the effect of changing one parameter while keeping the rest at default values. The first thing we need to do is to move the minimum of the previously mentioned well down and/or to the right. From figure 11.12, 11.13 and 11.15 we know that an increase in α , γ and ψ have this effect. Thus by using the parameter values of $(\alpha, \gamma, \psi) = (5, 5, 1)$ and all other parameters fixed at their default values we obtain the graph of $H(X_3)$ shown in figure 11.16. The steady state solution is given by $(X_{1ss}, X_{2ss}, X_{3ss}) = (0.1133, 0.1164, 0.4637)$ and it is locally stable.

Now we wish to increase $\max H'(X_3)$. From figure we know that an increase in ξ will give the desired effect. Using the parameters $(\alpha, \gamma, \psi, \xi) = (5, 5, 1, 4)$ we obtain three intersections and thereby three steady state solutions. This is shown in figure 11.17.

So we see that with a continuous change in parameters additional fixed points will emerge i.e a bifurcation occurs. A qualitative bifurcation diagram can be seen in figure 11.18. In this figure the qualitative change in number of fixed points and their local stability is seen as a function of ξ .

If we denote the steady state solutions as \mathbf{X}_{ssi} where $i \in \{1, 2, 3\}$ and letting the lowest value of i correspond to the lowest value of X_3 that appears in the steady state solution we get that $\mathbf{X}_{ss1} = (0.1170, 0.1199, 0.4779)$, $\mathbf{X}_{ss2} = (0.2223, 0.2018, 0.8039)$

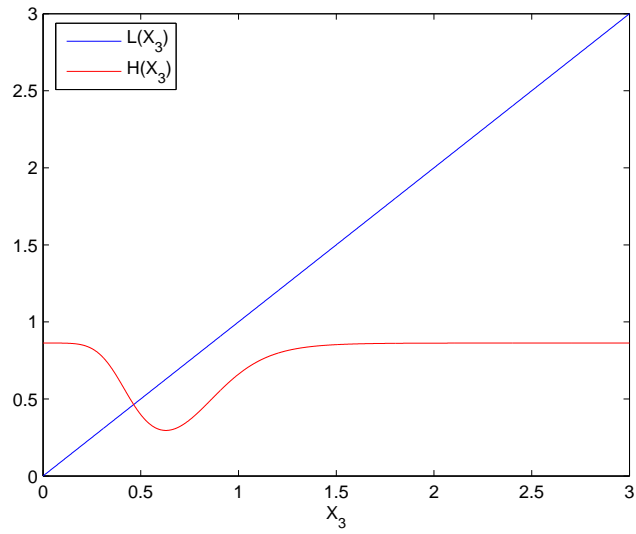


Figure 11.16: $H(X_3)$ for choice of parameters $(\alpha, \gamma, \psi) = (5, 5, 1)$ and all other parameters fixed at their default values.

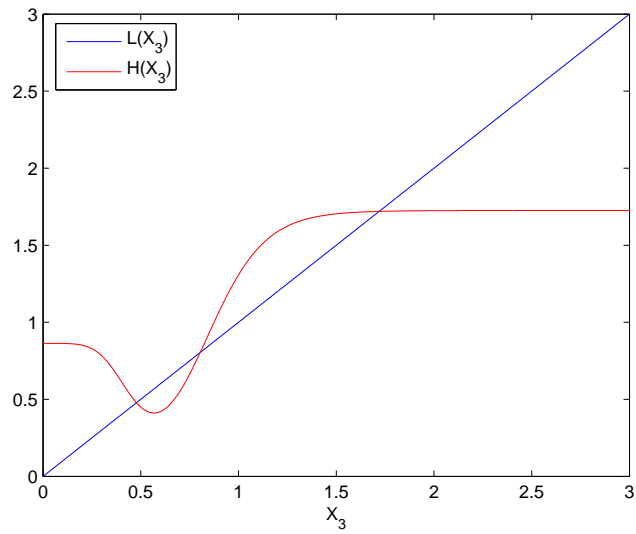


Figure 11.17: $H(X_3)$ for choice of parameters $(\alpha, \gamma, \psi, \xi) = (5, 5, 1, 4)$ and all other parameters fixed at their default values.

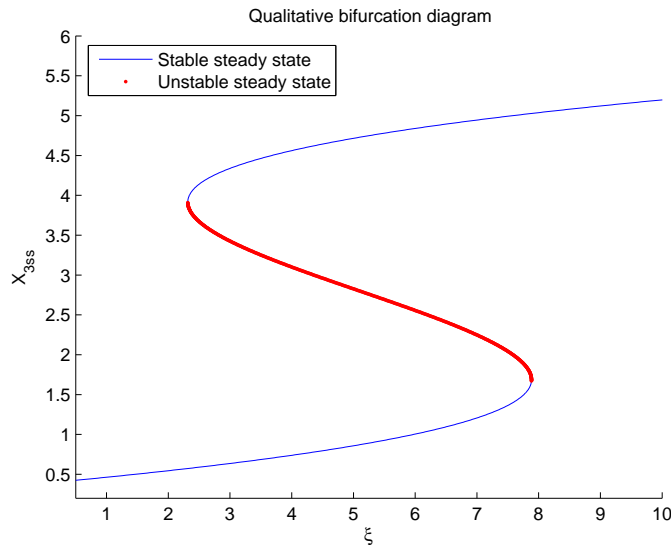


Figure 11.18: Qualitative bifurcation diagram. The number of fixed points and their local stability as a function of ξ .

and $\mathbf{X}_{ss3} = (0.7827, 0.4315, 1.7194)$. The eigenvalues of Jacobian evaluated at the three different steady state solutions are given in array 11.12.

$$\begin{aligned} \det(\mathbf{J}|_{\mathbf{X}_{ss1}} - \mathbf{I}\lambda) = 0 &\Leftrightarrow \lambda \in \{-4.8810, -0.5635 + 0.5096i, -0.5635 - 0.5096i\} \\ \det(\mathbf{J}|_{\mathbf{X}_{ss2}} - \mathbf{I}\lambda) = 0 &\Leftrightarrow \lambda \in \{-4.5500, -1.7146, 0.2567\} \\ \det(\mathbf{J}|_{\mathbf{X}_{ss3}} - \mathbf{I}\lambda) = 0 &\Leftrightarrow \lambda \in \{-4.7727, -1.0010, -0.2342\}. \end{aligned} \quad (11.12)$$

Thus from array 11.12 we see that the local stability of the three steady state solutions is such that \mathbf{X}_{ss1} is stable, \mathbf{X}_{ss2} is unstable and \mathbf{X}_{ss3} is locally stable.

To investigate the dynamics for these values of the parameters we have made a grid investigation of this system. The trapping region for this choice of parameters is $[0; 1.0431] \times [0; 1.0826] \times [0; 4.3137]$.

First we will investigate if all solutions enters the trapping region. This is done by making a grid investigation in the region $[0; 10] \times [0; 10] \times [0; 10]$ with a grid mask in the initial conditions of 1. The time of the simulation corresponds to three days. Four different colors are used to represent the different ending values as a function of initial conditions. Initial conditions with solutions converging towards \mathbf{X}_{ss1} are marked by a green dot. Initial conditions with solutions converging towards \mathbf{X}_{ss2} are marked by a black dot and initial conditions with solutions converging towards \mathbf{X}_{ss3} are marked by a yellow dot. The three steady state solutions are marked by a red ring and the solution value of the last simulated time are marked by a blue dot. The grid investigation is shown in figure 11.19.

As seen on figure 11.19 all solutions converge towards one of the two stable steady state solutions. Most of the solutions converge towards \mathbf{X}_{ss3} . We expect this to be

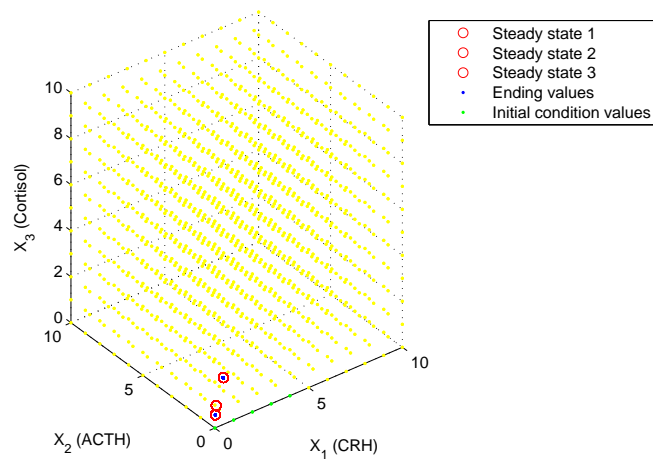


Figure 11.19: Investigation of points of convergence for different initial conditions. The initial conditions are marked by a yellow dot if the solution have converged to \mathbf{X}_{ss3} and a green dot if the solutions have converged to \mathbf{X}_{ss1} . For all solutions the last solution value was plotted as a blue dot. As seen these are all situated in the two stable steady states.

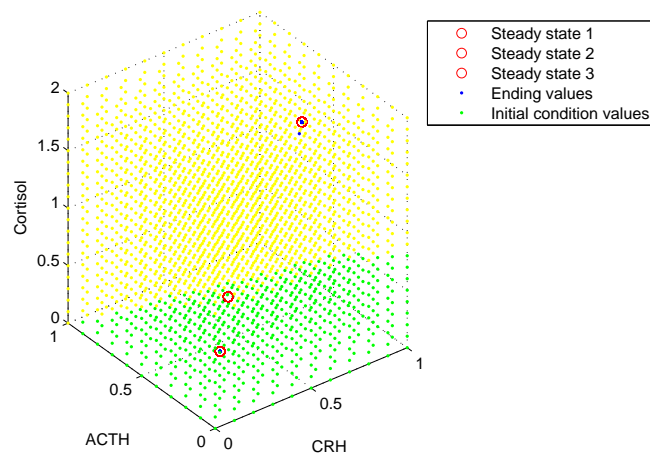


Figure 11.20: Investigation of points of convergence for different initial conditions. The initial conditions are marked by a yellow dot if the solution have converged to \mathbf{X}_{ss3} and a green dot if the solutions have converged to \mathbf{X}_{ss1} . For all solutions the last solution value was plotted as a blue dot. As seen these are all situated in the two stable steady states.

because most of the initial conditions are situated at much larger values for each component than the components of \mathbf{X}_{ss3} . In figure 11.19 we see that very few solutions converge to \mathbf{X}_{ss1} . Furthermore there are no solutions that do not converge to one of the two stable steady states. For this reason it does not seem likely that oscillations should occur even in the case of three steady state solutions.

Since the steady state solutions are situated close to each other and the solutions seems to converge towards these we have decided to make a smaller grid investigation. We make this in the region $[0; 1] \times [0; 1] \times [0; 2]$ with a grid masking of 0.1. This can be seen in figure 11.20

As seen the different initial conditions now cause the solutions to converge towards either \mathbf{X}_{ss1} or \mathbf{X}_{ss3} which are locally stable. Still there is no sign of oscillations.

In section 8.4 we presented a demand for a Hopf bifurcation to occur when $\xi > 0$. The demand was

$$\gamma/\tilde{c}_3 \geq \psi\gamma/\tilde{c}_3 \geq (\tilde{w}_2 + \tilde{w}_3)(\tilde{w}_1\tilde{w}_2 + \tilde{w}_1\tilde{w}_3 + \tilde{w}_2\tilde{w}_3) + \tilde{w}_1^2(\tilde{w}_2 + \tilde{w}_3). \quad (11.13)$$

If we insert the default parameter values we get

$$\gamma > 20.15. \quad (11.14)$$

This is an unreasonable high value of γ .

11.4 Summary of numerical analysis of the system including hippocampal mechanisms

The default parameters give $\max |H'(X_3)| < 1$ on the part of the trapping region corresponding to X_3 . This guarantees that a unique fixed point exists and it is globally stable. By varying one parameter at a time and keeping all other parameters fixed at their default values global stability of the unique fixed point is guaranteed for $\hat{w}_1\hat{w}_2\hat{w}_3 > 0.57142\tilde{w}_1\tilde{w}_2\tilde{w}_3$, $\alpha \in \{2, 3, 4\}$, $\gamma \in \{1, 2, 3, 4, 5\}$, $\rho = 1$ and $\hat{c}_3 = 2\tilde{c}_3$.

Perturbing one parameter within (what we consider as) reasonable values does not result in an unstable steady state. No limit cycles are detected within the trapping region.

Perturbing several parameters at the same time cause a bifurcation and thereby three steady state solutions. Two of the steady state solutions are locally stable and one is unstable with no complex eigenvalue with positive real part and non zero imaginary part. The grid investigation inside the trapping region for the system using these specific parameter values showed that solutions within the trapping region converge to one of the two stable fixed points.

The overall conclusion is that the chances of ultradian oscillations of the system seems to be minimal.

11.5 Including external function to model the circadian rhythm

In this section we wish to investigate how to model the circadian rhythm. In previous work this has been done by introducing a trigonometric function additively to the differential equation governing the concentration of CRH.

Since we are not able to achieve the desired ultradian oscillations this section will not be an in depth analysis but more an investigation out of interest.

In the following we have used the same approach as previously work. Since we do not have CRH data we will assume the circadian rhythm of ACTH to be the same as the circadian rhythm of CRH. We use fast Fourier transformation on our data to get the amplitudes of the first frequency. These frequencies and amplitudes will be our first guess to model the circadian rhythm. Since the previous work on estimation of parameters have been done on the healthy control people from the confidential data we will also use the mean circadian rhythm from these people.

To illustrate how to include the circadian rhythm we have chosen individual number eight from the confidential attachment. Using fast Fourier transformation we have masked the data. On figure 11.21 the data is presented using only the first 20 frequencies. Furthermore the circadian rhythm is shown. The circadian rhythm of this individual is

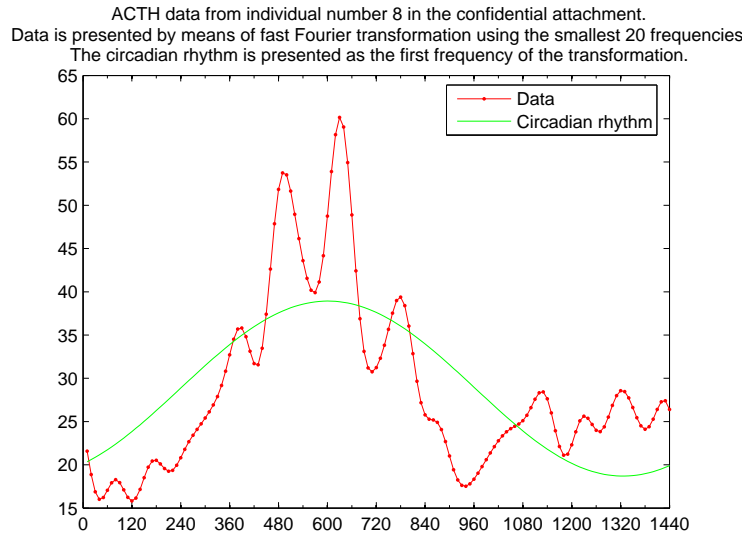


Figure 11.21: Masked data and circadian rhythm.

given as

$$f(t) = 28.8118 - 8.4992 \cos(2\pi/1440t) + 5.5438 \sin(2\pi/1440t) . \quad (11.15)$$

The units of the circadian rhythm is concentration. 28.8118 represents the mean value of ACTH. Since we wish to model the circadian rhythm on CRH and not on ACTH we express equation 11.15 in terms of the mean value \bar{x}_2 , that is

$$f(t) = \bar{x}_2 - 0.295\bar{x}_2 \cos(2\pi/1440t) + 0.1924\bar{x}_2 \sin(2\pi/1440t) . \quad (11.16)$$

Since we are now dealing with a single individual we wish to determine the specific parameters of this individual. We will use default parameters for all parameters except k_i . These parameters will be determined from the mean hormone level of this specific

individual. This is done as in chapter 10. The specific mean hormone concentrations of this individual is

$$\bar{x}_2 = 28.8118 \text{pg/ml} \quad (11.17)$$

$$\bar{x}_3 = 0.05 \cdot 5.0945 = 0.2547 \mu\text{g/dl} = 2.547 \text{ng/ml}. \quad (11.18)$$

The reader should remember that we only model the free cortisol but our data present the total amount of cortisol, both free and bound.

Since we do not have any data on CRH we will use the mean value of CRH that was presented in chapter 10. Estimating the parameters for this individual we get table 11.8.

Parameter	Our values
k_0	0.85876 ^{pg} /ml·min
k_1	0.17471 ¹ /min
k_2	8.0202·10 ⁻⁴ ¹ /min
w_1	0.17329 ¹ /min
w_2	0.034832 ¹ /min
w_3	0.0090726 ¹ /min
ρ	0.5
ψ	0.5
ξ	2
α	3
γ	3
c	2.547 ^{ng} /ml
c_3	1.1822 ^{ng} /ml

Table 11.8: Parameter values for the system including hippocampus for individual number 8 in the confidential attachment.

As we have seen in the previous sections a unique, stable fixed point exists. Then we investigate the effect of adding the circadian rhythm in the differential equations governing x_1 . The parameter A is the amplitude and the unit of A must be ¹/min. This parameter is necessary to avoid negative concentration.

So we achieve the following non autonomous system of differential equations

$$\begin{aligned} \frac{dx_1}{dt} &= k_0 \left(1 + \xi \frac{x_3^\alpha}{x_3^\alpha + c^\alpha} - \psi \frac{x_3^\gamma}{x_3^\gamma + c_3^\gamma} \right) - w_1 x_1 \\ &\quad + A (0.295 \cos(2\pi/1440t) + 0.1924 \sin(2\pi/1440t)) \\ \frac{dx_2}{dt} &= k_1 \left(1 - \rho \frac{x_3^\alpha}{x_3^\alpha + c^\alpha} \right) x_1 - w_2 x_2 \\ \frac{dx_3}{dt} &= k_2 x_2 - w_3 x_3. \end{aligned} \quad (11.19)$$

We have simulated this system with $A = 0.11$. The result for the concentration of ACTH is shown in figure 11.22 the simulation has been run for what corresponds to

three days. As seen it takes about a day for the system to be governed only of the time dependent input function.

On figure 11.23 the simulation of day three is shown, also the fitted circadian rhythm of ACTH is shown. We find the result reasonable compared to only changing the parameter A .

It seems that the peak of the circadian is shifted a little to the left. Therefore it seems as if the effect in hypothalamus does not affect the pituitary gland immediately. From figure 11.23 we see that the circadian rhythm seems to be shifted about 90 min. This means that if a phase difference about 90 min is reasonable we can model the circadian rhythm as

$$\begin{aligned}\frac{dx_1}{dt} &= k_0 \left(1 + \xi \frac{x_3^\alpha}{x_3^\alpha + c^\alpha} - \psi \frac{x_3^\gamma}{x_3^\gamma + c_3^\gamma} \right) - w_1 x_1 \\ &\quad + A (0.295 \cos(2\pi/1440(t + 90)) + 0.1924 \sin(2\pi/1440(t + 90))) \\ \frac{dx_2}{dt} &= k_1 \left(1 - \rho \frac{x_3^\alpha}{x_3^\alpha + c^\alpha} \right) x_1 - w_2 x_2 \\ \frac{dx_3}{dt} &= k_2 x_2 - w_3 x_3.\end{aligned}\tag{11.20}$$

If one wanted of course variation in amplitudes of both the sine and cosine function could give a better match.

In figure 11.24 and figure 11.25 we have plotted twenty first frequencies of the fast Fourier transformed data of person number eight along with the fitted diurnal rhythm and the simulation carried out using the above mentioned parameters for both ACTH and cortisol. These figures are without phase difference.

As seen in figure 11.24 and 11.25 the peak of the circadian rhythm seems to be shifted approximately 90 min. Therefore we have chosen to show the simulations from the system where there was a phase difference on 90 min on the external input in hypothalamus. These simulations are seen in figure 11.26 and 11.27.

As seen the amplitude of the simulated circadian rhythm of cortisol is too small. Maybe this can be improved by decreasing the value of the parameter ρ .

We find that the circadian rhythm imposed on the derivative of CRH in hypothalamus seems to give a good representation of the circadian rhythm in both cortisol and ACTH. We are a bit puzzled about the fact that a phase difference of 90 minutes gives a better fit of the position of the peak in the circadian rhythm. Furthermore there seems to be a delay of the circadian peak in cortisol compared to that of ACTH on around 90 minutes. This is seen in both the data and our simulation. We find it surprising that there seems to be an inherent delay between the two compartments. We have not studied enough data to know if this is a characteristic that the HPA axis is supposed to have. We therefore leave this for further studies.

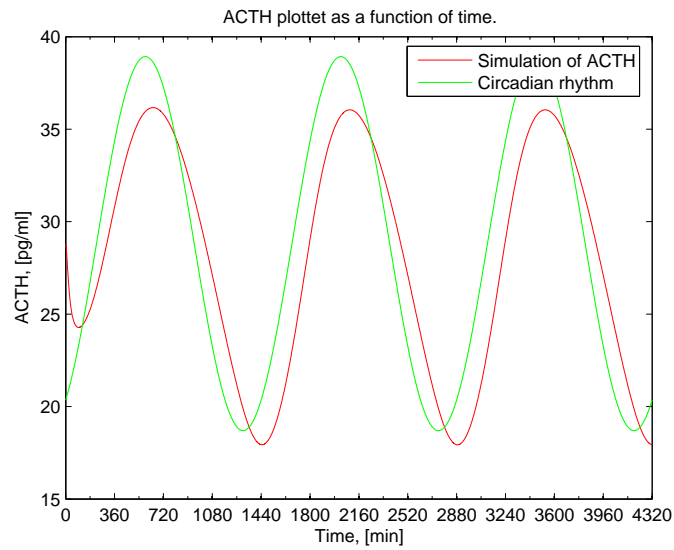


Figure 11.22: The circadian rhythm from fast Fourier transformation and the solution curve to array 11.19 of ACTH using the parameters given in table 11.8 and $A = 0.11$.

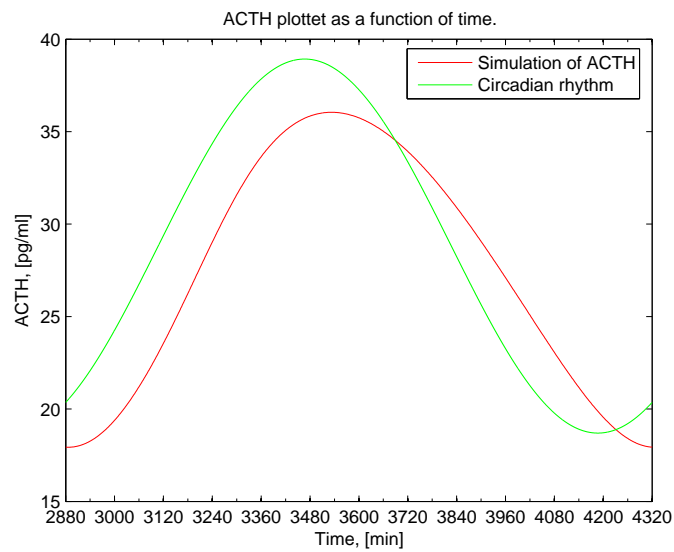


Figure 11.23: The circadian rhythm from fast Fourier transformation and the solution curve to array 11.19 of ACTH using the parameters given in table 11.8 and $A = 0.11$. Here we only show day three.

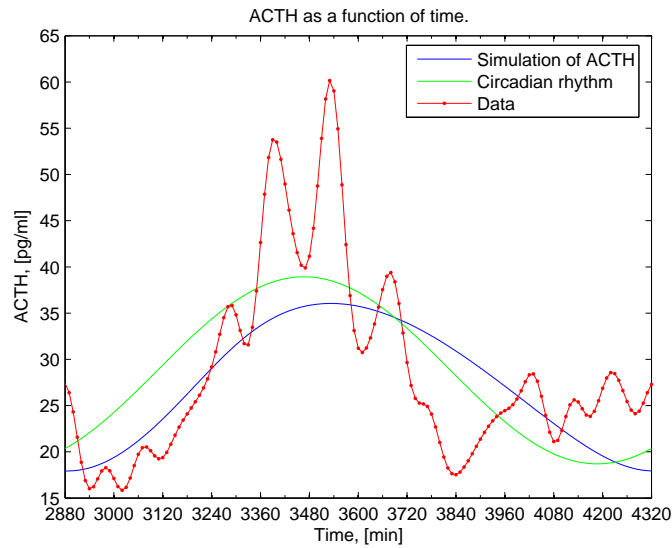


Figure 11.24: The twenty first frequencies of the fast Fourier transformed ACTH data from person number 20 in the confidential attachment. Along with the circadian rhythm and the simulation using the parameters given in table 11.8 and $A=0.11$.

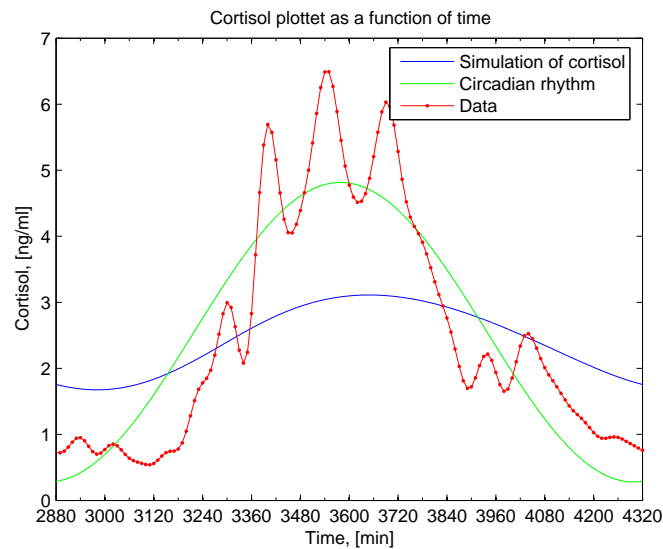


Figure 11.25: The twenty first frequencies of the fast Fourier transformed cortisol data from person number 20 in the confidential attachment. Along with the circadian rhythm and the simulation using the parameters given in table 11.8 and $A=0.11$.

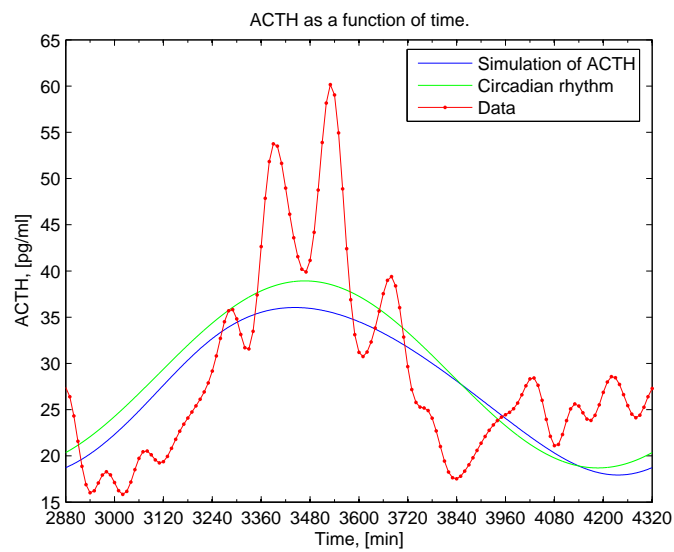


Figure 11.26: The twenty first frequencies of the fast Fourier transformed ACTH data from person number 20 in the confidential attachment. Along with the circadian rhythm and the simulation using the parameters given in table 11.8 and $A=0.11$. There has been implemented a phase difference of 90 min in the external function.

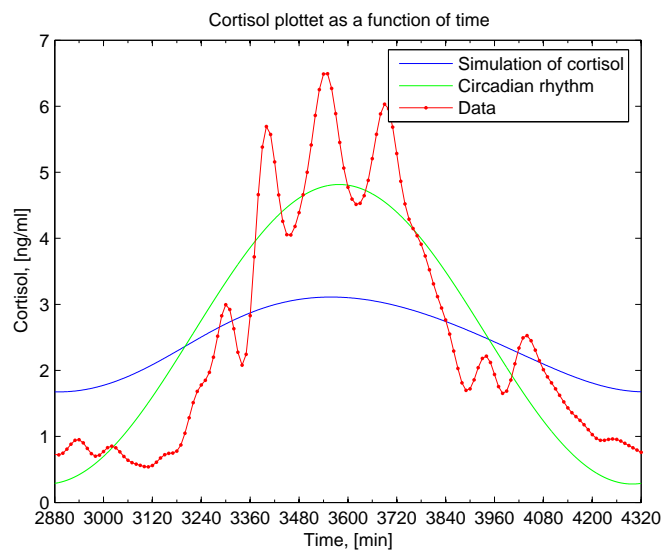


Figure 11.27: The twenty first frequencies of the fast Fourier transformed ACTH data from person number 20 in the confidential attachment. Along with the circadian rhythm and the simulation using the parameters given in table 11.8 and $A=0.11$. There has been implement a phase difference of 90 min in the external function.

12 Discussion

First we summarize some of the main results of our models. We have expanded the complexity of our models of the HPA axis and tried to generalize the arguments along with this. Quite often the same kind of arguments were used. However reusing arguments on different systems emphasize some common properties of the systems. Therefore it became possible to generalize after these special cases has been considered. In this overview we will revert the order and start with the most general results.

12.1 Most general results

With a scaling making concentrations and time dimensionless all our models are contained in the following differential equations 12.1. The autonomous system of differential equations is without circadian stimulation on the derivative of CRH.

$$\begin{aligned}\dot{X}_1 &= F_1(X_3) - \tilde{w}_1 X_1 \\ \dot{X}_2 &= F_2(X_3) X_1 - \tilde{w}_2 X_2 \\ \dot{X}_3 &= X_2 - \tilde{w}_3 X_3.\end{aligned}\tag{12.1}$$

with $\tilde{w}_1, \tilde{w}_2, \tilde{w}_3 > 0$ and with the following criteria on $F_1(X_3), F_2(X_3)$ (using $\tilde{D} \equiv \mathbb{R}_+ \cup \{0\}$)

$F_1, F_2 : \tilde{D} \rightarrow \tilde{D}, F_1(0) > 0, F_2(0) > 0, \sup(F_1(\tilde{D})) \leq M_1 \in \tilde{D}, \sup(F_2(\tilde{D})) \leq M_2 \in \tilde{D}, F_1, F_2 \in C^1, \forall X_3 \in \tilde{D}.$

F_1 and F_2 are bounded functions mapping non negative numbers to non negative numbers. The boundedness of the feedback functions can be justified by a saturation mechanism of the receptors that cortisol must occupy in order to perform a feedback. When there is no cortisol the feedback functions must not totally inhibit positive stimulation of hormone production. Therefore $F_1(0) > 0$ and $F_2(0) > 0$.

From this very general model we can conclude

- Existence and uniqueness of solutions is guaranteed by theorem 3.1.

Trapping region

- Non negative initial conditions lead to solutions that stay non negative for all future time.
- A trapping region exists $V = I_1(0) \times I_2(0) \times I_3(0)$ meaning that solutions in U stay the region stay bounded for all future time.
- Solutions with non negative initial conditions outside the trapping region converge to or enter the trapping region with increasing time. This assures the 'interesting' dynamics of the system is contained in the trapping region since e.g. fixed points and limit cycles cannot exist outside the trapping region.

Fixed points

- At least one fixed point exists within the trapping region.
 - If $\frac{1}{\bar{w}_1\bar{w}_2\bar{w}_3} \frac{d(F_1(X_3)F_2(X_3))}{dX_3} < 1$ on $I_3(0)$ then only one fixed point exists.
 - * $dF_1(X_3)/dX_3 < 0$ and $dF_2(X_3)/dX_3 < 0, \forall X_3 \in I_3(0)$ guarantees $\frac{1}{\bar{w}_1\bar{w}_2\bar{w}_3} \frac{d(F_1(X_3)F_2(X_3))}{dX_3} < 1, \forall X_3 \in I_3(0)$. Therefore if $F_1(X_3)$ and $F_2(X_3)$ corresponds to a negative feedback for all concentrations then the fixed point is unique.

Stability of fixed point(s)

- Assume $dF_2(X_3)/dX_3 < 0, \forall X_3 \in \tilde{D}$. This corresponds to a negative feedback from cortisol on ACTH. This assumption is used for the following characterization of fixed points and for our two models this assumption is also used.

The characteristic polynomial at the fixed point is on the form

$$P(\lambda) = \lambda^3 + \alpha_1\lambda^2 + \alpha_2\lambda + \alpha_3.$$

- If $dF_1(X_{3ss})/dX_3 < 0$ the stability of the fixed point is determined by $\text{sign}(\alpha_1\alpha_2 - \alpha_3)$.
 - If $\alpha_1\alpha_2 - \alpha_3 > 0$ the fixed point is stable.
 - If $\alpha_1\alpha_2 - \alpha_3 < 0$ the fixed point is unstable and the roots of the characteristic polynomial have one real, negative root and a set of complex conjugate roots with positive real part and non zero imaginary part.
 - If a continuous change in a parameter leads to continuous change in $\alpha_1\alpha_2 - \alpha_3$ from negative to positive values then a Hopf bifurcation occurs where a limit cycle is guaranteed (however it may be of physiologically irrelevant size).
- If $dF_1(X_{3ss})/dX_3 = 0$ the fixed point is stable.
- If $dF_1(X_{3ss})/dX_3 > 0$ the stability of the fixed point is determined by sign of α_3 .
 - If $\alpha_3 > 0$ the fixed point is stable.
 - If $\alpha_3 < 0$ the fixed point is unstable. There is at least one real, positive root of the characteristic polynomial. In case of complex roots with nonzero imaginary part then the real part is negative.
 - A Hopf bifurcation is impossible if a continuous change in a parameter leads to α_3 continuously changing from negative to positive values.

This listing of different cases will now proceed as we make some further restrictions on the feedback functions.

- If $\frac{1}{\bar{w}_1\bar{w}_2\bar{w}_3} \left| \frac{d(F_1(X_3)F_2(X_3))}{dX_3} \right| < 1, \forall X_3 \in I_3(0)$ then only one fixed point exists and the fixed point is globally asymptotically stable. This is a major result that eliminates the possibility of existence of limit cycles of systems where cortisol can exert positive as well as negative feedback on CRH.

12.2 Results of model including hippocampal dynamics

Now we focus on the results of our model including hippocampal mechanisms where four feedbacks occur. One negative feedback from cortisol on ACTH, a negative feedback from cortisol on CRH in hypothalamus and a negative as well as a positive feedback from cortisol on CRH acting through hippocampal receptors. This lead to the feedback functions

$$F_1(X_3) = 1 + \xi \frac{X_3^\alpha}{1 + X_3^\alpha} - \psi \frac{X_3^\gamma}{\tilde{c}_3^\gamma + X_3^\gamma}, \quad (12.2)$$

with $\xi \geq -1$, $\psi \in [0; 1 + \xi] \cap [0; 1]$, $\tilde{c}_3 > 0$ and α, γ are a positive integers.

$$F_2(X_3) = 1 - \rho \frac{X_3^\alpha}{1 + X_3^\alpha}, \quad (12.3)$$

with $\rho \in [0; 1]$.

- If

$$\frac{\xi\alpha}{\tilde{w}_1\tilde{w}_2\tilde{w}_3} \leq 1, \quad (12.4)$$

then exactly one fixed point exists.

- For small values of ξ only one fixed point exists. However increasing the value of ξ make more steady state solutions possible.
- A necessary condition for a Hopf bifurcation is $dF_1(X_{3ss})/dX_3 < 0$ at some fixed point and

$$\gamma/c_3 \geq \psi\gamma/c_3 \geq (\tilde{w}_2 + \tilde{w}_3)(\tilde{w}_1\tilde{w}_2 + \tilde{w}_1\tilde{w}_3 + \tilde{w}_2\tilde{w}_3) + \tilde{w}_1^2(\tilde{w}_2 + \tilde{w}_3) \quad \text{for } \xi \geq 0. \quad (12.5)$$

This condition requires unphysiologically large values of γ for physiologically values of \tilde{c}_3 , \tilde{w}_1 , \tilde{w}_2 and \tilde{w}_3 .

- Simulations show that in the case of one fixed point this is stable. Another observed case is three fixed points. In this case the larger and lower value of X_{3ss} corresponds to stable fixed points and the one in the middle is unstable with one real, positive root of the characteristic polynomial and no complex roots with nonzero imaginary parts have a positive real part. This means at this fixed point $\frac{dF_1(X_{3ss})}{dX_3} > 0$.

For all simulations the long term behavior of solutions showed 'convergence' to a fixed point. This was investigated for one and three fixed points of the system. Therefore the possibility of existence of limit cycles seems minimal. In the case of three fixed points the trapping region seemed to be divided into one basin of attraction for each stable fixed point.

Moreover we were able to determine conditions for each parameter that guaranteed global stability of a unique fixed point. This was determined when all other parameters were fixed at their default values. Using default values for all parameters guarantee a globally stable fixed point.

12.3 Results of the model excluding hippocampal mechanisms

Now we focus on our model not including hippocampal mechanisms which means that there is a negative feedback on CRH from cortisol

- $\frac{dF_1(X_3)}{dX_3} \leq 0$ on \tilde{D} ensures exactly one fixed point.

We have considered some specific choices of $F_1(X_3)$ and $F_2(X_3)$ based on receptor dynamics.

$$F_1(X_3) = 1 - \mu \frac{X_3^\alpha}{1 + X_3^\alpha} \quad (12.6)$$

$$F_2(X_3) = 1 - \rho \frac{X_3^\alpha}{1 + X_3^\alpha}, \quad (12.7)$$

with $\rho, \mu \in [0; 1]$ and α is an integer value.

- All solutions enter the trapping region in finite time.
- The fixed point is asymptotically stable for $\alpha < 8$ which means the fixed point is stable for reasonable values of α and a Hopf bifurcation of the fixed point is thus impossible.
- Physiologically relevant parameters are found from literature. The remaining parameters are estimated from an assumption that the fixed point value is at the mean value of the hormone levels.
 - All simulations show solution curves converging to the unique fixed point. However $\max \left| \frac{1}{\bar{w}_1 \bar{w}_2 \bar{w}_3} \frac{d(F_1(X_3)F_2(X_3))}{dX_3} \right| > 1$ using default parameters. We were able to determine the size of perturbation to one of the default parameters that caused $\max \left| \frac{1}{\bar{w}_1 \bar{w}_2 \bar{w}_3} \frac{d(F_1(X_3)F_2(X_3))}{dX_3} \right| < 1$ which analytically guarantees a globally stable fixed point.
 - All simulations of the long term behaviour of solutions converged to the fixed point. Therefore existence of limit cycles seem unlikely.

12.4 Comparing the results to state of the art models

This discussion aim trelate the results of this projecte to state of the art models of the HPA axis especially the models of Kyrylov et al and Jelic et al. that have already been described. Kyrylov et al. investigate a five dimensional model of the HPA axis [1]. Assuming fast dynamics between the bound forms of cortisol the model can be reduced to a three dimensional model. Except for the direct CRH -cortisol stimulation bypassing ACTH the model without bound forms of cortisol has also been investigated in a previous work of Kyrylov et al [23]. The idea of investigating a linear system first is used. Using (problematic) parameters the predominant result is a set of complex conjugate eigenvalues with non zero imaginary part and one real negative eigenvalue. Then non linearities are added. The non linearities ensure that hormones do not become negative and make sure that the derivative of the concentrations have an upper bound. No argument that the concentrations are bounded is used. Comparing to our model with or without hippocampus the saturation mechanisms from receptor dynamics make sure that the concentrations are bounded and also it is evident from the differential equations that the concentrations cannot become negative when the initial conditions are non negative. This means a trapping region exists for our system which is a physiological desirable property that makes sure solutions having 'reasonable' values at some time stay 'reasonable' for all future time. Thus in our model the non linearities are an inherent part of the model build on physiological reasoning.

Jelic et al. [2] describes the mechanisms of hippocampus that we have used in one of our models. However Jelic et al. disregards the feedback from cortisol on CRH and the

system of differential equations follow from a reaction scheme that lacks justification. The system is non trivially reduced from a four dimensional system to a two dimensional. Then a limit cycles exists due to the assumptions of the values of parameters and by use of Theorem of Poincaré-Bendixon that may only be applied on twodimensional systems.

The conclusion of our work is thus inconsistent with the conclusions in [2] and [1].

In our view the field in general is characterized by diverging papers. For example [6] argues that ACTH and CRH can be pooled in one compartment since the two concentrations 'have a strong and fast synchrony'. This is inconsistent with [2] where the CRH dynamics is considered slow compared to the ACTH dynamics thus leading to the assumption $d^{CRH}/dt = 0$ while still considering the dynamics of ACTH. Nevertheless [6] cites [2] without pointing out this important difference in the approaches. Another problem in general is the description of the ultradian oscillations of the system. Some authors [1, 2] argue that these should be inherent to the system. Other authors [3, 6] argue that the fixed points are stable. In case ultradian oscillations are considered this behavior is simply a response to an outer, ultradian stimuli (a forcing function with ultradian frequency) as in [3].

12.5 Typical mathematical approaches when non linear differential equations are used for modeling

Only rarely can a non linear system of differential equations be solved. However often it is still possible to show existence and uniqueness of solutions using theorem 3.6. In the two dimensional case the Poincaré Bendixson theorem may be used to guarantee existence of limit cycles. Comparing the model to reality can be done using numerical integration of the differential equations. This requires choice of parameters as well as initial conditions. This approach give a finite number of solutions of the differential equations for specific parameters and initial conditions. If e.g. no periodic solutions are observed then one may be tempted to say there is no periodic solutions of the system in general. However investigating a finite number of solution curves in a continuum of solution curves can never constitute a proof. Then what can be done? Some look for Hopf bifurcation of fixed points since this guarantees existence of a limit cycle (however the limit cycle may be so small that it is not physiologically relevant). This resembles the approach of Kyrylov et al. where the interesting results for the linear system is a set of complex conjugate eigenvalues with real part and one negative real eigenvalue.

Savic and Jelic [3] make models of the HPA axis using CRH, ACTH and cortisol as variables. They make models of increasing complexity as the model fail to show oscillations. Since the fixed point of their models are stable no Hopf bifurcations are possible. From this they conclude that no periodic solutions are present and the 'systems' are stable. However there is quite a long way from a fixed point being locally stable to globally stable. Their analysis showed that the system is locally stable and no simulations were used to show that initial conditions 'far' from the fixed point would be attracted to the fixed point. Because stability of fixed points is one of the few things that often can be analyzed rigorously then failure of limit cycles through Hopf bifurcations may wrongly be converted to an argument that no limit cycles exists for the system in general.

12.6 Inclusion of circadian rhythm

In analogy with previous work we decided to model the circadian rhythm additively in the differential equation governing CRH. Under the assumption that the circadian rhythm is caused by external factors like sunlight etc. a splitting of the dynamics of circadian and ultradian oscillations seems physiologically relevant.

Because of our access to data of ACTH and cortisol we reasoned that the circadian rhythm could be presented as the first component of the fast Fourier transformation. A hypothesis that the circadian rhythm in CRH could be modeled by a scaling of the circadian rhythm in ACTH gave reasonable results. Although we did not make an in depth analysis of the circadian rhythm we were able to conclude that adding a trigonometric function in the differential equation governing CRH was able to show the circadian rhythm in ACTH and cortisol. When reaching this conclusion we found it puzzling that a delay of 90 minutes lead to almost perfect fit in the peaks of the circadian rhythm in both ACTH and cortisol.

12.7 Conclusion

We have made two deterministic models of the HPA axis containing well known physiological mechanisms. A trapping region is found for both models and all solutions outside the trapping region converge to or enter the trapping region. This guarantees that solutions to the system correspond to reasonable levels in hormone concentration. All fixed points of the systems are located inside the trapping regions.

For the model without hippocampus a unique fixed point exists. For physiologically reasonable parameters it is analytically shown that this fixed point is stable thus a Hopf bifurcation causing a limit cycle is impossible.

We have made a thorough investigation of fixed points and stability of fixed points searching for ultradian oscillations. We put forward an easily applicable criteria on the feedback functions and parameters that guarantee existence of a globally stable fixed point. This criteria is fulfilled for some sets of physiologically reasonable parameter values for both models.

Using physiologically reasonable parameter values for both models no oscillating solutions are found. In some cases analytical arguments are applied and in some cases numerical investigations are used. All simulations showed the long term behaviour of a solution is convergence to a fixed point.

The generality of many of our results rules out existence of periodic solutions in a range of three dimensional models with feedback functions.

We can conclude that an external imposed function on CRH is able to produce the circadian rhythm in both ACTH and cortisol.

13 Discussion: Modeling of HPA axis including time delay

In the models of the HPA axis considered in this project the derivative of the cortisol concentration depends on the instant value of the ACTH concentration. However it takes some time for ACTH to move with the bloodstream and stimulate the adrenal glands to create cortisol. Therefore it makes sense to include a time delay τ which is needed before ACTH stimulate the cortisol production such that the derivative of cortisol depends on $\text{ACTH}(t - \tau)$ instead of $\text{ACTH}(t)$. The argument for a time delay from ACTH to cortisol can be made to all cites where one hormone is affecting another hormone. Either by a delay caused by the transport with the bloodstream and/or time of receptor binding.

Including a time delay in differential equations may have a destabilizing effect [19]. Therefore inclusion of time delays may force a stable fixed point into an unstable fixed point which may lead to a limit cycle.

Including time delays the system of differential equations with no diurnal input on the CRH derivative can be written (modifying array 8.5 by including time delays)

$$\begin{aligned}
 \frac{dx_1}{dt} &= k_0 \left(1 - \mu \frac{(x_3(t - \tau_1))^\alpha}{(x_3(t - \tau_1))^\alpha + c^\alpha} + \phi \frac{(x_3(t - \tau_2))^\alpha}{(x_3(t - \tau_2))^\alpha + c^\alpha} \right. \\
 &\quad \left. - \psi \frac{(x_3(t - \tau_3))^\gamma}{(x_3(t - \tau_3))^\gamma + \tilde{c}_3^\gamma} \right) - w_1 x_1 \\
 \frac{dx_2}{dt} &= k_1 \left(1 - \rho \frac{(x_3(t - \tau_4))^\alpha}{(x_3(t - \tau_4))^\alpha + c^\alpha} \right) x_1(t - \tau_5) - w_2 x_2 \\
 \frac{dx_3}{dt} &= k_2 x_2(t - \tau_6) - w_3 x_3.
 \end{aligned} \tag{13.1}$$

Since a fixed point solution has the property that $\mathbf{x}_{ss}(t_1) = \mathbf{x}_{ss}(t_2)$ for any t_1 and t_2 we can find the fixed points for the simpler case with $\tau_1 = \tau_2 = \tau_3 = \tau_4 = \tau_5 = \tau_6 = 0$. This means that there exists at least one fixed point due to our previous analysis. However when finding the stability of the fixed points the time delays cannot be neglected. It can be much more difficult to analyze this than the corresponding system without time delay.

The time delay model of Savic et al.

A model without hippocampal mechanisms has been investigated analytically by Savic et al. in [4]. The model corresponds to array 13.1 with the choice of parameters $\phi =$

$\psi = 0$ and $\alpha = 1$.

$$\begin{aligned}\frac{dx_1}{dt} &= k_0 \left(1 - \mu \frac{x_3(t - \tau_1)}{x_3(t - \tau_1) + c} \right) - w_1 x_1 \\ \frac{dx_2}{dt} &= k_1 \left(1 - \rho \frac{x_3(t - \tau_4)}{x_3(t - \tau_4) + c} \right) x_1(t - \tau_5) - w_2 x_2 \\ \frac{dx_3}{dt} &= k_2 x_2(t - \tau_6) - w_3 x_3.\end{aligned}\tag{13.2}$$

The analysis of Savic et al. can be categorized as

- The system with all time delays equal zero result in a stable fixed point (this also follows from our previous analysis).
- Rouché's theorem¹ is used to compare the eigenvalues of the system with zero time delays to the system with arbitrary, positive values of the time delays. This smart approach requires a choice of a contour that defines the domain where the eigenvalues from the two systems are compared.
- Savic et. al finds a sufficient criteria for the system to have a stable fixed point, that is $B > 0$ with

$$B \equiv abX_{3ss}^3 + (b(1 + 2a) - \mu)X_{3ss}^2 + (a + 2b - \mu b)X_{3ss} + 1.\tag{13.3}$$

Here $a = 1 - \mu$ and $b = 1 - \rho$. The value of $X_{3ss} = x_{3ss}/K_d$ is estimated from $x_{3ss} = 10\mu g/dL = 276nmol/L$, $K_d = 18nmol/L$ giving $X_{3ss} = 15$. Inserting this in 13.3 Savic et al. claims that $B > 0$. This means that no time delays can force the stable fixed point into an unstable fixed point.

We investigate the condition $B > 0$ by inserting for a and b .

$$\begin{aligned}B &= (1 - \mu)(1 - \rho)X_{3ss}^3 + (2(1 - \mu)(1 - \rho) + 1 - \mu - \rho)X_{3ss}^2 + \\ &((1 - \mu)(1 - \rho) + (1 - \mu) + (1 - \rho))X_{3ss} + 1.\end{aligned}\tag{13.4}$$

For $\mu = \rho = 1$ we get $B_{1,1} = -X_{3ss}^2 + 1$. Since $X_{3ss} \approx 15$ then $B_{1,1} < 0$. Thus for large values of μ and ρ the conditions for applying Rouché's theorem are not fulfilled by the argument of Savic et al. It is worth noting that Savic et al. assume $a \ll 1$, $b \ll 1$ meaning that μ and ρ are close to 1.

It should be noted that for $\rho = \tau_1 = \tau_4 = \tau_5 = 0$, $\mu = 1$ the system 13.2 is mathematically equivalent to a system modeling the testosterone production [19]. Here sufficiently large values of τ_6 leads to a Hopf bifurcation. Since this choice of parameters give a subset of the cases considered by [4] it should be clear that the argumentation of the asymptotic stable fixed point in [4] is deficient. However it may be the case that the fixed point in array 13.2 is stable for *physiologically relevant* parameters and time delays. It just means we have no knowledge about it.

¹ In [32] Rouché's theorem is stated for a complex variable z as: 'If two functions $f(z)$ and $g(z)$, are analytic inside and on the closed contour C , $f(z)$ has no zeros on C and $|f(z) - g(z)| < |f(z)|$ on C , then $g(z)$ and $f(z)$ have the same number of zeros inside C '.

A simpler model including delay differential equations by Savic and Jelic

Savic and Jelic [3] have investigated a system very similar to the model of testosterone but with the conclusion that physiologically relevant parameters does not lead to a Hopf bifurcation. We will discuss this now since we disagree with their reasoning and conclusion.

The model in [3] is contained in the model in [4] since array 13.2 reduce to the model in [3] by a restriction of parameters $\tau_1 = \tau_4 = \tau_5 = 0$.

$$\begin{aligned}\frac{dx_1}{dt} &= k_0 \left(1 - \mu \frac{x_3}{x_3 + c} \right) - w_1 x_1 \\ \frac{dx_2}{dt} &= k_1 \left(1 - \rho \frac{x_3}{x_3 + c} \right) x_1 - w_2 x_2 \\ \frac{dx_3}{dt} &= k_2 x_2 (t - \tau_6) - w_3 x_3.\end{aligned}\tag{13.5}$$

One fixed point exists and it is stable for $\tau_6 = 0$. The question is whether $\tau_6 > 0$ can lead to a Hopf bifurcation when the parameters of the model have reasonable values. Savic and Jelic conclude that the fixed point is stable for all time delays and reasonable choice of parameters which is consistent with their conclusion in [4]. However we do not consider this conclusion valid. We will not go through the entire paper but jump to the problematic part. We have from [3] (but using our notation from previous chapters)

$$\begin{aligned}X_{3ss} &= \frac{x_{3ss}}{c} \\ a &= 1 + X_{3ss}(1 - \rho) \\ b &= 1 + X_{3ss}(1 - \mu) \\ F &= \frac{X_{3ss}(\mu a + \rho b)}{(1 + X_{3ss})ab} - 1.\end{aligned}\tag{13.6}$$

Jelic and Savic formulate the condition that there exists a time delay, τ_6 causing a Hopf bifurcation as $F > 0$. $F \leq 0$ guarantees that no Hopf bifurcation occurs for any time delay. They find for $\mu = 0.98$ and $\rho = 0.72$ $F \leq 0$ for all $X_{3ss} \geq 0$ and this guarantee their conclusion. However there is no discussion of why μ and ρ should have these values though μ is assumed to be close to one. Inserting in F for array 13.6.

$$F = \frac{X_{3ss}}{1 + X_{3ss}} \left(\frac{\mu}{1 + X_{3ss}(1 - \mu)} + \frac{\rho}{1 + X_{3ss}(1 - \rho)} \right) - 1.\tag{13.7}$$

With $\mu, \rho \in [0, 1]$ we have F is increasing in μ and ρ and $F(\mu, \rho) \in [-1; \frac{2X_{3ss}}{1+X_{3ss}} - 1]$. This means $F(\mu, \rho, X_{3ss}) \leq F(1, 1, X_{3ss})$. This makes sense compared to our analysis of the system without hippocampus where $\mu = \rho = 1$ gave the case with largest chance of instability and Hopf bifurcation. Using $\mu = \rho = 1$ we get a bound for what values of X_{3ss} that can lead to Hopf bifurcation

$$\frac{X_{3ss}}{1 + X_{3ss}} \left(\frac{1}{1 + X_{3ss}(1 - 1)} + \frac{1}{1 + X_{3ss}(1 - 1)} \right) - 1 > 0 \Leftrightarrow X_{3ss} > 1.\tag{13.8}$$

This means that for $\mu = \rho = 1$ then a Hopf bifurcation occurs for some $\tau_6 > 0$ at the fixed point for $X_{3ss} > 1$. In [3] Savic and Jelic state that $X_{3ss} \in [50; 100]$ and

in [4] Savic and Jelic state that $X_{3ss} = 15$. In either case $X_{3ss} > 1$ which means a Hopf bifurcation occurs for some time delay which contradicts the conclusion of [3] and [4]. However this is a promising outcome for future modeling of the HPA-axis using delay differential equations since a limit cycle is then guaranteed. Of course the time delay(s) cannot attain physically irrelevant size(s) which must be investigated in depth in future research. However the analysis above show that when the remaining parameters have physiologically relevant size then a Hopf bifurcation is possible when a time delay is included.

13.1 Inclusion of time delay in our system

In this section we will show that introducing a time delay in our model will give an unstable steady state. The solutions are showing oscillations like the diurnal oscillations that are seen in data. The aim of this thesis have not been to include time delay so this section could serve as an appetizer for future work.

Since it seems as if an inclusion of hippocampal mechanisms have a stabilizing effect on the system we will not include hippocampal mechanisms in this section.

A time delay can be explained as the hormones have to move with the bloodstream in order to reach receptors in different parts of the body. Furthermore it could take some time from the hormone reach the receptor until the receptor delivers the effect of a feedback.

Throughout this work we have gathered knowledge of the effect each parameter has on the stability of the system. We know that large α , μ and ρ have a destabilizing effect (This is at least true when considering global stability). Therefore we will set $\alpha = 5$ and $\rho = \mu = 1$. w_i is not changed and k_i will be determined in the same way as in chapter 10. This gives the following values of the parameters $k_0 = 2.6543$, $k_1 = 0.191$, $k_2 = 0.0013$ and $c = 3.055$. The steady state will be given as $\mathbf{x}_{ss} = (7.6508^{pg/ml}, 21^{pg/ml}, 3.055^{ng/ml})$. The system simulated is given as

$$\begin{aligned}\dot{x}_1 &= k_0 \left(1 - \mu \frac{(x_3(t - \tau))^\alpha}{c^\alpha + (x_3(t - \tau))^\alpha} \right) - w_1 x_1 \\ \dot{x}_2 &= k_1 \left(1 - \rho \frac{(x_3(t - \tau))^\alpha}{c^\alpha + (x_3(t - \tau))^\alpha} \right) x_1 - w_2 x_2 \\ \dot{x}_3 &= k_2 x_2(t - \tau) - w_3 x_3.\end{aligned}\tag{13.9}$$

Simulating this system with a time delay ($\tau = 19$ min) we are capable of producing oscillations in the system. The Matlab file used for producing this simulation can be seen in appendix B.4. These are seen on figure 13.1.

Thus it is possible to obtain inner oscillations in the system. Furthermore a lot of different time delays could be implemented. Surely a time delay of 19 minutes can not be explained by the time it takes for the hormones to travel with the bloodstream. But we see that oscillations are possible. If anyone can give a reasonable explanation of why a delay of this magnitude is reasonable this could be an idea to pursue. But this must be left for future work.

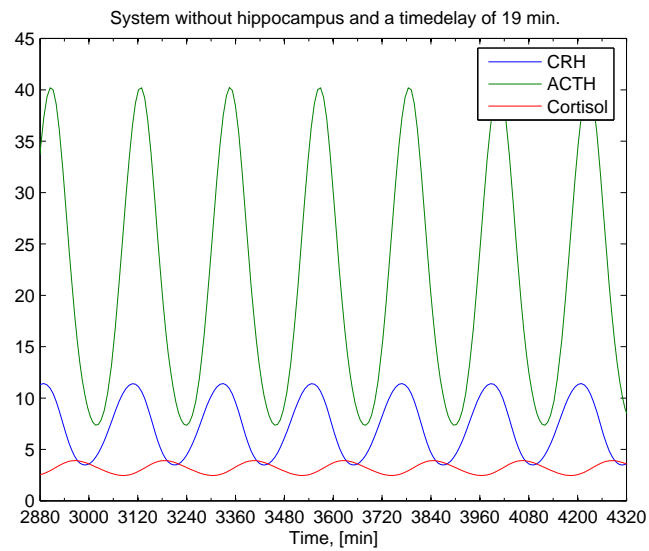


Figure 13.1: The system given in array 13.9 simulated with a time delay of 19 min and the parameters mentioned in this section. The figure shows oscillations in all three hormones. The unit of CRH is pg/ml the unit of ACTH is pg/ml and the units of cortisol is ng/ml .

A Proof of the Routh Hurwitz Criteria

The RHC for a third order polynomial is often used in this project so here is a proof. In general a RHC is valid for an n 'th degree polynomial but for the third order case the proof can be based on 'brute force'. First the theorem is restated from chapter 3.

Theorem A.1

Routh Hurwitz Criteria

Given

$$P(\lambda) = \lambda^3 + \alpha_1\lambda^2 + \alpha_2\lambda + \alpha_3, \quad \alpha_1, \alpha_2, \alpha_3 \in \mathbb{R} \quad (\text{A.1})$$

Then all of the roots of $P(\lambda)$ are negative or have negative real part if and only if $\alpha_1 > 0$, $\alpha_3 > 0$ and $\alpha_1 \cdot \alpha_2 > \alpha_3$.

Proof

Using complex numbers any third order polynomial has three roots (not necessarily distinct). These can be used to factorize the polynomial. A third order polynomial has at least one real root. This is due to the fact that for a large absolute value of λ , the term λ^3 dominates in the expression for P . Thus for a sufficiently large λ , P is positive, and for a sufficiently small λ , P is negative. Since P is continuous in λ by the intermediate value theorem [17, p. 75] there must exist a λ_1 such that $P(\lambda_1) = 0$. Factorizing P using this solution one gets

$$P(\lambda) = (\lambda - \lambda_1)(\lambda^2 + b\lambda + c), \quad b, c \in \mathbb{R} \quad (\text{A.2})$$

Finding the roots of the second factor in equation A.2 one gets

$$\lambda_+ = \frac{-b + \sqrt{d}}{2}, \quad \lambda_- = \frac{-b - \sqrt{d}}{2}, \quad d \equiv b^2 - 4ac. \quad (\text{A.3})$$

If d is negative λ_- is the complex conjugate of λ_+ , which is seen from splitting equation A.3 in real and imaginary parts. In that case we define $\mu = -b/2$ and $\omega = \sqrt{-d}/2$ and then the roots can be written $\lambda_+ = \mu + i\omega$ and $\lambda_- = \mu - i\omega$ where ω is not zero. For $d \geq 0$ the two real roots are named λ_2 and λ_3 . Thus we are left with two different ways of factorizing P depending on the sign of d .

$$P_{d \geq 0} = (\lambda - \lambda_1)(\lambda - \lambda_2)(\lambda - \lambda_3) \quad (\text{A.4})$$

$$P_{d < 0} = (\lambda - \lambda_1)(\lambda - \mu - i\omega)(\lambda - \mu + i\omega), \quad (\text{A.5})$$

where $\lambda_1, \lambda_2, \lambda_3, \mu, \omega \in \mathbb{R}, \omega \in \mathbb{R}_+$.

This proof is simply a brute force comparison of equation A.4 and equation A.5 with the statements $\alpha_1 > 0 \wedge \alpha_3 > 0 \wedge \alpha_1\alpha_2 - \alpha_3 > 0$ resulting in table A.1 which will now

be justified. We begin with the case of only real roots, $P_{d \geq 0}$. Expanding equation A.4 one gets

$$P_{d \geq 0} = \lambda^3 - (\lambda_1 + \lambda_2 + \lambda_3) \lambda^2 + (\lambda_1 \lambda_2 + \lambda_1 \lambda_3 + \lambda_2 \lambda_3) \lambda - \lambda_1 \lambda_2 \lambda_3. \quad (\text{A.6})$$

Now it is straightforward to identify α_1, α_2 and α_3

$$\alpha_1 = -(\lambda_1 + \lambda_2 + \lambda_3) \quad (\text{A.7})$$

$$\alpha_2 = (\lambda_1 \lambda_2 + \lambda_1 \lambda_3 + \lambda_2 \lambda_3) \quad (\text{A.8})$$

$$\alpha_3 = -\lambda_1 \lambda_2 \lambda_3. \quad (\text{A.9})$$

$$\alpha_1 \alpha_2 - \alpha_3 = -(\lambda_1 + \lambda_2 + \lambda_3) (\lambda_1 \lambda_2 + \lambda_1 \lambda_3 + \lambda_2 \lambda_3) + \lambda_1 \lambda_2 \lambda_3 \Leftrightarrow \quad (\text{A.10})$$

$$\alpha_1 \alpha_2 - \alpha_3 = -(\lambda_2 + \lambda_3) (\lambda_1 \lambda_2 + \lambda_1 \lambda_3 + \lambda_2 \lambda_3) - \lambda_1^2 (\lambda_2 + \lambda_3). \quad (\text{A.11})$$

- If $\lambda_1, \lambda_2, \lambda_3 < 0$ we see that $\alpha_1, \alpha_3 > 0$ and from equation A.11 it can be seen that $\alpha_1 \alpha_2 - \alpha_3$ consists of two positive terms such that $\alpha_1 \alpha_2 - \alpha_3 > 0$.
- If one or more roots are zero then α_3 is zero and thus cannot be positive.
- If exactly one root is non negative, α_3 cannot be positive.
- If exactly two roots are positive and one negative, say $\lambda_1 < 0, \lambda_2, \lambda_3 > 0$ then $\alpha_3 > 0$. In general if we require $\alpha_1 > 0, \alpha_3 > 0$ and $\alpha_1 \alpha_2 - \alpha_3 > 0$ this clearly leads to $\alpha_2 > 0$ as a necessary condition. If $\alpha_2 > 0$ we look at the expression for $\alpha_1 \alpha_2 - \alpha_3$ in equation A.11 remembering that the second factor is α_2 .

$$\alpha_1 \alpha_2 - \alpha_3 = -(\lambda_2 + \lambda_3) \alpha_2 - \lambda_1^2 (\lambda_2 + \lambda_3). \quad (\text{A.12})$$

Since we assumed $\lambda_1 < 0, \lambda_2, \lambda_3 > 0$ we have $\alpha_1 \alpha_2 - \alpha_3 < 0$. The proof should also be done in the case $\lambda_2 < 0, \lambda_1, \lambda_3 > 0$ and also when $\lambda_3 < 0, \lambda_1, \lambda_2 > 0$ but since $\alpha_1, \alpha_2, \alpha_3$ are symmetric in λ_1, λ_2 and λ_3 then so is $\alpha_1 \alpha_2 - \alpha_3$, and all cases are thus covered by covering one.

- If all three roots are positive then $\alpha_3 < 0$.

For the case of real roots of P we have now been through all relevant scenarios showing that RHC holds in each case. Now we just need to do the same when there is one real root and two complex conjugate roots of P . Expanding equation A.5 one gets

$$P_{d < 0} = \lambda^3 - (2\mu + \lambda_1) \lambda^2 + (\mu^2 + \omega^2 + 2\mu\lambda_1) \lambda - \lambda_1 (\mu^2 + \omega^2). \quad (\text{A.13})$$

Identifying the coefficients of the polynomials now with a prime not to be confused with the case $d \geq 0$.

$$\alpha'_1 = -(2\mu + \lambda_1) \quad (\text{A.14})$$

$$\alpha'_2 = \mu^2 + \omega^2 + 2\mu\lambda_1 \quad (\text{A.15})$$

$$\alpha'_3 = -\lambda_1 (\mu^2 + \omega^2) \quad (\text{A.16})$$

$$\alpha'_1 \alpha'_2 - \alpha'_3 = -(2\mu + \lambda_1) (\mu^2 + \omega^2 + 2\mu\lambda_1) + \lambda_1 (\mu^2 + \omega^2) \Leftrightarrow$$

$$\alpha'_1 \alpha'_2 - \alpha'_3 = -2\mu (\mu^2 + \omega^2 + 2\mu\lambda_1 + \lambda_1^2) \Leftrightarrow$$

$$\alpha'_1 \alpha'_2 - \alpha'_3 = -2\mu \left((\mu + \lambda_1)^2 + \omega^2 \right). \quad (\text{A.17})$$

Now the real part of the roots are only two numbers, λ_1 and μ .

P_d	Real part of roots	$\alpha_1 > 0 \wedge \alpha_3 > 0 \wedge \alpha_1\alpha_2 - \alpha_3 > 0$
$d \geq 0$	$\lambda_1 < 0 \wedge \lambda_2 < 0 \wedge \lambda_3 < 0$	true
$d \geq 0$	$\lambda_1 = 0 \vee \lambda_2 = 0 \vee \lambda_3 = 0$	false
$d \geq 0$	Exactly one root > 0	false
$d \geq 0$	Exactly two roots > 0	false
$d \geq 0$	$\lambda_1 > 0 \wedge \lambda_2 > 0 \wedge \lambda_3 > 0$	false
$d < 0$	$\lambda_1 < 0 \wedge \mu < 0$	true
$d < 0$	$\lambda_1 \geq 0$	false
$d < 0$	$\mu \geq 0$	false

Table A.1: Proof of RHC

- If $\mu < 0$, $\lambda_1 < 0$ then α_1 consists of two positive terms and is thus guaranteed positive. α_3 is positive since it is a product of two positive factors. Regarding $\alpha_1\alpha_2 - \alpha_3$ the factor in the brackets is a sum of a positive and a non negative term and is thus positive. Multiplied with a positive factor makes $\alpha_1\alpha_2 - \alpha_3$ positive.
- If λ_1 is nonnegative then α_3' cannot be positive.
- If $\mu \geq 0$ then

$$\alpha_1'\alpha_2' - \alpha_3' \leq 0, \quad (\text{A.18})$$

since it is a result of a negative number multiplied by a positive. The equality sign only applies for $\mu = 0$.

Now all the different classes of roots of P have been considered and the result is proving the RHC summarized in table A.1.

B Matlab codes

In this appendix the various Matlab codes used throughout this thesis is presented.

B.1 Fast Fourier transformation

Listing B.1: Main file transforming the confidential raw data by means of fast Fourier transformation.

```
1 function [x z X Z y]=fourierACTH(h)
2 %Enkeltpersoner
3 close all
4 clear x y X Y z x1 X1 D
5 %først hentes data
6 Carroll_data_som_matrix;
7
8 %Nu defineres hvilket af gennemsnittene vi vil undersøge (data fra
   enkeltpersoner kan ligeledes benyttes)
9 %For y=mean(*)', hvor * kan være HyperACTH, HyperCortisol, ControlACTH,
   %ControlCortisol, LowACTH, LowCortisol. Husk at ændre figurtekster!
10
11
12 %h giver person nummer. h=1:29
13 h=5;
14 y=ACTH(:,h);
15 %when doing fft of a discontinous point, the average has to be used.
16 %Important for endpoints
17 x(1,1)=(y(145)+y(1))/2;
18 x(145,1)=x(1,1);
19 x(2:144)=y(2:144);
20 %Nu er y det ønskede datasæt, og x er identisk med y bortset fra i
21 %endepunkterne
22
23 %diskret, endelig fouriertransformation udregnes
24 X=fft(x);
25
26 %Nu konstrueres en form for filter i frekvensdomænet. Z dannes som en
27 %73x145 matrice. I første søjle medtages 1 frekvens, i næste 2 osv.
28
29 Z=zeros(73,145);
30 for i=0:72;
31 Z(i+1,1:i+2)=X(1:i+2);
32 Z(i+1,145-i:145)=X(145-i:145);
33 %z er en 73x145 matrice hvor den i'te søjle er den i'te inverse fourier
34 %transformerede af den i'te søjle i Z
35 z(i+1,1:145)=ifft(Z(i+1,1:145));
36 end
37 t=1:145;
38 %test af z er ren reel. da er imag_del_lig_nul=0
```

```

39 imag_del_lig_nul=sum(sum(imag(z).^2));
40
41 k1=0;
42 if k1==0
43
44 %Nu plottes x mod de forskelllige søjler i z. Dvs nu kommer (en tegneserie
45 )
46 %en følge af grafer hvor et stigende antal frekvenser medtages
47
48     plot(t.*10,z(20,:), 'b.-')
49     %D(i) er den summerede, kvadrerede afstand mellem datasæt og z(i,:)
50     D(i) = sqrt(sum((x'-z(i,:)).^2));
51     pause(0.1)
52
53 end
54 hold on
55 h=10;
56 y=ACTH(:,h);
57 %when doing fft of a discontinous point, the average has to be used.
58 %Important for endpoints
59 x(1,1)=(y(145)+y(1))/2;
60 x(145,1)=x(1,1);
61 x(2:144)=y(2:144);
62 %Nu er y det ønskede datasæt, og x er identisk med y bortset fra i
63 %endepunkterne
64
65 %diskret, endelig fouriertransformation udregnes
66 X=fft(x);
67
68 %Nu konstrueres en form for filter i frekvensdomænet. Z dannes som en
69 %73x145 matrice. I første søjle medtages 1 frekvens, i næste 2 osv.
70
71 Z=zeros(73,145);
72 for i=0:72;
73     Z(i+1,1:i+2)=X(1:i+2);
74     Z(i+1,145-i:145)=X(145-i:145);
75     %z er en 73x145 matrice hvor den i'te søjle er den i'te inverse fourier
76     %trasnformerede af den i'te søjle i Z
77     z(i+1,1:145)=ifft(Z(i+1,1:145));
78 end
79 t=1:145;
80 %test af z er ren reel. da er imag_del_lig_nul=0
81 imag_del_lig_nul=sum(sum(imag(z).^2));
82
83 k1=0;
84 if k1==0
85
86 %Nu plottes x mod de forskelllige søjler i z. Dvs nu kommer (en tegneserie
87 )
88 %en følge af grafer hvor et stigende antal frekvenser medtages
89
90     plot(t.*10,z(20,:), 'r.-')
91     %D(i) er den summerede, kvadrerede afstand mellem datasæt og z(i,:)
92     D(i) = sqrt(sum((x'-z(i,:)).^2));
93     pause(0.1)
94
95 end
96 h=27;
97 y=ACTH(:,h);

```

```

96 %when doing fft of a discontinuous point, the average has to be used.
97 %Important for endpoints
98 x(1,1)=(y(145)+y(1))/2;
99 x(145,1)=x(1,1);
100 x(2:144)=y(2:144);
101 %Nu er y det ønskede datasæt, og x er identisk med y bortset fra i
102 %endepunkterne
103
104 %diskret, endelig fouriertransformation udregnes
105 X=fft(x);
106
107 %Nu konstrueres en form for filter i frekvensdomænet. Z dannes som en
108 %73x145 matrice. I første søjle medtages 1 frekvens, i næste 2 osv.
109
110 Z=zeros(73,145);
111 for i=0:72;
112 Z(i+1,1:i+2)=X(1:i+2);
113 Z(i+1,145-i:145)=X(145-i:145);
114 %z er en 73x145 matrice hvor den i'te søjle er den i'te inverse fourier
115 %trasnformerede af den i'te søjle i X
116 z(i+1,1:145)=ifft(Z(i+1,1:145));
117 end
118 t=1:145;
119 %test af z er ren reel. da er imag_del_lig_nul=0
120 imag_del_lig_nul=sum(sum(imag(z).^2));
121
122 k1=0;
123 if k1==0
124
125 %Nu plottes x mod de forskelllige søjler i z. Dvs nu kommer (en tegneserie
126 %)
127 %en følge af grafer hvor et stigende antal frekvenser medtages
128 plot(t.*10,z(20,:), 'g.-')
129 %D(i) er den summerede, kvadrerede afstand mellem datasæt og z(i,:)
130 D(i) = sqrt(sum((x'-z(i,:)).^2));
131 pause(0.1)
132
133 end
134 %title({'ACTH data presented by means of fast Fourier transformation';'
135 using the smallest 20 frequencies.'})
136 xlabel('time□,□[min]')
137 ylabel('ACTH□concentration, □[pg/ml]')
138 legend('Hypercortisol□depressive', 'Normal', 'Lowcortisol□depressive')
139 axis([0 1440 0 60])
140 set(gca, 'XTick', 0:120:1440)
141 set(gca, 'XMinorTick', 'on')
142
143 %Tilsvarende laves for cortisol
144 h=5;
145 y=Cortisol(:,h);
146 %when doing fft of a discontinuous point, the average has to be used.
147 %Important for endpoints
148 x(1,1)=(y(145)+y(1))/2;
149 x(145,1)=x(1,1);
150 x(2:144)=y(2:144);
151 %Nu er y det ønskede datasæt, og x er identisk med y bortset fra i
152 %endepunkterne

```

```

153 %diskret, endelig fouriertransformation udregnes
154 X=fft(x);
155
156 %Nu konstrueres en form for filter i frekvensdomænet. Z dannes som en
157 %73x145 matrice. I første søjle medtages 1 frekvens, i næste 2 osv.
158
159 Z=zeros(73,145);
160 for i=0:72;
161 Z(i+1,1:i+2)=X(1:i+2);
162 Z(i+1,145-i:145)=X(145-i:145);
163 %z er en 73x145 matrice hvor den i'te søjle er den i'te inverse fourier
164 %trasnformerede af den i'te søjle i Z
165 z(i+1,1:145)=ifft(Z(i+1,1:145));
166 end
167 t=1:145;
168 %test af z er ren reel. da er imag_del_lig_nul=0
169 imag_del_lig_nul=sum(sum(imag(z).^2));
170
171 k1=0;
172 if k1==0
173
174 %Nu plottes x mod de forskelllige søjler i z. Dvs nu kommer (en tegneserie
175 %)
176 %en følge af grafer hvor et stigende antal frekvenser medtages
177 figure
178 plot(t.*10,z(20,:), 'b.-')
179 %D(i) er den summerede, kvadrerede afstand mellem datasæt og z(i,:)
180 D(i) = sqrt(sum((x'-z(i,:)).^2));
181 pause(0.1)
182 end
183 hold on
184 h=10;
185 y=Cortisol(:,h);
186 %when doing fft of a discontinuous point, the average has to be used.
187 %Important for endpoints
188 x(1,1)=(y(145)+y(1))/2;
189 x(145,1)=x(1,1);
190 x(2:144)=y(2:144);
191 %Nu er y det ønskede datasæt, og x er identisk med y bortset fra i
192 %endepunkterne
193
194 %diskret, endelig fouriertransformation udregnes
195 X=fft(x);
196
197 %Nu konstrueres en form for filter i frekvensdomænet. Z dannes som en
198 %73x145 matrice. I første søjle medtages 1 frekvens, i næste 2 osv.
199
200 Z=zeros(73,145);
201 for i=0:72;
202 Z(i+1,1:i+2)=X(1:i+2);
203 Z(i+1,145-i:145)=X(145-i:145);
204 %z er en 73x145 matrice hvor den i'te søjle er den i'te inverse fourier
205 %trasnformerede af den i'te søjle i Z
206 z(i+1,1:145)=ifft(Z(i+1,1:145));
207 end
208 t=1:145;
209 %test af z er ren reel. da er imag_del_lig_nul=0
210 imag_del_lig_nul=sum(sum(imag(z).^2));

```

```

211
212 k1=0;
213 if k1==0
214
215 %Nu plottes x mod de forskelllige søjler i z. Dvs nu kommer (en tegneserie
    )
216 %en følge af grafer hvor et stigende antal frekvenser medtages
217
218     plot(t.*10,z(20,:), 'r.-')
219     %D(i) er den summerede, kvadrerede afstand mellem datasæt og z(i,:)
220     D(i) = sqrt(sum((x'-z(i,:)).^2));
221     pause(0.1)
222
223 end
224 h=27;
225 y=Cortisol(:,h);
226 %when doing fft of a discontinous point, the average has to be used.
227 %Important for endpoints
228 x(1,1)=(y(145)+y(1))/2;
229 x(145,1)=x(1,1);
230 x(2:144)=y(2:144);
231 %Nu er y det ønskede datasæt, og x er identisk med y bortset fra i
232 %endepunkterne
233
234 %diskret, endelig fouriertransformation udregnes
235 X=fft(x);
236
237 %Nu konstrueres en form for filter i frekvensdomænet. Z dannes som en
238 %73x145 matrice. I første søjle medtages 1 frekvens, i næste 2 osv.
239
240 Z=zeros(73,145);
241 for i=0:72;
242     Z(i+1,1:i+2)=X(1:i+2);
243     Z(i+1,145-i:145)=X(145-i:145);
244     %z er en 73x145 matrice hvor den i'te søjle er den i'te inverse fourier
245     %trasnformerede af den i'te søjle i Z
246     z(i+1,1:145)=ifft(Z(i+1,1:145));
247 end
248 t=1:145;
249 %test af z er ren reel. da er imag_del_lig_nul=0
250 imag_del_lig_nul=sum(sum(imag(z).^2));
251
252 k1=0;
253 if k1==0
254
255 %Nu plottes x mod de forskelllige søjler i z. Dvs nu kommer (en tegneserie
    )
256 %en følge af grafer hvor et stigende antal frekvenser medtages
257     plot(t.*10,z(20,:), 'g.-')
258     %D(i) er den summerede, kvadrerede afstand mellem datasæt og z(i,:)
259     D(i) = sqrt(sum((x'-z(i,:)).^2));
260     pause(0.1)
261
262 end
263 %title({'Cortisol data presented by means of fast Fourier transformation
    '; 'using the smallest 20 frequencies.'})
264 xlabel('time□,□[min]')
265 ylabel('Cortisol□concentration ,□[\mug/dl]')
266 legend('Hypercortisol□depressive', 'Normal', 'Lowcortisol□depressive')

```

```

267 axis([0 1440 0 20])
268 set(gca,'XTick',0:120:1440)
269 set(gca,'XMinorTick','on')

```

B.2 Calculation of parameters

Listing B.2: File calculating the default parameter values.

```

1  %%This m-file gives an approximate value for unknown parameters
2  %First we define the parameters we know
3  clear all
4
5  %The mean value of the concentrations
6  x1=7.6588; %pg/ml
7  x2=21; %pg/ml
8  x3=3.055; %ng/ml
9
10 %The half lifes
11 half_life_CRH=4; %min
12 half_life_ACTH=19.9; %min
13 half_life_Cortisol=76.4; %min
14
15 %The elimination constants
16 w1=log(2)/half_life_CRH;
17 w2=log(2)/half_life_ACTH;
18 w3=log(2)/half_life_Cortisol;
19
20 %The parameters in the feedback functions
21
22 mu=1; %hypothalamic feedback
23 phi=0; %hippocampal feedforward
24 psi=0; %hippocampal feedback
25
26 xi=phi-mu; %sum of hippocampal and hypothalamic GR potential
27
28 rho=1; %pituary feedback
29 alpha=5; %GR exponent
30 gamma=3; %MR exponent
31 c=x3; % GR affinity
32 c3=(1/10)^(1/gamma)*c^(alpha/gamma); % MR affinity
33
34 %Defining steady state to be in the meanvalues gives the k's
35
36 k0=w1*x1/(1+xi*(x3^alpha/(c^alpha+x3^alpha))-psi*(x3^gamma/(x3^gamma+c3^
    gamma)))
37 k1=w2*x2/((1-rho*(x3^alpha/(c^alpha+x3^alpha)))*x1)
38 k2=w3*x3/x2
39
40 %The parameters in the reduced system can now be determined
41
42 d0=(k0*k1*k2/c)^(1/3)
43 d1=(c*k0^2/(k1*k2))^(1/3)
44 d2=(c^2*k0*k1/k2^2)^(1/3)
45 d3=c
46 w1tilde=w1/d0
47 w2tilde=w2/d0
48 w3tilde=w3/d0

```

```

49 c3tilde=c3/d3
50 theta=d0

```

B.3 Main file used for the numerical analysis

Listing B.3: Main file used for numerical analysis.

```

1  %% This file shows the dynamics of a parameterset in the model with and
   without hippocampal dynamics
2  close all
3  clear all
4  run k_values_from_mean_values
5  %1. The system without reduction
6  %2. The reduced system
7
8  %loading the parameter values
9  %k_values_from_mean_values
10 %% Additional cell used to plot circadian rhythm
11 ta=0:0.001:3*1440;
12 a=28.8118-8.4592*cos(2*pi/1440.*ta)+5.5438*sin(2*pi/1440*ta);
13 b=(5.0945-4.5157*cos(2*pi/1440.*ta)+0.42192*sin(2*pi/1440*ta))/2;
14
15 %% Define the initial values as fractions of the mean values
16 a1=2;
17 a2=1;
18 a3=1;
19 xstart=[a1*x1 a2*x2 a3*x3];
20 tspan=[0 3*1440];
21
22 %% This cell evaluates the Jacobian at a given point
23 System_steady_state_matrix=System_Jacobian([x1 x2 x3], xi, k0, k1, k2, psi
   , rho, alpha, gamma, c, c3, w1, w2, w3)
24 Eigenvalues_of_System_Steady_state_Jacobian_SS=eig(
   System_steady_state_matrix);
25
26 %% This cell makes a one- and a three dimensional plot of the
27 %% solutioncurves of the unreduced system
28 %This solves the full system
29 Options = odeset('Jacobian',@System_Jacobian,'RelTol',1e-8,'AbsTol',1e-8);
30 [t, x] = ode15s(@Ikke_reduceret_system_med_hippocampus, tspan, xstart,
   Options, k0, k1, k2, w1, w2, w3, xi, psi, rho, alpha, gamma, c, c3, x1
   );
31 figure
32 plot(t,x(:,1),'b')
33 %legend('CRH')
34 title('CRH plottet as a function of time')
35 xlabel('Time, [min]')
36 ylabel('CRH, [pg/ml]')
37 figure
38 plot(t,x(:,2),'b',ta,a,'g',10*Tk,Z,'r.-')
39 title('ACTH as a function of time.')
40 legend('Simulation of ACTH','Circadian rhythm','Data')
41 xlabel('Time, [min]')
42 ylabel('ACTH, [pg/ml]')
43 set(gca,'XLim',[2*1440 3*1440])
44 set(gca,'XTick',2*1440:120:3*1440)
45 set(gca,'XMinorTick','on')

```

```

46 figure
47 plot(t,x(:,3),'b',ta,b,'g',10*Tk,ZCortisol/2,'r.-')
48 title('Cortisol plottet as a function of time')
49 legend('Simulation of cortisol','Circadian_rhythm','Data')
50 set(gca,'XLim',[2*1440 3*1440])
51 set(gca,'XTick',2*1440:120:3*1440)
52 set(gca,'XMinorTick','on')
53 xlabel('Time,[min]')
54 ylabel('Cortisol,[ng/ml]')
55 figure
56 %Tredimensionelt plot af alle concentrationer
57 plot3(x(:,1),x(:,2),x(:,3),'-b',xstart(1),xstart(2),xstart(3),'or',x1,x2,
58     x3,'og')
59 title('Three dimensional plot of the solution curve')
60 xlabel('CRH,[pg/ml]')
61 ylabel('ACTH,[pg/ml]')
62 zlabel('Cortisol,[ng/ml]')
63 legend('Solution_curve','Starting_value','Steady_state')
64 grid on
65
66 %% This cell does the same as the previous cell but for the reduced system
67 xstart=[a1*x1/d1 a2*x2/d2 a3*x3/d3]
68 tspan=[0 10*d0*1440];
69 %This solves the reduced system
70
71 alpha=61;
72 %'Jacobian',@Reduced_system_Jacobian,
73 Options = odeset('RelTol',1e-8,'AbsTol',1e-8); %Options = odeset('RelTol
74     ',1e-8,'AbsTol',1e-10);
75 [t, x] = odel5s(@Reduceret_system_med_hippocampus, tspan, xstart, Options
76     , xi, psi, rho, alpha, gamma, c3tilde, w1tilde, w2tilde, w3tilde);
77 figure
78 plot(t,x(:,1),'b')
79 %legend('X_1 (CRH)')
80 title('X_1 plottet as a function of \theta')
81 xlabel('\theta(time)')
82 ylabel('X_1(CRH)')
83 figure
84 plot(t,x(:,2),'r')
85 %legend('ACTH')
86 title('X_2 plottet as a function of \theta')
87 xlabel('\theta(time)')
88 ylabel('X_2(ACTH)')
89 figure
90 plot(t,x(:,3),'g')
91 title('X_3 plottet as a function of \theta')
92 legend('Cortisol')
93 xlabel('\theta(time)')
94 ylabel('X_3(Cortisol)')
95 figure
96 %Tredimensionelt plot af alle concentrationer
97 %,'or',z1,z2,z3,'og'
98 plot3(x(:,1),x(:,2),x(:,3),'-b',xstart(1),xstart(2),xstart(3))
99     )
100 title('Three dimensional plot of the solution curve in the reduced system')
101 xlabel('X_1(CRH)')
102 ylabel('X_2(ACTH)')
103 zlabel('X_3(Cortisol)')

```

```

101 legend('Solution_curve','Starting_value','Steady_state')
102 grid on
103 %% Here it is grapically shown where the intersection(s) of the two curves
104 %% that determine the steady state solution(s) of cortisol is.
105 %Define tmax (The length of the desired interval)
106 xi=2.98
107 psi=1
108 %rho=0.5
109 alpha=5
110 gamma=5
111 %k=k+1
112 tmax=3;
113 t=0:.001:tmax;
114 y=(1/(w1tilde*w2tilde*w3tilde))*(1+xi*(t.^(alpha)./(1+t.^(alpha))))-psi*(t.^(gamma)./(c3tilde^gamma+t.^(gamma)))*(1-rho*(t.^(alpha)./(1+t.^(alpha)))));
115 yprime=(1/(w1tilde*w2tilde*w3tilde))*((xi*alpha*t.^(alpha-1)./((1+t.^(alpha)).^2)-psi*gamma*c3tilde^gamma*t.^(gamma-1)./((c3tilde^gamma+t.^(gamma)).^2))*(1-rho*(t.^(alpha)./(1+t.^(alpha))))-(rho*alpha*t.^(alpha-1)./((1+t.^(alpha)).^2))*(1+xi*(t.^(alpha)./(1+t.^(alpha))))-psi*(t.^(gamma)./(c3tilde^gamma+t.^(gamma)))));
116 maxgradient=max(yprime)
117 mingradient=min(yprime)
118 %This is only interesting when positve feedback is included
119 tmaxgradient=fsolve(@(t)((1/(w1tilde*w2tilde*w3tilde))*((xi*alpha*t.^(alpha-1)./(1+t.^(alpha)).^2)-psi*gamma*c3tilde^gamma*t.^(gamma-1)./(c3tilde^gamma+t.^(gamma)).^2)*(1-rho*(t.^(alpha)./(1+t.^(alpha))))-(rho*alpha*t.^(alpha-1)./(1+t.^(alpha)).^2)*(1+xi*(t.^(alpha)./(1+t.^(alpha))))-psi*(t.^(gamma)./(c3tilde^gamma+t.^(gamma)))))-maxgradient),1)
120 tmingradient=fsolve(@(t)((1/(w1tilde*w2tilde*w3tilde))*((xi*alpha*t.^(alpha-1)./(1+t.^(alpha)).^2)-psi*gamma*c3tilde^gamma*t.^(gamma-1)./(c3tilde^gamma+t.^(gamma)).^2)*(1-rho*(t.^(alpha)./(1+t.^(alpha))))-(rho*alpha*t.^(alpha-1)./(1+t.^(alpha)).^2)*(1+xi*(t.^(alpha)./(1+t.^(alpha))))-psi*(t.^(gamma)./(c3tilde^gamma+t.^(gamma)))))-mingradient),0.5)
121 y_maxgradient=(1/(w1tilde*w2tilde*w3tilde))*(1+xi*(tmaxgradient^(alpha)./(1+tmaxgradient^(alpha))))-psi*(tmaxgradient^(gamma)./(c3tilde^gamma+tmaxgradient^(gamma)))*(1-rho*(tmaxgradient^(alpha)./(1+tmaxgradient^(alpha)))));
122 y_mingradient=(1/(w1tilde*w2tilde*w3tilde))*(1+xi*(tmingradient^(alpha)./(1+tmingradient^(alpha))))-psi*(tmingradient^(gamma)./(c3tilde^gamma+tmingradient^(gamma)))*(1-rho*(tmingradient^(alpha)./(1+tmingradient^(alpha)))));
123 figure
124 plot(t,t,'b',t,y,'r');
125 %,'tmaxgradient',y_maxgradient,'mo'
126 %,['Maximum grad=',num2str(maxgradient),]
127 %legend('H(X_3)', 'L(X_3)', ['Minimum grad=',num2str(mingradient),], ['Maximum grad=',num2str(maxgradient),])
128 %title('H(X_3) for different parameter values')
129 legend('L(X_3)', 'H(X_3)',2)
130 xlabel('X_3')
131 %figure
132 %plot(t,t,t,y)
133 %legend('L(X_3)', '~c_3=0.5c_3', '~c_3=c_3', '~c_3=2c_3',4)
134 %xlabel('X_3')
135 %axis([0 1.5 0 1.5])
136 %Investigate this figure for number of intersections. If there are one go
137 %to the cells evaluating for one solution. If there are three solutions go
138 %to the cells evaluating for three solutions.

```

```

139 %% These cells evaluate the solutions for one solution
140
141 %go to file Reduced_system_Jacobian and remove t to evaluate this cell
142
143 %Give an estimate of the steady state solution
144 %for c3tilde=[0.5*frank frank 2*frank]
145 L_R_equal_zero=1;
146 z3=fzero(@(x)ZerosofRx3Lx3(x, xi, psi, rho, alpha, gamma, c3tilde, w1tilde
, w2tilde, w3tilde),L_R_equal_zero);
147 z1=(1+xi*(z3^alpha/(1+z3^alpha))-psi*(z3^gamma/(c3tilde^gamma+z3^gamma)))/
w1tilde;
148 z2=(1-rho*(z3^alpha/(1+z3^alpha)))*z1/w2tilde;
149 %Then the steady state vector is given as
150 SteadyStateVector=[z1 z2 z3]
151 %The Jacobian at steady state is evaluated and the eigenvalues is computed
152 Jacobian_SS=Reduced_system_Jacobian([z1 z2 z3], xi, psi, rho, alpha, gamma
, c3tilde, w1tilde, w2tilde, w3tilde);
153 Eigenvalues_of_Jacobian_SS=eig(Jacobian_SS)
154 %end
155 %% This cell will evaluate how the ending positions depend on the starting
156 %% positions. On the reduced system.
157 figure
158 gridstart=0;
159 gridmask=.2;
160 gridend=4.6;
161 %This solves the reduced system
162 for x01=gridstart: gridmask: gridend;
163     for x02=gridstart: gridmask: gridend;
164         for x03=gridstart: gridmask: gridend;
165             xstart = [x01 x02 x03];
166             %Tidsintervallet der skal simuleres bestemmes
167             tspan=[0 d0*1440];
168             %Her løses differential ligningerne
169             Options = odeset('Jacobian',@Reduced_system_Jacobian,'RelTol',1e-8,'AbsTol
',1e-8); %Options = odeset('RelTol',1e-8,'AbsTol',1e-10);
170             [t, x] = ode15s(@Reduceret_system_med_hippocampus, tspan, xstart, Options
, xi, psi, rho, alpha, gamma, c3tilde, w1tilde, w2tilde, w3tilde);
171             plot3(SteadyStateVector(1),SteadyStateVector(2),SteadyStateVector(3),'or',
x(numel(t),1),x(numel(t),2),x(numel(t),3)'.b',x01,x02,x03,'g. ')
172 hold on
173         end
174     end
175 end
176 title('Ending values as a function of initial conditions')
177 xlabel('X_1(CRH)')
178 ylabel('X_2(ACTH)')
179 zlabel('X_3(Cortisol)')
180 legend('Steady state','Ending values','Initial conditions')
181 grid on
182
183
184
185
186 %% These cells evaluate the solutions for three steady state solutions.
187
188 %go to file Reduced_system_Jacobian and remove t to evaluate this cell
189
190 % Define minimum and maximum(gradient=0)
191 grad_L_equal_to_zero_min=0.1;

```

```

192 grad_L_equal_to_zero_max=1;
193 %Here the exact value is calculated
194 zmin=fminsearch(@(x)ZerosofRx3Lx3(x, xi, psi, rho, alpha, gamma, c3tilde,
    w1tilde, w2tilde, w3tilde),grad_L_equal_to_zero_min)
195 zmax=fminsearch(@(x)minusZerosofRx3Lx3(x, xi, psi, rho, alpha, gamma,
    c3tilde, w1tilde, w2tilde, w3tilde),grad_L_equal_to_zero_max)
196 %Here we are finding the intersection of R(x_3) og L(x3)
197 z31=fzero(@(x)ZerosofRx3Lx3(x, xi, psi, rho, alpha, gamma, c3tilde,
    w1tilde, w2tilde, w3tilde),[0 zmin]);
198 z32=fzero(@(x)ZerosofRx3Lx3(x, xi, psi, rho, alpha, gamma, c3tilde,
    w1tilde, w2tilde, w3tilde),[zmin zmax]);
199 z33=fzero(@(x)ZerosofRx3Lx3(x, xi, psi, rho, alpha, gamma, c3tilde,
    w1tilde, w2tilde, w3tilde),[zmax tmax]);
200 z=y-t;
201 plot(t,z,'b',zmin,ZerosofRx3Lx3(zmin, xi, psi, rho, alpha, gamma, c3tilde,
    w1tilde, w2tilde, w3tilde),'ro',zmax,ZerosofRx3Lx3(zmax, xi, psi, rho
    , alpha, gamma, c3tilde, w1tilde, w2tilde, w3tilde),'ro')
202 legend('L(x_3)-R(x_3)', 'Minimum', 'Maximum');
203 xlabel('cortisol');
204
205 %% This cell finds the steady state concentrations of all variables and
    for
206 %% all fixpoints
207 %First we calculate the other staedy state concentrations
208 %For CRH
209 z11=(1+xi*(z31^alpha/(1+z31^alpha))-psi*(z31^gamma/(c3tilde^gamma+z31^
    gamma)))/w1tilde;
210 z12=(1+xi*(z32^alpha/(1+z32^alpha))-psi*(z32^gamma/(c3tilde^gamma+z32^
    gamma)))/w1tilde;
211 z13=(1+xi*(z33^alpha/(1+z33^alpha))-psi*(z33^gamma/(c3tilde^gamma+z33^
    gamma)))/w1tilde;
212 %For ACTH
213 z21=(1-rho*(z31^alpha/(1+z31^alpha)))*z11/w2tilde;
214 z22=(1-rho*(z32^alpha/(1+z32^alpha)))*z12/w2tilde;
215 z23=(1-rho*(z33^alpha/(1+z33^alpha)))*z13/w2tilde;
216 %A matrix is computed with the steady state concentrations as column
    vectors
217 SteadyStateMatrix=[z11 z12 z13; z21 z22 z23; z31 z32 z33]
218 %The Jacobian is computed
219 Jacobian_SS1=Reduced_system_Jacobian([z11 z21 z31], xi, psi, rho, alpha,
    gamma, c3tilde, w1tilde, w2tilde, w3tilde)
220 Eigenvalues_of_Jacobian_SS1=eig(Jacobian_SS1)
221 Jacobian_SS2=Reduced_system_Jacobian([z12 z22 z32], xi, psi, rho, alpha,
    gamma, c3tilde, w1tilde, w2tilde, w3tilde)
222 Eigenvalues_of_Jacobian_SS2=eig(Jacobian_SS2)
223 Jacobian_SS3=Reduced_system_Jacobian([z13 z23 z33], xi, psi, rho, alpha,
    gamma, c3tilde, w1tilde, w2tilde, w3tilde)
224 Eigenvalues_of_Jacobian_SS3=eig(Jacobian_SS3)
225 %% This cell will evaluate how the ending positions depend on the starting
    %% positions. On the reduced system.
226 x_gridstart=0;
227 x_gridmask=.1;
228 x_gridend=1;
229 y_gridstart=0;
230 y_gridmask=.1;
231 y_gridend=1;
232 z_gridstart=0;
233 z_gridmask=.1;
234 z_gridend=2;

```

```

236 %This solves the reduced system
237 for x01=x_gridstart: x_gridmask: x_gridend;
238     for x02=y_gridstart: y_gridmask: y_gridend;
239         for x03=z_gridstart: z_gridmask: z_gridend;
240 xstart = [x01 x02 x03];
241 %Tidsintervallet der skal simuleres bestemmes
242 tspan=[0 d0*2*1440];
243 %Define the size of the small omegn around steady state.
244 epsilon=0.1;
245 %Her løses differential ligningerne
246 Options = odeset('Jacobian',@Reduced_system_Jacobian,'RelTol',1e-8,'AbsTol',
    '1e-8'); %Options = odeset('RelTol',1e-8,'AbsTol',1e-10);
247 [t, x] = ode15s(@Reduceret_system_med_hippocampus, tspan, xstart, Options
    , xi, psi, rho, alpha, gamma, c3tilde, w1tilde, w2tilde, w3tilde);
248 if x(numel(t),1)>SteadyStateMatrix(1,1)-epsilon & x(numel(t),1)<
    SteadyStateMatrix(1,1)+epsilon & x(numel(t),2)>SteadyStateMatrix(2,1)-
    epsilon & x(numel(t),2)<SteadyStateMatrix(2,1)+epsilon & x(numel(t)
    ,3)>SteadyStateMatrix(3,1)-epsilon & x(numel(t),3)<SteadyStateMatrix
    (3,1)+epsilon
249 plot3(SteadyStateMatrix(1,1),SteadyStateMatrix(2,1),SteadyStateMatrix(3,1)
    , 'or',SteadyStateMatrix(1,2),SteadyStateMatrix(2,2),SteadyStateMatrix
    (3,2), 'or',SteadyStateMatrix(1,3),SteadyStateMatrix(2,3),
    SteadyStateMatrix(3,3), 'or',x(numel(t),1),x(numel(t),2),x(numel(t),3),
    'b',x01,x02,x03,'g. ')
250 xlabel('CRH')
251 ylabel('ACTH')
252 zlabel('Cortisol')
253 legend('Steady_state_1','Steady_state_2','Steady_state_3','Ending_value','
    Initial_condition')
254 hold on
255 grid on
256 elseif x(numel(t),1)>SteadyStateMatrix(1,2)-epsilon & x(numel(t),1)<
    SteadyStateMatrix(1,2)+epsilon & x(numel(t),2)>SteadyStateMatrix(2,2)-
    epsilon & x(numel(t),2)<SteadyStateMatrix(2,2)+epsilon & x(numel(t)
    ,3)>SteadyStateMatrix(3,2)-epsilon & x(numel(t),3)<SteadyStateMatrix
    (3,2)+epsilon
257 plot3(SteadyStateMatrix(1,1),SteadyStateMatrix(2,1),SteadyStateMatrix(3,1)
    , 'or',SteadyStateMatrix(1,2),SteadyStateMatrix(2,2),SteadyStateMatrix
    (3,2), 'or',SteadyStateMatrix(1,3),SteadyStateMatrix(2,3),
    SteadyStateMatrix(3,3), 'or',x(numel(t),1),x(numel(t),2),x(numel(t),3),
    'b',x01,x02,x03,'k. ')
258 xlabel('CRH')
259 ylabel('ACTH')
260 zlabel('Cortisol')
261 legend('Steady_state_1','Steady_state_2','Steady_state_3','Ending_values',
    'Initial_condition')
262 elseif x(numel(t),1)>SteadyStateMatrix(1,3)-epsilon & x(numel(t),1)<
    SteadyStateMatrix(1,3)+epsilon & x(numel(t),2)>SteadyStateMatrix(2,3)-
    epsilon & x(numel(t),2)<SteadyStateMatrix(2,3)+epsilon & x(numel(t)
    ,3)>SteadyStateMatrix(3,3)-epsilon & x(numel(t),3)<SteadyStateMatrix
    (3,3)+epsilon
263 plot3(SteadyStateMatrix(1,1),SteadyStateMatrix(2,1),SteadyStateMatrix(3,1)
    , 'or',SteadyStateMatrix(1,2),SteadyStateMatrix(2,2),SteadyStateMatrix
    (3,2), 'or',SteadyStateMatrix(1,3),SteadyStateMatrix(2,3),
    SteadyStateMatrix(3,3), 'or',x(numel(t),1),x(numel(t),2),x(numel(t),3),
    'b',x01,x02,x03,'y. ')
264 xlabel('X_1_(CRH)')
265 ylabel('X_2_(ACTH)')
266 zlabel('X_3_(Cortisol)')

```

```

267 legend('Steady_state_1','Steady_state_2','Steady_state_3','Ending_values',
          'Initial_condition_values')
268 else
269     plot3(SteadyStateMatrix(1,1),SteadyStateMatrix(2,1),SteadyStateMatrix
           (3,1),'or',SteadyStateMatrix(1,2),SteadyStateMatrix(2,2),
           SteadyStateMatrix(3,2),'or',SteadyStateMatrix(1,3),
           SteadyStateMatrix(2,3),SteadyStateMatrix(3,3),'or',x(numel(t),1),x(
           numel(t),2),x(numel(t),3),'.b',x01,x02,x03,'m0')
270 end
271     hold on
272     end
273     end
274 end
275
276
277
278 %% In this cell we wish to investigate the effect of a time delay in the
279 %% reduced system
280 %%Definition of the starting values making these the same as previous
281 %%starting values.
282 %%xstart1=xstart(1);
283 %%xstart2=xstart(2);
284 %%xstart3=xstart(3);
285 %%Define the timespan
286 tspan=[0, d0*1440];
287 %%sincematlab cannot solve for a timedelay equal to zero. A timedelay equal
288 %%to zero will be defined as 1e-16
289 alpha=5;
290 tau1=200*theta; %min (Time for cortisol to activate GR in hypothalamus)
291 tau2=200*theta; %min (Time for cortisol to activate GR in hippocampus)
292 tau3=400*theta; %min (Time for cortisol to activate MR in hippocampus)
293 tau4=20*theta; %min (Time for cortisol to activate GR in adrenal glands)
294 tau5=1*theta; %min (Time for CRH give positive stimulus in adrenal glands)
295 tau6=400*theta; %min (Time for ACTH give positive stimulus in pituitary
           gland)
296 timedelay=[tau1, tau2, tau3, tau4, tau5, tau6];
297 options=[];
298 sol = dde23(@Reduced_system_Delaymodel, timedelay,
           @Reduced_System_delaymodel_History, tspan, options, mu, phi, psi, rho,
           alpha, gamma, c3tilde, w1tilde, w2tilde, w3tilde);
299 figure
300 plot(sol.x,sol.y)
301 %axis([1430 2870 0 3])
302 %title(['All graphs with a timedelay of',num2str(tidsforsinkelse),'
           minuttes, k_0=',num2str(k_0),'', k_1=',num2str(k_1),'', k_2=',num2str(
           k_2),'', my=',num2str(my),'', rho=',num2str(rho),]);
303 xlabel('Time_in_minuttes');
304 ylabel('Solutions');
305 legend('CRH','ACTH','Cortisol')
306 %% In this cell we investigate the effect of a time delay in the unreduced
307 %% system including hippocampal mecanisms.
308 tspan=[0, 14400];
309 alpha=5;
310 rho=1;
311 xi=-1;
312 psi=0;
313 tau1=19; %min (Time for cortisol to activate GR receptors)
314 tau2=19; %min (Time for cortisol to activate MR receptors)
315 tau3=19; %min (Time for ACTH to activate release of cortisol)

```

```

316 timedelay=[tau1, tau2, tau3];
317 options=[];
318 sol = dde23(@unreduced_system_med_hippocampus_delay_model, timedelay,
    @unreduced_System_med_hippocampus_delaymodel_History, tspan, options,
    k0, k1, k2, w1, w2, w3, xi, psi, rho, alpha, gamma, c, c3, x1);
319 figure
320 plot(sol.x, sol.y)
321 title('System without hippocampus and a timedelay of 19 min. ')
322 legend('CRH', 'ACTH', 'Cortisol')
323 set(gca, 'XLim', [2*1440 3*1440])
324 set(gca, 'XTick', 2*1440:120:3*1440)
325 set(gca, 'XMinorTick', 'on')
326 xlabel('Time, [min]')
327 %dette er brugt til lundbeck præsentation og artikel 1.
328 figure
329 plot(sol.x, 2*sol.y(2,:))
330 %legend('ACTH')
331 set(gca, 'XLim', [2*1440-30 3*1440-30])
332 set(gca, 'XTick', 2*1440-30:120:3*1440-30)
333 set(gca, 'XMinorTick', 'on')
334 ylabel('ACTH, [pg/ml]')
335 xlabel('Time, [min]')
336 figure
337 plot(sol.x, 2*sol.y(3,:))
338 %legend('Cortisol')
339 set(gca, 'XLim', [2*1440-30 3*1440-30])
340 set(gca, 'XTick', 2*1440-30:120:3*1440-30)
341 set(gca, 'XMinorTick', 'on')
342 ylabel('Cortisol, [\mug/dl]')
343 xlabel('Time, [min]')
344 %ny vektor defineres således at nulpunktet er hvor man ønsker
345 sol.X=sol.x-(2*1440-30);
346 figure
347 plot(sol.X, 2*sol.y(2,:))
348 %legend('ACTH')
349 set(gca, 'XLim', [0 1440])
350 set(gca, 'XTick', 0:120:3*1440)
351 set(gca, 'XMinorTick', 'on')
352 ylabel('ACTH, [pg/ml]')
353 xlabel('Time, [min]')
354 figure
355 plot(sol.X, 2*sol.y(3,:))
356 %legend('Cortisol')
357 set(gca, 'XLim', [0 1440])
358 set(gca, 'XTick', 0:120:1440)
359 set(gca, 'XMinorTick', 'on')
360 ylabel('Cortisol, [\mug/dl]')
361 xlabel('Time, [min]')
362 figure
363 plot(sol.X, sol.y)
364 title('System without hippocampus and a timedelay of 19 min. ')
365 legend('CRH', 'ACTH', 'Cortisol')
366 set(gca, 'XLim', [0 1440])
367 set(gca, 'XTick', 0:120:1440)
368 set(gca, 'XMinorTick', 'on')
369 xlabel('Time, [min]')

```

B.4 Files loaded by the main file used for numerical analysis

Listing B.4: The Jacobian of the unreduced system.

```

1 function F=System_Jacobian(t, x, xi, k0, k1, k2, psi, rho, alpha, gamma, c
, c3, w1, w2, w3, x1);
2 F=[-w1 0 k0*(xi*alpha*(x(3)^(alpha-1)*c^alpha/(c^alpha+x(3)^alpha)^2)-
psi*gamma*c3^gamma*(x(3)^(gamma-1)/(c3^gamma+x(3)^gamma)^2))
3 k1*(1-rho*(x(3)^alpha/(c^alpha+x(3)^alpha))) -w2 -k1*rho*alpha*(x(3)
^(alpha-1)*c^alpha/(c^alpha+x(3)^alpha)^2)*x(1)
4 0 k2 -w3];

```

Listing B.5: The differential equations of the unreduced system.

```

1 function xdot=Ikke_reduceret_system_med_hippocampus(t, x, k0, k1, k2, w1,
w2, w3, xi, psi, rho, alpha, gamma, c, c3, x1)
2 %De afledte til tiden nul bestemmes
3 xdot=zeros(3,1);
4 %Systemet defineres
5 xdot(1)=k0*(1+xi*(x(3)^alpha/(c^alpha+x(3)^alpha))-psi*(x(3)^gamma/(x(3)^
gamma+c3^gamma))-w1*x(1)+0.11*(-0.295*x1*cos(2*pi/1440*(t+90))
+0.1924*x1*sin(2*pi/1440*(t+90)));
6 xdot(2)=k1*(1-rho*(x(3)^alpha/(c^alpha+x(3)^alpha)))*x(1)-w2*x(2);
7 xdot(3)=k2*x(2)-w3*x(3);
8
9 %xdot(1)=(1+xi*(x(3)^alpha/(1+x(3)^alpha))-psi*(x(3)^gamma/(c3tilde^gamma+
x(3)^gamma)))-w1tilde*x(1);
10 %xdot(2)=(1-rho*(x(3)^alpha/(1+x(3)^alpha)))*x(1)-w2tilde*x(2);
11 %xdot(3)=x(2)-w3tilde*x(3);
12
13
14 %k0=w1*x1/(1+xi*(x3^alpha/(c^alpha+x3^alpha))-psi*(x3^gamma/(x3^gamma+c3^
gamma)))
15 %k1=w2*x2/((1-rho*(x3^alpha/(c^alpha+x3^alpha)))*x1)
16 %k2=w3*x3/x2

```

Listing B.6: The Jacobian of the reduced system.

```

1 function F=Reduced_system_Jacobian(x, t, xi, psi, rho, alpha, gamma,
c3tilde, w1tilde, w2tilde, w3tilde);
2 F=[-w1tilde 0 xi*alpha*(x(3)^(alpha-1)/(1+x(3)^alpha)^2)-psi*gamma*
c3tilde^gamma*(x(3)^(gamma-1)/(c3tilde^gamma+x(3)^gamma)^2)
3 (1-rho*(x(3)^alpha/(1+x(3)^alpha))) -w2tilde -rho*alpha*(x(3)^(alpha
-1)/(1+x(3)^alpha)^2)*x(1)
4 0 1 -w3tilde];

```

Listing B.7: The differential equations of the reduced system.

```

1 function xdot=Reduceret_system_med_hippocampus(t, x, xi, psi, rho, alpha,
gamma, c3tilde, w1tilde, w2tilde, w3tilde)
2 %De afledte til tiden nul bestemmes
3 xdot=zeros(3,1);
4 %Systemet defineres
5 xdot(1)=(1+xi*(x(3)^alpha/(1+x(3)^alpha))-psi*(x(3)^gamma/(c3tilde^gamma+x
(3)^gamma))-w1tilde*x(1);
6 xdot(2)=(1-rho*(x(3)^alpha/(1+x(3)^alpha)))*x(1)-w2tilde*x(2);
7 xdot(3)=x(2)-w3tilde*x(3);

```

Listing B.8: The function $H(X_3) - L(X_3)$.

```

1 function f=ZerosofRx3Lx3(x, xi, psi, rho, alpha, gamma, c3tilde, w1tilde,
   w2tilde, w3tilde)
2 f=(1/(w1tilde*w2tilde*w3tilde))*(1+xi*(x^(alpha)/(1+x^(alpha)))-psi*(x^(
   gamma)/(c3tilde^gamma+x^(gamma)))*(1-rho*(x^(alpha)/(1+x^(alpha))))-x
   ;

```

Listing B.9: The function $L(X_3) - H(X_3)$.

```

1 function f=minusZerosofRx3Lx3(x, xi, psi, rho, alpha, gamma, c3tilde,
   w1tilde, w2tilde, w3tilde)
2 f=-1*((1/(w1tilde*w2tilde*w3tilde))*(1+xi*(x^(alpha)/(1+x^(alpha)))-psi*(x
   ^gamma)/(c3tilde^gamma+x^(gamma)))*(1-rho*(x^(alpha)/(1+x^(alpha))))
   -x);

```

Listing B.10: The differential equations for the system including timedelays.

```

1 function ydot=unreduced_system_med_hippocampus_delay_model(t, y, Z, k0, k1
   , k2, w1, w2, w3, xi, psi, rho, alpha, gamma, c, c3, x1)
2 %De afledte til tiden nul bestemmes
3 ylag1=Z(:,1);
4 ylag2=Z(:,2);
5 ylag3=Z(:,3);
6 %The system with time delay is defined
7
8 ydot=[k0*(1+xi*(ylag1(3)^alpha/(c^alpha+ylag1(3)^alpha))-psi*(ylag2(3)^
   gamma/(ylag2(3)^gamma+c^gamma))-w1*y(1)%+0.7*(-0.295*x1*cos(2*pi
   /1440*(t+90))+0.1924*x1*sin(2*pi/1440*(t+90)))
9 k1*(1-rho*(ylag1(3)^alpha/(c^alpha+ylag1(3)^alpha)))*y(1)-w2*y(2)
10 k2*ylag3(2)-w3*y(3)];
11
12
13 %xdot(1)=(1+xi*(x(3)^alpha/(1+x(3)^alpha))-psi*(x(3)^gamma/(c3tilde^gamma+
   x(3)^gamma))-w1tilde*x(1);
14 %xdot(2)=(1-rho*(x(3)^alpha/(1+x(3)^alpha)))*x(1)-w2tilde*x(2);
15 %xdot(3)=x(2)-w3tilde*x(3);
16
17
18 %k0=w1*x1/(1+xi*(x3^alpha/(c^alpha+x3^alpha))-psi*(x3^gamma/(x3^gamma+c3^
   gamma)))
19 %k1=w2*x2/((1-rho*(x3^alpha/(c^alpha+x3^alpha)))*x1)
20 %k2=w3*x3/x2

```

Listing B.11: The history file used in the differential equations for the system including timedelays.

```

1 function s = unreduced_System_med_hippocampus_delaymodel_History(t, k0, k1
   , k2, w1, w2, w3, xi, psi, rho, alpha, gamma, c, c3, x1)
2 % Der skal defineres en historiefunktion, her er den bare konstant.
3 s = [2, 21, 11];

```

Bibliography

- [1] Vadim Kyrylov, Liudmila A. Severyanova, and Amandio Vieira. Modeling robust oscillatory behaviour of the hypothalamic-pituitary-adrenal axis. *IEEE Transactions on Biomedical Engineering*, 52, 2005.
- [2] Smiljana Jelic, Zeljko Cupic, and Ljiljana Kolar-Anic. Mathematical modeling of the hypothalamic-pituitary-adrenal system activity. *Mathematical Biosciences*, 197, 2005.
- [3] Danka Savic and Smiljana Jelic. A mathematical model of the hypothalamo-pituitary-adrenocortical system and its stability analysis. *Chaos, Solitons & Fractals*, 26, 2005.
- [4] Danka Savic and Smiljana Jelic. Stability of a general delay differential model of the hypothalamo-pituitary-adrenocortical system. *International Journal of Bifurcation and Chaos*, 16, 2006.
- [5] Gerard J. Tortora and Bryan Derrickson. *Principles of Anatomy and Physiology, 11th edition*. John Wiley & Sons, Inc., 2006.
- [6] Matthias Conrad, Christian Hubold, Bernd Fischer, and Achim Peters. Modeling the hypothalamus-pituitary-adrenal system: homeostasis by interacting positive and negative feedback. *J Biol Phys*, 35, 2009.
- [7] George Chrousos. Editorial: Ultradian, circadian, and stress-related hypothalamic-pituitary-adrenal axis activity- a dynamic *Digital-to-Analog* modulation. *Endocrinology*, 139, 1998.
- [8] James E. Griffin and Sergio R. Ojeda. *Textbook of Endocrine Physiology, Fifth Edition*. Oxford University Press, Inc, 2004.
- [9] B. J. Carroll, F. Cassidy, D. Naftolowitz, N. E. Tatham, W. H. Wilson, A. Iranmanesh, P. Y. Liu, and J. D. Veldhuis. Pathophysiology of hypercortisolism in depression. *Acta Psychiatrica Scandinavia*, 115, 2007.
- [10] Jean D. Wilson and Daniel W. Foster. *Williams Textbook of Endocrinology, Eighth Edition*. W. B. Saunders Company, 1992.
- [11] Philip Felig and Lawrence A. Frohman. *Endocrinology & Metabolism, Fourth Edition*. McGRAW-HILL, Inc., 2001.
- [12] Karen Collatz Christensen, Kristófer Hannesson, Daniel Frank Hansen, Luminita Felicia Jensen, and Kenneth Hagde Mandrup Nielsen. Matematisk modellering af hpa-aksen. Master's thesis, Roskilde Universitetscenter, 2007.
- [13] Martin Braun. *Differential Equations and Their Applications, Fourth Edition*. Springer-Verlag New York, Inc., 1993.
- [14] Linda J. S. Allen. *An Introduction to Mathematical Biology*. Pearson Education, Inc., 2007.
- [15] William E. Boyce and Richard C. Dippima. *Elementary Differential Equations and Boundary Value Problems, eighth edition*. John Wiley & Sons, Inc, 2005.

-
- [16] Jens Starke, Mads Peter Sørensen, Poul Hjort, John Bagterp Jørgensen, Kirsten Riber Philipsen, Lasse Engbo Christiansen, and Henrik Madsen. *An Introduction to Mathematical Modelling, Nonlinear Dynamics, Stochastic and Complex Systems*. 2009.
- [17] William R. Wade. *An Introduction to Analysis, Third Edition*. Pearson Education, Inc., 2004.
- [18] John Guckenheimer and John Holmes. *Nonlinear Oscillations, Dynamical Systems, and Bifurcations of Vector Fields*. Springer-Verlag New York, Inc., 1983.
- [19] J.D. Murray. *Mathematical Biology:I. An Introduction, Third Edition*. Springer, 2002.
- [20] J. Hale and H. Kocak. *Dynamics and Bifurcations*. Springer-Verlag New York, Inc., 1991.
- [21] Vasile I. Istratescu. *Fixed Point Theory, Second Edition*. D. Reidel Publishing Company, 1981.
- [22] Yi-Wei Liu, Zhi-Hong Hu, Jian-Hua Peng, and Bing-Zheng Liu. A dynamical model for the pulsatile secretion of the hypothalamo-pituitary-adrenal axis. *Mathematical and Computer Modelling*, 29(4):103–110, 1999.
- [23] Vadim Kyrlyov, Liudmila A. Severyanova, and Anatoly Zhiliba. The ultradian pulsatility and nonlinear effects in the hypothalamic-pituitary-adrenal axis. *The 2004 International Conference on Health Sciences Simulation (HSS 2004), San Diego, California*, 2004.
- [24] Thomas D. Geraciotti JR., David N. Orth, Nosa N. Ekhatior, Bennett Blumenkopf, and Peter T. Loosen. Serial cerebrospinal fluid corticotropin-releasing hormone concentrations in healthy and depressed humans*. *Journal of Clinical Endocrinology and Metabolism*, 74(6):1325–1330, 1992.
- [25] L.D. Landau and E.M. Lifshitz. *Course of Theoretical Physics Volume 5, Statistical Physics 3rd Edition Part 1*. Copyright ©1980, Elsevier Ltd, 2008.
- [26] Donald Voet and Judith G. Voet. *Biochemistry, Third Edition*. John Wiley & Sons, Inc., 2004.
- [27] Danka Savic and Smiljana Jelic. A theoretical study of hypothalamo-pituitary-adrenocortical axis dynamics. *Annals New York Academy of Sciences*, 1048:430–432, 2005.
- [28] Frank Vinther, Morten Andersen, and Johnny Tom Ottesen. Standard model of the hypothalamic-pituitary-adrenal axis. *Journal of Mathematical Biology*, 2010. Sent to review.
- [29] Christoph Kellendonk, Peter Gass, Oliver Kretz, Günther Schütz, and Francois Tronche. Corticosteroid receptors in the brain: Gene targeting studies. *Brain Research Bulletin*, 57(1):73–83, 2002.
- [30] Kozo Hashimoto, Tatsuya Nishioka, Yukiko Numata, Takashi Ogasa, Jingo Kageyama, and Shuso Suemaru. Plasma levels of corticotropin-releasing hormone in hypothalamic-pituitary-adrenal disorders and chronic renal failure. *Acta Endocrinol*, 128(6):503–507, 1993.
- [31] Liu Bingzhenga, Zhao Zhenye, and Chen Liansong. A mathematical model of the regulation system of the secretion of glucocorticoids. *Journal of Biological Physics*, 17(4):221–233, 1990.
- [32] Walter Rudin. *Real and Complex Analysis, Second Edition*. McGraw-Hill, Inc., 1974.